

*Calcium homeostasis and role of ryanodine receptor
type 1 (RyR1) in immune cells*

Inauguraldissertation

zur

**Erlangung der Würde eines Doktors der Philosophie
vorgelegt der
Philosophisch-Naturwissenschaftlichen Fakultät
der Universität Basel**

von

Mirko Vukcevic

aus Belgrad (Serbien)

Basel, 2010

**Genehmigt von der Philosophisch-Naturwissenschaftlichen
Fakultät auf Antrag von:**

Prof. Dr. Jean Pieters

Prof. Dr. Hans-Rudolf Brenner

PD Dr. Susan Treves

Basel, den 08. Dezember 2009

Prof. Dr. Eberhard Parlow

Dekan

ACKNOWLEDGMENTS

First of all I would like to thank PD Dr. Susan Treves for her scientific support and always good will to give me advice and to answer with a lot of patience any question I may have. I appreciate very much her enormous energy, kindness, enthusiasm and power to create perfect atmosphere for work in our group.

Special thanks to Dr. Franceso Zorzato for his support, scientific passion and always right criticism that allow all our projects to reach the best scientific answers.

I sincerely thank Professor Giulio Spagnoli for supporting my thesis and sharing with us his great insight and novel ideas.

In addition I would like to thank all present and past members of the Perioperative Patient Safety group (Thierry Girard, Soledad Levano, Anne-Sylvie Monnet, Martine Singer, Antonio Teixeira, Marcin Maj, Jin-Yu Xia and Raphael Thurnheer for their help and very pleasant and friendly atmosphere they create in the lab.

I would like to also acknowledge the support of the Anesthesia department and thank Professor Albert Urwyler for believing in us.

I want to express my gratitude to my family and friends for moral support and their forgiveness for not spending enough time with them.

I cordially thank Professor Jean Pieters and Professor Hans Rudolf Brenner who accepted to be members of my PhD committee.

CONTENTS

ABSTRACT	1
LIST OF ABBREVIATIONS	5
CHAPTER 1: INTRODUCTION	8
I. Dendritic cells and their role in innate immunity	8
<i>I.1 Initiate immunity and pattern recognition; general</i>	
<i>Introduction</i>	8
<i>I.2 Dendritic cells and antigen sampling and processing</i>	11
<i>I.3 Formation of immunological synapse and T cell activation</i>	20
II. Calcium homeostasis and the role of calcium as a second messenger in muscle and immune cells	22
<i>II.1 Ca²⁺ entry mechanisms</i>	23
<i>II.1.1 Voltage Gated Ca²⁺ channels</i>	24
<i>II.1.2 Store-operated channels (SOCs)</i>	27
<i>II.2 Ca²⁺ release from internal stores</i>	30
<i>II.3 Role of Ca²⁺ as a second messenger in skeletal and cardiac muscle excitation-contraction coupling</i>	34
<i>II.4 Role of Ca²⁺ signalling in immune cells</i>	38
III. RYANODINE RECEPTORS AND NEUROMUSCULAR DISORDERS	42
<i>III.1. The Ryanodine receptor calcium channels</i>	42
<i>III.1.1. Isoforms of ryanodine receptor and their structure</i>	42
<i>III.1.2. RyR modulators</i>	46
<i>III.2. Genetic linkage and functional effects of RYR1 mutations</i>	52
<i>III.3. Neuromuscular disorders</i>	56

<i>III.3.1 Malignant Hyperthermia</i>	57
<i>III.3.2 Central Core Disease</i>	62
<i>III.3.3 Multi-minicore disease</i>	63
<i>III.3.4 Centronuclear myopathy (CNM)</i>	65
CHAPTER 2: RESULTS	66
I. Ca²⁺ homeostasis and role of RyR1 in dendritic cells	66
<i>I.1 Introduction to publications</i>	66
<i>I.2 publications</i>	67
II. Functional properties of RyR1 mutations linked to malignant hyperthermia and central core disease	97
<i>II.1 Introduction to publications</i>	97
<i>II.2 publications</i>	98
CHAPTER 3: GENERAL CONCLUSION AND PERSPECTIVES	114
REFERNCES	119
CURRICULUM VITAE	144

ABSTRACT

Ryanodine receptors are intracellular Ca^{2+} release channels located in the membrane of the Endoplasmic/Sarcoplasmic Reticulum. Ryanodine receptor 1 isoform is preferentially expressed in skeletal muscle where it is responsible for release of Ca^{2+} from the SR, an event that leads to muscle contraction. Point mutations in the gene encoding ryanodine receptor 1 have been linked to disease such as Malignant Hyperthermia, Central core disease and Multi-minicore disease.

Malignant Hyperthermia is a pharmacogenetic disorder with autosomal dominant inheritance and abnormal Ca^{2+} homeostasis in skeletal muscle in response to triggering agents. In susceptible individuals, a malignant hyperthermia crisis may be triggered by commonly used halogenated anaesthetics (halothane, isoflurane) or muscle relaxants (succinylcholine). The main symptoms are hypermetabolism and muscle rigidity. Without treatment, death would occur in more than 80% of cases. Although a genetic-chip based diagnostic approach is under development, the invasive *in vitro* contracture test remains the “gold standard” to diagnose this disorder.

Central core disease is a slowly progressive myopathy characterized by muscle weakness and hypotonia. Central core disease is characterized histologically by the presence of central cores running along longitudinal axis of the muscle fiber.

Multi-minicore disease disease is a more severe, rare, autosomal recessive myopathy characterized histologically by the presence of multi-minicores in only a small number of sarcomeres. So far, no effective therapy has been developed to treat muscle weakness in central core disease and multi-minicore disease patients and their diagnosis is difficult on the basis of clinical findings alone. Histological examination of muscle tissue in these diseases is essential.

Recent data has shown that ryanodine receptor 1 is also expressed in some areas of the central nervous system as well as in cells of the immune system, specifically B-lymphocytes and dendritic cells.

The first part of my thesis focuses on the role of the ryanodine receptor 1 in dendritic cell. We first show that both immature and mature *in vitro* derived dendritic cells as well as circulating plasmacytoid cells express the ryanodine receptor 1 Ca^{2+} release channel within the endoplasmatic reticulum. Pharmacological activation of the ryanodine receptor 1 leads to the rapid release of Ca^{2+} from intracellular stores, and in the presence of sub-optimal concentrations of microbial stimuli, provides synergistic signals resulting in dendritic cell maturation and stimulation of T cell function. Furthermore, we were interested in unravelling more direct roles of this receptor in dendritic cells function. Interestingly, ryanodine receptor 1 activation in dendritic cells causes a very rapid increase in surface expression of major histocompatibility complex II molecules. In order to dissect the physiological route of ryanodine receptor 1 activation *in vivo* we hypothesized that a possible functional partner of ryanodine receptor 1 in dendritic cells could be, an L-type Ca^{2+} channel. We were able to show that human dendritic cells express the cardiac isoform of the L-type Ca^{2+} channel, which acts as a ryanodine receptor 1 functional partner on the plasma membrane of dendritic cells. We show that depolarization of dendritic cells by the addition of potassium chloride activates L-type Ca^{2+} channels initiating Ca^{2+} influx and activation of Ca^{2+} release via ryanodine receptor 1 and that this process could be prevented by nifedipine or ryanodine. Physiologically potassium could be released from dying cells within an inflamed tissue or from T- cells into immunological synapse during dendritic cell T-cell engagement and these events could be possible routes for activation of L-type Ca^{2+} channel- ryanodine receptor 1 signalling in dendritic cells *in vivo*. Thus, *in vivo*, activation of the ryanodine receptor 1 signalling cascade may be important during the early stages of infection, providing the immune system with rapid mechanisms to initiate an early response, facilitating the presentation of antigens to T cells.

While continuing our investigation on Ca^{2+} homeostasis in dendritic cells we noticed that spontaneous Ca^{2+} oscillations occur in immature dendritic cells but not in dendritic cells stimulated to undergo maturation with lipopolysaccharide or other toll like-receptor agonists. We investigated the mechanism and role of spontaneous Ca^{2+} oscillations in immature dendritic cells and found that they are mediated by the inositol-1,4,5-trisphosphate receptor since they were blocked by pre-treatment of cells with the inositol-

1,4,5-trisphosphate receptor antagonist Xestospongin C and 2-Aminoethoxydiphenyl borate. A component of the Ca^{2+} signal is also due to influx from the extracellular environment. As to the biological function of these high frequency oscillations, our results indicate that they are associated with the translocation of a Ca^{2+} dependent transcription factor (nuclear factor of activated T-cells) into the nucleus of immature dendritic cells. In fact, once the Ca^{2+} oscillations are blocked with the 2-aminoethoxydiphenyl borate or by treating cells with lipopolysaccharide, nuclear factor of activated T-cells remains cytoplasmic.

The results from the first part of my thesis provide novel insights into the physiology of dendritic cells, role of ryanodine receptor 1 signaling and Ca^{2+} as an important second messenger in these cells.

The second aim of my thesis deals with functional properties of ryanodine receptor 1 carrying mutations linked to neuromuscular disorders, which is important from diagnostic point of view but also to understand the basic pathophysiological mechanism leading to these different diseases.

Since functional ryanodine receptors 1 are expressed in B-lymphocytes we investigated Ca^{2+} homeostasis in B-lymphocytes transformed with Epstein Barr virus from patients carrying the mutation linked to malignant hyperthermia and healthy donors.

In the first study from the Swiss population we investigated four novel mutations found in malignant hyperthermia susceptible pedigrees: (p.D544Y, p.R2336H, p.E2404K and p.D2730G). We found that the resting Ca^{2+} levels were significantly higher in cells from all four mutations bearing individuals compared to controls. These four mutations were also found to significantly affect either 4-chloro-m-cresol or caffeine dose response curves suggesting higher sensitivity of ryanodine receptor 1 to pharmacological activation in patients carrying these mutations.

In the second study we examined patients from the Swedish population carrying five different novel mutations (p.E1058K, p.R1679H, p.H382N, p.K1393R and p.R2508G). The first 4 patients had serious malignant hyperthermia clinical reactions and thereafter have tested by the in vitro contracture test and classified as malignant hyperthermia susceptible; the patient with the fifth mutation, p.Arg2508Gly, had been diagnosed as a central core disease. In this study as well functional studies were performed on Epstein

Barr virus transformed B-lymphocytes from patients carrying mutations and healthy donors. Our results from the Swedish population suggest that ryanodine receptor 1 mutations also lead to abnormal Ca^{2+} homeostasis. Results from these and other studies support the use of Epstein Barr virus transformed B-lymphocytes as an alternative, non-invasive, protocol for the diagnosis and the functional proof that a mutation in the ryanodine receptor causes alterations in Ca^{2+} homeostasis. This is a pre-requisite for the molecular diagnosis of malignant hyperthermia. These results also provide new concepts for the treatment of muscular pathologies involving mutations in ryanodine receptor 1.

LIST OF ABBREVIATIONS

AMP	Adenosine monophosphate
APCs	Antigen presenting cells
ATP	Adenosine triphosphate
Ca ²⁺	Calcium
CACNA1	Voltage-dependent calcium channel alpha 1
CaM	Calmoduline
CCD	Central core disease
CCE	Capacitative calcium entry
CICR	Calcium induce calcium release
CNM	Centronuclear myopathy
cSMAC	Centralized supramolecular activation cluster
DAG	Diacylglycerol
DCs	Dendritic cells
DHPR	Dihydropyridine receptor
EBV	Epstein-Barr virus
EC	Excitation-contraction
ECCE	Excitation coupled Ca ²⁺ entry
ER	Endoplasmic reticulum
FKBP12	12 kDa FK-506-binding protein
GM-CSF	Granulocyte-macrophage colony-stimulating factor
GSH	Glutathion
GSSG	Glutathion disulphide

ICAM 1	Inter-Cellular Adhesion Molecule 1
iDCs	Immature dendritic cells
IL	Interleukin
IP3	Inositol 1, 4, 5-trisphosphate
IP3R	Inositol 1, 4, 5-trisphosphate receptor
mDCs	Mature dendritic cells
IVCT	In Vitro Contracture Test
LFA-1	Lymphocyte function-associated antigen 1
LPS	Lipopolysaccharides
MH	Malignant hypethermia
MHC	Major Histocompatibility Complex
MHE	Malignant hyperthermia equivocal
MHN	Malignant hyperthermia normal
MHS	Malignant hyperthermia susceptible
MmD	Multi-minicore disease
Na+	Sodium
NF-AT	Nuclear factor of activated T cells
NF- κ B	Nuclear factor κ B
NK	Natural killer
NO	Nitric oxide
PAMPS	Pathogen-associated molecular patterns
PBS	Phosphate-buffered saline
PDC	Plasmacytoid cells
PK	Protein kinase
PLC	Phospholipase C
PMCA	Plasma membrane calcium ATPase
PRR	Pattern recognition receptors
ROCs	Receptor-operated channels
RyR	Ryanodine receptor
SMOCs	Second messenger operated channels
SOCs	Store-operated channels

SERCA	Sarcoplasmic/endoplasmic reticulum Ca ²⁺ -ATPase
SR	Sarcoplasmic reticulum
STIM	Stromal interaction molecule
TCR	T cell antigen receptors
TLR	Toll-like receptor
VOCs	Voltage-operated Ca ²⁺ channels

CHAPTER 1: INTRODUCTION

I. Dendritic cells and their role in innate immunity

I.1 Initiate immunity and pattern recognition; general introduction

Vertebrates display two main kinds of immunity, innate immunity and adaptive immunity. The first line and evolutionary ancient part of host defence is innate immunity. On the other hand the evolutionary younger adaptive immune response that comes in the second stage of host defence provides specific recognition of foreign antigens and allows generation of “immunological memory”, which in a subsequent encounter with the same antigen, generates a more efficient immune response.

Many cells participate in innate immune response such as macrophages, dendritic cells (DCs), mast cells, neutrophils, eosinophils, and NK cells. These cells express pattern-recognition receptors, which are germ line encoded and recognize conserved repetitive antigenic structures called PAMPs (pathogen-associated molecular patterns) (Janeway and Medzhitov, 2002).

The innate immune response recognizes foreign antigens by way of a variety of pattern recognition receptors (PRR). PRR are expressed on the cells surface, in intracellular compartments or secreted into the bloodstream and tissue fluids. The principal functions of PRR include opsonisation, activation of the complement and coagulation cascades, phagocytosis, activation of proinflammatory signalling pathways, and induction of apoptosis. Antigen presenting cells also use pattern recognition receptors to become

activated and efficiently present antigens to antigen specific lymphocytes and successfully connect innate and adaptive immune responses. Janeway proposed that antigen-presenting cells of the innate immune system perform their own self-nonself discrimination. This is based on their ability to innately recognize the signatures of bacterial presence, through these receptors. This hypothesis of contribution of innate immunity to self-nonself distinction is still not completely elaborated and does not explain for example the lack of response to symbiotic bacteria of gut flora that also possess PAMPs. Contrary to this hypothesis Matzinger introduced the “danger theory”. This theory suggests that the immune system is controlled by the detection of damage to the body, not detection of antigen or bacterial products. Matzinger proposed the existence of endogenous mediators produced by damaged or stressed cells, which activate the immune system through cells of the innate immune system. On the other hand in the absence of “danger signals” the cells of the innate immune system can actively suppress an immune response. This dynamic process is known as the mechanism of peripheral tolerance (Germain, 2004; Janeway and Medzhitov, 2002; Matzinger, 1994; Matzinger, 2002).

The Toll-like receptor (TLR) family is the best characterized class of PRRs in mammalian species. Most mammalian species express about 10 to 15 different TLRs which are encoded by a yet to be defined number of genes. Different TLRs recognize different PAMPs. Lipopolysaccharide (LPS) is detected by TLR4 and mice with a targeted deletion of TLR4 gene are unresponsive to LPS (Hoshino et al., 1999). Ligands for TLR2 constitute a large list and include lipoproteins and lipoteichoic acids. TLR5 recognize flagellin, the protein subunits that make up bacterial flagella (Hayashi et al., 2001). The unmethylated CpG DNA of bacteria and viruses are detected by TLR9, double stranded RNA by TLR3 and single stranded viral RNA detected by TLR7 (Diebold et al., 2004; Heil et al., 2004; Lund et al., 2004)

Innate recognition of PAMPs through TLRs initiates an inflammatory response characterized by the recruitment of cells to the sites of infection to induced killing of pathogens and to stop their spread (Iwasaki and Medzhitov, 2004). Upon recognition of their ligands, TLRs induced the expression of many different host defence genes. These include inflammatory cytokines and chemokines, antimicrobial peptides, costimulatory

molecules, MHC molecules and other effectors necessary for successful activation of immune response and finally host defence.

Different TLRs direct different types of adaptive immune responses and probably activate different intracellular signalling pathways. The canonical signalling pathway for TLRs following PAMP ligation involves the interaction of the adaptor molecule MyD88, with TLR. MyD88 has both a TIR (Toll/Interleukin-1 receptor) domain and death domain, and the recruitment of MyD88 to a TLR occurs via a TIR-TIR homotypic interaction. The death domain of MyD88 then binds to the death domain of a serine/threonine kinase, usually interleukin-1-receptor-associated kinase (IRAK), and the signal is propagated via a specific member of the TNF-receptor-associated factor (TRAF) family, TRAF6, ultimately leading to the activation of NF- κ B mitogen activated protein (MAP) kinases, and the transcription of genes connected with activation of the immune response. There are other signalling pathways downstream of TLRs that do not require IRAK-4. Activation of TIRF pathway, for example, leads to the production of antiviral gene products via the transcription factor, IRF3, suggesting signalling specificity that may be relevant to the type of infection (Kopp and Medzhitov, 2003). In order to protect the host against a highly diverse microbial world the innate immune system is very complex and has diversities to recognize through different TLRs the different products of microbial infection. DCs are the key cell type that couples TLR-mediated innate immune recognition to the initiation of the specific immune response by activating T- and B-lymphocytes.

1.2 Dendritic cells and antigen sampling and processing

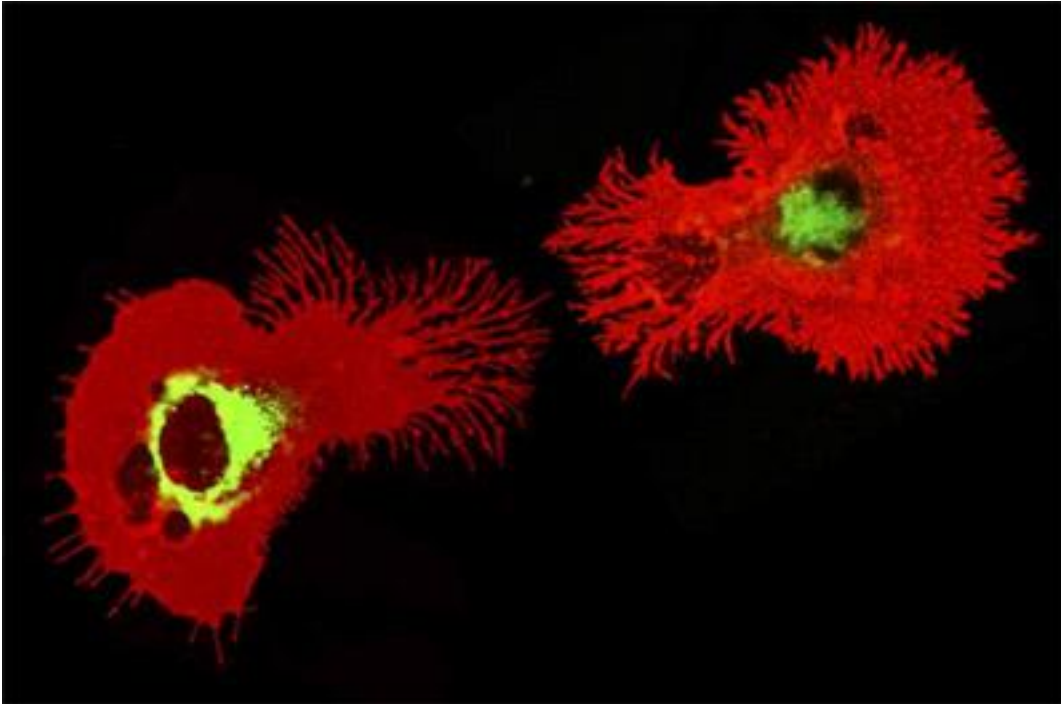


Figure 1-1: Two Dendritic cells. The nucleus is shown in green while the cell body is in red. At certain development stages dendritic cells grow branched projections, the dendrites, which give the cell its name.

http://www.wehi.edu.au/faculty_members/research_projects/what_dendritic_cells_do

DCs are the most potent, professional, antigen presenting cells (Fig 1-1). They play an essential role in connecting innate and adaptive immune responses. Due to their efficiency in antigen-presentation and their unique migration behaviour, dendritic cells are the cells responsible for the activation of naive T-lymphocytes.

DCs were first discovered by Paul Langerhans in 1868 during experiments to characterize the cellular constituents of skin (Jolles, 2002; Kimber et al., 2009). The term “dendritic” cell was coined by Steinman and Cohn in 1973 (Steinman and Cohn, 1973).

In general DCs exist in two forms immature DCs (iDCs) and mature DCs (mDCs). Immature DCs reside in the peripheral tissues, where they actively and constantly sample their environment by endocytosis for the presence of foreign antigens. After capturing antigens and being stimulated by cytokines, bacterial compounds and “danger” signals, they become activated and migrate to lymphoid tissues. During migration, DCs undergo profound phenotypical changes and convert into professional antigen-presenting cells, the so-called mDC. This maturation process is followed by downregulation of endocytic activity, upregulation of co-stimulatory molecules and increase of surface expression of major histocompatibility complex molecules that are involved in antigen presentation to T cells (Banchereau and Steinman, 1998; Lanzavecchia, 1996; Trombetta and Mellman, 2005).

Ag-sampling:

Immature DCs have the capacity to internalize a broad range of antigens using specific and non-specific uptake modes.

There are three general types of endocytic routes that can be distinguished in antigen presenting cells (Fig 1-2):

1. receptor mediated endocytosis
2. macropinocytosis
3. phagocytosis

Endocytosis

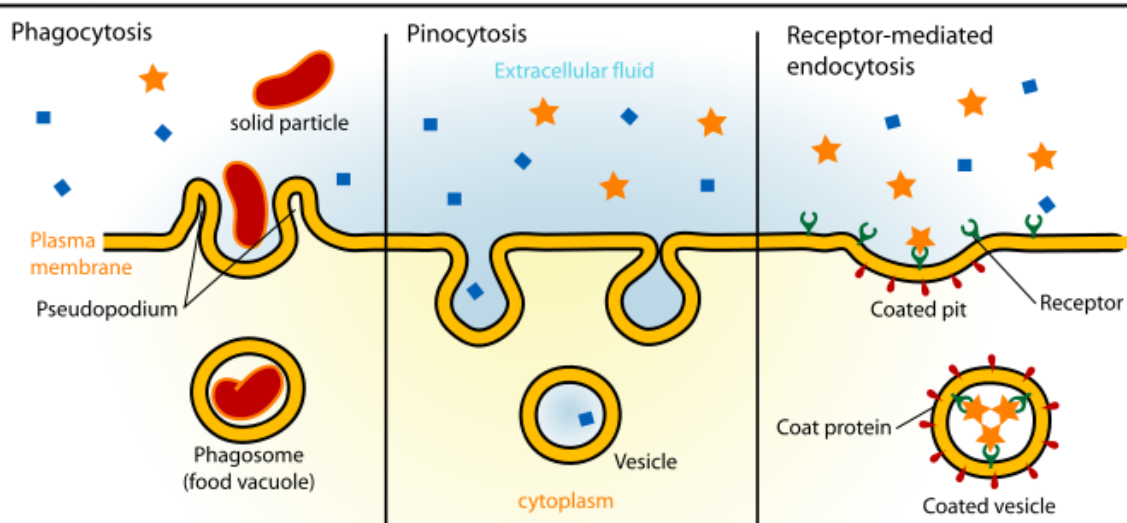


Figure 1-2: Endocytosis. (1) **phagocytosis** is the process by which cells ingest large objects, such as bacteria, or the remnants of cells, which have undergone apoptosis. The membrane invaginates enclosing the wanted particles in a pocket, then engulfs the object by pinching it off, and the object is sealed off into a large vacuole known as a phagosome. (2) **pinocytosis** is the process responsible for the uptake of soluble and single molecules such as proteins. (3) **receptor mediated endocytosis** is a more specific active event where the cytoplasm membrane folds inward to form coated pits. In this case, proteins lock into receptors/ ligands in the cell's plasma membrane and than get engulfed.

1.Receptor mediated endocytosis

Receptor mediated endocytosis allows the efficient internalization of antigens, which enables the APCs to present antigens also in the case of their low concentration (Lanzavecchia, 1990).

Antigen presenting cells express a broad range of surface receptors that mediate endocytosis including: C-type lectin receptors, which function as PRRs, like the macrophage mannose receptor and DEC205 expressed on DCs. In addition Fc receptors can also mediate endocytosis and provide delivery of captured antigens to the intracellular compartment of APCs. There is one important difference between mannose receptors and FcR in terms of recycling, FcR are degraded together with their cargo whereas mannose receptors release their ligand at endosomal pH and get recycled, thus allowing uptake and accumulation of many ligands by a small number of receptors (Fig.1-2) (Banchereau and Steinman, 1998; Jiang et al., 1995; Sallusto and Lanzavecchia, 1994; Sallusto et al., 1995).

2.Macropinocytosis

Macropinocytosis is a cytoskeleton dependent type of fluid phase endocytosis mediated by membrane ruffling and the formation of large vesicles (1-3 μm). In iDCs this process is constitutive and enables a single cell to take up a very large volume of fluid (half of the cell's volume per hour) on the other hand in macrophages and epithelial cells macropinocytosis is stimulated by growth factors (Lanzavecchia, 1996; Sallusto et al., 1995). Macropinosome formation starts at the cell periphery by extension of a large planar membrane ruffle that folds back to form the vesicle (Araki et al., 1996).

3. Phagocytosis

Phagocytosis is the process by which cells ingest large particles, such as apoptotic cells, bacteria, yeasts or parasites. The membrane invaginates enclosing the ingested particle in a pocket, then engulfs the object by pinching it off, and the object is sealed off into a large vacuole known as a phagosome. Phagocytosis serves uptake of antigens in the process of antigen sampling but more importantly represents an innate host defence mechanism. Besides killing of microbes the phagosomal contents represent a major source of exogenous antigens. A number of the endocytic receptors that can recognize ligands free in solution also contribute to the phagocytic process by recognizing their ligands on the surface of microbes. These include FcγRs, complement receptors, and a variety of lectins (Fig.1-2) (Trombetta and Mellman, 2005).

Antigen processing:

Internalized antigens need to be further processed to generate peptide ligands for surface presentation on MHC molecules. There are two pathways for antigen processing (Fig.1-3):

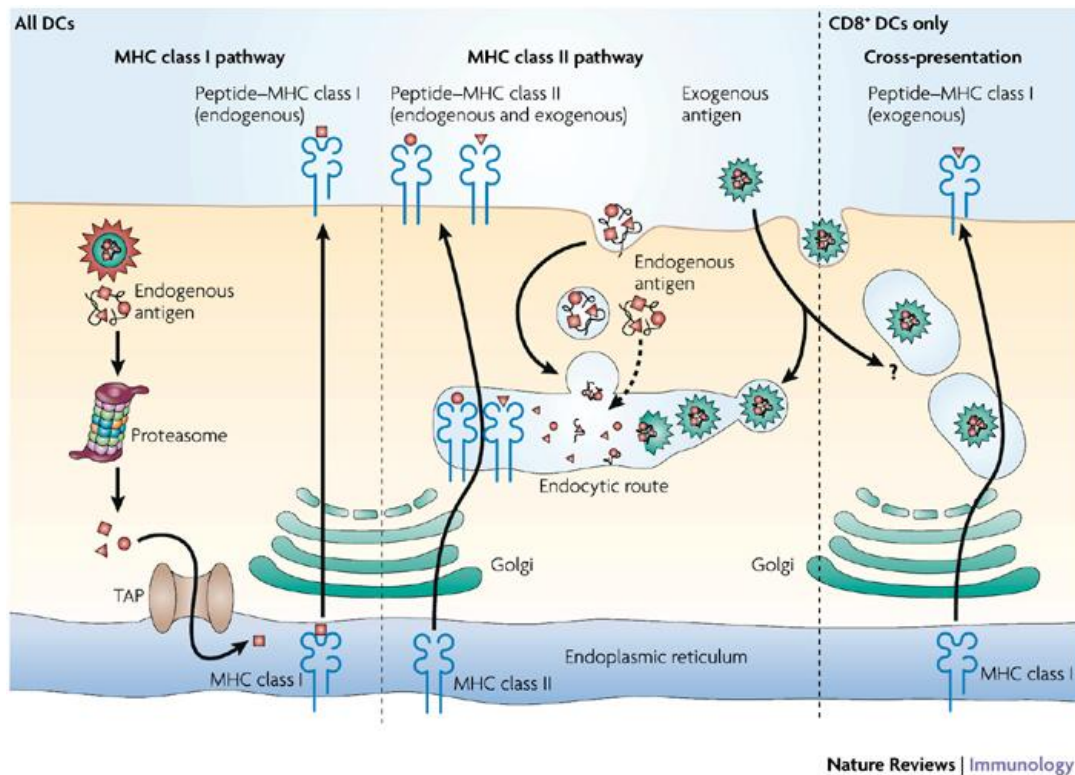


Figure 1-3: Ag-processing pathways. MHC class I molecules present peptides that are derived from proteins degraded mainly in the cytosol, whereas MHC class II molecules present exogenous antigens generated by proteolytic degradation in endosomal compartments and also endogenous components, such as plasma membrane proteins, components of the endocytic pathway and cytosolic proteins that access the endosomes by autophagy. Cross-presentation pathway represents possibility that exogenous antigens get delivered to MHC class I pathway. (José A. Villadangos & Petra Schnorrer, Nature Reviews Immunology 7, 543-555 (July 2007).

1. The MHC class I pathway

MHC class I molecules are found on every nucleated cell of the body (and thus not on red blood cells and platelets). They are heterodimers consisting of a membrane-spanning heavy chain, which is non-covalently associated with a β -chain, called microglobulin. The peptides bind in a cleft generated by the folding of alpha 1 and alpha 2 domains of the heavy chain (Bjorkman et al., 1987). MHC I ligands are derived from endogenous cytosolic proteins. Proteasome, a cytosolic multi-enzyme complex (Baumeister et al., 1998), plays a critical role in cleaving the ubiquitinated proteins into peptides of 10-20 aa length. Peptides presented on MHC class I molecules are recognized by CD8⁺ T-cells.

2. The MHC class II pathway

MHC class II molecules are normally expressed only on professional APCs (macrophages, DCs and B cells). They are composed of two transmembrane glycoproteins, the alpha and beta chain. MHC-II ligands are exogenous, encountering MHC-II molecules following endocytosis. For proteolytic processing proteins are transported into the acidic lysosomal compartment where they are cleaved into shorter peptides by proteases, which include cysteine proteases, the cathepsins as well as asparaginyl endopeptidase (Chapman, 1998; Manoury et al., 1998). MHC class II loading takes place in a specialized endocytic compartment called MHC class II compartment (MIIC) and once loaded the peptide-MHC class II complexes are transported to the surface of APC where they are recognized by CD4⁺T cells.

, MHC-I can present peptides derived from exogenous antigens, and MHC-II can present intracellular antigens that do not come from the extracellular space; these events are called “cross-presentation.” (Bevan, 1976; Trombetta and Mellman, 2005).

Process of DCs maturation:

One of the most important yet at the same time most complex processes concerning DCs is maturation. It is clear that maturation of DCs is crucial for the initiation of immunity and the critical link between innate and many forms of adaptive immunity. Immature DCs begin to mature during the antigen collection stage immediately after receiving adequate stimuli, such as microbial and inflammatory products. In vitro DC maturation can be stimulated by TLR ligands such as LPS. Different cytokines such as IL1, GM-CSF and TNF-alpha are also responsible for DCs maturation but other factors recognized as “danger” signals such as different factors released from dead cells as well. Upon activation DCs travel to lymphoid tissues such as spleen and lymph nodes. There, DCs may complete their maturation process under the influence of signals (e.g. CD40 ligand) received from T cells to which they present antigens. During activation and migration DCs drastically change their phenotype. First there is induction in surface expression of MHC-II, co-stimulatory and MHC-I molecules. Activation of TLRs induces the expression of selectin, and chemokine receptor genes that regulate cell migration to the sites of inflammation (Huang et al., 2001). Secondly there are also drastic morphological changes of iDCs; they develop extensions and membrane folds that give them increased surface area and this further increases the probability of binding to T cells (Mosmann and Livingstone, 2004). An increase in surface area makes the mDC more suitable for antigen presentation rather than collection, maximizing the chance of binding with a T-cell receptive to the specific structures of the presented antigen. Function versus phenotype of mDCs is further complicated by the fact that different maturation stimuli may produce qualitatively different DCs that can produce distinct ways of immunostimulation, selectively polarizing Th1 versus Th2 responses (Lanzavecchia and Sallusto, 2001). Furthermore certain types of stimuli responsible for production of DCs with “intermediate” phenotypes (high MHC-II, low or moderate CD86) may produce tolerogenic effect (Inaba et al., 1997; Steinman et al., 1997).

Different DCs subsets:

In both humans and mouse, distinct DCs subsets occupy special niches defined by their anatomical location and their ability to respond to certain types of pathogens (Iwasaki and Medzhitov, 2004). In humans two main DCs subsets have been identified: CD11c+ myeloid DCs (MDC) and CD11c- CD123+ plasmacytoid cells (PDC). MDC include Langerhans cells, dermal DCs and interstitial DCs, and populations widely distributed throughout the body. PDC are primarily located in the blood and secondary lymphoid organs, but they can be recruited to sites of inflammation. Besides location, the difference between MDC and PDC is manifested by cytokine secretion and TLR expression pattern. MDC secrete high levels of interleukin-12 (IL-12), whereas PDC are thought to play an important role in the innate immune response to different viruses by producing interferon alpha (IFN α) (Asselin-Paturel and Trinchieri, 2005; Colonna et al., 2004).

In vitro monocyte derived dendritic cells, produced by culturing monocytes with granulocyte-macrophage colony-stimulating factor (GM-SCF) and interleukin 4 (IL4), are phenotypically equivalent to iDCs residing in peripheral tissues. They can undergo maturation when stimulated by agonist such as LPS and reach the mature stage exhibiting all phenotypic characteristics of mDCs found in secondary lymphoid tissues.

Research on DCs was enhanced since the discovery that DCs could be produce in-vitro from monocytes in the presence of cytokines such as IL4 and GM-CSF (Sallusto et al., 1995).

1.3 Formation of immunological synapse and T cell activation:

A critical event in the initiation of the adaptive immune response is the activation of T lymphocytes. This is mediated by the interaction of T cell antigen receptors (TCRs) with their ligands, major histocompatibility molecule-peptide complexes (MHC-peptide). Signaling via the TCR results in the intracellular activation of transcription factors such as NF κ B, AP-1 and NF-AT (Cantrell, 1996). Together these factors promote transcription and secretion of the T-cell growth factor IL-2 and other cytokines, leading to T-cell proliferation, differentiation and induction of its effector functions.

The signals generated via TCR are not sufficient for full T cell activation. Some other signals are also triggered by activation of accessory molecules present on the surface of the antigen-presenting cells (APC). Efficient T cell activation and initiation of immune response require TCR engagement and signalling for many minutes or hours. To fulfil this requirement T cells and APCs form special structures at the contact site, the immunological synapse, which allows them to be in close contact for a long enough period of time (fig.1-4). In the center of the synapse, the so-called centralized supramolecular activation cluster (cSMAC), TCR/CD3 complex and CD28 accumulate. A second group of molecules including the adhesion receptor LFA-1 which interacts with ICAM-1 on the opposing APC form a ring around the cSMAC, termed peripheral SMAC (Bromley et al., 2001). The interaction between T cells and DCs in immunological synapses is a dialog rather than a monolog in which DCs also respond to signals from T cells through different surface molecules but also via release of cytokines and other molecules from activated T cells. During this communication DCs conclude their maturation process and undergo further changes, which make antigen presentation even more efficient.

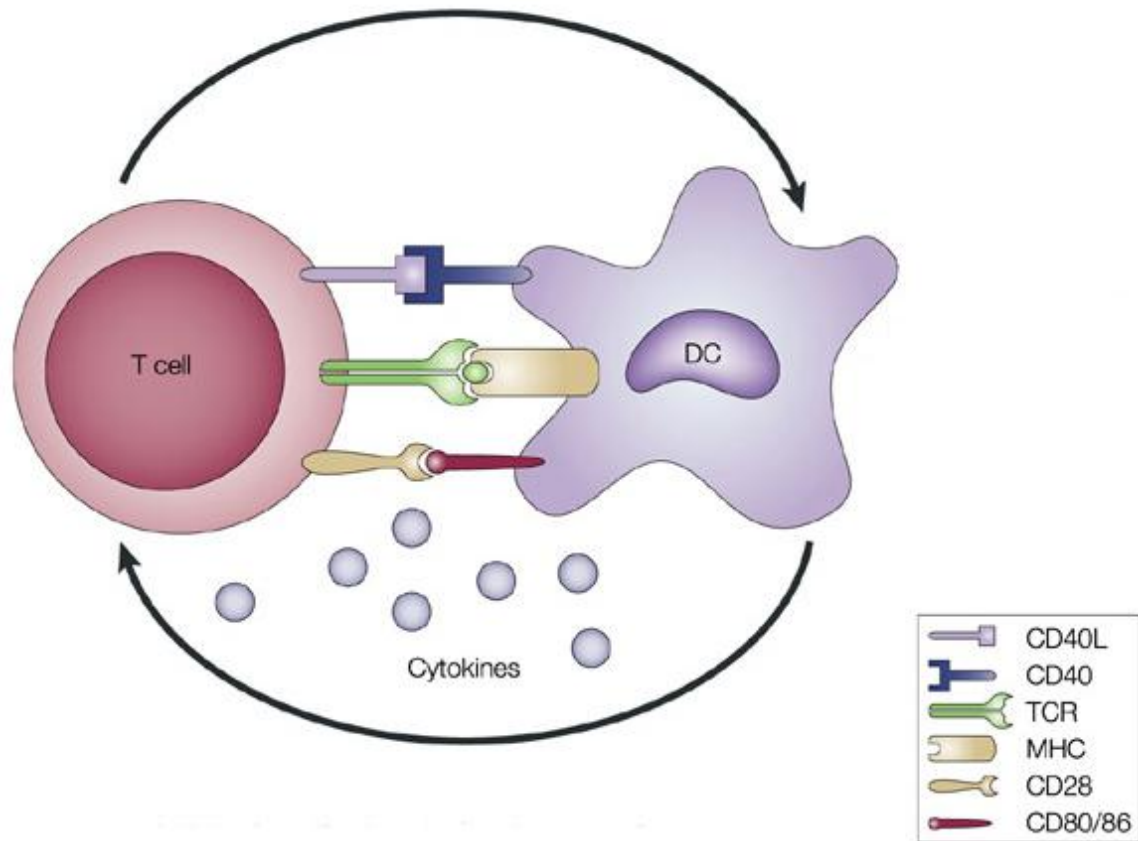


Figure 1-4: Immunological synapse formed between DC and T cell. The key interaction is driven by the recognition of antigenic peptide–major histocompatibility complex (MHC) dimers by T cells bearing T-cell receptors (TCRs) with high affinity for the complex. However, this signal alone is not sufficient for initiation and amplification of specific T-cell responses. Co-stimulatory signals (that is, CD28 recognition of CD80/CD86) and the production of pro-inflammatory cytokines, provide the 'infectious context' by which the full activation of antigen-specific T cells is achieved.

II. Calcium homeostasis and the role of calcium as a second messenger in muscle and immune cells

Calcium was established very early on as a possible second messenger when Ringer demonstrated for the first time its importance for contraction of the heart (Ringer, 1883). Changes in the intracellular free Ca^{2+} concentration regulate a variety of functions in eukaryotic cells from muscle contraction and neuronal excitability to gene expression, cell proliferation, secretion, metabolism and apoptosis (Berridge et al., 1998).

Genome-wide screens have identified over 300 different genes (Feske et al., 2001; Lanahan and Worley, 1998) and approximately 30 transcription factors that are regulated by the concentration of intracellular calcium. The processes regulated by changes in Ca^{2+} concentration are within extremely different time frames, from microseconds (exocytosis), minutes and hours (gene expression) to months and years (memory processes) (Petersen et al., 2005).

Unlike many others second messenger molecules calcium cannot be metabolized so cells are enforced to create specific calcium stores and tightly regulate intracellular levels of Ca^{2+} through numerous binding and specialized extrusion proteins (Clapham, 1995). Under resting conditions, eukaryotic cells maintain the cytoplasmic calcium concentration at very low levels (about 100nM) in comparison with the extracellular concentration which is 1-2mM, but upon stimulation its concentration raises dramatically (more than 1000-fold) in just a few milliseconds and both the amplitude and the frequency of the Ca^{2+} signal can be sensed by specific proteins allowing a cell to respond appropriately to specific signals. One of the most important questions in Ca^{2+} signalling is, how cells interpret these diverse Ca^{2+} signals and convert them into specific responses. To efficiently utilize Ca^{2+} as second messenger, cells are equipped with an essential toolbox kit composed of a variety of proteins that allow Ca^{2+} ions to flow into the cytoplasm and be removed from the cytoplasm, proteins that store/buffer Ca^{2+} and

proteins acting as a sensor after Ca^{2+} binding as well as Ca^{2+} regulated enzyme. Calcium is stored in special compartments, organelles (or subregions of organelles) inside of cell and at the same time these stores represent Ca^{2+} reservoirs that could be used when necessary. These cellular compartments are: endoplasmatic/sarcoplasmatic reticulum (ER/SR), the Golgy apparatus (Hu et al., 2000), mitochondria, secretory granules, and the nuclear envelope. In order to keep the free Ca^{2+} concentration low in the cytoplasm during the resting phase, cells use also different buffer proteins, exchangers and pumps. Since Ca^{2+} concentration in the cell is not static, but, on the contrary dynamic, we can divide Ca^{2+} homeostasis into several functional units:

1. Signalling that is triggered by a stimulus that generates various Ca^{2+} mobilizing signals.
2. "On" phase that feed Ca^{2+} into the cytoplasm.
3. Effector phase where Ca^{2+} binds to numerous Ca^{2+} sensors, which produce specific cellular effects.
4. "Off" phase where cells using different tools such as pumps, exchangers, or organelles (such as mitochondria) remove Ca^{2+} from the cytoplasm to restore the resting state (Berridge et al., 2000).

During the "on" phase previously received stimuli induce both entry of external Ca^{2+} and formation of second messengers that lead to the release of Ca^{2+} from intracellular stores.

II.1 Ca^{2+} entry mechanisms

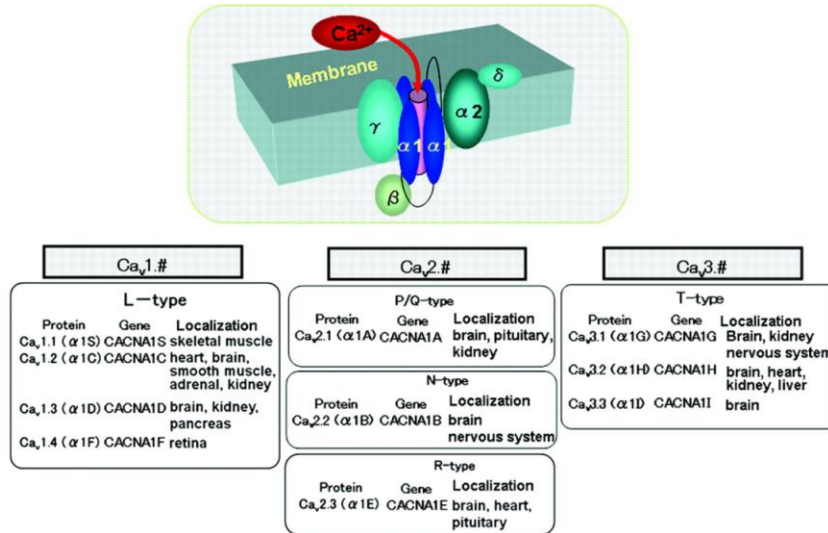
Entry of Ca^{2+} is driven by the presence of a large electrochemical gradient across the plasma membrane.

Two different categories of plasma membrane Ca^{2+} channels, which allow Ca^{2+} entry, can be distinguished: voltage-operated Ca^{2+} channels (VOCs) and voltage independent channels. Thus, plasma membranes Ca^{2+} channels can be activated by voltage or extracellular and intracellular signals and stretch (Chakrabarti and Chakrabarti, 2006).

II.1.1 Voltage Gated Ca²⁺ channels

In excitable cells, such neurons and muscle cells Ca²⁺ entry mostly occurs through voltage-operated channels (VOCs). These mediate calcium influx in response to membrane depolarization and regulate intracellular processes such as muscle contraction, secretion, neurotransmission, and gene expression. The Ca²⁺ channels that have been characterized biochemically are complex proteins composed of four or five distinct subunits, which are encoded by multiple genes. The $\alpha 1$ subunit of 190–250 kDa is the largest subunit, and it encompasses the conduction pore, the voltage sensor and gating apparatus, and the known sites of channel regulation by second messengers, drugs, and toxins. Mammalian $\alpha 1$ subunits are encoded by at least ten distinct genes. Six families of VOCs have been identified L-, P-, Q-, N-, R-, T-type, however as new Ca²⁺ channel genes are cloned, it seems that this alphabetical nomenclatures is too simple and that Ca²⁺ channels should be renamed using the chemical symbol of the principal permeating ion (Ca) with the principal physiological regulator (voltage) indicated as a subscript (CaV). The numerical identifier would correspond to the CaV channel $\alpha 1$ subunit gene family (1 through 3 at present) and the order of discovery of the $\alpha 1$ subunit within that family (1 through m). According to this nomenclature, the CaV1 family (CaV1.1 through CaV1.4) includes channels containing $\alpha 1S$, $\alpha 1C$, $\alpha 1D$, and $\alpha 1F$, which mediate L-type Ca²⁺ currents. The CaV2 family (CaV2.1 through CaV2.3) includes channels containing $\alpha 1A$, $\alpha 1B$, and $\alpha 1E$, which mediate P/Q-type, N-type, and R-type Ca²⁺ currents, respectively. The CaV3 family (CaV3.1 through CaV3.3) includes channels containing $\alpha 1G$, $\alpha 1H$, and $\alpha 1I$, which mediate T-type Ca²⁺ currents (Fig.1-5) (Ertel et al., 2000).

Ca²⁺ channel structure and nomenclature



Hayashi, K. et al. Circ Res 2007;100:342-353

Circulation Research

Copyright ©2007 American Heart Association

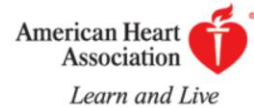


Figure 1-5: Ca²⁺ channel structure and nomenclature. These are formed as a complex of several different subunits: α1, α2δ, β1-4, and γ. The α1 subunit forms the ion-conducting pore while the associated subunits have several functions including modulation of gating. α1 subunit possesses main characteristics of the channel and is encoded by *CACNA1* gene family consisting of 10 genes represented by nomenclature in this figure.

L-Type calcium channels:

L-type Ca^{2+} currents require a strong depolarization for activation, are long lasting, and are blocked by organic L-type Ca^{2+} channel antagonists, including dihydropyridines, phenylalkylamines, and benzodiazepines. These channels are called also dihydropyridine receptors (DHPRs) according to one of their antagonists. L-type Ca^{2+} channels are composed of a $\alpha 1$ subunit (Cav), which spans the membrane and contains the pore region, and four additional subunits $\beta 1$, $\alpha 2$, γ , and δ . There are at least four genes encoding $\alpha 1$ subunits (Cav1.1-Cav1.4), and all mediate L-type Ca^{2+} currents, although their products are preferentially expressed in different tissues/subcellular locations (Catterall, 2000; Catterall et al., 2005).

Cav1.1 is localized in the transverse tubules and is involved in skeletal muscle excitation-contraction coupling; Cav1.2 is expressed in cardiac and smooth muscle cells, endocrine cells, and pancreatic β cells as well as in neuronal cell bodies and is involved in cardiac excitation-contraction coupling, hormone release, transcription regulation, and synaptic integration. Cav1.3 and Cav1.4 have a more widespread distribution, including neuronal cell bodies, dendrites, pancreatic β cells, cochlear hair cells, adrenal gland, and mast cells where they are involved in hormone/neurotransmitter release, regulation of transcription, and synaptic regulation (Catterall et al., 2005).

Recently, new form of store operated Ca^{2+} entry in muscle cells called excitation coupled Ca^{2+} entry (ECCE) has been demonstrated. Physiological stimuli that do not produce substantial depletion of stores, rapidly activate Ca^{2+} entry through channels having properties corresponding to those of store operated Ca^{2+} channels (Cherednichenko et al., 2004). This Ca^{2+} influx channel has pharmacological properties identical to those of the CAV1.1 (Bannister et al., 2009).

II.1.2 Store-operated channels (SOCs)

There are many others Ca^{2+} entry channels that open in response to different external signals, such as receptor-operated channels (ROCs), second messenger operated channels (SMOCs) or store-operated channels (SOCs). In this section, only store-operated channels will be described.

SOCs are Ca^{2+} permeable channels located on the plasma membrane that are activated in response to depletion of intracellular Ca^{2+} stores. Giving rise to the phenomenon of store operated calcium entry also known as capacitative Ca^{2+} entry. The concept of store-operated Ca^{2+} entry was proposed in 1986 by Putney (Putney, 1986). The idea originated from a series of experiments in parotid acinar cells aimed at investigating the relationship between Ca^{2+} release from internal stores, Ca^{2+} entry, and store refilling. On the basis of this work, and a few eclectic observations in the literature, it was suggested that the amount of Ca^{2+} in the stores controlled the extent of Ca^{2+} influx in nonexcitable cells. When stores are full, Ca^{2+} influx did not occur but as the stores emptied, Ca^{2+} entry developed. The first time SOC currents were characterized, was in mast cells where they were identified as the Ca^{2+} release-activated Ca^{2+} (CRAC) current (Hoth and Penner, 1992). This current had been previously identified by Lewis and Cahalan in T-cells, but at the time it was not recognized as a store operated current (Lewis and Cahalan, 1989). The existence of SOC current in T cells was confirmed later (Zweifach and Lewis, 1993). Other groups demonstrated the existence of capacitative Ca^{2+} entry in excitable cells, first in skeletal myotubes cultured in vitro (Hopf et al., 1996) and later in adult skeletal muscle fibers (Kurebayashi and Ogawa, 2001).

However, the molecular mechanism remained undefined until recently. The key breakthroughs came from RNAi screening experiments, which first identified STIM proteins as the molecular link from ER Ca^{2+} store depletion to Store Operated Calcium Entry (SOCE) and CRAC channel activation in the plasma membrane, and then identified Orai proteins that comprise the CRAC channel pore-forming subunit.

Almost simultaneously, two laboratories discovered the role of STIM1 (initially *Drosophila* Stim) in capacitative Ca^{2+} entry by use of limited RNAi screens for

modulators of thapsigargin-activated Ca^{2+} entry in *Drosophila* S2 cells (Roos et al., 2005) and in mammalian HeLa cells (Liou et al., 2005). *Drosophila* has a single STIM gene, whereas mammals have two, STIM1 and STIM2. STIM1 and STIM2 are both single-pass transmembrane proteins with paired N-terminal EF-hands located in the ER lumen and protein interaction domains located both in the ER lumen and in the cytoplasm (Stathopoulos et al., 2008). Both STIM1 and STIM2 are functional ER Ca^{2+} sensors that can trigger store-operated Ca^{2+} entry through CRAC channels in activated (store-depleted) cells (Fig.1-6). STIM1 activates SOCE upon Ca^{2+} store depletion, whereas its homolog STIM2 seems to be more implicated in the control of basal cytosolic and ER Ca^{2+} levels, presumably because the affinity of STIM2 EF-hands for Ca^{2+} is two-fold lower than that of STIM1 EF-hands (Brandman et al., 2007; Oh-Hora et al., 2008).

Orai1 was first reported (and named) by Feske et al. through a combination of gene mapping in a family with an immunodeficiency attributed to loss of CRAC and a whole-genome screen of *Drosophila* S2 cells (Feske et al., 2006).

Orai1 has since been demonstrated to be the pore subunit of the prototypic store-operated CRAC channel of blood cells (Prakriya et al., 2006; Vig et al., 2006; Yeromin et al., 2006). Co-expression of STIM1 and Orai1 generates robust CRAC currents in a number of expression systems (Peinelt et al., 2006).

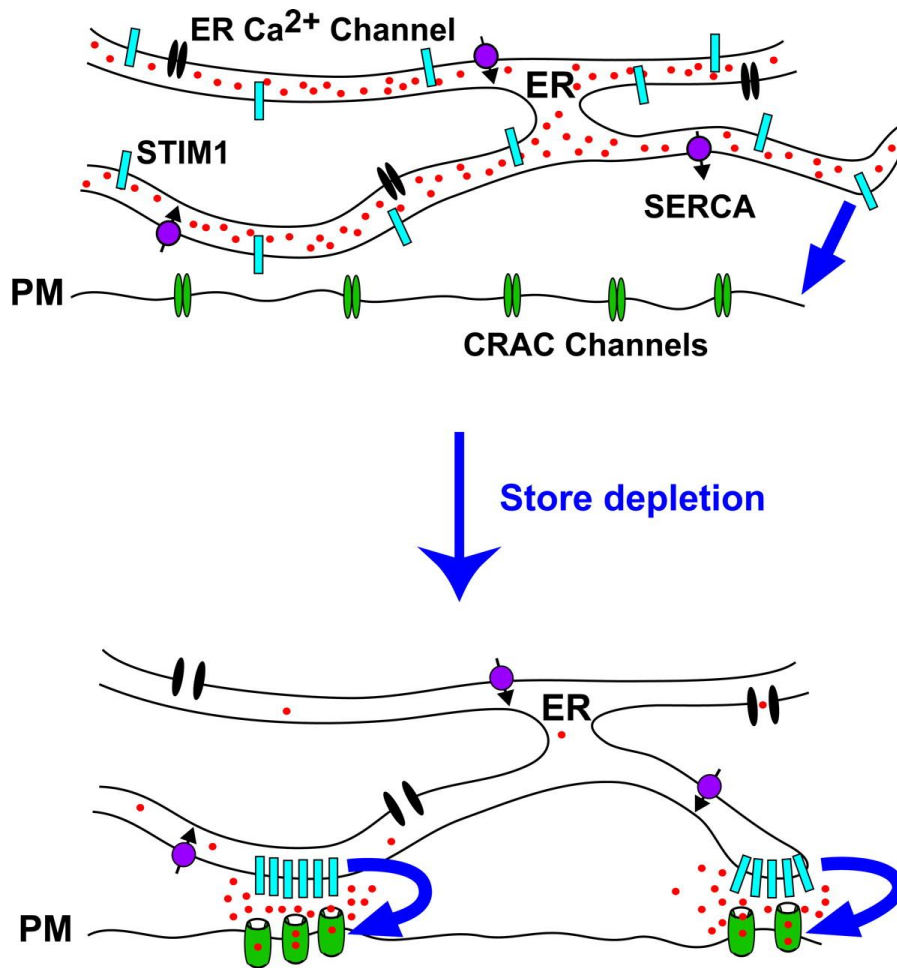


Figure 1-6: Local activation of CRAC channels by STIM1 at ER-plasma membrane junctions. Store depletion causes STIM1 to accumulate in pre-existing and newly formed regions of ER, whereas Orai1 accumulates in apposed regions of the plasma membrane. CRAC channels open only in the close vicinity of the STIM1 puncta. The convergence of STIM1 and Orai1 at ER-plasma membrane junctions creates the elementary unit of SOCE. (Luik R. M. et.al. J. Cell Biol. 2008:174:815-825)

II.2 Ca²⁺ release from internal stores

Aside the Ca²⁺ entry pathways, the main source of Ca²⁺ utilized for signalling, are the internal stores that are located primarily in the ER/SR, of which Ins(1,4,5)P₃Rs and RyRs are the main intracellular Ca²⁺ release channels. These two channels are sensitive to Ca²⁺ and this phenomenon of Ca²⁺ induces Ca²⁺ release (CICR) is thought to contribute to the rapid rise of Ca²⁺ levels during the “on” reaction. In addition to Ca²⁺, these channels are regulated by a variety of factors that operate on both the luminal and cytosolic surface of the channels.

In the case of Ins(1,4,5)P₃Rs, the primary agonists are Ins(1,4,5)P₃ and Ca²⁺. The binding of Ins(1,4,5)P₃ increases the sensitivity of the receptor to Ca²⁺, which has a biphasic action, it activates at low concentrations, but inhibits at high concentrations. This Ca²⁺ regulation is mediated by the direct action of Ca²⁺ on the receptor as well as indirectly through calmodulin (CaM) (Nadif Kasri et al., 2002; Taylor and Laude, 2002). A variety of ligands activate receptors coupled to phospholipase C (PLC) to generate Ins(1,4,5)P₃ which in turn releases Ca²⁺ from the internal stores. There are several PLC isoforms that are activated by different mechanisms, such as G-protein-coupled receptors (PLC β), tyrosine-kinase-coupled receptors (PLC γ), Ca²⁺ activated (PLC δ) or Ras activated (PLC ϵ).

Excitable cells, which need to respond to signals within milliseconds, are equipped with RyR calcium channels (Berridge et al., 2000). Regulation of the latter class of proteins is not mediated by the generation of a second messenger but rather through direct coupling with the L-type Ca²⁺ channel present on the plasma membrane (Catterall, 2000). In fact, in cardiac and skeletal muscles, signalling to the RyR is coupled to the dihydropyridine receptor (DHPR), L-type Ca²⁺ channels, which sense changes in membrane potential thereby activating Ca²⁺ release from the sarcoplasmic reticulum.

During the “on” phase Ca²⁺ flows into the cytoplasm increasing drastically the intracellular concentration. Of the cytoplasmic calcium however, only a small amount stays free, because most of it is rapidly bound to the different calcium binding proteins. There are around 200 genes in the human genome, which encode either for Ca²⁺ buffer or effectors (Carafoli et al., 2001). The buffers, which become loaded with Ca²⁺ during the

“on” phase and unload during the “off” phase, function to fine-tune the spatial and temporal properties of Ca^{2+} signals. They can alter both the amplitude and the recovery time of individual Ca^{2+} transients. These buffers have different properties and expression patterns. For example, calbindin D-28 (CB) and calretinin (CR) are fast buffers, whereas parvalbumin (PV) has much slower binding kinetics and a high affinity for Ca^{2+} . These are mobile buffers that increase the diffusional range of Ca^{2+} (John et al., 2001). Once the “On” mechanisms have generated a Ca^{2+} signal, various Ca^{2+} sensitive processes translate this into a cellular response. Several different Ca^{2+} effectors (sensors) have been described and classified into 4 categories: (1) Ca^{2+} -binding proteins (calmodulin, troponin C, etc.), (2) Ca^{2+} -sensitive enzymes (kinases, phosphatases, proteases, nitric oxide synthases, calcineurin, etc.), (3) ion channels (potassium channels such as SK, IK and BK and chloride channels) and (4) Ca^{2+} -sensitive transcription factors (NFATc, CREB, DREAM and CREB-binding protein) (Berridge et al., 2003). In the case of transcription factors, Ca^{2+} itself or Ca^{2+} -dependent intracellular pathways activate or inhibit the transcription factors and consequently regulate the expression of certain genes. Activation of the nuclear factor of activated T cells (NFAT), a well characterized Ca^{2+} dependent transcription factor requires, Ca^{2+} elevation. NFAT translocates from the cytoplasm into the nucleus in response to dephosphorylation of several of its serins by the Ca^{2+} Calmodulin (CaM) phosphatase calcineurin (Clipstone and Crabtree, 1992; Okamura and Rao, 2001). Calcineurin binds some NFAT isoforms and translocates into the nucleus as a complex with NFAT, where it maintains NFAT in the dephosphorylated state as long as Ca^{2+} remains elevated. As soon as Ca^{2+} signalling stops, kinases in the nucleus rapidly phosphorylate NFAT, which then leaves the nucleus and transcription of NFAT responsive genes ceases (Fig.1-7) (Shibasaki et al., 1996). Calcineurin is a serine- and threonine-specific protein phosphatase that is conserved in all eukaryotes and is unique among phosphatases for its ability to sense Ca^{2+} through its activation by calmodulin. Identified and characterized in pioneering work by Claude Klee and Philip Cohen in the late 1970s, calcineurin catapulted to center stage when the groups of Stuart Schreiber and Irving Weissman discovered that it is the target of the immunosuppressants cyclosporin A and FK506 (Aramburu et al., 2004). Thus explaining its action as an immunosuppressant drug and leading to its wide spread use in transplanted patients.

Nuclear factor kappa B (NFκB) is another transcription factor that is regulated by Ca^{2+} . NFκB translocates into the nucleus after phosphorylation and degradation of an inhibitory subunit IκB (Stancovski and Baltimore, 1997). A single spike of Ca^{2+} is sufficient to trigger IκB degradation and NFκB translocation into the nucleus, where it persists for at least 30 min until IκB is replenished (Dolmetsch et al., 1997).

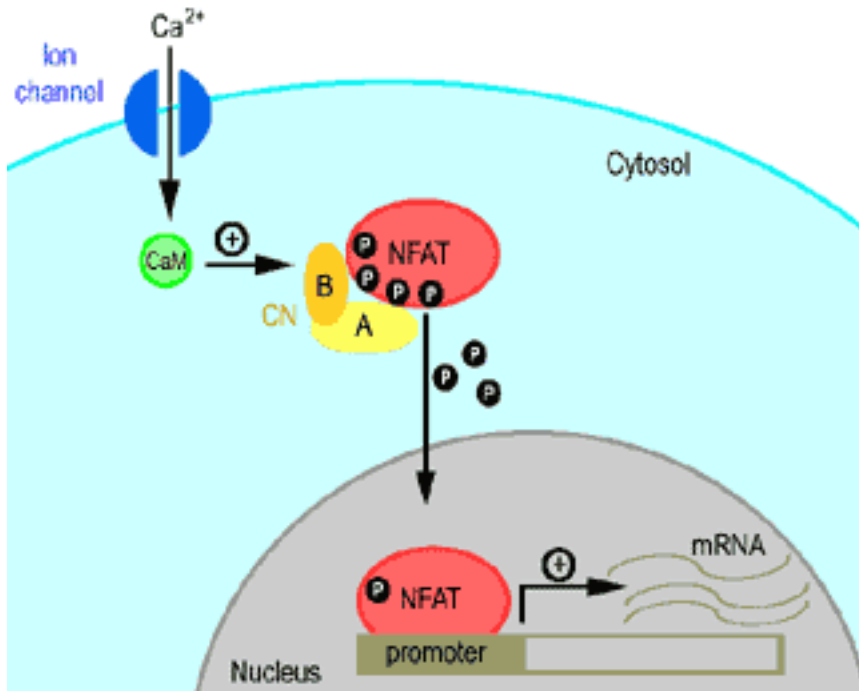


Figure 1-7: The Calcineurin-NFAT signalling pathway. An increase of intracellular calcium levels activates the cellular phosphatase Calcineurin (CN) through its interaction with Calmodulin (CaM). Activated CN is able to dephosphorylate NFAT (Nuclear Factor of Activated T-cells), and allows the nuclear translocation of this transcription factor. In the nucleus, NFAT binds to specific DNA motifs within the promoter of numerous genes and induce their transcription. (http://www.angiobodies.com/figuras/uam_fig2.gif)

During the “off” phase various pumps and exchangers are activated in order to decrease the levels of cytosolic Ca^{2+} and to terminate the signal. There are four different pumping mechanisms that are responsible for maintaining or bringing back the Ca^{2+} levels at approximately 100nM and ensure that the internal stores are loaded. The plasma membrane Ca^{2+} -ATPase (PMCA) pumps and $\text{Na}^+/\text{Ca}^{2+}$ exchangers extrude Ca^{2+} to the outside whereas the sarco-endoplasmic reticulum ATPase (SERCA) pumps return Ca^{2+} to the internal stores. These pumps use energy from ATP hydrolysis and from the Na^+ electrochemical gradient to transport Ca^{2+} against its electrochemical gradient.

The fourth component of this machinery is the mitochondrial uniporter. Mitochondria extrude protons to create an electrochemical gradient that allows ATP synthesis and the same gradient is used to drive Ca^{2+} uptake through a uniporter that has a low sensitivity to Ca^{2+} (half-maximal activation around 15 μM). This low sensitivity means that mitochondria accumulate Ca^{2+} more effectively when they are close to Ca^{2+} release channels (Rizzuto et al., 1993). The mitochondrion has an enormous capacity to accumulate Ca^{2+} and the mitochondrial matrix contains buffers that prevent its concentration from rising too high. Once the cytosolic Ca^{2+} has returned to its resting level, a mitochondrial $\text{Na}^+/\text{Ca}^{2+}$ exchanger pumps the large load of Ca^{2+} back into the cytoplasm, from which it is either returned to the ER or removed from the cell. Ca^{2+} can also leave the mitochondrion through a permeability transition pore (PTP) (Bernardi, 1999; Duchen, 1999), which has all the elements of Ca^{2+} -induced Ca^{2+} release because it is activated by the build up of Ca^{2+} within the mitochondrial matrix (Ichas et al., 1997). On the other hand, PMCA and SERCA pumps have lower transport rates but high affinities, which means that they can respond to modest elevations in Ca^{2+} levels and set basal Ca^{2+} levels.

II.3 Role of Ca^{2+} as a second messenger in skeletal and cardiac muscle excitation-contraction coupling

One of the main roles of Ca^{2+} as a second messenger in muscle cells is to promote contraction. The release of Ca^{2+} from the SR and generation of Ca^{2+} signal responsible for muscle contraction differ between skeletal and cardiac muscles. To accomplish this special function and generate Ca^{2+} signals skeletal muscle cells are equipped with specialized proteins, namely L-type VOC ($\alpha 1S/CaV1.1$), the dihydropyridine receptor (DHPR) located on the plasma membrane and RyR1 located on the SR terminal cisternae junctional face membrane. The DHPR interacts directly with the large cytoplasmic head of the RyR1. Membrane depolarization induces a conformational change in $\alpha 1S$ subunit of DHPR that is transmitted directly to the RyR1, causing it to release Ca^{2+} from the SR (Fig.1-8) (Ikemoto et al., 1994; Marty et al., 1994). Ca^{2+} conductance through DHPRs in skeletal muscle is not essential for excitation-contraction coupling. The Ca^{2+} released from the SR mediates the interaction between thick and thin filaments resulting in muscle contraction. At the same time Ca^{2+} is pumped back into the SR by SR Ca^{2+} -ATPases (SERCA) (Ebashi et al., 1969; Hasselbach, 1964; Sandow, 1965).

Electron microscopy investigations have demonstrated that skeletal muscle DHPRs are arranged in tetrads, clusters of four receptors, corresponding to the homotetrameric structure of RyR1. Experimental evidence supports a physical interaction between the two proteins and activation of DHPR by membrane depolarization elicits opening of RyR (Bers and Stiffel, 1993; Franzini-Armstrong et al., 1998). The coupling is bidirectional, in addition to orthograde signal transmitted from skeletal DHPR to the RyR1, the DHPR also receives a retrograde signal from the RyR enhancing L-type Ca^{2+} currents.

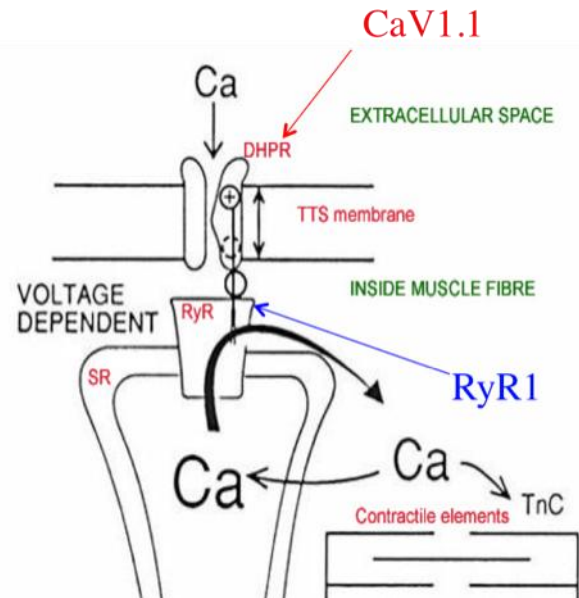
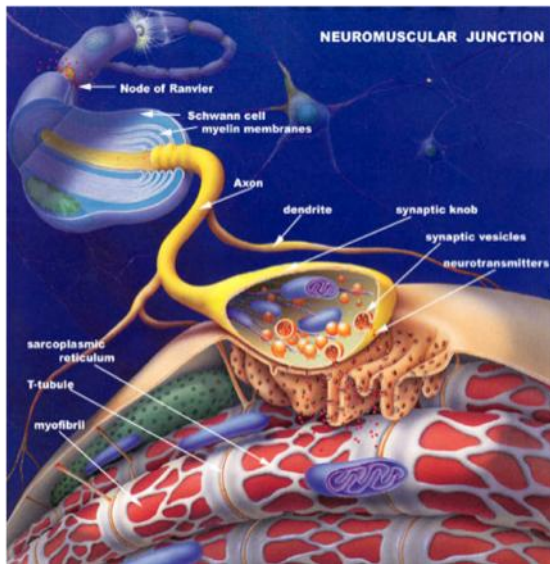


Figure 1-8: Neuromuscular junction and skeletal muscle type of EC coupling

Action potential from a motor neuron results in local depolarization of the sarcolemma and activation of DHPR (Cav1.1), that cause conformational changes of the channel and direct interaction with RyR1, opening of RyR1 and release SR Ca^{2+}

(<http://www.bio.miami.edu/~cmallery/150/neuro/neuromuscular-sml.jpg>)

In contrast to skeletal muscle cells, cardiac muscle cells are equipped with different isoforms of L-type Ca^{2+} channels and RyRs: They express alpha1C/ CaV1.2 L-type VOC and RyR2 isoforms. The nature of the coupling between these two players in cardiac cells is different. In heart, the action potential depolarizes the membrane, opens the DHPR and causes entry of extracellular Ca^{2+} that diffuses across the junctional zone to stimulate RyR2 to release Ca^{2+} from the SR. The process is named calcium-induce calcium-release

(CICR) (Bers, 2002). As the Ca^{2+} entry activates a cluster of 4-6 RyR2s Ca^{2+} release from the SR is much larger and results in a considerable amplification of the initial Ca^{2+} influx. After its release from the SR, Ca^{2+} then diffuses from the junctional zone to induce muscle contraction by activating sarcomeres that are situated in the immediate vicinity (Fig. 1-9). Calcium homeostasis is particularly important in cardiac cells, since during every heart beat there is a large circulation of Ca^{2+} . Thus the same amount of Ca^{2+} that is released by the RyR2s is returned to the SR by the SERCA pump.

The force of contraction can be adjusted by varying the amount of Ca^{2+} that circulates during each on/off cycle. The positive inotropic response that is produced by β -adrenergic stimulation is mediated by cyclic AMP/PKA, which has three main actions on Ca^{2+} signalling. First, it stimulates the L-type VOCs to increase the amount of Ca^{2+} that enters during each action potential. Second, it phosphorylates phospholamban to reduce its inhibitory effect on the SERCA pump, which is then able to increase the luminal Ca^{2+} concentration so that more Ca^{2+} is released from the SR and an increase in the activity of the SERCA pump is also enhanced by cADPR (Lukyanenko et al., 2001). Third, cAMP/PKA phosphorylates the RyR2, thereby enhancing their ability to release Ca^{2+} (Marx et al., 2000). In contrast to skeletal muscle, dihydropyridine receptors in cardiac muscle are located randomly relative to the RyR2 tetramers (Berridge et al., 2003).

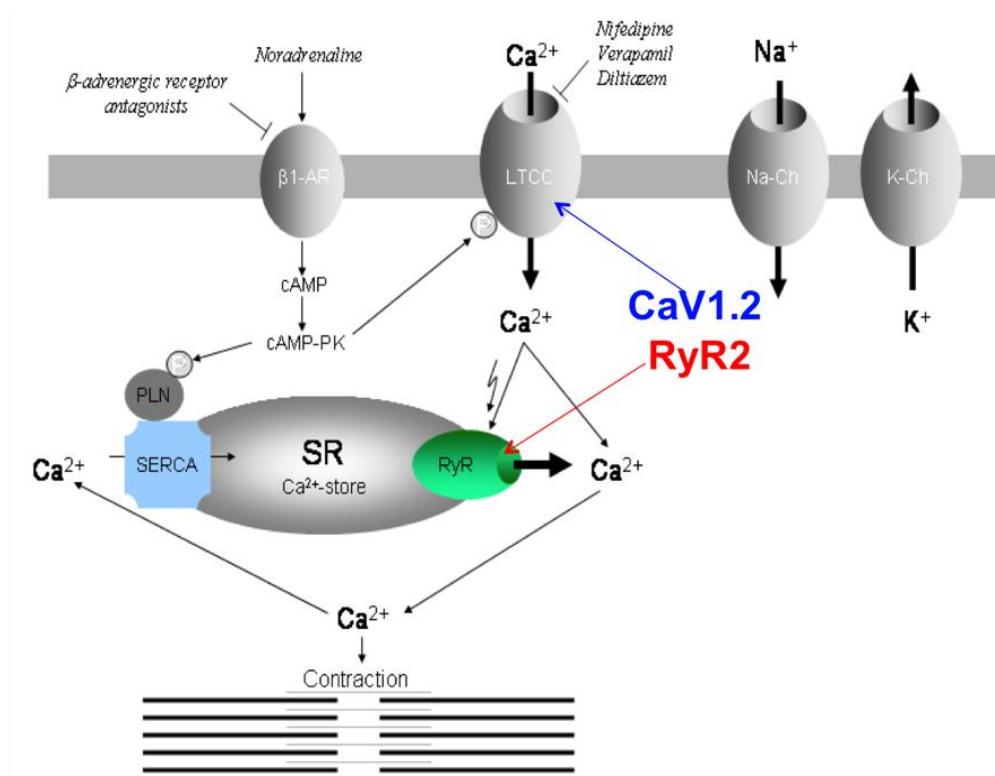


Figure 1-9: EC coupling in cardiac muscle Ca^{2+} induce Ca^{2+} release mechanism

Calcium release from RyR2 is triggered by Ca^{2+} entry through the nearby L-type Ca^{2+} channel (CaV1.2 isoform). Ca^{2+} that flows into the cell activates RyR2 channels and amplifies Ca^{2+} signal. (<http://calcium.ion.ucl.ac.uk/images/contraction-heart.gif>).

II.4 Role of Ca²⁺ signalling in immune cells

In the cells of the immune system calcium signals are essential for diverse cellular functions including differentiation, migration, effector functions and gene transcription.

An increase in intracellular calcium concentration occurs after the engagement of immunoreceptors, such as B-cell and T-cell receptors and Fc receptors on mast cells, natural killer (NK) cells, DCs or macrophages as well as chemokine receptors. Many important immune receptors initiate Ca²⁺ signals through the production and accumulation of the soluble second messenger InsP₃. InsP₃ is produced by the hydrolysis of the membrane lipid phosphatidylinositol-4,-5-bisphosphate (PtdIns(4,5)P₂; also known as PIP₂), a process that also produces the lipid second messenger diacylglycerol (DAG) (Brose et al., 2004). PIP₂ hydrolysis is mediated by members of the PLC enzyme family, which is constituted of several differentially regulated isoforms (Rhee, 2001). An important distinction among the various PLC isoforms is that 7-transmembrane spanning G-protein-coupled receptors (GPCRs) activate PLCβ isoform through the heterotrimeric G-protein G_q and related subunits, whereas tyrosine-kinase-linked receptors, including many growth factor receptors, the T-cell receptor (TCR), the BCR and activating Fc receptors (FcRs), activate PLCγ isoform through tyrosine phosphorylation.

InsP₃ binds to the IP₃Rs on the ER membrane and causes the release of Ca²⁺ from ER-bound intracellular stores. The reduced ER Ca²⁺ concentration is sensed by STIM molecules, which are located on the ER membrane, and its conformational change leads to activation of Orail and CRAC channels on the plasma membrane and consequently to sustained Ca²⁺ influx into the cell. As a result, several Ca²⁺-dependent signalling proteins and their target transcription factors are activated, including the phosphatase calcineurin and its target NFAT (nuclear factor of activated T cells), CaMK (Ca²⁺-calmodulin-dependent kinase) and its target CREB (cyclic-AMP-responsive-element-binding protein) MEF2 (myocyte enhancer factor 2) which is activated by both the calcineurin and CaMK pathways, and NFκB (nuclear factor κB). Simultaneously, DAG production activates the Ras-mitogen activated protein kinase (MAPK) and protein kinase C (PKC) pathways, which in turn lead to activation of the transcription factors AP-1 (a transcriptional

complex formed by c-Jun and c-Fos) and NFκB (Karin and Gallagher, 2005; Schulze-Luehrmann and Ghosh, 2006).

Beside SOCE, which is the most studied Ca^{2+} entry pathway in immune cells, the existence of other Ca^{2+} entry pathways has been reported, such as L-type voltage-gated Ca^{2+} channels (CaV channels), TRP (transient receptor potential) and ATP-responsive purinergic (P2X) receptors (Oh-hora, 2009). Several studies have shown that CD4+ and CD8+ T cells express high levels of the Cav1 pore-forming subunit subfamily ($\alpha 1\text{S}$, $\alpha 1\text{C}$, $\alpha 1\text{D}$, and $\alpha 1\text{F}$) at levels comparable to those in excitable cells in which these channels are critical for Ca^{2+} entry (Badou et al., 2006; Gomes et al., 2004; Kotturi et al., 2003; Matza and Flavell, 2009). Other studies have also shown that these channels are widely expressed in various immune cell types, such as dendritic cells (DCs), B-lymphocytes, and monocytes (Grafton et al., 2003; Vukcevic et al., 2008). It has been shown that CaV channels are required for T cell functions *in vitro* and *in vivo*. The DHP antagonist, nifedipine and related compounds, clearly reduce *in vitro* T cell proliferation, IL2 secretion, and Ca^{2+} entry (Colucci et al., 2009; Gomes et al., 2004; Grafton and Thwaite, 2001). In DCs CaV1.2 activation influences process of maturation and the mechanisms that lead to fast induction in surface expression of MHC class II molecules (Vukcevic et al., 2008). Although InsP_3 is a key messenger regulating Ca^{2+} concentration, some studies have postulated the possibility that the ryanodine receptor (RyR) contributes to the InsP_3 -insensitive component of Ca^{2+} signalling in immune cells (Sei et al., 1999). Particularly in B-lymphocytes and DCs pharmacological activation gives rise to a rapid and transient increase in the intracellular Ca^{2+} concentration. Furthermore in freshly isolated B-lymphocytes, activation of the RyR1 leads to the rapid release of the proinflammatory cytokine IL1β (Bracci et al., 2007; Ducreux et al., 2006; Girard et al., 2001; Goth et al., 2006; O'Connell et al., 2002). Interestingly in some cells the Ca^{2+} signal is also encoded by high frequency oscillations of the cytosolic Ca^{2+} concentration. This is an interesting mechanism through which decoding of both the amplitude and the frequency of the oscillations can convey different messages leading to activation of different cell functions.

For some functions of immune cells such as activation of T-lymphocytes by antigen, repetitive oscillation of the intracellular Ca^{2+} concentration are the result of the activation

of the phosphoinositide signalling pathway through cell-surface receptors (Lewis, 2003). Furthermore positive selection of T cells has been shown to depend on Ca^{2+} oscillations in thymocytes. Thus immune cells are equipped with a variety of components to handle Ca^{2+} homeostasis and decode messages underlining specific Ca^{2+} signals. The close coordination of CRAC channels and PMCA pumps allows the PMCA pumps to respond rapidly to local changes in Ca^{2+} concentration and thereby to significantly influence the frequency and amplitude of intracellular Ca^{2+} oscillations and/or the peak cytosolic Ca^{2+} concentration triggered by CRAC channel activation.

Thus Ca^{2+} signalling is integrated with other signalling pathways and the integration occurs at the level of the binding of transcription factors to DNA response elements, resulting in cell proliferation and cytokine gene expression. The functional consequences of Ca^{2+} entry have been very well documented in T cells and mast cells where differences between short term and long term increases in intracellular Ca^{2+} levels have been observed.

Short-term functions of Ca^{2+} signals:

The regulation of lymphocyte motility and immunological synapse formation are Ca^{2+} dependent processes. Several studies using *in vitro* and *in vivo* imaging of T cells have shown that an increase in the intracellular Ca^{2+} concentration results in reduced mobility and rounding of otherwise polymorphic T cells (Delon et al., 1998; Negulescu et al., 1996). This “stop” signal seems to sustain the interaction between a CD4^+ T cells and APCs and favour the formation of the immunological synapse. An immunological synapse is also formed between CTLs and their target cells, such as virus-infected cells and tumor cells. Synapse formation is accompanied by a rise in the intracellular Ca^{2+} concentration of CTLs, which is required for granule exocytosis and target-cell killing (Lyubchenko et al., 2001; Poenie et al., 1987; Treves et al., 1987). Similarly, mast cell degranulation also involves granule exocytosis triggered by Ca^{2+} entry, in this case degranulation is initiated by binding of antigen –immunoglobulin E (IgE) complexes to

the mast cell Fc receptor, and leads to the release of variety of mediators including histamine and leukotrienes (Perrimon and Mathey-Prevot, 2007).

Long-term functions of Ca²⁺ signals:

The long-term responses involve transcriptional programs initiated by sustained Ca²⁺ signalling. They include proliferation, differentiation and acquisition of effector function by “naive” T and B lymphocytes following their first encounter with antigen, as well as transcription of cytokine, chemokine and other activation-associated genes by differentiated “effector” T cells upon secondary exposure to antigen.

It also has been known that increases in the intracellular Ca²⁺ concentration participate in the regulation and maturation of dendritic cells (Czerniecki et al., 1997; Koski et al., 1999). Probably the best studied Ca²⁺-responsive signalling pathway in T cells involves the phosphatase calcineurin, which dephosphorylates NFAT proteins following an increase in intracellular Ca²⁺ concentration and leads to its nuclear translocation. NFAT is regulated in a highly dynamic manner by Ca²⁺ levels because a decrease in intracellular Ca²⁺ level results in the almost instantaneous phosphorylation and export of NFAT from the nucleus. As a consequence, NFAT-dependent gene transcription is only poorly activated in response to a single pulse of high intracellular Ca²⁺ levels but requires prolonged elevation of Ca²⁺ levels (Dolmetsch et al., 1997). This is in contrast to another transcription factor, nuclear factor- κ B (NF- κ B), for which a transient increase in intracellular Ca²⁺ concentration is sufficient for activation and subsequent target gene expression. Calcineurin–NFAT signalling pathway is responsible for activation of transcription of diverse cytokines and several hundreds other genes (Cristillo and Bierer, 2002; Feske et al., 2001). These studies also indicated that Ca²⁺ signals exert both stimulatory and inhibitory effects on gene expression. As to the long term functions of Ca²⁺ signals in DCs there are reports of CRAC activity in DCs. Its activation in these cells has been reported to be linked to the induction of maturation (Hsu et al., 2001).

III. RYANODINE RECEPTORS AND NEUROMUSCULAR DISORDERS

III.1. The Ryanodine receptor calcium channels

III.1.1. Isoforms of ryanodine receptor and their structure

Ryanodine receptors are intracellular Ca^{2+} release channels of which at least three different isoforms that have been identified and extensively characterized biochemically, functionally and at the molecular level (Bers, 2004; Franzini-Armstrong and Protasi, 1997; Sutko and Airey, 1996). The three isoforms share an overall amino acid identity of approximately 60% and experimental evidence suggests that they are structurally similar, with a large hydrophilic NH₂-terminal domain and a hydrophobic C-terminal domain containing several transmembrane domains as well as the channel pore (Samso et al., 2005; Serysheva et al., 2005). Type 1 RyR, also called skeletal type RyR because it was identified for the first time in skeletal muscles (Takeshima et al., 1989; Zorzato et al., 1990) is encoded by a gene on human chromosome 19 and is mainly expressed in skeletal muscle where it mediates Ca^{2+} release from the sarcoplasmic reticulum, following depolarization of the plasmalemma. RyR1 is also expressed to a lower extent in Purkinje cells and recent reports have demonstrated its expression in some cells of the immune system (Hosoi et al., 2001) particularly B-lymphocytes and DCs. Mutations in this gene are associated with the rare neuromuscular disorders malignant hyperthermia, central core disease, and some forms of multi-minicore disease, Centronuclear myopathy and

King Denborough syndrome (Robinson et al., 2006; Treves et al., 2005). Type 2 RyR encoded by a gene located on chromosome 1 is mainly expressed in cardiac muscle and in certain areas of the cerebellum and is activated through a Ca^{2+} induced Ca^{2+} release mechanism (McPherson and Campbell, 1993; Otsu et al., 1990). Mutations in its gene are associated with genetic variants of congestive heart failure, namely catecholaminergic polymorphic ventricular tachycardia and arrhythmogenic right ventricular dysplasia (George et al., 2007; Wehrens and Marks, 2003).

Type 3 RyR encoded by a gene located on a chromosome 15 is expressed in a variety of excitable tissues, including central nervous system, as well as in developing muscle cells. Its expression in some tissues appears to be developmentally regulated (Sorrentino et al., 1993; Tarroni et al., 1997).

RyRs are large homotetramers made up of four subunits with a mass of around 560kD, each composed of about 5000 amino acids. Each subunit can bind one molecule of the 12KDa protein FKBP12. Accessory proteins, including CaM, calcineurin and S100 (MacKrell, 1999; Meissner, 1994) have been shown to form a complex with RyRs giving rise to a huge macromolecular complex with a total molecular mass greater than 2 million Da making the RyR the largest known ion channel. The RyR protomer contains a large hydrophilic domain and a relatively small hydrophobic COOH-terminal domain containing several transmembrane (TM) segments. Depending on the model, the exact number of TM segments ranges between 4 and 12. Primary sequence and hydropathy plot analysis by Takeshima et al. (1989) suggest an arrangement of four transmembrane spanning α -helices and a final tail facing the SR lumen. In a second model, Zorzato et al., proposed 10 transmembrane domains (Takeshima et al., 1989; Zorzato et al., 1990).

More recently a model consisting of 6-8 TM domains was proposed (Fig. 1-10) (Du et al., 2002). This arrangement places both the N-terminal and C-terminal domain of RyR in the cytoplasm. However, determination of the exact number TM segments will require further investigations at high EM resolution. The transmembrane sequences from each of the four monomers interact to form the ion-conducting pore (Lai et al., 1989) whereas the large cytoplasmic region regulates gating via interaction with a variety of intracellular messengers. Many of the mutations that produce human disease are located in the cytoplasmic region (Du et al., 2002).

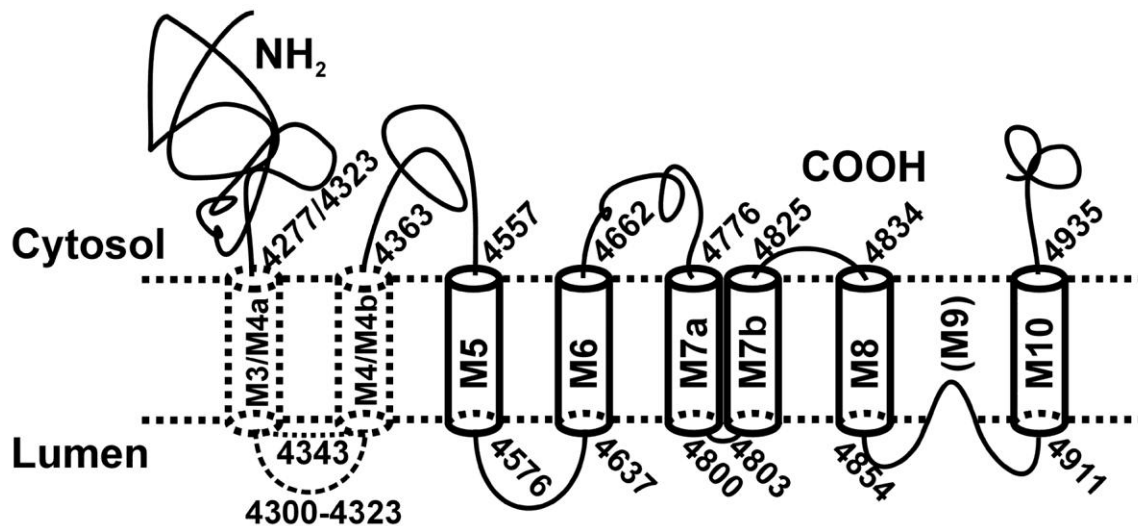


Figure 1-10: Model for the transmembrane regions of RyR1. Proposal for the transmembrane topology of rabbit skeletal muscle RYR1 according to the model of Du. Model shows eight transmembrane sequences with cytosolic N- and C-terminal domain.

Over the last 10 years, single-particle cryoelectron microscopy (cryo-EM) was the method of choice to unravel the structure of the RyRs and recently reconstructions of RyR1 have reached subnanometer resolution (Fig. 1-11). RyRs have a mushroom shape with 4-fold symmetry (Ludtke et al., 2005). Image analyses revealed a quatrefoil or coverleaf-shaped channel with a large square cytoplasmic domain (29x29x12nm) and a narrower transmembrane domain spanning 7nm from the center of the cytoplasmic domain. A 2-3nm cylindrical hole, which could be occluded by a “plug” mass, in the center of the channel, may correspond to the transmembrane Ca^{2+} conducting pathway. Single-particle cryo-EM has been used to generate images of RyR1 in different conformational states to explore the structural transitions associated with RyR gating. Such studies have shown the existence of conformation changes between open and closed states of the channel (Ikemoto and el-Hayek, 1998; Samsó and Wagenknecht, 1998). Global conformational changes associated with the closed-open transition of the RyR

channel were detected in both the cytoplasmic region and the transmembrane region. Channel opening was proposed to be similar to the opening-closing of the iris in a camera diaphragm (Hamilton and Serysheva, 2009).

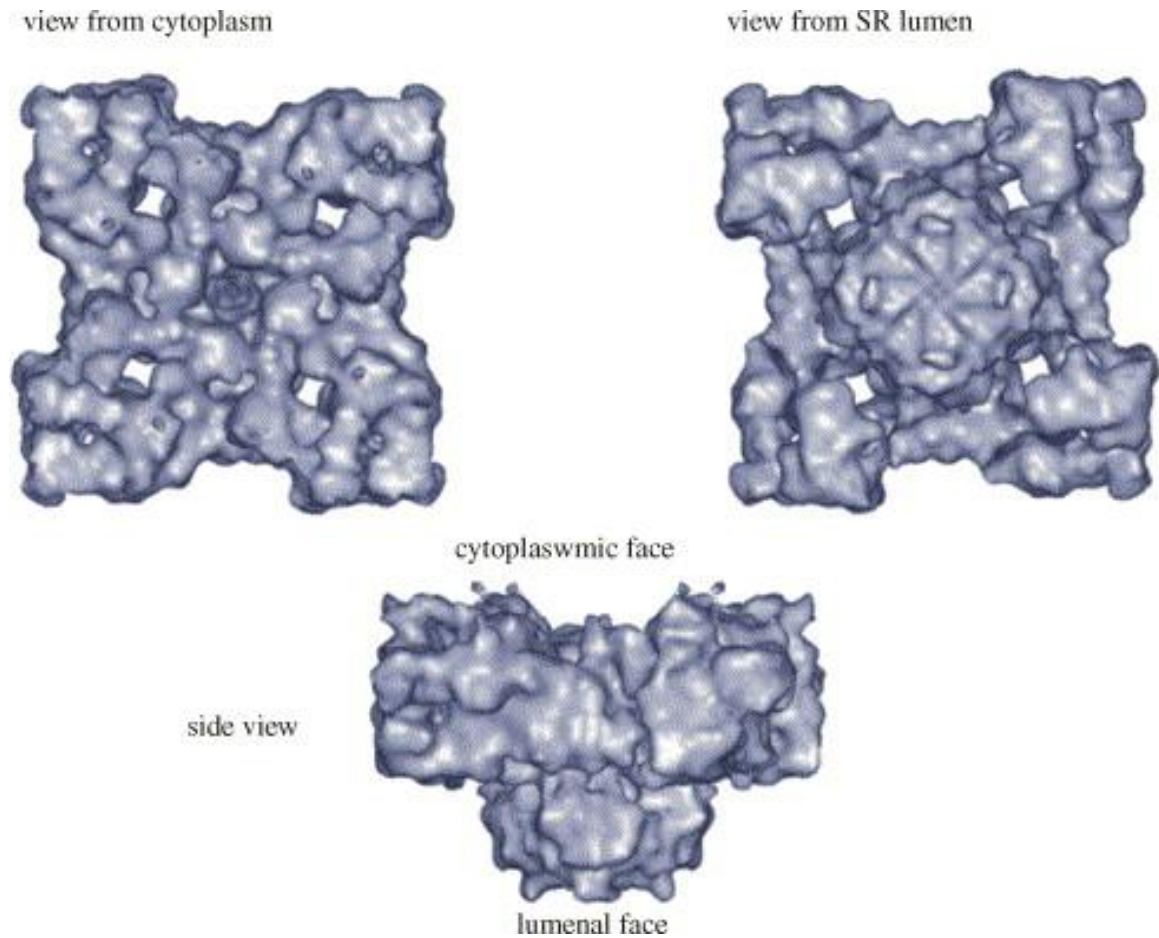


Figure 1-11: Three-dimensional structure of RyR1 at 14 Å resolution. (from I.I. Serysheva, S.L. Hamilton, W. Chiu and S.J. Ludtke, *J. Mol. Biol.* 345 (2005))

III.1.2.RyR modulators

The activities of all three RyR isoforms are modulated by a large number of substances. These compounds can act as activators or inhibitors and most of them bind to the cytoplasmic domain of the RyRs and allosterically regulate the opening of the Ca^{2+} conduction pathway in the transmembrane region. RyR activity can also be modulated by post-translational modifications such as phosphorylation, oxidation and S-nitrosylation. To address the mechanisms and nature of the channel regulation by individual modulators it is important to identify sites of interaction on the primary/secondary sequence of the RyR as well as their location in the three-dimensional structure of RyR. Single-particle cryo-EM has been used to analyze macromolecular interactions between the RyR and some of its larger modulators, such as FKBP12 and calmoduline (Wagenknecht et al., 1996; Zorzato et al., 1990).

Endogenous modulators:

1. Calcium:

All RyR isoforms are activated by Ca^{2+} : RyR1 shows a bell-shaped Ca^{2+} -dependent activation curve with low Ca^{2+} concentrations (1-10 μM range) activating the channel and higher concentrations (500 μM to 10 mM range) inhibiting channel activity (Meissner et al., 1997). Interestingly RyR2 show a small inactivation at high Ca^{2+} concentrations (over 100 mM). This biphasic Ca^{2+} dependent behavior of RyR1 suggests the existence of at least two different Ca^{2+} binding sites: high affinity sites, which stimulate Ca^{2+} release and low affinity binding sites, which are less selective and inhibit Ca^{2+} release. In RyR1 potential Ca^{2+} binding sites have been identified between residues 1861 and 2094 and between 3657 and 3776 (Chen and MacLennan, 1994). In another study Treves et al. generated an antibody to a peptide encoded by sequence from amino acid 4380-4625 and found that this antibody could block Ca^{2+} dependent RyR1 activation. They speculated

that this could be the Ca^{2+} activating site. Interestingly several motifs within the primary sequence of RyRs have been suggested to act like Ca^{2+} binding EF hand motifs. Two such putative sites are located at amino acids 4079-4092 and at 4115-4126 (Xiong et al., 1998). On the other hand little is known about the inactivation low affinity site. Both Zorzato et al. and Hayek et al. suggested that the low affinity inhibitory Ca^{2+} binding site falls within the negatively charged region between residues 1872 and 1923 (Hayek et al., 2000; Zorzato et al., 1990).

2. Magnesium:

Mg^{2+} is a key regulator of RyRs function and in general of normal skeletal and cardiac muscle contraction. Mg^{2+} is believed to inhibit RyRs by two mechanisms: it can inhibit RyRs by competing with Ca^{2+} for the activation sites (Dunnett and Nayler, 1978; Meissner, 1986) or it can bind to the low affinity Ca^{2+} binding site and close the RyRs (Laver et al., 1997; Soler et al., 1992). There is a difference between RyR1 and RyR2 in their sensitivity to inhibition by Mg^{2+} since the low affinity Ca^{2+} binding sites have a 10 fold lower affinity for Mg^{2+} in RyR2 than in RyR1. This is translated into differences in Mg^{2+} inhibition of RyR1 and RyR2 at elevated cytoplasmic Ca^{2+} levels (Laver et al., 1997; Laver et al., 1995). In resting skeletal muscle, where the free Mg^{2+} concentration is approximately 1mM, Mg^{2+} is the primary inhibitor of Ca^{2+} release from the SR preventing CICR and uncontrolled contraction of resting muscles. This concept was highlighted in experiments by Lamb and Stephenson (Lamb and Stephenson, 1994; Owen et al., 1997) which showed that a reduction of cytoplasmic free Mg^{2+} from physiological levels (approximately 1 mM) to 0.2 mM or lower in skinned muscle preparations, released Ca^{2+} from the SR. Furthermore during t-tubule depolarization and activation of the RyR by the DHPR, the sensitivity of RyRs to inhibition by Mg^{2+} is reduced by more than ten fold (Lamb and Stephenson, 1991). Thus during EC coupling, DHPRs somehow relieve Mg^{2+} 's inhibition and thus permit RyR activation by ATP and Ca^{2+} (the Mg^{2+} de-repression hypothesis) (Lamb and Stephenson, 1992).

Cytosolic Mg^{2+} may also be involved in the regulation of RyR1 by SR luminal Ca^{2+} . Recent work suggests that luminal Ca^{2+} influences RyR gating indirectly, by decreasing

the affinity of the cytosolic Ca^{2+} activation site for Mg^{2+} (Laver et al., 2004). Thus, pharmacological activators of the RyR must overcome Mg^{2+} inhibition to produce Ca^{2+} release from the SR. Interestingly, increasing evidence suggests that defects in the regulation of RyR by Mg^{2+} may be connected with MH susceptibility (Laver et al., 1997; Owen et al., 1997).

3. Adenine nucleotides

Adenine nucleotides including ATP and ADP are RyR activators (Galione and Churchill, 2000; Pessah et al., 1987). ATP strongly activates RyR1 at resting (nM) cytoplasmic Ca^{2+} concentration and in conjunction with Ca^{2+} , can cause almost full activation. The cardiac isoform RyR2 is not appreciably activated by ATP in the absence of Ca^{2+} , but ATP enhances its activation by Ca^{2+} (Kermode et al., 1998; Meissner et al., 1988). RyR3 also appears to be less sensitive to ATP.

4. Redox modifications of RyR:

RyR channels have been proposed to act as intracellular redox sensors (Eu et al., 2000; Hidalgo et al., 2005). Each RyR monomer has 100 cysteine residues (Liu et al., 1994) and about half of them are free. This large number of free thiol groups makes RyRs sensitive to modification by reactive oxygen intermediates. In particular, many recent studies have reported modifications of RyR cysteines by non-physiological redox compounds (Hamilton and Reid, 2000; Hidalgo et al., 2002; Pessah et al., 2002). For example thimerosal enhances single RyR channel activity in lipid bilayers (Marengo et al., 1998). Thimerosal also stimulates CICR from SR vesicles isolated from mammalian skeletal muscle (Donoso et al., 2000; Hidalgo et al., 2000). Endogenous redox components include the free radicals nitric oxide (NO) and superoxide anion, which through

enzymatic or non-enzymatic chemical reactions can be readily converted into non-radical species of lower reactivity but longer half-life such as S-nitrosoglutathione (GSNO) or hydrogen peroxide (H₂O₂). These endogenous redox components can modify RyR function (Hidalgo et al., 2004) and both skeletal and cardiac RyR isoforms have been shown to be endogenously S-nitrosylated (Eu et al., 2000; Xu et al., 1998b; Zahradnikova et al., 1997), suggesting that nitric oxide (NO) and NO-adducts are physiological effectors of excitation contraction-coupling. Incubation with NO or NO donors also modifies RyR channel activity (Salama et al., 2000; Suko et al., 1999; Xu et al., 1998a). Additionally, RyR channels are highly susceptible to modification by other endogenous redox agents, including glutathione (GSH), glutathione disulphide (GSSG), NADH, and by changes in the GSH/GSSG ratio (Hidalgo et al., 2004).

5. Phosphorylation of RyRs:

Endogenous kinases and phosphatases which modulate RyRs include cAMP-dependent protein kinase (PKA), cGMP-dependent protein kinase (PKG), protein kinase C (PKC), and calmodulin-dependent protein kinase II (CaMK). According to sequence analysis, several serine and threonine residues have been identified as possible phosphorylation sites on the RyR1. Phosphorylation of Ser2843 by endogenous kinase (Varsanyi and Meyer, 1995) and *in vitro* phosphorylation of Ser2843 by cAMP-, cGMP- and CaM-dependent protein kinases (Suko et al., 1993) have been reported. In addition phosphorylation of Ser2809 by PKA and Ser2815 by CaMKII of cardiac isoform RyR2 are thought to be involved in activation of channel gating (Bers, 2006). In failing human hearts PKA phosphorylation of RyR2 is significantly elevated. Since PKA phosphorylation of RyR2 inhibits FKBP12.6 binding, which is normally bound to the RyR complex and stabilizes the channel, hyperphosphorylated RyR2 in failing heart results in increased Ca²⁺ sensitivity for activation and elevated channel activity associated with destabilization of the tetrameric channel complex. These modifications of the channel lead to defective channel functions and possibly underline the pathological mechanism in failing heart (Marx et al., 2000).

Exogenous modulators:

1. Ryanodine:

In 1948, Rogers purified ryanodine, a plant alkaloid, from *Ryania speciosa*. Ryanodine specifically binds to RyRs and gives the receptor its name. Ryanodine has two opposite effects on Ca^{2+} release: at submicromolar concentrations it increases the channel's activity whereas at high micromolar concentrations it decreases SR Ca^{2+} release. Consequently, ryanodine has been proposed to bind at multiple (high- and low- affinity) sites on the ryanodine receptor but the number and exact location of these sites are still unknown. The high-affinity site may be located on the carboxy-terminal domain of the channel and since RyR monomers do not able to bind ryanodine, it has been assumed that the tetrameric structure is necessary for ligand binding where binding of ryanodine favours the open RyR conformation and modifies the conductance properties of the channel (Fill and Copello, 2002; Fryer et al., 1989).

2. Caffeine:

Caffeine a methylxanthine, promotes Ca^{2+} release and CICR at millimolar concentrations (Pessah et al., 1987). By an allosteric interaction, caffeine appears to increase the sensitivity of the Ca^{2+} activator site for Ca^{2+} and even to reverse Mg^{2+} inhibition. RyR2 is more sensitive to caffeine than RyR1. Caffeine and adenosine nucleotides seem to have a synergistic effect, suggesting that their respective binding sites are in close proximity or even overlap with each other.

3. Volatile anaesthetics:

In skeletal muscle, at a concentration of 0.002-3.8% gas, halothane increases Ca^{2+} efflux via the RyR by increasing the open probability of the channel (Kim et al., 1984). The response of the channel to halothane stimulation is pH and Ca^{2+} -dependent but adenosine

nucleotide independent. Effects similar to those of halothane have been observed with other volatile anaesthetics such as isoflurane and enflurane (2.5 to 4%).

4. 4-chloro-m-cresol:

It is a specific RyR1 activator (Herrmann-Frank et al., 1996; Zorzato et al., 1993). It seems to have a similar effect to that of caffeine but opens the channel at lower concentrations (micromolar versus millimolar concentrations). It is a more potent and specific drug than halothane and caffeine.

5. Ruthenium red:

It is an inorganic polyamine and a polycationic dye. It has been demonstrated to inhibit the SR- Ca^{2+} release in both skeletal and cardiac muscles. Ruthenium red blocks the channel in an asymmetrical and voltage-dependent mode. In particular it completely blocks CICR and therefore is often used to verify RyR-dependent leakage from the SR (Chamberlain et al., 1984; Chiesi et al., 1988).

6. Dantrolene

It is a highly lipophilic hydantoin (anticonvulsant) derivate. It is classified as a direct-acting skeletal muscle relaxant. It is currently the only specific and effective treatment for malignant hyperthermia. The therapeutic concentration is about $10\mu\text{M}$ (Flewellen et al., 1983). Dantrolene depresses excitation-contraction coupling in skeletal muscle by binding to the ryanodine receptor 1. *In vivo*, dantrolene may target RyR1 and RyR3 but not RyR2 (Zhao et al., 2001).

7. Doxorubicin:

Doxorubicin also known as Adriamycin, was first described to induce Ca^{2+} -release from isolated skeletal muscle SR vesicles and from skinned muscle fibres (Zorzato et al.,

1985). The same behavior was also found in cardiac muscle, where doxorubicin increases the [3H] ryanodine– binding to the ryanodine receptor. Doxorubicin, an anthraquinone, is a widely used antineoplastic and chemotherapeutic agent. Although its acute effects are completely reversible, chronic clinical treatment may cause cardiotoxicity, possibly due to the long term sensitization of RyRs to Ca^{2+} (Abramson et al., 1988; Pessah et al., 1990).

III.2. Genetic linkage and functional effects of RYR1 mutations

The RyR1 is encoded by a gene composed of 106 exons, which produces one of the largest known proteins (5038 amino acids). The first 4000 amino acids are predicted to form the hydrophilic domain while the last 1000 residues encode the hydrophobic COOH-terminal domain containing the transmembrane segments and the pore region.

Mutations in the *RYR1* gene have been linked to several neuromuscular disorders such as MH, CCD, MmD, CNM and King Denborough syndrome (D'Arcy et al., 2008; Jungbluth et al., 2007; Robinson et al., 2006; Treves et al., 2005; Wu et al., 2006; Zhou et al., 2007).

To date over 100 mutations (substitutions or small deletions) in the *RYR1* have been associated with MH susceptibility and CCD/MmD phenotypes while a few with CNM (Ghassemi et al., 2009; Jungbluth et al., 2007). Most MH and CCD causing mutations are located in one of the three “hot spot” regions. The first hotspot is clustered between amino acid residues 35 and 614 (MH/CCD region 1), the second region between amino acid residues 2129 and 2458 (MH/CCD region 2) and the third between amino acid residues 3916 and 4942 (MH/CCD region 3)(Fig. 1-12) (Robinson et al., 2006; Treves et al., 2005). The majority of MH-linked mutations are present in the heterozygous state, within the myoplasmic foot regions 1 and 2, while in most CCD-affected individuals mutations are also in heterozygous state, but appear to be concentrated in the transmembrane/luminal domain. Though some patients affected by CCD have also been phenotyped as MHS, these results must be interpreted with caution, particularly since (i)

any underlying muscular disorder can potentially influence the outcome of the in vitro contracture test and (ii) the threshold values for caffeine and halothane sensitivity in the in vitro contracture test have been defined for the “general population”, unaffected by neuromuscular disorders. Since both MH and CCD are due to a dysregulation of Ca^{2+} homeostasis it appears risky to classify CCD patients as MHN or MHS. For those MmD patients harbouring *RYR1* mutations, these appear to be evenly distributed along the gene and present either in homozygous state at the genomic level, or homozygously expressed in muscle due to imprinting of the mutated allele (Zhou et al., 2007).

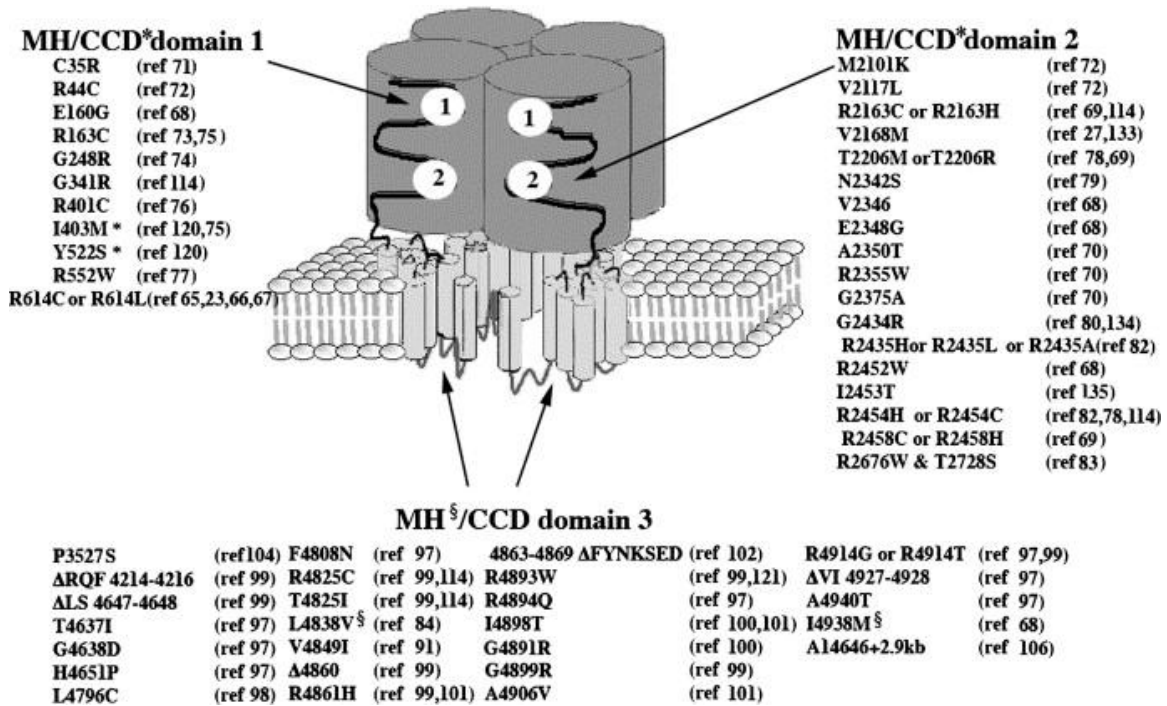


Figure 1-12: Cartoon depicting the ryanodine receptor tetramer inserted into a lipid bilayer. The mutations identified in the different domains as well as their association with MH and CCD are indicated (from Treves et al., 2005)

Functional effects of *RYR1* mutations:

It appears that *RYR1* mutations result in four different channel defects (Treves et al., 2008): (i) one class of mutations (mostly associated with the MHS phenotype) cause Ca^{2+} channels to become hypersensitive to membrane depolarization and pharmacological activation; (ii) a second class of mutations causes the RyR1 channels to become leaky (iii) a third class of mutations renders the Ca^{2+} channel unable to conduct Ca^{2+} and/or uncouples RyR1 from the voltage sensor (Xu et al., 2008) (mutation class 2 and 3 are mostly associated to CCD); (iv) the fourth class of mutations found in MmD patients where only one allele is expressed (hemizygous) results in protein Ca^{2+} channel instability which ultimately leads to a decrease of the expression level within muscle (Monnier et al., 2008; Zhou et al., 2006b). In order to elucidate possible pathophysiological mechanisms of neuromuscular disorders linked to *RYR1* mutations it is essential to define the mutation class by studying the functional properties of channels harbouring clinically relevant amino acid substitutions.

Functional studies have revealed that most Malignant Hyperthermia causing mutations disturb normal calcium homeostasis by shifting the sensitivity to pharmacological activation to lower agonist concentrations and/or by causing an increase in the resting Ca^{2+} concentration (Ducreux et al., 2004; Girard et al., 2001; Lopez et al., 2000). A recent model proposed by Kobayashi et al. (Shimamoto et al., 2008) concerning channel regulation suggests inter-domain interactions between the N-terminal and the central domain of RyR1 serving as “domain switches” for calcium regulation. In the resting state, these domains make close contacts within several subdomain regions and any mutation in these regions could cause partial unzipping or weakening of domain switches resulting in the hypersensitivity of the RyR1 to agonists. The existence of such inter-domain interactions between N-terminal and central RyR1 domains has been experimentally confirmed (Zorzato et al., 1996). The recently hypothesized flip-state theory (Steinbach, 2008) could further explain the increased sensitivity of mutated *RyR1* to agonists. Flip-state was recently proposed for the acetylcholine receptor but could also be applied to the RyR1. “Flip” is an intermediate state between an initial inert drug-effector complex and the receptor with the channel open. MH-causing mutations could

promote the entry of the RyR channel into the flip-state; as a consequence, after binding the agonist, the mutated receptors are more able to “flip” and therefore pass into the “open” state. Alternatively, Malignant hyperthermia causing mutations might increase the stability of the flip-state. The flip-state theory is attractive for ion channels which are large proteins composed of several subunits and whose activation involves a considerable conformational change that probably takes place in a series of steps.

Two hypotheses have been suggested to explain the functional effect of CCD-linked *RYR1* mutations: the first one, leaky channel hypothesis, suggests that these mutations lead to leaky channels, depletion of SR Ca^{2+} stores and consequently muscle weakness (Lynch et al., 1999; Rossi and Dirksen, 2006; Tilgen et al., 2001; Treves et al., 2005; Zorzato et al., 2003). According to the second hypothesis, the “EC uncoupling hypothesis” CCD mutations in the hot spot domain 3 lead to functional uncoupling of sarcolemma depolarization from release of Ca^{2+} from the SR Ca^{2+} stores (Dirksen and Avila, 2004; Rossi and Dirksen, 2006). The main difference between these two hypothesis concerns the Ca^{2+} load in the lumen of the SR (Treves et al., 2005). In the case of the uncompensated Ca^{2+} leak hypothesis, a decrease of the SR is present, while the EC uncoupling hypothesis predicts that the muscle weakness does not result from major changes in the SR Ca^{2+} levels, but rather is due to a defect in excitation contraction coupling mechanism (Rios et al., 2006).

In MmD patients harbouring *RYR1* mutations the situation is more complicated in terms of alterations of RyR1 function. The first functional study of MmD-related *RYR1* mutations demonstrated that the p.P3527S and p.V4849I substitutions are associated with a slightly elevated resting Ca^{2+} concentration, but not depleted intracellular stores (Ducreux et al., 2006). Interestingly, cells carrying the homozygous P3527S *RYR1* mutation were found to release significantly less Ca^{2+} after pharmacological activation. In another study it was shown that RyR macromolecular complexes carrying the p.N2283H heterozygous mutations increased the sensitivity of the RyR1 activation by KCl and caffeine but this is probably caused by its MHS linkage phenotype. The same study however, a patient with the compound heterozygous p.N2283H + p.S71Y mutations lead to “unstable” channels which lost their activity during purification. Other compound

heterozygous mutations such as p.A1577T + p.G2060C and p.R109W + p.M485V lead to a decrease in the amount of RyR1 expressed in skeletal muscle, to a decrease of Ca^{2+} release as well as [^3H]ryanodine binding (Zhou et al., 2006b). Finally in some MmD patients, particularly those with ophthalmoplegia, the clinical phenotype may be at least partly explained by a decrease of the RyR1 channel density in the junctional sarcoplasmic reticulum membrane, as demonstrated by Western blot analysis with anti-RyR Ab (Zhou et al., 2006a; Zhou et al., 2006b; Zhou et al., 2007) (Monnier et al., 2003).

III.3. Neuromuscular disorders

Ca^{2+} is an important second messenger and in skeletal muscle is a key player in the development of contractile force. The intracellular Ca^{2+} concentration is finely regulated and any alteration in the proteins involved in Ca^{2+} handling can potential lead to pathological condition. Thus defects in genes encoding proteins of the SR have been found to cause several pathologies (MacLennan, 2000) including Brody disease (BD) the first described disorder of skeletal muscle. That is due to a dysfunctional in SERCA1a (Brody, 1969; Odermatt et al., 1996).Furthermore Malignant Hyperthermia (MH; MIM#145600), Central Core Disease (CCD; MIM#11700), specific forms of multi-minicore (MmD; MIM#255320) disease and centronuclear myopathy (CNM) associated with *RYR1* mutation.

III.3.1 Malignant Hyperthermia

Malignant hyperthermia (called also Malignant hyperpyrexia) is an autosomal dominant, potentially lethal, pharmacogenetic disorder manifesting itself as a hypermetabolic response triggered by volatile halogenated anaesthetics such as halothane, sevoflurane, desflurane, isoflurane, enflurane and/or depolarizing muscle relaxant succinylcholine and rarely, in humans, by stress, vigorous exercise and heat. MH is a classical example of a pharmacological disease since almost all patients who are MH susceptible have no phenotypic changes without anaesthesia. Numerous publications in the anaesthesia literature have reported that also patients with disorders leading to Ca^{2+} dysregulation such as Duchenne muscular dystrophy (DMD) (Brownell et al., 1983) and Becker dystrophy (BD) can experience a variety of life-threatening complications during and after general anaesthesia and are at an increased risk of developing a MH episode. Furthermore patients with diseases connected with *RYR1* mutation such as CCD (Denborough et al., 1973) and MmD are also at risk of developing an MH reaction. MH like crisis may also develop after administration of some drugs such as neuroleptics.

Epidemiology:

The first time an MH reaction was clearly identified in a patient, was at the beginning of the 20th Century by Denborough and Lovell in 1960. Since then the number of publications reporting MH reactions has grown exponentially and it is now established that the incidence of MH episode is about 1 in 5000 to 1 in 15000 anaesthesias in children and about 1 in 50000 to 1 in 100000 in adults (Loke and MacLennan, 1998; Rosenberg et al., 2007). MH episodes are a major cause of anaesthetic related deaths in young, fit individuals (Kaus and Rockoff, 1994). Reactions develop more frequently in males than females with males having a greater fatality rate (Brady et al., 2009; Strazis and Fox, 1993). It is so far unclear why age and sex differences influence the incidence of MH. It has been suggested that young males are more likely candidates for general anaesthesia and surgical interventions such as orthopaedic, eye, dental operations, ear,

nose and throat trauma in which triggering drugs are frequently used, compared to females. All ethnic groups are affected in all parts of the world. It should be mentioned however that the reported incidences are probably underestimated because of the difficulty in defining mild reactions and since many MH susceptible individuals are never anesthetized and also since many individuals who develop an MH reaction do so after being subjected to other general anaesthetics without developing a reaction (Loke and MacLennan, 1998). MH crises develop not only in humans but also in other species particularly pigs, which have been a valuable source for research. Reactions have also been described in horses, dogs and other animals (Britt, 1985). Over the years mortality in humans has been reduced from 80% to 10% and even 0% in developed countries. This is possible under present-day standard anaesthetic practice where heart rate, blood pressure, body temperature and other parameters are closely monitored during anaesthesia and if necessary the antidote dantrolene is available (Harrison, 1975). Nevertheless neurological, muscle and kidney damage still contribute to the morbidity resulting from an MH reaction.

Clinical description:

MH may occur at any time during anaesthesia and in the early postoperative period. The earliest signs are tachycardia, rise in end-expired carbon dioxide concentration despite increased minute ventilation, accompanied by muscle rigidity, especially following succinylcholine administration. Body temperature elevation is a dramatic but often late sign of MH. Other signs include acidosis, tachypnea and hyperkalemia. The progression of the syndrome may be very rapid. Uncontrolled hypermetabolism leads to cellular hypoxia that is manifested by a progressive and worsening metabolic acidosis. If untreated, continuing myocyte death and rhabdomyolysis result in life-threatening hyperkalemia. Thus muscle damage brings about electrolyte imbalance, with early elevation of serum K^+ and Ca^{2+} and later elevation of muscle proteins such as creatine kinase and myoglobin in the blood and urine myoglobinuria may lead to acute renal

failure. Additional life-threatening complications include disseminated intravascular coagulation, congestive heart failure, bowel ischemia, and compartment syndrome of the limbs secondary to profound muscle swelling, and renal failure from rhabdomyolysis. Indeed, when body temperature exceeds approximately 41°C, disseminated intravascular coagulation is the usual cause of death.

For patients known or suspected of being MHS or even for patients with other myopathies, anaesthetic management should be changed to avoid contact with trigger agents. All inhalation anaesthetics except nitrous oxide (NO) act as trigger agents for MH. Thus in patients at risk for developing a MH reaction a combination of non-triggering anaesthetics such as barbiturates, tranquilizers, narcotics, propofol, ketamin, NO, and local anaesthetics should be used.

Laboratory diagnostic methods:

The “gold standard” for diagnosis of MH is currently the in-vitro contracture test (IVCT), which is based on contracture of muscle fibres in the presence of halothane or caffeine. This test was developed and standardized by the European Malignant Hyperthermia Group (EMGH, www.emgh.org) to exclude the MH risk of family members who had a MH reaction. The test is invasive because for each test muscle fibres from biopsied skeletal muscle need to be removed. In Switzerland, phenotypic assessment by the IVCT has been performed since 1986 in the MH laboratory of the Departments of Anaesthesia and Research, Kantonsspital Basel.

Summarized protocol:

The biopsy is preferably performed from the quadriceps muscle (vastus medialis or vastus lateralis) under regional anaesthesia. The patient fully recovers from the biopsy within 8 to 11 days. After excision, muscle bundles are immediately placed in precarboxygenated Krebs-Ringer solution at room temperature at a pH of 7.4. The muscle should be transported to the lab with minimal delay between the surgical removal of the muscle

strip and the IVCT performance; this time should not exceed 5 hours. The muscle biopsy is dissected into strips (15-25mm length x 2-3mm thickness) free of connective tissues. A strip is suspended in a bath of Krebs-Ringer solution at 37°C. It is stretched to its optimal length and allowed to equilibrate in order to develop a stable resting tension; viability is demonstrated by recording twitches elicited by electrical stimulation. Once the baseline tension is obtained, muscle strips are tested successively for their sensitivity to increasing concentrations of caffeine and halothane. The threshold of positivity is an increase of $\geq 2\text{mN}$ in the resting tension to caffeine concentration $\leq 2\text{mM}$ and to halothane concentration $\leq 0.44\text{mM}$ (2% vol) (Fig 1-13). According to the European guidelines, patients are diagnosed as MHS if results are positive for both substances, MHN if results are negative for both substance and MHE when only one test is positive. For research, MHE patients are treated separately, while for clinical purposes they are considered as MHS.

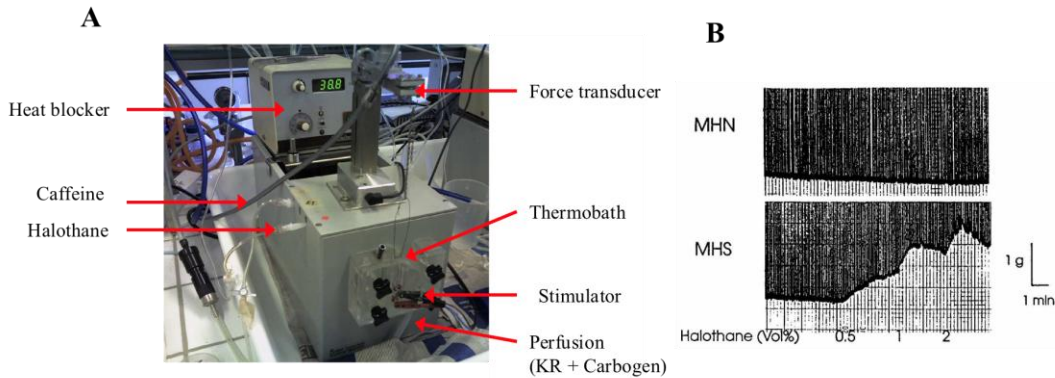


Figure 1-13: In Vitro Contracture Test. (A) set up for IVCT. (B) Original traces with resting tension and absolute twitch tension. The test with halothane in a normal and a MHS individual is shown. The increase of resting tension of MHS reflects the development of a contracture.

The IVCT carries a good sensitivity (99%) and specificity (93.6%) (Ording et al., 1997). A slightly different protocol for testing MH susceptibility evolved in North America and is referred as the caffeine-halothane contracture test (CHCT). The test is associated with a lower specificity (78%) and sensitivity (97%) than the European protocol (Allen et al., 1998). Japan also has a different standard protocol for testing MH susceptibility. It relies on the detection of an accelerated rate of calcium-induced calcium-release (CICR) from SR of skinned muscle fibres in comparison to reference values previously measured in healthy controls. In this test, the sarcolemma of skeletal muscle fibres is chemically destroyed, thus allowing the stimulation of calcium release from sarcoplasmic reticulum using external calcium solutions of five different concentrations. If the patient's CICR values are 1.5 SD above the normal average values at two or more calcium concentrations in two or more skinned fibres, the CICR rate is defined as being clearly enhanced. Otherwise, CICR test results are reported as abnormally enhanced or not enhanced (Ibarra et al., 2006). Nevertheless, all test procedures carry the potential risk of false-positives and false-negatives. Moreover, people with other neuromuscular disorders can have a positive IVCT. The major drawbacks of the IVCT are false positive and false negative results, the invasiveness of the test since surgical procedure is required, the test is expensive and commitment of a specialized testing center.

Modifications of EMHG protocol include the use of ryanodine (Bendahan et al., 2004) which binds selectively to the calcium release channel, 4-chloro-m-cresol (Rueffert et al., 2002) but to date these agents have not been included in the standard protocol.

Further problems arising from the presently used diagnostic method are linked to the fact that supplies of halothane are becoming limited. Possible alternative trigger agents are the fluorinated ether and sevoflurane. Even if the IVCT is the “gold standard” research is focusing on the development of less invasive but equally sensitive tests for MH diagnosis.

Measurements of other physiologic parameters potentially associated with MH pathology such as abnormal lymphocyte or hepatocytes intracellular calcium mobilization in response to anaesthetics have not been proven as sufficiently useful for clinical diagnosis of MH (Fletcher et al., 1990; Klip et al., 1987; Klip et al., 1986; Ording et al., 1990)

(Iaizzo et al., 1991). DNA analysis, however, offers an alternative to IVCT, requiring only a blood sample, which can be sent to specialized testing laboratories. Since about 50% of MH cases have been linked to mutations in the *RYR1* gene and over 100 different point mutations have been identified in MH families, genetic identification of a proven *RYR1* causing mutation can theoretically substitute the IVCT, however, patients with negative genetic tests still require an IVCT.

III.3.2 Central Core Disease

Central core disease (CCD) is a rare, nonprogressive, or slowly progressing myopathy, presenting in infancy, with main clinical symptoms such as hypotonia and proximal muscle weakness. CCD is usually inherited as an autosomal dominant (AD) trait (Jungbluth, 2007) but recessive inheritance has been recently described in few families (Kossugue et al., 2007; Wu et al., 2006; Zhou et al., 2006b; Zhou et al., 2007). Marked clinical variability, often within the same family, has been recognized. Orthopaedic complications such as congenital dislocation of the hips (Ramsey and Hensinger, 1975), scoliosis which may be present from birth (Merlini et al., 1987) and foot deformities including talipes equinovarus and pes planus (Gamble et al., 1988) are common in CCD. Almost all patients with CCD achieve the ability to walk independently, except the most severe neonatal cases and those with congenital dislocation of the hips.

More severe presentations within the range of the foetal akinesia syndrome (Romero et al., 2003) have been reported associated with recessive inheritance or *de novo* dominant mutations. Inability to bury eyelashes completely may be the only manifestation of some patients presenting with mild symptoms. Bulbar involvement is untypical in the dominant form and extra-ocular muscle involvement has been considered a clinical exclusion

criterion by some authors however, both features may be observed in the most severely affected neonates due to recessive inheritance (Romero et al., 2003).

Beside the clinical diagnosis by a neurologist, pathological examination of a muscle biopsy from CCD patients shows muscle fibre, with areas of reduced or absent oxidative enzyme activity running along the longitudinal axis (Dubowitz and Pearse, 1960). These areas are called cores and they are observed upon histological staining of the muscle biopsies from patients. Type I fibre predominance is common in CCD. Electron microscopy shows variable degrees of disintegration of the contractile apparatus within the core region, from Z line streaming to total loss of myofibrillar structure

Many patients with CCD are positive for the malignant hyperthermia susceptibility (MHS) trait on IVST (Robinson et al., 2002; Shuaib et al., 1987) and should therefore be considered at risk for MH episode during anaesthesia. An association between CCD and MHS had been suspected early, as individuals with MHS may have central cores on muscle biopsy (Denborough et al., 1973) and patients with CCD may be prone to malignant hyperthermia episodes (Eng et al., 1978; Frank et al., 1980; Shuaib et al., 1987). In most cases, patients with dominant CCD carry mutations in *RYR1* gene and with few exceptions these are clustered in the hydrophobic COOH-terminal pore-forming region of the molecule (domain 3) (Robinson et al., 2006; Treves et al., 2005; Wu et al., 2006).

III.3.3 Multi-minicore disease

MmD disease is an autosomal recessive early onset congenital myopathy (Engel et al., 1971). The diagnosis of MmD is based on the presence, in most muscle fibres, of multiple mini-cores, which occur in both type 1 and type 2 fibres and typically run to a limited extent along the longitudinal muscle fibre axis. By electron microscopy mini-cores appear as unstructured lesions with amorphous material, misalignment of

myofibrils and absence of mitochondria. The most common phenotype of MmD or “classical” MmD form is characterized by the axial predominance of muscle weakness, scoliosis with spinal rigidity and respiratory insufficiency; because of early respiratory failure, most patients require mechanical ventilation. A second group of patients shows moderate phenotype with generalized muscle weakness predominantly in the hip girdle region, amyotrophy and hyperlaxity. In this group of patients, scoliosis and respiratory impairments are mild or absent. Other patients may also have partial or complete ophthalmoplegia. The clinical heterogeneity of MmD is reflected in its genetic heterogeneity having been linked to recessive mutations both in the selenoprotein 1 (*SEPNI*) gene and the skeletal muscle *RYR1* gene (Ferreiro et al., 2002; Godfrey et al., 2006; Jungbluth et al., 2002; Moghadaszadeh et al., 2001). Although genotype-phenotype correlations have not been fully established, it appears that extra-ocular muscle involvement is more common in the *RYR1*-related form of MmD, while severe scoliosis and respiratory impairment requiring ventilatory support are more prevalent in *SEPNI*-related ‘classical’ MmD (Ferreiro et al., 2002; Jungbluth et al., 2002; Monnier et al., 2003). The association with malignant hyperthermia (MH) is not as well documented as in CCD due to dominant *RYR1* mutations (Denborough et al., 1973), but clinical MH episodes have been recognized in a few cases of MmD (Koch et al., 1985; Osada et al., 2004); Mini-cores have also been noted in muscle biopsies from families with MH susceptibility due to *RYR1* mutations but no other clinical features of a congenital myopathy (Barone et al., 1999; Guis et al., 2004). Precautions during general anaesthesia are necessary especially in the cases of MmD with *RYR1* mutation.

III.3.4 Centronuclear myopathy (CNM)

Centronuclear myopathy is a rare and genetically heterogeneous congenital myopathy. On examination of muscle biopsies from CNM patients, the nuclear material is located predominantly in the center of the muscle cells with a central aggregation of oxidative enzymes and type 1 fibre predominance. Mutations in the myotubularin (*MTM1*) gene on chromosome Xq28 are implicated in the X-linked variant of disease and mutation in the dynamin 2 (*DNM2*) gene on chromosome 19p13 have been recently associated with a dominant form of CNM (Bitoun et al., 2005; Laporte et al., 1996; Laporte et al., 1997). Interestingly a *de novo* dominant *RYR1* mutation has been reported in a sporadic case of CNM. The latest findings between *RYR1* missense mutations (c.12335C > T; Ser4112Leu) and CNM clinical manifestations indicate that *RYR1* screening should be considered in CNM patients without *MTM1* or *DNM2* mutations (Jungbluth et al., 2007).

CHAPTER 2: RESULTS

I. Ca^{2+} homeostasis and role of RyR1 in dendritic cells

1.1 Introduction to publications

Recent data has shown that the skeletal muscle isoform of the RyR (RyR1) is expressed in cells of the immune system, specifically B-lymphocytes and DCs.

In the first publication of our study we confirmed the expression of RyR1 in B-lymphocytes, immature and mature monocyte derived DCs and Plasmacytoid cells.

We investigated the role of RyR1 in dendritic cells by following the changes in intracellular Ca^{2+} concentration and phenotypical changes of DCs, upon pharmacological activation of RyR1. In particular, since previous publications had noticed a role for Ca^{2+} in maturation, we were interested in investigating the involvement of RyR1 in the maturation process of DCs and possible synergy between TLR engagement (LPS induced maturation) and RyR1 activation. We evaluated the expression of genes associated with DCs maturation as well as the capacity of DCs to stimulate T-cell responses. We also investigated the involvement of RyR1 induced Ca^{2+} release in calcineurin (Ca^{2+} /calmodulin phosphatase) dependent processes.

We were also interested (paper 2) in identifying the possible physiological routes of RyR1 activation in DCs in-vivo and whether in these cells as well, the L-type Ca^{2+} channel is a functional partner leading to RyR1 induced Ca^{2+} release. The underlining hypothesis being that in cardiac and skeletal muscles, signalling to the RyR1 is coupled to the L-type Ca^{2+} channel, which senses changes in membrane potential thereby activating Ca^{2+} release from the SR.

In the third part of our study (manuscript 3) we further investigated Ca^{2+} homeostasis in DCs since we had noticed that immature DCs exhibit unstimulated changes in their intracellular Ca^{2+} concentration. In particular our studies show that spontaneous Ca^{2+}

oscillations occur in immature human monocyte-derived dendritic cells, but not in dendritic cells stimulated to undergo maturation with LPS or other toll like-receptor agonists. We investigated the mechanism and role of spontaneous Ca^{2+} oscillations in immature dendritic cells. Amplitude and frequency of specific Ca^{2+} signals are precise codes that cell is using to decode and take right messages form different stimulus. Spontaneous Ca^{2+} oscillations have been observed in a number of excitable and non-excitable cells, but in most cases their biological role remains elusive.

1.2 publications

- 1.** Laura Bracci*, Mirko Vukcevic*, Giulio Spagnoli, Sylvie Ducreux, Francesco Zorzato and Susan Treves. Ca^{2+} signalling through ryanodine receptor 1 enhances maturation and activation of human dendritic cells
J Cell Sci. 2007 Jul 1;120(Pt 13):2232-40. Epub 2007 Jun 13. Erratum in: J Cell Sci. 2007 Jul 15;120(Pt 14):2468.
* These authors contributed equally to this work
- 2.** Mirko Vukcevic, Giulio C. Spagnoli, Giandomenica Iezzi, Francesco Zorzato and Susan Treves. Ryanodine Receptor Activation by Cav1.2 Is Involved in Dendritic Cell Major Histocompatibility Complex Class II Surface expression
J Biol Chem. 2008 Dec 12;283(50):34913-22. Epub 2008 Oct 16.
- 3.** Mirko Vukcevic, Francesco Zorzato, Giulio Spagnoli and Susan Treves.
Frequent calcium oscillations lead to NFAT activation in human immature dendritic cells
J. Biol Chem. 2010 May 21;285(21):16003-11. Epub 2010 Mar 26.

Ca²⁺ signaling through ryanodine receptor 1 enhances maturation and activation of human dendritic cells

Laura Bracci, Mirko Vukcevic, Giulio Spagnoli, Sylvie Ducreux, Francesco Zorzato and Susan Treves

Journal of Cell Science 120, 2468 (2007) doi:10.1242/jcs.017590

There was an error published in *J. Cell Sci.* **120**, 2232-2240.

The address for Mirko Vukcevic was incorrectly assigned in the e-press version.

In addition, in both the online and print versions, the addresses for Susan Treves were incorrectly assigned.

The correct version is shown below.

Laura Bracci^{1,*,‡}, Mirko Vukcevic^{2,*}, Giulio Spagnoli¹, Sylvie Ducreux², Francesco Zorzato³ and Susan Treves^{2,3,§}

¹Institute of Surgical Research and ²Departments of Anesthesia and Research, Basel University Hospital, Hebelstrasse 20, 4031 Basel, Switzerland

³Department of Experimental and Diagnostic Medicine, General Pathology Section, University of Ferrara, 44100 Ferrara, Italy

*These authors contributed equally to this work

[‡]Present address: Department of Cell Biology and Neurosciences, Istituto Superiore di Sanità, 00161, Rome, Italy

[§]Author for correspondence (e-mail: susan.treves@unibas.ch)

Ca²⁺ signaling through ryanodine receptor 1 enhances maturation and activation of human dendritic cells

Laura Bracci^{1,*,#}, Mirko Vukcevic^{2,*}, Giulio Spagnoli¹, Sylvie Ducreux², Francesco Zorzato³ and Susan Treves^{2,§}

¹Institute of Surgical Research and ²Departments of Anesthesia and Research, Basel University Hospital, Hebelstrasse 20, 4031 Basel, Switzerland

³Department of Experimental and Diagnostic Medicine, General Pathology Section, University of Ferrara, 44100 Ferrara, Italy

*These authors contributed equally to this work

[†]Present address: Department of Cell Biology and Neurosciences, Istituto Superiore di Sanità, 00161, Rome, Italy

[§]Author for correspondence (e-mail: susan.treves@unibas.ch)

Accepted 5 May 2007

Journal of Cell Science 120, 2232-2240 Published by The Company of Biologists 2007

doi:10.1242/jcs.007203

Summary

Increases in intracellular Ca²⁺ concentration accompany many physiological events, including maturation of dendritic cells, professional antigen-presenting cells characterized by their ability to migrate to secondary lymphoid organs where they initiate primary immune responses. The mechanism and molecules involved in the early steps of Ca²⁺ release in dendritic cells have not yet been defined. Here we show that the concomitant activation of ryanodine receptor-induced Ca²⁺ release together with the activation of Toll-like receptors by suboptimal concentrations of microbial stimuli provide synergistic signals, resulting in dendritic cell maturation and

stimulation of T cell functions. Furthermore, our results show that the initial intracellular signaling cascade activated by ryanodine receptors is different from that induced by activation of Toll-like receptors. We propose that under physiological conditions, especially when low suboptimal amounts of Toll-like receptor ligands are present, ryanodine receptor-mediated events cooperate in bringing about dendritic cell maturation.

Key words: Dendritic cell, Maturation, Ryanodine receptor, Signaling

Introduction

Ryanodine receptors (RyR) are intracellular Ca²⁺ channels mainly found in excitable tissues, mediating Ca²⁺ release from intracellular stores (Sutko and Airey, 1996; Franzini-Armstrong and Protasi, 1997). The functional Ca²⁺ release channel is composed of four ryanodine receptor monomers (each of which has a molecular mass of approximately 560 kDa), which assemble into a large macromolecular structure with a molecular mass of more than 2 × 10⁶ Da (Bers, 2004; Serysheva et al., 2005; Samso et al., 2005). Three isoforms of the RyR have been identified at the molecular level: they share an overall amino acid identity of approximately 60% and experimental evidence suggests that they are structurally similar, with a large hydrophilic NH₂-terminal domain and a hydrophobic C-terminal domain containing several transmembrane domains as well as the channel pore (Bers, 2004; Serysheva et al., 2005; Samso et al., 2005). Type 1 RyR (RyR1), encoded by a gene located on human chromosome 19, is mainly expressed in skeletal muscle where it mediates Ca²⁺ release from the sarcoplasmic reticulum, following depolarization of the plasmalemma (Phillips et al., 1996; Takeshima et al., 1989; Zorzato et al., 1990). Type 2 RyR, encoded by a gene located on chromosome 1, is mainly expressed in the heart and in certain areas of the cerebellum and is activated through a Ca²⁺-induced Ca²⁺-release mechanism (Otsu et al., 1990; McPherson and Campbell, 1993). Type 3 RyR, encoded by a gene located on chromosome 15, is expressed in several tissues, including the central nervous system; its expression in some tissues appears to be

developmentally regulated (Sorrentino et al., 1993; Tarroni et al., 1997). In recent years, more detailed investigations have revealed that this isoform-specific tissue distribution of RyR may in fact be more complex. Sei et al. (Sei et al., 1999) and Hosoi et al. (Hosoi et al., 2001) showed that circulating leukocytes, as well as leukocyte-derived cell lines, express different RyR transcripts. We have shown that Epstein Barr Virus (EBV)-immortalized B-lymphocytes express the transcript, the protein and the functional RyR1 Ca²⁺-release channel (Girard et al., 2001), and O'Connell et al. (O'Connell et al., 2002) have demonstrated that the RyR1 is expressed in immature mouse dendritic cells (DCs). Immature DCs (iDCs) act as sentinels in peripheral tissues, continuously sampling the antigenic environment. Upon Toll-like receptor engagement by microbial products or tissue debris, DCs undergo maturation and become the most potent antigen-presenting cells. At this point, Toll-like receptor-activated DCs upregulate costimulatory and antigen-presenting molecules and migrate to secondary lymphoid organs for the interaction with naive T-cells and the priming of immune responses in vivo (Banchereau and Steinman, 1998). For several years it has been known that increases in the intracellular calcium concentration ([Ca²⁺]_i) participate in the regulation and maturation of DCs (Koski et al., 1999; Czerniecki et al., 1997), although the mechanism and molecules involved in the early steps of the Ca²⁺-release event have not been clearly defined.

As part of an investigation aimed at identifying the role of RyR1 in cells of the immune system, we showed that in freshly isolated human B-lymphocytes, activation of the RyR1 leads

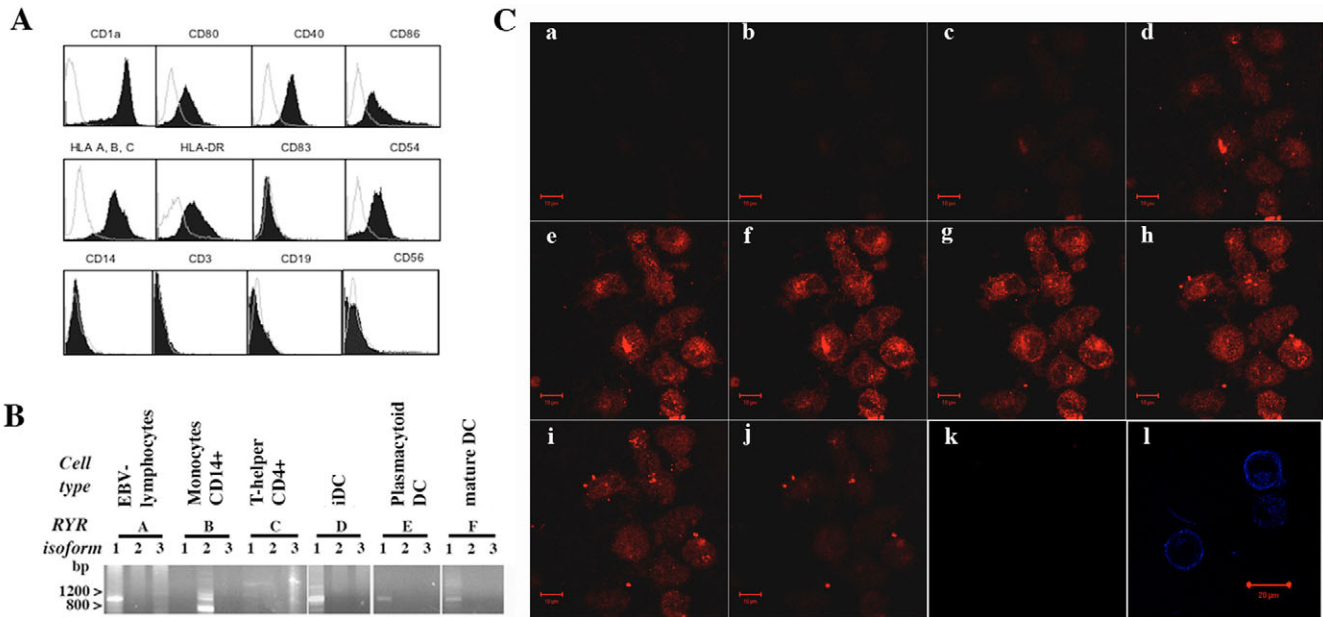


Fig. 1. Expression of RyR in human DCs. Peripheral blood monocytes were induced to differentiate into iDCs by 5-day culture in IL4 and GM-CSF. (A) Cells were then washed and incubated in the presence of fluorochrome-labeled monoclonal antibodies (mAbs) recognizing the indicated surface markers. Specific fluorescence (full histograms) was evaluated by taking advantage of a FACSCalibur flow cytometer equipped with Cell Quest software (Becton Dickinson) using, as negative controls, isotype-matched irrelevant reagents (empty histograms). One representative experiment out of five is shown. (B) Total RNA was extracted from immature (iDCs), LPS-matured (mature DCs) and from other cell types, and the expression of genes encoding the different RYR isoforms was evaluated by RT-PCR. RNA from EBV-transformed lymphocytes was used as control for RYR1 isoform gene expression. (C) Immunofluorescence analysis of iDCs. Cells were stained with goat anti-RyR polyclonal Ab followed by Alexa Fluor-555-conjugated anti-goat Ab (a-j), Alexa Fluor-555-conjugated anti-goat Ab alone (k) or with allophycocyanine-conjugated anti-CD1a (l). Immunofluorescence analysis on acetone:methanol-fixed iDCs reveals strong perinuclear RyR fluorescence that extends into the endoplasmic reticulum network. Panels a-j show 1 μ m optical slices from the bottom upwards; bar, 10 μ m. Images were acquired with a 100 \times Plan Neofluar oil immersion objective (NA 1.3) mounted on a Zeiss Axiovert 100 confocal microscope. Panel l: paraformaldehyde fixed DCs display typical plasma membrane fluorescence for the CD1a marker (bar, 20 μ m).

to the rapid release of the proinflammatory cytokine IL1B. Furthermore, cells from patients with the malignant hyperthermia susceptible phenotype, a pharmacogenetic hypermetabolic disease caused by *RYR1* mutations (Treves et al., 2005), released more proinflammatory cytokines than cells from controls, indicating that one of the downstream effects of human RyR1 activation is coupled to cytokine release (Girard et al., 2001). In the present study we investigated the effects of pharmacological activation of RyR1 in human DCs. Our results show that treatment of iDCs with RyR1 agonists is accompanied by an increase in the intracellular calcium concentration. Furthermore, treatment of iDCs with a suboptimal concentration of bacterial lipopolysaccharide (LPS) in the presence of RyR1 agonists induces activation of cytokine transcription and upregulation of surface markers that are typically associated with cell maturation as well as with an increased capacity to stimulate allospecific T-cells. These effects are specifically associated with RyR1 activation as they could be blocked by pretreatment with the RyR1 antagonist dantrolene (Zhao et al., 2001) and could not be induced by addition of ATP, an agonist releasing calcium through IP₃ mobilization (Ralevic and Burnstock, 1998; Schnurr et al., 2004). These results provide for the first time evidence for the involvement of RyR1 in DC maturation and indicate a functional cooperation between RyR1-mediated and Toll-like receptor-mediated intracellular signaling.

Results

Fig. 1A shows that peripheral blood monocytes cultured for 5 days in the presence of GM-CSF and IL4 differentiate into iDCs (Sallusto and Lanzavecchia, 1994). These cells display a typical immature phenotype in as much as they express the surface markers CD1a, CD80, CD40, CD86 and CD54 and are negative for CD83 (maturation marker) and CD14 (monocyte marker). Furthermore, no positivity for CD3 (T-lymphocytes), CD19 (B-lymphocyte marker) and CD56 (NK cell marker) could be detected. Immature CD1a-positive DCs can be matured by treatment with Toll-like receptor agonists, including bacterial LPS (Sallusto et al., 1998). Fig. 1B shows that, irrespective of their degree of maturation, DCs express the gene encoding the skeletal muscle RyR1 but not the other isoforms. This transcript is not expressed by other peripheral blood leukocyte populations such as monocytes (which express the RyR2 isoform transcript) and T-lymphocytes (Fig. 1B), but is expressed by plasmacytoid DCs, which are natural circulating DCs isolated from peripheral blood as opposed to cells obtained upon in vitro culture. Immunofluorescence analysis shows that the intracellular distribution of the RyR1 in in vitro-derived CD1a-positive DCs is concentrated in a reticulum extending from the perinuclear area towards the plasma membrane. Confocal analysis of 1 μ m optical slices shows no surface fluorescence, confirming that the RyR1 is expressed in intracellular membrane compartments, most likely the endoplasmic reticulum (Fig. 1C).

Single-cell intracellular Ca^{2+} measurements on fura-2-loaded iDCs show that addition of 10 mM caffeine leads to a rapid and transient increase in the $[\text{Ca}^{2+}]_i$ (Fig. 2A). Data presented in Fig. 2B confirm that the RyR1 can also be activated pharmacologically with specific agonists such as caffeine and 4-chloro-m-cresol (Zucchi and Ronca-Testoni, 1997) as well as by KCl. The addition of 100 μM ATP, which induces Ca^{2+} release through InsP_3 receptor activation in many cell types (Ralevic and Burnstock, 1998; Schnurr et al., 2004), was also accompanied by an increase in $[\text{Ca}^{2+}]_i$ in iDCs (Fig. 2C). Interestingly, the peak amplitude induced by ATP was significantly larger than that observed after RyR1 activation (compare Fig. 2B and Fig. 2D; $P < 0.00001$). These results unequivocally demonstrate that increases in intracellular $[\text{Ca}^{2+}]_i$ in human iDCs can be stimulated both by InsP_3 mobilizing agonists as well as by RyR1 activators. We next investigated whether the Ca^{2+} released through RyR1 activation plays a specific function in DC maturation.

Immature DCs generated by culturing peripheral blood monocytes for 5 days in the presence of IL4 and GM-CSF were induced to mature by 18 hours of incubation with increasing concentrations of LPS (from 1 ng/ml to 1 $\mu\text{g}/\text{ml}$) in the

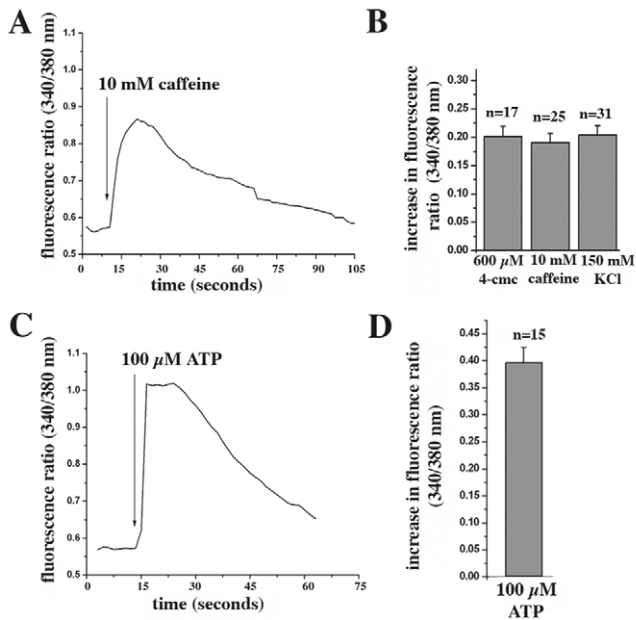


Fig. 2. Single-cell intracellular calcium imaging on iDCs. (A,C) Single-cell intracellular calcium measurements in fura-2-loaded iDCs obtained after 5 days of culture. The traces show changes in fura-2 fluorescence ratio (340/380 nm) in a single iDC after addition of caffeine or ATP. Experiments were performed in Krebs-Ringer containing 1 mM Ca^{2+} . (B,D) Average peak increases in fluorescence ratio induced by the addition of the indicated agonists to fura-2-loaded iDCs. Results represent the mean Δ increase in fluorescence (calculated by subtracting the peak fluorescent ratio from the resting fluorescent ratio) obtained after addition of 600 μM 4-chloro-m-cresol, 10 mM caffeine or 150 mM KCl (B) or 100 μM ATP (D). No difference was found in the peak Ca^{2+} in response to RyR activation ($P = 0.820$), but the amount of Ca^{2+} released by 100 μM ATP was significantly higher ($P < 0.00001$). Results represent the mean (\pm s.e.m.) Δ increase in fluorescence in DCs isolated from four different donors.

presence of 10 mM caffeine. The expression of genes associated with DC maturation and their capacity for stimulating T-cell responses was then evaluated. Fig. 3 shows the results obtained in a typical experiment representative of data obtained with four different donors. Low (sub-optimal) concentrations (1 ng/ml) of LPS only slightly activated the transcription of the genes under investigation, whereas the addition of an optimal LPS concentration (1 $\mu\text{g}/\text{ml}$) strongly stimulated the transcription of genes encoding the maturation marker CD83 and $\text{IFN}\alpha$, IL12B and IL23A, cytokines that are associated with a high capacity of stimulating T-cell responses. Importantly, costimulation of DCs for 18 hours with 10 mM caffeine plus 1 ng/ml LPS stimulated transcription of all the genes under investigation to extents similar to those obtained using a 1000-fold higher concentration of LPS alone. The involvement of RyR1 activation is supported by the fact that pretreatment of cells with the RyR1 antagonist dantrolene followed by the addition of caffeine and LPS inhibited the synergistic effects of caffeine and LPS on gene expression (Fig. 3A). Quantitatively and qualitatively similar results were obtained when iDCs were treated with 4-chloro-m-cresol and LPS, but in some cases the presence of the latter RyR1 agonist was accompanied by apoptosis, resulting in more variable results (data not shown). Fig. 3B shows that in human DCs Ca^{2+} release mediated by the activation of the InsP_3 -signaling pathway induced by 100 μM ATP in the presence of 1 ng/ml LPS could only partially activate DCs, as detected by the expression of the *IL23A* gene, albeit at a fourfold lower extent than that observed upon RyR1 activation. By contrast, it was not potent enough to induce transcription of the genes encoding CD83, IL12B and $\text{IFN}\alpha$. The addition of 10 mM caffeine alone (i.e. in the absence of LPS) caused an increase in *IL23A* gene expression, but did not affect transcription of the other genes under investigation (Fig. 3B, right panel).

Finally, increasing concentrations of caffeine (from 1-10 mM + 1 ng/ml LPS) resulted in a proportional increase of *IL23A* gene transcription, reflecting the calcium-dependent nature of this activation event (Fig. 3C); this result was further confirmed by the observation that addition of 1 μM thapsigargin [an inhibitor of sarcoplasmic and endoplasmic reticulum Ca^{2+} -ATPases (SERCA)] in the presence of 1 ng/ml LPS resulted in the activation of *IL23A* gene transcription (Fig. 3C).

We then examined in more detail the functional consequences of the maturation signals generated by simultaneous RyR1 and Toll-like receptor activation. The capacity of iDCs treated with LPS plus caffeine to stimulate allospecific T-cell proliferation was assayed by measuring [^3H]thymidine incorporation. As shown in Fig. 3D, iDCs are relatively poor allostimulatory cells (white bars) and the low dose of LPS used to activate DCs in this assay (1 ng/ml) was also not so efficient, causing a 1.6-fold increase in T-cell proliferation (grey bars). Incubation of iDCs with 100 μM ATP (which induces a large $[\text{Ca}^{2+}]_i$ transient) plus 1 ng/ml LPS did not significantly improve [^3H]thymidine incorporation by T cells (horizontally lined bars), as compared with LPS treatment alone. However, treatment of iDCs with 10 mM caffeine plus 1 ng/ml LPS provided synergistic signals resulting in a twofold increase in [^3H]thymidine incorporation in T cells (hatched bars). This effect was specific as it could be blocked by inhibiting RyR1-mediated Ca^{2+} signaling by pretreating iDCs

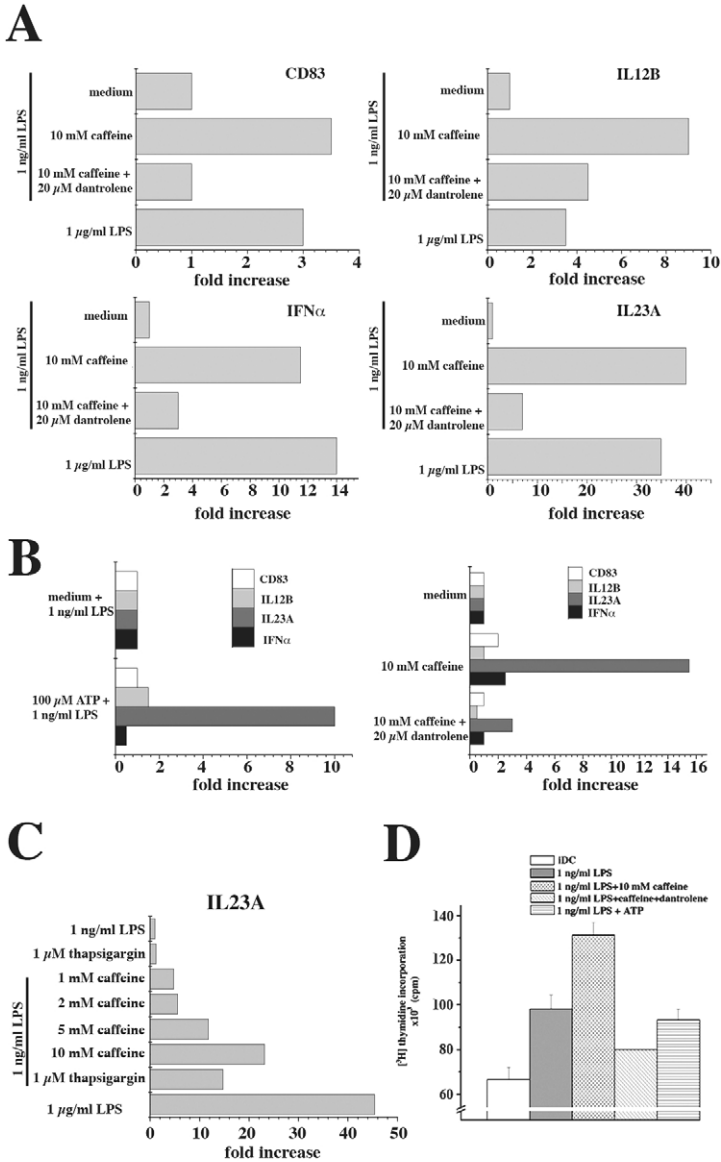


Fig. 3. RyR activation induces transcription of genes involved in DC maturation and potentiates allospecific T-cell stimulation. (A) In vitro-derived iDCs were cultured for 18 hours in the presence of the indicated concentrations of LPS and with 10 mM caffeine and 20 μM dantrolene, as indicated. Total RNA was extracted and *CD83*, *IFNα*, *IL12B* and *IL23A* gene expression was evaluated by quantitative real-time PCR. Gene expression results are expressed as fold-increase as compared with values obtained in iDCs treated with medium + 1 ng/ml LPS. One representative experiment out of four is shown. (B) Experiment as in A except that in vitro-derived iDCs were cultured for 18 hours in the presence of 1 ng/ml LPS + 100 μM ATP (left panel) or in the presence of 10 mM caffeine and 20 μM dantrolene, as indicated (right panel). Gene expression results are expressed as fold-increase as compared with values obtained in iDCs treated with medium + 1 ng/ml LPS (left panel; ATP experiments) or as fold-increase as compared with values obtained in iDCs treated with medium alone (right panel). One representative experiment out of four is shown. (C) Experiment as in A except that in vitro-derived iDCs were cultured for 18 hours in the presence of 1 μM thapsigargin, or the indicated concentration of caffeine or 1 μM thapsigargin + 1 ng/ml LPS. Total RNA was extracted and *IL23A* gene expression was evaluated by quantitative real-time PCR. One representative experiment out of four is shown. (D) Immature DCs were harvested on day 5 of differentiation and stimulated with 1 ng/ml LPS (grey box), with 10 mM caffeine + 1 ng/ml LPS (hatched box), with 20 μM dantrolene + 10 mM caffeine + 1 ng/ml LPS (diagonal lines) or with 100 μM ATP + 1 ng/ml LPS (horizontal lines), or left untreated (empty box). DCs were then washed and added to allogenic PBMC at a ratio of 10:1 for 5 days. [³H] thymidine was then added and cells were cultured for another day. The bars indicate the mean value of c.p.m. (± s.e.m.) from triplicate samples from one donor. The experiment was repeated with similar results at least four times with different donors.

with 20 μM dantrolene, prior to the addition of 10 mM caffeine and 1 ng/ml LPS (diagonally lined bars). Taken together, these results suggest that the signals generated in human DCs through Toll-like receptors (by the addition of LPS) and by RyR1 activation are different, and that their combined activation results in synergistic effects.

Although RyR1 can be pharmacologically activated by a variety of agonists, how its activation occurs in iDCs in vivo remains puzzling. We were intrigued by the finding that the addition of KCl causes a rise in the $[Ca^{2+}]_i$ in iDCs and reasoned that this may have physiological relevance. In fact, cells dying in the vicinity of iDCs in a restricted microenvironment such as an inflamed tissue could release their intracellular K^+ into the extracellular milieu, thereby providing the necessary costimulating signal(s) to iDCs residing in neighboring areas. In order to verify our hypothesis, we set up a series of experiments; first we tested whether the effects of caffeine on DC maturation could be monitored by flow cytometry, by following the surface expression of CD83,

a good phenotypic indicator of DC maturation (Zhou and Tedder, 1996; Lachmann et al., 2002). Fig. 4A shows that as early as 4 hours after stimulation 1 μg/ml LPS induced significant surface expression of CD83; this incubation time was chosen for all subsequent experiments and the results obtained by adding different stimuli were compared with those obtained by treating cells with 1 μg/ml LPS, which was set at 100% induction of CD83 expression. Fig. 4A shows that addition of 10 mM caffeine alone, 100 μM ATP plus 1 ng/ml LPS, or pretreatment of cells with 20 μM dantrolene followed by the addition of 10 mM caffeine plus 1 ng/ml LPS did not result in significant induction of CD83 expression. Pretreatment of DCs with 20 μM dantrolene did not affect the induction of CD83 surface expression stimulated by 1 μg/ml LPS. However, the addition of 10 mM caffeine plus 1 ng/ml LPS caused a significant induction of CD83 surface expression ($P < 0.001$; Student's *t*-test).

We followed the same protocol to verify whether the hypothesis that KCl or the content of necrotic cells could

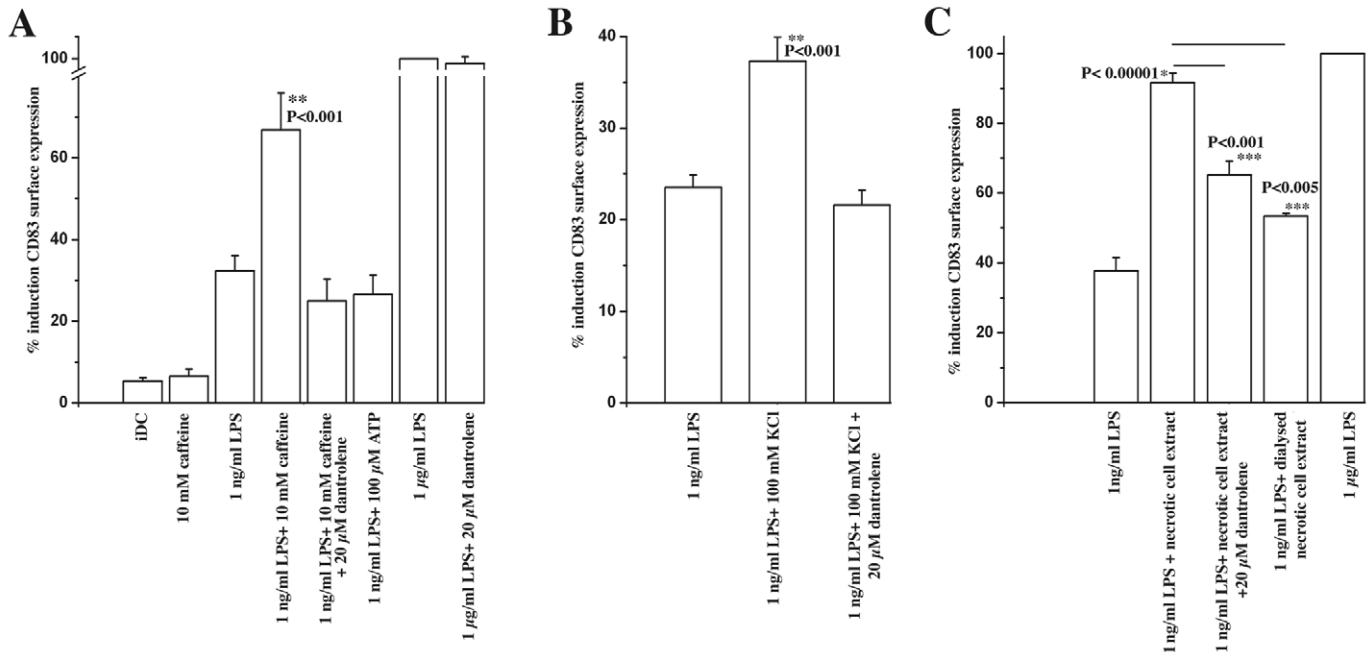


Fig. 4. Incubation of iDCs with KCl or soluble extracts from necrotic cells promotes surface expression of CD83. iDCs were treated for 4 hours as indicated and the percent positive CD83 cells was determined by flow cytometry. (A) Stimulation with 10 mM caffeine alone or 100 μM ATP + 1 ng/ml LPS did not significantly increase CD83 surface expression; incubation with 10 mM caffeine + 1 ng/ml LPS significantly increased CD83 surface expression ($P<0.001$). This effect was blocked by pretreatment with 20 μM dantrolene. (B) When KCl was added, cells were incubated with Krebs-Ringer saline (in which the NaCl had been substituted for KCl) for 30 minutes at 37°C; they were then centrifuged, and fresh medium containing 1 ng/ml LPS was added and cells were incubated at 37°C for 4 hours. (C) For experiments in which iDCs were incubated with the supernatant from necrotic HEK293 cells, extracts were prepared as described in the Materials and methods section and either used directly (+ necrotic cell extract ± 20 μM dantrolene) or dialysed overnight against 1×PBS (dialysed necrotic cell extract). Results are expressed as mean (± s.e.m.) percentage induction of CD83 surface expression of at least three experiments performed on iDCs purified from blood of different donors; values obtained by treating iDCs with 1 μg/ml LPS was considered 100%. * P and ** P , significant difference in the treated population compared with iDCs treated with 1 ng/ml. *** P , significant difference from iDCs treated with 1 ng/ml LPS + necrotic cell extracts.

mimic the synergistic effects of caffeine on iDC maturation. Immature DCs were incubated with Krebs-Ringer in which NaCl was substituted for KCl (in order to maintain the osmolarity), plus 1 ng/ml LPS for 30 minutes at 37°C; the medium was then replaced by differentiation medium containing 1 ng/ml LPS and the cells were incubated for 4 hours. The KCl-washout step was necessary as iDCs were sensitive to prolonged exposure to KCl. As shown in Fig. 4B, the addition of KCl and sub-optimal LPS (1 ng/ml) to iDCs promoted surface expression of CD83, which could be inhibited by pretreatment with 20 μM dantrolene. Fig. 4C shows that the addition of filtered soluble extracts from necrotic HEK293 cells in the presence of 1 ng/ml LPS caused a significant number of cells to express surface CD83; this stimulation of CD83 surface expression was significantly decreased by preincubation with 20 μM dantrolene ($P<0.0001$), or by dialysis of the filtered extracts ($P<0.005$). In the former cases, however, some induction of CD83 expression was still present, indicating that other factors promoting iDC maturation independently of RyR activation are also released from dying cells.

In order to dissect the intracellular pathways involved in Toll-like receptor and RyR activation, we examined (1) the effects of LPS and caffeine on the translocation of p65 (RelA, a component of the NF-κB complex) to the nucleus and (2) the

sensitivity of DC maturation to cyclosporine A, which would suggest the involvement of the Ca^{2+} /calmodulin phosphatase, calcineurin. Fig. 5A (top panels) shows that in untreated iDCs and in cells treated for 5 minutes with 10 mM caffeine and/or 1 ng/ml LPS, p65 was mainly distributed in the cytoplasm; however, incubation with 1 μg/ml LPS for 60 minutes caused its nuclear translocation in a large number of cells (Fig. 5A, bottom panel, arrowheads). Caffeine stimulation of iDCs evokes a low-amplitude calcium signal (Fig. 2), and this low-amplitude calcium signal alone or in combination with 1 ng/ml LPS is not sufficient to activate the nuclear translocation of NF-κB. These results support the hypothesis that some intracellular signals generated by LPS-mediated activation of Toll-like receptors in DCs are led by NF-κB-dependent events, whereas caffeine-activated pathways are NF-κB independent.

We next investigated whether the caffeine low-amplitude calcium signal is sufficient to activate an alternative signaling pathway, namely Ca^{2+} /calmodulin-dependent phosphatase calcineurin. We probed the effect of caffeine on maturation of iDCs by using the calcineurin pathway inhibitors cyclosporine A (Barford, 1996) and deltamethrin (Enan and Matsumara, 1992). Fig. 5B shows that the synergistic effects of 1 ng/ml LPS and 10 mM caffeine (light-grey bars) on maturation of iDCs could be completely abrogated by pretreatment of iDCs with 2 μM cyclosporine A and 10 μM deltamethrin. These

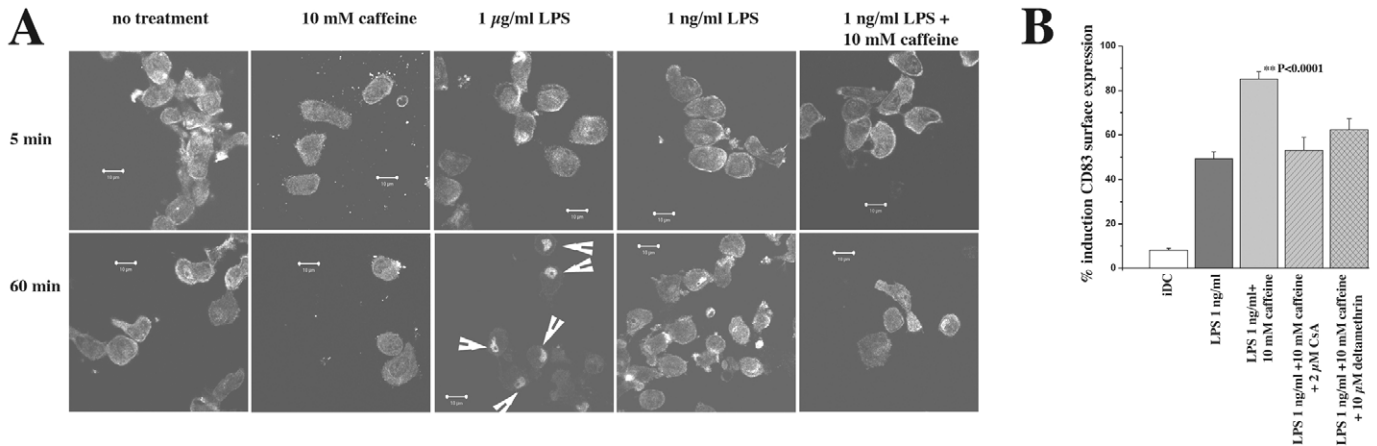


Fig. 5. LPS but not caffeine induces nuclear translocation of NF- κ B, whereas caffeine-induced maturation is sensitive to cyclosporine A (CsA). iDCs were left untreated or stimulated for 5 or 60 minutes at 37°C, as indicated. Cells were allowed to stick to poly-L-lysine-treated coverslips and permeabilized with acetone:methanol. Cells were incubated with rabbit anti-p65 polyclonal antibodies (Ab), followed by Alexa Fluor-488-labeled secondary Ab and visualized with a confocal microscope as indicated in the Materials and Methods section. Arrowheads indicate nuclear fluorescence. Images were acquired with a 100 \times Plan Neofluar oil immersion objective (NA 1.3) mounted on a Zeiss Axiovert 100 confocal microscope. Horizontal bar, 10 μ m. Arrowheads point to nuclear translocation of p65. (B) Surface expression of CD83 in unstimulated iDCs (empty bars) or iDCs stimulated with 1 ng/ml LPS (dark-grey bars) \pm 10 mM caffeine (light-grey bars) or pretreated with 2 μ M CsA for 30 minutes and then with 10 mM caffeine + 1 ng/ml LPS (slashed grey bars), or pretreated with 10 μ M deltamethrin for 30 minutes and then with 10 mM caffeine + 1 ng/ml LPS (hatched grey bars). Results are expressed as percent (mean \pm s.e.m.; $n=3$) induction of CD83 surface expression: 100% was the value obtained by stimulating cells with 1 μ g/ml LPS for 4 hours. ** P , significant difference in the treated population compared with iDCs treated with 1 ng/ml.

results are consistent with the idea that in addition to NF- κ B the Ca²⁺-calcineurin-sensitive signaling pathway is also involved in the maturation of human DCs.

Discussion

The present study shows that activation of RyR1 in iDCs generates, through a calcineurin-sensitive pathway, a costimulatory signal that enhances the sensitivity of iDCs to bacterial stimuli, leading to their maturation. These effects are unveiled when subthreshold concentrations of LPS are used. DCs express both IP₃R and RyR1 intracellular Ca²⁺ channels (Hosoi et al., 2001; Stolk et al., 2006; Goth et al., 2006) and the involvement of Ca²⁺-dependent signaling events in their activation has been clearly established. In fact, (1) treatment of human iDCs with the Ca²⁺ ionophore A23187 induces upregulation of major histocompatibility complex (MHC) and costimulatory molecules and CD83 expression (Czerniecki et al., 1997) and activates the transcription of *IL23A* (this study), and (2) promotes T-cell activation (Faries et al., 2001). Moreover, (3) treatment of mature human DCs with ionomycin triggers release of pro-IL-1 β (Gardella et al., 2001).

As to the types of intracellular Ca²⁺-release channels involved in DC activation and/or maturation, Stolk et al. recently showed the RyRs are not indispensable because bone marrow precursors obtained from the liver of RyR1 knockout (KO) mice injected into sublethally irradiated congenic hosts could still be induced to differentiate and mature into normal DCs (Stolk et al., 2006). Notably, however, the Ca²⁺ signaling machinery possesses a vast array of toolkit components, which can be mixed and matched to deliver Ca²⁺ signals (Berridge et al., 2003). Thus, one can assume that in the DC precursors obtained from (lethal) RyR1 KO mice other molecules involved in intracellular Ca²⁺ signaling are compensating for

the depletion of RyR1. Clearly, under physiological conditions RyR1 activation, together with signals generated through triggering of Toll-like receptors, generates costimulatory signals involved in the maturation of human DCs.

An interesting observation arising from this study is that addition of KCl to iDCs is accompanied by a rapid and transient increase in [Ca²⁺]_i. In skeletal muscle, depolarization of the plasma membrane is sensed by an L-type Ca²⁺ channel, which undergoes a conformational change allowing it to interact directly with the RyR, thereby activating Ca²⁺ release from the sarcoplasmic reticulum (Sutko and Airey, 1996; Franzini-Armstrong and Protasi, 1997). Although DCs are not electrically excitable, one can envisage that massive release of KCl from cells dying in the vicinity of DCs may activate sensitive channels present on the plasma membrane coupled to the RyR1, thereby leading to RyR1 activation and thus Ca²⁺ release. Such a conclusion is supported by two sets of data: (1) the demonstration that treatment of iDCs with KCl promotes surface expression of CD83, which can be antagonized by dantrolene, and (2) the fact that incubation of iDCs with filtered soluble extracts, but not dialysed extracts, from necrotic cells promoted surface expression of CD83 that could partially be prevented by the addition of dantrolene. Similar results were reported by Sauter et al. (Sauter et al., 2000), who showed that incubation of iDCs with extracts from necrotic cells, but not apoptotic cells, induces DC maturation. Clearly, some of the signals generated by necrotic cells are capable of activating the iDC RyR, providing maturation stimuli. Based on these results, we propose that the intracellular contents released from dying cells in the vicinity of iDCs provide RyR1-dependent costimulatory signal(s), leading to full maturation of DCs even in the presence of suboptimal concentrations of bacterial stimuli. A schematic representation of our hypothesis concerning the signals

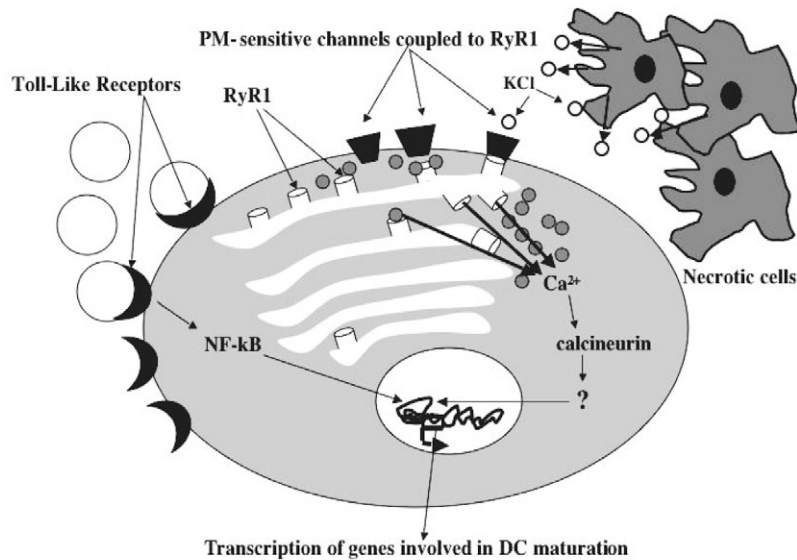


Fig. 6. Cartoon depicting signaling pathways involved in DC maturation. In the presence of sub-optimal Toll-like receptor ligand, the signal(s) generated from cells dying in the vicinity of iDCs bind to receptors that are coupled to the RyR1, activating calcium release. This intracellular pathway leading to DC maturation through RyR1 activation is dependent upon the activity of calcineurin as it could be blocked by cyclosporine A and deltamethrin. PM, plasma membrane.

underlying RyR1 activation and their involvement in the event leading to iDC maturation is illustrated in Fig. 6.

As to the involvement of specific transcription factors in DC maturation and function, NF- κ B has been shown to play a role in the regulation of transcription of several genes, including those encoding *IL1A* and *IL1B*, *IL6*, *IL8*, *IL12B*, *TNF α* and *IFN γ* and *CD86* (Ghosh et al., 1998; Grohmann et al., 1998; Lee et al., 1999). Under resting conditions NF- κ B forms an inactive complex (NF- κ B1+RelA+I κ B) detectable in the cytoplasm, which upon activation translocates to the nucleus where it binds to specific promoter sequences and functions as a transcriptional activator. Although it is well-established that the activation of Toll-like receptors by LPS induces nuclear translocation of NF- κ B (Ghosh et al., 1998; Lee et al., 1999) (and this study), this does not occur with caffeine, suggesting the involvement of other (Ca^{2+} -dependent) transcriptional regulators. In a previous study we showed that RyR1 activation in human myotubes leads to cyclosporine-A-sensitive IL6 release (Duceux et al., 2004). In DCs, the effects of cyclosporine A are controversial: one report suggests that pretreatment with cyclosporine A increases maturation and CD80 expression (Ciesek et al., 2005), whereas others report that cyclosporine A inhibits IL12 production and upregulation of costimulatory molecules induced by LPS (Lee et al., 1999; Tajima et al., 2003). Our results support and extend the latter conclusion. The synergistic effects of caffeine on LPS-induced maturation are sensitive to cyclosporine A and deltamethrin, implying the involvement of calcineurin (Barford, 1996; Enan and Matsumara, 1992) in RyR1-induced maturation of DCs. In addition, our data demonstrate that the low-amplitude calcium signal mediated by RyR synergizes with LPS in inducing DC maturation, whereas the large Ca^{2+} transient induced by ATP does not promote the expression of genes associated with DC maturation. On the basis of these data, one may postulate that amplitude modulation of the Ca^{2+} signal is a mechanism contributing to the maturation of DCs. A similar control by amplitude modulation of the Ca^{2+} signal has been proposed to play an important role in B-lymphocyte signaling (Dolmetsch et al., 1997). High LPS concentrations may engage a sufficient number of Toll-like receptors, and thereby the cooperation of

additional signaling pathways is not required to fully activate DCs. The model emerging from our data indicates that NF- κ B and calcineurin signaling pathways may ultimately converge to regulate the transcription of a set of genes involved in DC maturation. A similar complex regulatory mechanism has been reported for the transcription of the *IL4* gene in T cells, which is under the control of several transcription factors, including NF- κ B, NF-AT and NF-IL6 (Li-Weber et al., 2004).

Finally, on a lighter note, based on these findings one may envisage that by drinking caffeine-containing beverages containing up to 85 mg/150 ml caffeine (Barone and Roberts, 1996) (i.e. 3 mM), iDCs residing in the gut may be exposed to concentrations of caffeine sufficient to activate them, especially in the presence of low levels of bacterial derivatives (Iwasaki and Kelsall, 1999), thereby enhancing their antigen-presenting capacity. Thus, relatively small amounts of antigens may be sufficient to induce effective T-cell responses and protection against enteric infections.

Materials and Methods

DC generation and stimulation

iDCs were generated from human peripheral blood mononuclear cells (PBMC) as previously described (Schnurr et al., 2004). Briefly, monocytes were purified by positive sorting using anti-CD14-conjugated magnetic microbeads (Miltenyi Biotec, Bergisch Gladbach, Germany). The recovered cells (95–98% purity) were cultured for 5 days at 3×10^5 /ml in differentiation medium containing: RPMI, 10% FCS glutamine, non-essential amino acids and antibiotics (all from Invitrogen, Basel, Switzerland), supplemented with 50 ng/ml GM-CSF (Laboratory Pablo Cassarà, Buenos Aires, Argentina) and 1000 U/ml IL4 (a gift from A. Lanzavecchia, Institute for Research in Biomedicine, Bellinzona, Switzerland). Maturation was induced by an 18-hour culture, unless otherwise stated, in the presence of the Toll-like receptor-4 agonist LPS (from *Salmonella abortus equi*; Sigma Chemicals, St Louis, MO) at the doses indicated in the different experiments. The phenotype of the cells was evaluated prior to and after maturation by flow cytometry. Briefly, cells were washed and resuspended in phosphate-buffered saline (PBS). They were then incubated for 30 minutes at 4°C in the presence of 1:20 dilutions of fluorochrome-labeled commercial monoclonal antibodies recognizing the following surface markers: CD1a, CD14, CD40, CD80, CD86, CD83, CD54, HLA-ABC, HLA-DR, CD3, CD19 and CD56, or isotype-matched controls (BD Pharmingen, Basel, Switzerland). After two washes, specific fluorescence was evaluated by flow cytometry, by using a FACSCalibur instrument equipped with Cell Quest software (Becton Dickinson, San José, CA). Plasmacytoid DCs were magnetically isolated from peripheral blood using BDCA-2 DC isolation kits (Miltenyi Biotec, Bergisch Gladbach, Germany) according to the manufacturer's instructions. The number and viability of DCs was determined by trypan blue exclusion and purity was assessed by flow cytometry. For functional experiments, in vitro-derived iDCs were cultured

in the presence of the indicated concentration of LPS \pm 10 mM caffeine \pm 20 μ M dantrolene or a standard, optimal concentration of LPS (1 μ g/ml) as control for the indicated time period. In some experiments, iDCs were stimulated with 100 μ M ATP as indicated or with 100 mM KCl plus 1 ng/ml LPS for 30 minutes, followed by removal of KCl and addition of differentiation medium containing 1 ng/ml LPS for 4 hours. When the latter protocol was applied, NaCl was substituted for KCl in order to maintain osmolarity of the medium. For experiments in which iDCs were incubated with the supernatant of necrotic cells, experiments were performed essentially as described by Sauter et al. (Sauter et al., 2002); briefly, 6×10^6 HEK293 cells were rinsed twice with PBS, resuspended in 3 ml PBS and subjected to five cycles of freeze-thawing. Viability was assessed by trypan blue exclusion and was $>95\%$. Cells were centrifuged, the resulting supernatant was filtered through a 0.2 μ m Millipore filter and one half was added to iDC cultures (0.8×10^6 cells) in 1 ml differentiation medium plus a final concentration of 1 ng/ml LPS; the other half was added to iDCs that had been pretreated with 20 μ M dantrolene for 30 minutes and then processed as described above. Cells were incubated for 4 hours at 37°C. For experiments in which iDCs were incubated with the dialysed supernatant of necrotic cells, experiments were performed as described above, except that the supernatants were dialysed overnight against 1 \times PBS, filtered and then added to iDCs.

Ryanodine receptor isoform expression

Total RNA was isolated from leukocyte populations and reverse transcribed into cDNA as previously described (Girard et al., 2001). The expression of genes encoding ryanodine receptor isoforms was investigated by PCR analysis using previously reported specific primers and conditions (Hosoi et al., 2001).

Immunofluorescence analysis and single-cell intracellular Ca²⁺ measurements

Immunofluorescence analysis was performed on paraformaldehyde-fixed DCs using allophycocyanine-conjugated anti-CD1a (BD Pharmingen), or on acetone:methanol (1:1)-fixed iDCs, using a goat anti-RyR raised against the NH₂-terminus and recognizing the three RyR isoforms (Santa Cruz Biotech), followed by Alexa Fluor-555-conjugated donkey anti-goat antibodies (Molecular Probes) or rabbit anti-NF- κ B (sc-109; Santa Cruz Biotech), followed by Alexa Fluor-488-conjugated chicken anti-rabbit antibodies (Molecular Probes), as previously described (Duceux et al., 2004). Fluorescence was visualized using a 100 \times Plan Neofluar oil immersion objective (NA 1.3) mounted on a Zeiss Axiovert 100 confocal microscope.

Single-cell intracellular calcium measurements were performed on fura-2-loaded iDCs attached to poly-L-lysine-treated glass coverslips mounted onto a 37°C thermostated chamber that was continuously perfused with Krebs-Ringer medium containing 1 mM CaCl₂. Individual cells were stimulated with the indicated agonist in Krebs-Ringer (plus 1 mM CaCl₂) by way of a 12-way 100 mm diameter quartz micromanifold computer-controlled microperfuser (ALA Scientific, Westbury, NY), as previously described (Duceux et al., 2004). Online (340 nm, 380 nm and ratio) measurements were recorded using a fluorescent Axiovert S100 TV inverted microscope (Carl Zeiss, Jena, Germany) equipped with a 40 \times oil immersion Plan Neofluar objective (0.17 NA), filters (BP 340/380, FT 425, BP 500/530) and attached to a Hamamatsu multiformat CCD camera. The cells were analyzed using an Openlab imaging system and the average pixel value for each cell was measured at excitation wavelengths of 340 and 380 nm, as previously described (Duceux et al., 2004).

Quantitative gene expression analysis

Eighteen hours after stimulation, total RNA was extracted from DCs (Qiagen, Basel, Switzerland) and treated with Deoxyribonuclease I (DNase I) (Invitrogen, Carlsbad, CA) to eliminate contaminant genomic DNA. After reverse transcription using the Moloney Murine Leukemia Virus Reverse Transcriptase (M-MLV RT) (Invitrogen), cDNA was amplified by quantitative real-time PCR in the ABI PrismTM 7700 using the TaqMan[®] technology. Commercially available exon-intron junction-designed primers for GAPDH, CD83, IFN α , IL12B and IL23A (Applied Biosystems, Foster City, CA) were used. Gene expression was normalized using self-GAPDH as reference.

Allostimulatory properties of DCs

Allostimulatory capacity of DCs treated with different concentrations of LPS alone or with 100 μ M ATP, 10 mM caffeine plus or minus 20 μ M dantrolene, was assayed by standard mixed lymphocyte reaction (MLR) tests by culturing cells in the presence of allogenic PBMC in RPMI medium supplemented with 5% pooled human serum at a 10:1 ratio (Mohty et al., 2002). Lymphocyte proliferation was evaluated by [³H]-thymidine incorporation.

Activation of intracellular signaling pathways

NF- κ B translocation was monitored by indirect immunofluorescence on DCs treated with LPS and/or caffeine (10 mM) as indicated, for 5 or 60 minutes at 37°C. Cells were fixed with acetone:methanol and processed as described above for RyR immunofluorescence, using rabbit anti-NF- κ B [anti-p65 (RelA) polyclonal antibodies; Santa Cruz Biotech], followed by Alexa Fluor-488-conjugated chicken anti-rabbit antibodies (Molecular Probes).

Involvement of the calcium/calmodulin-dependent calcineurin signaling pathway

was determined by studying the sensitivity of CD83 surface expression to cyclosporine A or deltamethrin. Briefly, iDCs were pretreated with carrier, cyclosporine A (2 μ M) (Sigma Chemicals) or deltamethrin (10 μ M) (Fluka Chemicals, Buchs, Switzerland) for 30 minutes, followed by incubation for 4 hours with 1 μ g/ml LPS or sub-optimal concentrations of LPS in the presence or absence of 10 mM caffeine. Cells were harvested and surface expression of CD83 was investigated by flow cytometry using FITC-labeled anti-CD83 monoclonal antibodies (BD Pharmingen).

Statistical analysis and software programs

Statistical analysis was performed using the Student's *t*-test for unpaired samples; means were considered statistically significant when the *P* value was <0.05 . The Origin computer program (Microcal Software, Northampton, MA) was used to generate graphs and for statistical analysis; figures were assembled using Adobe Photoshop.

This work was supported by the Departments of Anesthesia and Surgery of the Basel University Hospital, by grants 3200-067820.02, 3200B0-114597, 3200B0-04060/1 of the SNF and grants from the Swiss Muscle Foundation and Association Française Contre les Myopathies. We also wish to thank Chantal Feder-Mengus for her support in performing real-time PCR.

References

- Banchereau, J. and Steinman, R. M. (1998). Dendritic cells and the control of immunity. *Nature* **392**, 245-252.
- Barford, D. (1996). Molecular mechanisms of the protein serine/threonine phosphatases. *Trends Biochem. Sci.* **21**, 407-412.
- Barone, J. J. and Roberts, H. R. (1996). Caffeine consumption. *Food Chem. Toxicol.* **34**, 119-129.
- Berridge, M., Bootman, M. D. and Roderick, H. L. (2003). Calcium signalling: dynamics, homeostasis and remodelling. *Nat. Rev. Mol. Cell Biol.* **4**, 517-529.
- Bers, D. M. (2004). Macromolecular complexes regulating cardiac ryanodine receptor function. *J. Mol. Cell. Cardiol.* **37**, 417-429.
- Ciesek, S., Ringe, B. P., Strassburg, C. P., Klempnauer, J., Manns, M. P., Wedemeyer, H. and Becker, T. (2005). Effects of cyclosporine on human dendritic cell subsets. *Transplant. Proc.* **27**, 20-24.
- Czerniecki, B. J., Carter, C., Rivoltini, L., Koski, G. K. H., Kim, I., Weng, D. E., Roros, J. G., Hijazi, Y. M., Xu, S., Rosenberg, S. A. et al. (1997). Calcium ionophore-treated peripheral blood monocytes and dendritic cells rapidly display characteristics of activated dendritic cells. *J. Immunol.* **159**, 3823-3837.
- Dolmetsch, R. E., Lewis, R. S., Goodnow, C. C. and Healey, J. I. (1997). Differential activation of transcription factors induced by Ca²⁺ response amplitude and duration. *Nature* **386**, 856-858.
- Duceux, S., Zorzato, F., Müller, C. R., Sewry, C., Muntoni, F., Quinlivan, R., Restagno, G., Girard, T. and Treves, S. (2004). Effect of ryanodine receptor mutations on interleukin-6 release and intracellular calcium homeostasis in human myotubes from malignant hyperthermia-susceptible individuals and patients affected by central core disease. *J. Biol. Chem.* **279**, 43838-43846.
- Enan, E. and Matsumara, F. (1992). Specific inhibition of calcineurin by type II synthetic pyrethroid insecticides. *Biochem. Pharmacol.* **15**, 1777-1784.
- Faries, M. B., Bedrosian, I., Xu, S., Koski, G., Roros, J. G., Moise, M. A., Nguyen, H. Q., Friederike, H., Engels, H. C., Cohen, P. A. et al. (2001). Calcium signaling inhibits interleukin-12 production and activates CD83(+) dendritic cells that induce Th2 cell development. *Blood* **98**, 2489-2497.
- Franzini-Armstrong, C. and Protasi, F. (1997). Ryanodine receptors of striated muscles: a complex channel capable of multiple interactions. *Physiol. Rev.* **77**, 699-729.
- Gardella, S., Andrei, C., Lotti, L. V., Poggi, A., Torrisi, M. R., Zocchi, M. R. and Rubarteli, A. (2001). CD8(+) T lymphocytes induce polarized exocytosis of secretory lysosomes by dendritic cells with release of interleukin-1beta and cathepsin D. *Blood* **98**, 2152-2159.
- Ghosh, S., May, M. J. and Kopp, E. B. (1998). NF- κ B and Rel proteins: evolutionary conserved mediators of immune responses. *Annu. Rev. Immunol.* **16**, 225-260.
- Girard, T., Cavagna, D., Padovan, E., Spagnoli, G., Urwyler, A., Zorzato, F. and Treves, S. (2001). B-lymphocytes from malignant hyperthermia-susceptible patients have an increased sensitivity to skeletal muscle ryanodine receptor activators. *J. Biol. Chem.* **276**, 48077-48082.
- Goth, S. R., Chu, R. A., Gregg, J. P., Cjerednichenko, G. and Pessah, I. N. (2006). Uncoupling of ATP-mediated calcium signaling and dysregulated interleukin-6 secretion in dendritic cells by nanomolar thimerosal. *Environ. Health Perspect.* **114**, 1083-1091.
- Grohmann, U., Belladonna, M. L., Bianchi, R., Orabona, C., Ayroldi, E., Fioretti, M. C. and Puccetti, P. (1998). IL-12 acts directly on DC to promote nuclear translocation of NF- κ B and primes DC for IL-12 production. *Immunity* **9**, 315-323.
- Iwasaki, A. and Kelsall, B. L. (1999). Mucosal immunity and inflammation. I. Mucosal dendritic cells: their specialized role in initiating T cell responses. *Am. J. Physiol.* **276**, G1074-G1078.
- Hosoi, E., Nishizaki, C., Gallagher, K. L., Wyre, H. W., Matsuo, Y. and Sei, Y. (2001). Expression of the ryanodine receptor isoforms in immune cells. *J. Immunol.* **167**, 4887-4894.

- Koski, G. K., Schwartz, G. N., Weng, D. E., Czerniecki, B. J., Carter, C., Gress, R. E. and Cohen, P. A. (1999). Calcium mobilization in human myeloid cells results in acquisition of individual dendritic cell-like characteristics through discrete signaling pathways. *J. Immunol.* **163**, 82-92.
- Lachmann, M., Berchtold, S., Hauber, J. and Steinkasserer, A. (2002). CD83 on dendritic cells: more than just a marker for maturation. *Trends Immunol.* **23**, 273-275.
- Lee, J., Ganster, R. W., Geller, D. A., Burckart, G. J., Thomson, A. W. and Lu, L. (1999). Cyclosporine A inhibits the expression of co-stimulatory molecules on in vitro-generated dendritic cells. *Transplantation* **68**, 1255-1263.
- Li-Weber, M., Giasi, M., Baumann, S., Palfi, K. and Krammer, P. H. (2004). NF- κ B synergizes with NF-AT and NF-IL6 in activation of the IL-4 gene in T cells. *Eur. J. Immunol.* **34**, 1111-1118.
- McPherson, P. S. and Campbell, K. P. (1993). Characterization of the major brain form of the ryanodine receptor/ Ca^{2+} release channel. *J. Biol. Chem.* **268**, 13765-13768.
- Mohty, M., Isnardon, D., Charbonnier, A., Lafag-Pochitaloff, M., Merlin, M., Sainty, D., Olive, D. and Gaugler, B. (2002). Generation of potent T(h)1 responses from patients with lymphoid malignancies after differentiation of B lymphocytes into dendritic-like cell. *Int. Immunol.* **14**, 741-750.
- O'Connell, P. J., Klyachko, V. A. and Ahern, G. P. (2002). Identification of functional type 1 ryanodine receptors in mouse dendritic cells. *FEBS Lett.* **512**, 67-70.
- Otsu, K., Willard, H. F., Khanna, V. J., Zorzato, F., Green, N. M. and MacLennan, D. H. (1990). Molecular cloning of cDNA encoding the Ca^{2+} release channel (ryanodine receptor) of rabbit cardiac muscle sarcoplasmic reticulum. *J. Biol. Chem.* **265**, 13472-13483.
- Phillips, M., Fujii, J., Khanna, V. K., DeLeon, S., Yokobata, K., de Jong, P. J. and MacLennan, D. H. (1996). The structural organization of the human skeletal muscle ryanodine receptor (RYR1) gene. *Genomics* **34**, 24-41.
- Ralevic, R. and Burnstock, G. (1998). Receptors for purines and pyrimidines. *Pharmacol. Rev.* **50**, 413-455.
- Sallusto, F. and Lanzavecchia, A. (1994). Efficient presentation of soluble antigen by cultured human dendritic cells is maintained by granulocyte/macrophage colony-stimulating factor plus interleukin 4 and downregulated by tumor necrosis factor alpha. *J. Exp. Med.* **179**, 1109-1118.
- Sallusto, F., Schaerli, P., Loetscher, P., Schaniel, C., Lenig, D., Mackay, C. R., Qin, S. and Lanzavecchia, A. (1998). Rapid and coordinated switch in chemokine receptor expression during dendritic cell maturation. *Eur. J. Immunol.* **28**, 2760-2769.
- Samso, M., Wagenknecht, T. and Allen, P. D. (2005). Internal structure and visualization of transmembrane domains of the RyR1 calcium release channel by cryo-EM. *Nat. Struct. Mol. Biol.* **12**, 539-544.
- Sauter, B. B., Albert, M. L., Francisco, L., Larsson, M., Somersan, S. and Bhardwaj, N. (2000). Consequences of cell death: exposure to necrotic tumor cells but not primary tissue cells or apoptotic cells, induces the maturation of immunostimulatory dendritic cells. *J. Exp. Med.* **191**, 423-433.
- Schnurr, M., Shin, A., Hartmann, G., Rothenfusser, S., Soellner, J., Davis, I. D., Cebon, J. and Maraskovsky, E. (2004). Role of adenosine receptors in regulating chemotaxis and cytokine production of plasmacytoid dendritic cells. *Blood* **103**, 1391-1397.
- Sei, Y., Gallagher, K. L. and Basile, A. S. (1999). Skeletal muscle type ryanodine receptor is involved in calcium signaling in human B lymphocytes. *J. Biol. Chem.* **274**, 5995-6002.
- Serysheva, I. I., Hamilton, S. L., Chiu, W. and Ludtke, S. J. (2005). Structure of Ca^{2+} release channel at 14 Å resolution. *J. Mol. Biol.* **21**, 427-431.
- Sorrentino, V., Giannini, G., Malzac, P. and Mattei, M. G. (1993). Localization of a novel ryanodine receptor gene (RYR3) to human chromosome 15q14-q15 by in situ hybridization. *Genomics* **18**, 163-165.
- Stolk, M., Leon-Ponte, M., Merrill, M., Ahern, G. P. and O'Connell, P. J. (2006). IP3Rs are sufficient for dendritic cell Ca^{2+} signaling in the absence of RyR1. *J. Leuk. Biol.* **80**, 651-658.
- Sutko, J. L. and Airey, J. A. (1996). Ryanodine receptor Ca^{2+} release channels: does diversity in form equal diversity in function? *Physiol. Rev.* **76**, 1027-1071.
- Tajima, K., Amakawa, R., Ito, T., Miyaji, M. and Takebayashi, M. (2003). Immunomodulatory effects of cyclosporine A on peripheral blood dendritic cell subsets. *Immunology* **108**, 321-328.
- Takeshima, H., Nishimura, S., Matsumoto, T., Ishida, H., Kangawa, K., Minamino, N., Matsuo, H., Ueda, M., Hanaoka, M., Hirose, T. et al. (1989). Primary structure and expression from complementary DNA of skeletal muscle ryanodine receptor. *Nature* **339**, 439-445.
- Tarroni, P., Rossi, D., Conti, A. and Sorrentino, V. (1997). Expression of the ryanodine receptor type 3 calcium release channel during development and differentiation of mammalian skeletal muscle cells. *J. Biol. Chem.* **272**, 19808-19813.
- Treves, S., Anderson, A. A., Ducreux, S., Divet, A., Bleuven, C., Grasso, C., Paesante, S. and Zorzato, F. (2005). Ryanodine receptor 1 mutations, dysregulation of calcium homeostasis and neuromuscular disorders. *Neuromuscul. Disord.* **15**, 577-587.
- Zhao, F., Li, P., Chen, S. R., Louis, C. F. and Fruen, B. R. (2001). Dantrolene inhibition of ryanodine receptor Ca^{2+} release channels. Molecular mechanism and isoform selectivity. *J. Biol. Chem.* **276**, 13810-13816.
- Zhou, L. J. and Tedder, T. F. (1996). CD14+ blood monocytes can differentiate into functionally mature CD83+ dendritic cells. *Proc. Natl. Acad. Sci. USA* **93**, 2588-2592.
- Zorzato, F., Fujii, J., Otsu, K., Phillips, M., Green, N. M., Lai, F. A., Meissner, G. and MacLennan, D. H. (1990). Molecular cloning of cDNA encoding human and rabbit forms of the Ca^{2+} release channel (ryanodine receptor) of skeletal muscle sarcoplasmic reticulum. *J. Biol. Chem.* **265**, 2244-2256.
- Zucchi, R. and Ronca-Testoni, S. (1997). The sarcoplasmic reticulum Ca^{2+} channel/ryanodine receptor: modulation by endogenous effectors, drugs and disease states. *Pharmacol. Rev.* **49**, 1-51.

Ryanodine Receptor Activation by $\text{Ca}_v1.2$ Is Involved in Dendritic Cell Major Histocompatibility Complex Class II Surface Expression*

Received for publication, June 11, 2008, and in revised form, October 10, 2008. Published, JBC Papers in Press, October 16, 2008, DOI 10.1074/jbc.M804472200

Mirko Vukcevic[‡], Giulio C. Spagnoli[§], Giandomenica Iezzi[§], Francesco Zorzato[¶], and Susan Treves^{‡1}

From the [‡]Departments of Anaesthesia and Biomedicine and [§]Institute of Surgical Research, Basel University Hospital, 4031 Basel, Switzerland and the [¶]Department of Experimental and Diagnostic Medicine, General Pathology section, University of Ferrara, 44100 Ferrara, Italy

Dendritic cells express the skeletal muscle ryanodine receptor (RyR1), yet little is known concerning its physiological role and activation mechanism. Here we show that dendritic cells also express the $\text{Ca}_v1.2$ subunit of the L-type Ca^{2+} channel and that release of intracellular Ca^{2+} via RyR1 depends on the presence of extracellular Ca^{2+} and is sensitive to ryanodine and nifedipine. Interestingly, RyR1 activation causes a very rapid increase in expression of major histocompatibility complex II molecules on the surface of dendritic cells, an effect that is also observed upon incubation of mouse BM12 dendritic cells with transgenic T cells whose T cell receptor is specific for the I-A^{bm12} protein. Based on the present results, we suggest that activation of the RyR1 signaling cascade may be important in the early stages of infection, providing the immune system with a rapid mechanism to initiate an early response, facilitating the presentation of antigens to T cells by dendritic cells before their full maturation.

Ca^{2+} signals regulate a variety of functions in eukaryotic cells from muscle contraction and neuronal excitability to gene transcription, cell proliferation, and cell death. To efficiently utilize Ca^{2+} as a second messenger, cells are equipped with an essential toolbox kit composed of a variety of proteins that allow Ca^{2+} ions to flow into the cytoplasm and be removed from the cytoplasm, proteins that store/buffer Ca^{2+} in intracellular organelles, and proteins acting as sensors for intracellular Ca^{2+} levels as well as Ca^{2+} -regulated enzymes (1, 2). In both excitable and non-excitable cells, generation of an intracellular Ca^{2+} transient is due to the release of Ca^{2+} from intracellular stores via inositol 1,4,5-trisphosphate or ryanodine receptors (RyRs)²

present on the endoplasmic (ER)/sarcoplasmic reticulum membranes and opening of Ca^{2+} channels present on the plasma membrane. Both the amplitude and the frequency of the Ca^{2+} signal can be sensed by specific proteins allowing a cell to respond appropriately to signals, which apparently only give rise to an increase in the intracellular Ca^{2+} concentration ($[\text{Ca}^{2+}]_i$). In general, non-excitable cells are endowed with inositol 1,4,5-trisphosphate receptors which open in response to the generation of the receptor coupled second messenger inositol 1,4,5-trisphosphate, allowing Ca^{2+} to flow out of the ER. On the other hand, excitable cells, which need to respond to signals within milliseconds, are equipped with RyR Ca^{2+} channels (1). Regulation of the latter class of proteins is not mediated by the generation of a second messenger but rather through coupling with another protein component present on the plasma membrane, the L-type Ca^{2+} channel (3). In fact, in cardiac and skeletal muscles, signaling to the RyR is coupled to the dihydropyridine receptor (DHPR) L-type Ca^{2+} channels, which sense changes in membrane potential thereby activating Ca^{2+} release from the sarcoplasmic reticulum. L-type Ca^{2+} channels are composed of an α_1 subunit (Ca_v), which spans the membrane and contains the pore region, and the four additional subunits β_1 , α_2 , γ , and δ . There are at least four genes encoding the α_1 subunits ($\text{Ca}_v1.1$ – $\text{Ca}_v1.4$), and all mediate L-type Ca^{2+} currents, although their products are preferentially expressed in different tissues/subcellular locations (3, 4). $\text{Ca}_v1.1$ is localized in the transverse tubules and is involved in skeletal muscle excitation-contraction coupling; $\text{Ca}_v1.2$ is expressed in cardiac and smooth muscle cells, endocrine cells, and pancreatic β cells as well as in neuronal cell bodies and is involved in cardiac excitation-contraction coupling, hormone release, transcription regulation, and synaptic integration. $\text{Ca}_v1.3$ and $\text{Ca}_v1.4$ have a more widespread distribution, including neuronal cell bodies, dendrites, pancreatic β cells, cochlear hair cells, adrenal gland, and mast cells where they are involved in hormone/neurotransmitter release, regulation of transcription, and synaptic regulation (4).

Ryanodine receptors belong to a family of intracellular Ca^{2+} release channels composed of at least three different isoforms that have been characterized extensively biochemically, functionally, and at the molecular level (5–7). Type 1 RyRs are

* This work was supported by Swiss National Science Foundation Grants 3200B0-114597, 31600-117383 and 3200B0-104060 and by Swiss Muscle Foundation and Association Française Contre les Myopathies. The costs of publication of this article were defrayed in part by the payment of page charges. This article must therefore be hereby marked "advertisement" in accordance with 18 U.S.C. Section 1734 solely to indicate this fact.

¹ To whom correspondence should be addressed: Depts. of Anesthesia and Biomedical Research, Basel University Hospital, Hebelstrasse 20, 4031 Basel, Switzerland. Tel.: 41-61-2652373; Fax: 41-61-2653702; E-mail: susan.treves@unibas.ch.

² The abbreviations used are: RyR, ryanodine receptor; MHC, major histocompatibility complex; $[\text{Ca}^{2+}]_i$, intracellular calcium concentration; DC, dendritic cell; iDC, immature DC; DHPR, dihydropyridine receptor; ER, endoplasmic reticulum; LPS, lipopolysaccharide; bis-oxonol, bis-(1,3-diethylthiobarbiturate)-trimethineoxonal; PBS, phosphate-buffered

saline; FITC, fluorescein isothiocyanate; PE, phycoerythrin; Abs, antibody; HLA, human leukocyte antigens; ABM, anti-BM12.

RyR1 Signaling in Dendritic Cells

encoded by a gene on human chromosome 19 and are mainly expressed in skeletal muscle and to a lower extent in Purkinje cells. Mutations in this gene are associated with the rare neuromuscular disorders malignant hyperthermia, central core disease, and some forms of multimimicore disease (8, 9). Type 2 RyR is mainly expressed in cardiac muscles and cerebellum. Mutations in its gene are associated with genetic variants of congestive heart failure, namely catecholaminergic polymorphic ventricular tachycardia and arrhythmogenic right ventricular dysplasia (10, 11). Type 3 RyRs are expressed in a variety of excitable tissues as well as in immature muscle cells (12). Recent reports have demonstrated that type 1 RyRs are also expressed in some cells of the immune system (13), particularly B-lymphocytes and dendritic cells (DCs) where their pharmacological activation gives rise to a rapid and transient increase in the intracellular Ca^{2+} concentration (14–19).

Although both B-lymphocytes and DCs can act as antigen presenting cells and initiate T cell-driven immune responses (20), DCs play a central role in the immune system; they are strategically located in peripheral tissues where they continuously sample their environment for the presence of antigens. Upon encounter with microbial products or tissue debris, immature DCs (iDCs) stop endocytosing, undergo maturation, and become the most potent antigen presenting cells known. Mature DCs up-regulate co-stimulatory molecules and antigen-presenting molecules, transcribe mRNA for specific cytokines, and migrate to secondary lymphoid organs where they interact with naïve T cells to initiate specific immune responses (21). Complete maturation of DCs is thought to require at least 10–20 h (22, 23). The involvement of Ca^{2+} signaling events in DC maturation had been postulated for a number of years, but only recently was it demonstrated that RyR1-mediated Ca^{2+} signals can act synergistically with signals generated via Toll-like receptors driving DC maturation (17, 19). Experimentally, iDCs can be induced to undergo maturation by treatment with high (μM) concentrations of lipopolysaccharide. Physiologically, however, an inflamed region most likely contains a mixture of bacterial components, tissue and cellular debris, and other cellular components, including ions released from dying cells.

Several questions emerge concerning the role(s) of RyRs in DCs. (i) Why do these cells utilize the rapid acting RyRs to achieve such a slow process such as maturation; are RyRs involved in other aspects of DC function? (ii) What is the physiological route of RyR1 activation in DCs? In skeletal muscle the $\text{Ca}_v1.1$ subunit of the DHPR L-type Ca^{2+} channel present on the transverse tubular membrane acts as a voltage sensor and interacts directly with the RyR1 to initiate Ca^{2+} release. Are DCs equipped with a similar signaling pathway?

In the present report we show that DCs are endowed with a DHPR which is activated by membrane depolarization and triggers Ca^{2+} release via RyR1. More importantly we show that activation of this signaling pathway is both necessary and sufficient to cause the rapid release of an intracellular pool of MHC class II molecules onto the plasma membrane. We hypothesize that a such a rapid signaling machinery may be important under specific conditions, namely in the very early phases of an immune response when T cells and iDCs may become inti-

mately connected; engagement of T cell receptors with the MHC class II molecules on the surface of iDCs rapidly activates T cells to release factors stimulating an increase in the level of expression of MHC class II molecules on the surface of iDCs, possibly supporting very early activation steps of T cells.

EXPERIMENTAL PROCEDURES

Isolation and Generation of Dendritic Cells—Human iDCs were generated from peripheral blood mononuclear leukocytes as previously described (17). Briefly monocytes were purified by positive sorting using anti-CD14 conjugated magnetic microbeads (Miltenyi Biotech, Bergisch Gladbach, Germany). Sorted monocytes were cultured for the following 5 days in differentiation medium containing RPMI, 10% fetal calf serum, glutamine, nonessential amino acids, and antibiotics (Invitrogen) supplemented with 50 ng/ml granulocyte-macrophage colony-stimulating factor (Laboratory Pablo Cassarà, Buenos Aires, Argentina) and 1000 units/ml interleukin 4 (a gift from A. Lanzavecchia, Bellinzona, Switzerland).

Murine dendritic cells were isolated by positive sorting from spleens treated with collagenase D (1 mg/ml; Worthington Biotech; Lakewood, NJ) using anti-CD11c-coated magnetic MicroBeads according to the manufacturer's instructions (Miltenyi Biotech). The phenotype of cells was evaluated before experiments by flow cytometry using a FACSCalibur instrument equipped with Cell Quest software (BD Biosciences) as previously described (17).

Preparation of Necrotic Cell Extracts—Extracts were prepared essentially as described (17); briefly, cultured HEK293 cells ($1\text{--}1.5 \times 10^7$) were harvested, rinsed twice with PBS, resuspended in PBS, and subjected to 5 cycles of freeze-thawing. Viability was assessed by trypan blue exclusion and was $<5\%$. Large cellular debris were removed by centrifugation, and their supernatant was filtered twice through a $0.22\text{-}\mu\text{m}$ Millipore filter and stored at -70°C . Where indicated, extracts were dialyzed overnight at room temperature against PBS using a 3000 Da cut-off Spectrapore dialysis membrane (Spectrum Laboratories). Extracts were then centrifuged and filtered twice through $0.22\text{-}\mu\text{m}$ Millipore filters.

Stimulation of iDC and CD83 Expression—*In vitro* derived iDCs were cultured for 4 h at 37°C in the presence of $1\ \mu\text{g/ml}$ LPS (from *Salmonella abortus equi*, Sigma) or in the presence of $1\ \text{ng/ml}$ LPS supplemented with supernatants from necrotic cells. Briefly, necrotic cell extracts obtained from 1×10^7 cells ($1.2\ \text{ml}$) were added to 0.8×10^6 iDCs cultured in $1\ \text{ml}$ of differentiation medium plus $1\ \text{ng/ml}$ LPS; when nifedipine or dantrolene were used iDCs were pretreated at 37°C for 45 min in the dark with $10\ \mu\text{M}$ nifedipine (Calbiochem) or $20\ \mu\text{M}$ dantrolene (Sigma) before the addition of the necrotic extract. Cells were harvested, and surface expression of CD83 was investigated by flow cytometry using FITC-labeled anti-CD83 monoclonal antibodies (BD Pharmingen) on paraformaldehyde (1% in PBS) fixed cells.

Single-cell Intracellular Ca^{2+} Measurements—Measurements were performed on fura-2 (Molecular Probes, Eugene, OR)-loaded iDCs. In some experiments fura-2 loading and incubation with $500\ \mu\text{M}$ ryanodine (Calbiochem) were performed simultaneously. After loading, cells were rinsed once,

resuspended in Krebs-Ringer medium and allowed to adhere to glass coverslips, which were then mounted onto a 37 °C thermostatted chamber that was continuously perfused with Krebs-Ringer medium containing 1 mM CaCl₂. Individual cells were stimulated with the indicated agonist by way of a 12-way 100-mm diameter quartz micromanifold computer-controlled microperfuser (ALA Scientific, Westbury, NY) as previously described (15). Online (340 nm, 380 nm, and ratio) measurements were recorded using a fluorescent Axiovert S100 TV inverted microscope (Carl Zeiss, Jena, Germany) equipped with a 40× oil immersion Plan Neofluar objective (0.17 NA) and filters (BP 340/380, FT 425, BP 500/530) and attached to a Hamamatsu multiformat CCD camera. Cells were analyzed using an Openlab imaging system, and the average pixel value for each cell was measured at excitation wavelengths of 340 and 380 nm, as previously described (15).

Membrane Potential Measurements—Changes in membrane potential were assessed after the changes in fluorescence of the lipophilic dye bis-(1,3-diethylthiobarbiturate)-trimethineoxonal (bis-oxonol) as described by the manufacturer (Molecular Probes). iDCs (0.65 × 10⁶ cells/ml) were rinsed, resuspended in PBS, and added to a cuvette containing 200 nM bis-oxonol in PBS. After allowing the dye to equilibrate, changes in fluorescence were monitored with a PerkinElmer Life Sciences LS50 spectrofluorometer equipped with magnetic stirrer and thermostatted at 37 °C.

Immunofluorescence Analysis—Immunofluorescence analysis was performed as indicated on methanol-fixed or methanol:acetone (1:1)-fixed iDCs using rabbit anti-Ca_v1.2 antibody (anti-CCAT, a gift from Natalia Gomez-Ospina and Prof. Ricardo Dolmetsch, Department of Neurobiology, Stanford University School of Medicine, Stanford CA), goat anti-RyR (Santa Cruz Biotechnology Inc.), mouse anti-human HLA DR (Caltag Laboratories, Burlingame CA) followed by Alexa Fluor-488-conjugated chicken anti-rabbit IgG, Alexa Fluor-555-conjugated donkey anti-goat IgG (Molecular Probes), or PE-conjugated goat anti-mouse IgG (Southern Biotech). Fluorescence was visualized using a 100× Plan NEOFLUAR oil immersion objective (NA 1.3) mounted on a Zeiss Axiovert 100 as previously described (17).

Immunoblotting and Reverse Transcription PCR Analysis—For Western blots iDCs (1 × 10⁷ cells) were washed 3 times with PBS, and the pellet was then resuspended in 500 μl of detergent extraction buffer containing 1% Nonidet, 0.5% sodium deoxycholate, 150 mM NaCl, 5 mM EDTA, 50 mM Tris-HCl, pH 8.0, plus anti-proteases (EDTA-free, Roche Applied Science), passed through a 25-gauge needle, and incubated for 5 min at 95 °C. The solubilized proteins from 1 × 10⁶ cells were loaded in each lane and separated on a 6% SDS-PAGE. Proteins were transferred onto nitrocellulose, and the blots were probed with a rabbit anti-Ca_v1.2 antibody (1:2000) followed by peroxidase-conjugated protein G (1:50000, Fluka Biochemicals, Buchs, Switzerland). The immunopositive bands were visualized by autoradiography using the Super signal West Dura chemiluminescence kit from Thermo Scientific.

Reverse transcription PCR was performed as previously described (15). Total RNA was isolated from 8 × 10⁶ iDCs using the ULTRASPEC RNA isolation system (Biotex Labs) and

reverse-transcribed using a cDNA synthesis kit following the instructions provided by the manufacturer (Roche Applied Science). Approximately 100 ng of cDNA were used per PCR amplification using an Applied Biosystems 2720 thermal cycler. The following primers spanning exons 15–16 were used to amplify the Ca_v1.2 transcript: forward, 5'-AAA TTT CCCT GGG ACTG TTG; reverse, 5'-GGT TAT GCCC TCCC CTG. Such primers yield a DNA fragment of ~300 bp when amplifying cDNA; amplification from genomic DNA would be highly unlikely under normal PCR conditions as the expected fragment is too large (~2800 bp). Amplification conditions were 5 min at 95 °C followed by 35 cycles of 30 s annealing at 92 °C, 40 s extension at 50 °C, and 40 s denaturation at 72 °C followed by a final extension for 5 min at 72 °C using the 2.5× Master Mix Taq polymerase from Eppendorf. The products of the PCR reaction were separated on a 6% polyacrylamide gel, and the bands were visualized by ethidium bromide staining.

Functional Properties of iDCs—Endocytosis was studied by incubating iDCs in RPMI medium containing FITC-labeled dextran (final concentration 0.5 mg/ml; Fluka Chemicals, Buchs, Switzerland) for 30 min at 37 °C. Cells were washed in ice-cold PBS 2 times and fixed with 1% paraformaldehyde, and the number of FITC-positive cells was assessed by flow cytometry.

Surface expression of MHC class I and class II molecules was monitored in iDCs stimulated with 10 mM caffeine for 1–60 min at 37 °C or on iDCs stimulated with 100 mM KCl, necrotic cell extracts, 100 μM ATP, or 1 μg/ml LPS for 1 min. To monitor surface expression of MHC class I and II molecules, stimulated cells were washed with ice-cold PBS, labeled, and analyzed by flow cytometry using FITC-labeled anti-human HLA DR and HLA A, B, C or, in the case of mouse CD11c+ cells, with FITC-labeled anti mouse I-A^b monoclonal antibody (BD Pharmingen).

In Vivo Investigation of Mouse DC-T Cell Interactions; Increase in [Ca²⁺]_i and Rapid MHC Class II Induction—CD11c positive DCs were isolated from the spleens of either B6.C-H-2bm12Ly 5.1 mice (abbreviated BM12DC) or B6.Ly 5.1 mice (a generous gift of Prof. Ed Palmer, Department of Biomedicine, Basel University Hospital, Basel, Switzerland). T-lymphocytes were isolated from the lymph nodes of ABM Rg^{-/-} mice. These T cells recognize the I-A^{bm12} protein expressed on the surface of B6.C-H-2bm12.Ly5.1 DCs but do not recognize the I-A^b protein expressed on the surface of B6.Ly5.1 DCs (24). T-lymphocytes were divided in two groups; one group was left untreated, whereas the other was incubated with 100 nM charybdotoxin (Alexa Biochemicals) for 45 min to block K⁺ channels (25), after which the cells were washed to remove excess toxin.

For Ca²⁺ imaging BM12DC were loaded with the fluorescent Ca²⁺ indicator fluo-4 AM (Invitrogen; 5 μM final concentration) for 60 min at 37 °C. In some experiments BM12DCs were simultaneously incubated with 500 μM ryanodine (Calbiochem) and fluo-4 AM. Cells were then washed and resuspended in Krebs-Ringer containing 1 mM CaCl₂ and 0.2% bovine serum albumin. BM12DC were allowed to adhere to glass coverslips which were then mounted on a 37 °C thermostatted chamber. Experiments were started by adding T-lymphocytes to the coverslip onto which the BM12DCs had been applied. Changes in

RyR1 Signaling in Dendritic Cells

fluo-4 fluorescence were monitored with a Nikon Eclipse TE2000-E fluorescent microscope equipped with a CFI APO TIRF 60 \times objective. Changes in fluorescence were detected by exciting at 488 nm and recording the emission at 510-nm via an electron multiplier C9100-13 Hamamatsu CCD camera. Image analysis was performed with the MetaMorph (Molecular Devices) analysis software package.

For MHC II induction untreated T-lymphocytes or T-lymphocytes preincubated with 100 nM charybdotoxin (Alexa Biochemicals) for 45 min and washed to remove excess toxin were used. Both batches of T cells were placed in 1.5-ml Eppendorf tubes together with the CD11c positive B6 or B6.C-H-2bm12 DCs. Cells were spun down for 30 s using a Tomy PMC-060 capsulifuge and incubated at 37 $^{\circ}$ C for an additional 5 min. They were then diluted with ice-cold PBS, washed, and labeled with FITC-anti-mouse I-A^b, biotin-labeled anti-CD11c plus APC (allophycocyanin)-labeled streptavidin, and PE-labeled anti-CD45.1 (all from BD Pharmingen). Expression of MHC class II molecules was determined on triple positive cells by flow cytometry.

Statistical Analysis and Software Programs—Statistical analysis was performed using the Student's *t* test for unpaired samples; means were considered statistically significant when the *p* value was <0.05. The Origin computer program (Microcal Software, Inc., Northampton, MA) was used to generate graphs and for statistical analysis. Figures were assembled using Photoshop Adobe.

RESULTS

Upstream Events Leading to RyR1 Activation—In an earlier report (17) we showed that (i) iDCs only express the type 1 RyR isoform, (ii) the addition of caffeine, 4-chloro-*m*-cresol, or KCl to iDC causes a RyR1-dependent increase in the intracellular Ca²⁺ concentration ([Ca²⁺]_i), and (iii) the signaling cascade activated by the Ca²⁺ increase acts synergistically with signals generated via Toll-like receptors, stimulating DC maturation (17). Because RyRs are present in intracellular membranes and are not directly accessible to stimulation, our first aim was to identify events upstream from RyR1 activation by first searching for, and then using a more physiological stimulus leading to DC maturation.

Fig. 1 shows that treatment of iDCs with a suboptimal concentration of lipopolysaccharide (LPS 1 ng/ml) for 4 h in the presence of necrotic cell extracts, a stimulus that has been shown to cause maturation (26), leads to a significant increase in the surface expression of CD83, a reliable phenotypic marker for DC maturation (17, 27, 28). The signals generated by the addition of the necrotic cell extracts and leading to maturation were significantly decreased by pretreatment of cells with dantrolene (*p* < 0.034), an inhibitor of the RyR1 (29) and nifedipine (*p* < 0.019), a well known L-type Ca²⁺ channel inhibitor (4). The functional involvement of a nifedipine- and ryanodine-sensitive Ca²⁺ signal was confirmed by direct measurements of the intracellular [Ca²⁺]_i (Fig. 2, A and B). Individual fura-2 loaded iDCs were stimulated with filtered extracts from necrotic cells. This treatment caused a transient and rapid increase in [Ca²⁺]_i, which was significantly decreased (*p* < 0.0001) by preincubation of iDCs with 500 μ M ryanodine (Fig.

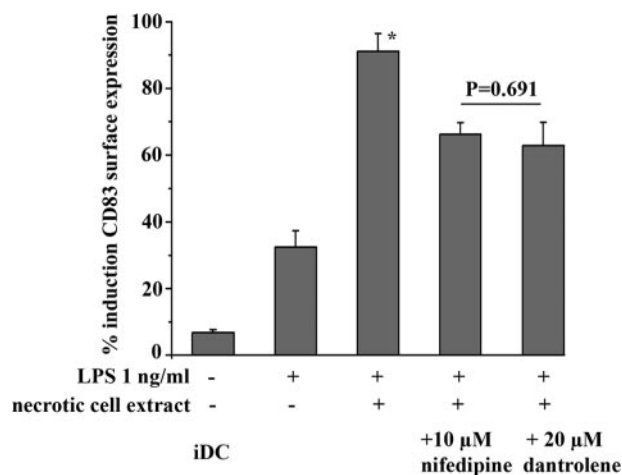


FIGURE 1. Surface expression of CD83 induced by necrotic cell extracts is sensitive to dantrolene and nifedipine. iDCs were treated for 4 h as indicated, and the number of positive CD83 cells was determined by flow cytometry on paraformaldehyde (1% in PBS) fixed cells. Stimulation with 1 ng/ml LPS alone induced a small increase CD83 surface expression; the concomitant presence of supernatants from necrotic HEK293 cells, prepared as described under "Experimental Procedures" increased CD83 significantly as compared with iDCs treated with 1 ng/ml LPS (*, *p* < 0.02). This effect was blocked by pretreatment of iDCs with the RyR1 inhibitor dantrolene (20 μ M; *p* < 0.034) or with the L-type Ca²⁺ channel inhibitor nifedipine (10 μ M; *p* < 0.019). Results are expressed as the mean (\pm S.E.) % induction of CD83 surface expression of at least three experiments carried out on iDCs purified from blood of different donors; values obtained by treating iDCs with 1 μ g/ml LPS were considered 100%.

2A, inset) (at high concentrations ryanodine blocks the RyR (30, 31); dantrolene, which is used to inhibit RyR-signaling events, is fluorescent and interferes with imaging when using fluorescent Ca²⁺ indicators) or 10 μ M nifedipine (*p* < 0.0001; Fig. 2A); in fact, the mean Δ fluorescence induced by necrotic extracts was 0.210 \pm 0.011 in untreated cells and 0.134 \pm 0.094 and 0.029 \pm 0.008 in cells pretreated with 500 μ M ryanodine or 10 μ M nifedipine, respectively. A similar result was observed after the addition of 100 mM KCl to iDCs (Fig. 2B). In the latter case, if the experiments were performed in the absence of extracellular Ca²⁺ and in the presence of 100 μ M La³⁺ to block Ca²⁺ influx (32) or on iDCs which had been pretreated with 500 μ M ryanodine or 10 μ M nifedipine, the mean increases in fluorescence induced by the addition of 100 mM KCl were significantly reduced (Fig. 2B; *p* < 0.0001), indicating that the intracellular Ca²⁺ transient is dependent on the activation of the RyR1, on influx of Ca²⁺ from the extracellular medium, and is sensitive to micromolar concentrations of nifedipine.

These results suggest that KCl and necrotic cell extracts may act in a similar fashion; KCl causes membrane depolarization, and this can be followed experimentally with the fluorescent membrane potential dye bis-oxonol whereby depolarization increases the fluorescence of bis-oxonol (Fig. 2C, left and central panels), whereas hyperpolarization causes a decrease in fluorescence. The addition of filtered necrotic cell extracts to iDCs causes plasma membrane depolarization (Fig. 2C, right panel), and the extent of depolarization is proportional to the number of cells from which the extracts were prepared (not shown); overnight dialysis of the necrotic extract against PBS with a 3000-Da cut-off membrane abolished its depolarizing effect (Fig. 2C, right panel).

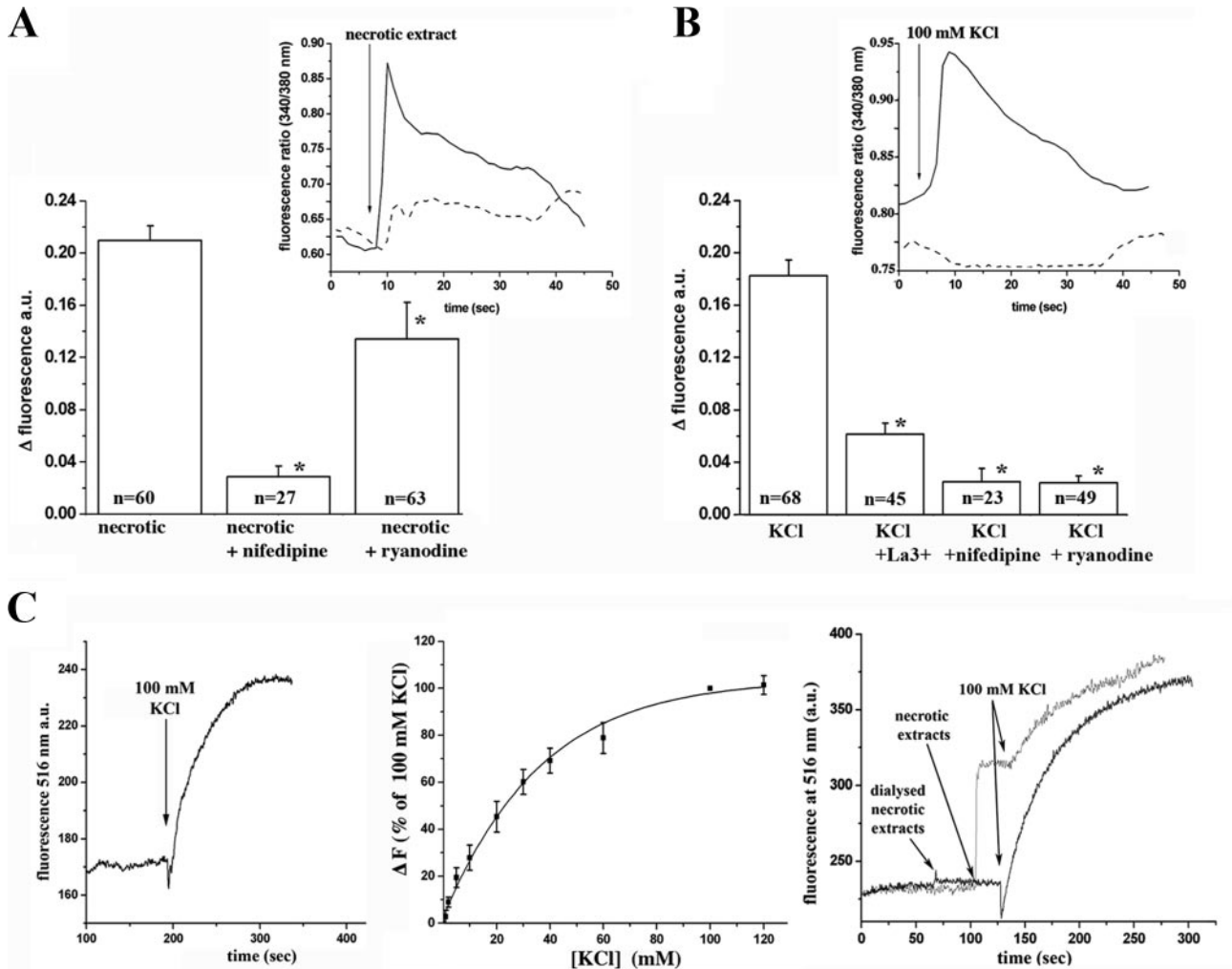


FIGURE 2. Necrotic cell extracts and KCl induce a nifedipine-sensitive increase in $[Ca^{2+}]_i$ in iDCs as well as membrane depolarization. *A* and *B*, single cell intracellular calcium measurements in fura-2-loaded iDCs. The traces in the insets show changes in the fura-2 fluorescence ratio (340/380 nm) in single iDC perfused with necrotic cell extracts (*A*) or 100 mM KCl (*B*). Continuous line, no pretreatment; dashed line, cells pretreated with 500 μ M ryanodine for 60 min. Experiments were performed in Krebs-Ringer containing 1 mM Ca^{2+} except when La^{3+} (100 μ M) was added, in which case only contaminating Ca^{2+} was present. When nifedipine or ryanodine were used, cells were preincubated with 10 μ M nifedipine or 500 μ M ryanodine during the fura-2 loading. The histograms represent the mean (\pm S.E. of the indicated *n* values) Δ increase in fluorescence, calculated by subtracting the peak fluorescence ratio—resting fluorescence ratio); *, $p < 0.0001$. *C*, membrane potential changes were monitored by following the change in fluorescence of bis-oxonol as detailed under “Experimental Procedures.” After allowing the dye to equilibrate, either KCl or filtered necrotic extracts obtained from 2.9×10^6 cells were added to the cuvette while continuously monitoring the emission at 516 nm. An upward deflection indicates membrane depolarization. Experiments were carried out at least three times giving similar results. The mean (\pm S.E.) of 4–6 values were used to generate the Δ fluorescence–KCl dose-dependent curve shown in panel *C* (center). a.u., arbitrary units.

In cardiac and skeletal muscles, signaling to the RyR1 is coupled to DHPR L-type Ca^{2+} channels, which sense changes in membrane potential thereby activating Ca^{2+} release from the sarcoplasmic reticulum. Because human iDCs express the $\beta 1$ subunit of the DHPR (33), we wondered whether the depolarization-coupled Ca^{2+} release observed in iDC could be due to the expression of a Ca_v1 isoform by these cells. Immunofluorescence analysis using confocal microscopy on methanol-fixed iDCs labeled with anti- $Ca_v1.2$ Abs followed by Alexa Fluor-488-conjugated anti-rabbit IgG (Fig. 3A, panel 1) and anti-MHCII Abs (Fig. 3A, panel 2) followed by PE-conjugated anti-mouse IgG confirmed partial co-localization of the two proteins on the plasma membrane of iDCs (Fig. 3A, panel 5). We next verified if there was co-localization between $Ca_v1.2$ and the RyR by performing immunofluorescence analysis on permeabilized acetone-methanol-fixed iDCs. Under these con-

ditions $Ca_v1.2$ appeared to be discretely distributed within iDCs (Fig. 3B, panel 1), whereas immunostaining for the RyR1 showed a more reticular pattern of distribution (Fig. 3B, panel 2); merging the two images shows that part of the positive fluorescent signals obtained with anti- $Ca_v1.2$ and anti-RyR overlap (Fig. 3B, panel 5), indicating that the two proteins co-localize within certain domains of iDCs. To confirm that the antibodies recognize a protein corresponding to $Ca_v1.2$, we performed Western blot analysis. Fig. 3C shows that the anti- $Ca_v1.2$ Abs we used, which were specifically raised against the COOH terminus of $Ca_v1.2$ (34), recognize a band in total iDC extracts migrating with an apparent molecular mass of 200 kDa as well as another immunopositive band with a slightly slower mobility; very similar results were obtained by Gomez-Ospina who used these Ab to identify $Ca_v1.2$ in neurons (34). Finally, reverse transcription-PCR using primers specifically designed

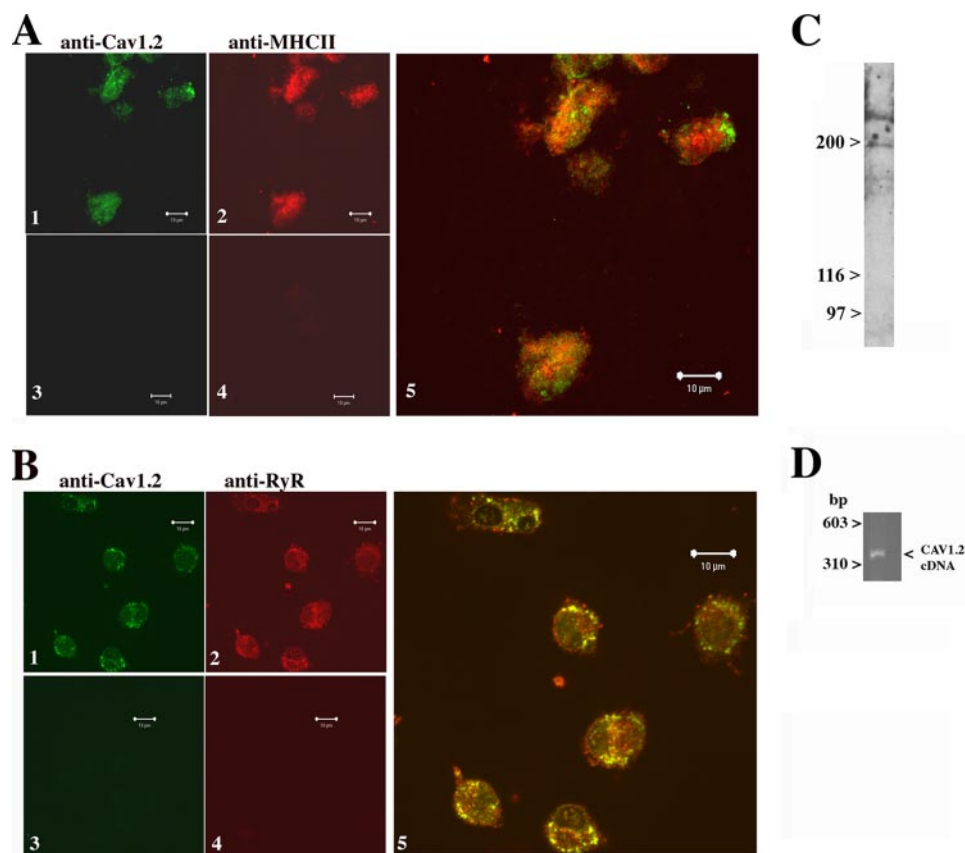


FIGURE 3. $Ca_v1.2$ is expressed in iDCs and shows partial co-localization with the RyR. *A*, immunofluorescence analysis on methanol fixed human iDCs. Shown are iDCs stained with rabbit anti-Cav1.2 polyclonal antibodies followed by Alexa Fluor-488-conjugated anti-rabbit IgGs (1) or Alexa Fluor-488 conjugated anti-rabbit IgGs alone (3) and mouse anti-MHC II (HLA DR) Abs followed by PE-conjugated goat anti-mouse Abs (2) or PE conjugate goat anti-mouse Abs alone (4). *Panel 5* shows the merged images, and *yellow-orange* pixels indicate overlapping fluorescent signal; *bars* indicate 10 μ m. *B*, immunofluorescence analysis on acetone: methanol fixed-iDCs (1). iDCs stained with rabbit anti- $Ca_v1.2$ polyclonal antibodies followed by Alexa Fluor-488-conjugated anti-rabbit Abs or Alexa Fluor-488-conjugated anti-rabbit Abs alone (3) or goat anti-RyR polyclonal Ab followed by Alexa Fluor-555 conjugated anti-goat Abs (2) or Alexa Fluor-555 conjugate Abs alone (4). *Panel 5* shows the merged images, and *yellow-orange* pixels indicate overlapping fluorescent signals; *bars* indicate 10 μ m. All images were acquired with a 100 \times Plan NEOFLUAR oil immersion objective (NA 1.3) mounted on a Zeiss Axiovert 100 confocal microscope. *C*, Western blot of total proteins of iDC (1×10^6 cell/lane) separated on a 6% SDS polyacrylamide gel. The blot was incubated with rabbit anti- $Ca_v1.2$ followed by protein-G peroxidase. The immunoreaction was visualized by chemiluminescence. *D*, reverse transcription-PCR confirms the presence of the transcript for human $Ca_v1.2$ in iDC (see "Experimental Procedures" for details of the experimental conditions and primers used).

to amplify the human $Ca_v1.2$ transcript generated a band corresponding to the expected size (Fig. 3D) when amplifying cDNA. PCR amplification using primers specific for human $Ca_v1.1$ and $Ca_v1.3$ failed to amplify any band from cDNA of DCs (results not shown).

Rapid Events Occurring after RyR1 Activation—We were also interested in investigating if activation of the RyR1 leads to any direct changes in DCs. Immature DCs are extremely efficient at endocytosing (20, 21), so our first experiments were aimed at determining whether pretreatment of cells with a RyR1 agonist affects their capacity to endocytose FITC-labeled dextran. No difference in mean fluorescent intensity was observed between untreated iDCs or cells treated with 10 mM caffeine or 100 mM KCl. In 5 different experiments the mean \pm S.E. % of FITC-positive cells was $98.5 \pm 18.7\%$ for cells pretreated with 100 mM KCl and 100% for iDCs ($p = 0.899$).

We next investigated whether RyR1 activation is linked to surface expression of MHC molecules. DCs express one pool of

MHC class I molecules that are synthesized and loaded with antigenic peptides in the ER and two main populations of MHC class II molecules; one pool is synthesized *de novo* and is loaded with processed antigenic peptides in the ER, whereas the other is preformed and located within re-cycling endosomes (20). Immature dendritic cells were stimulated for 1–60 min with the RyR1 agonist caffeine, stained with anti-MHC I or anti-MHC II antibodies, and processed by flow cytometry. Fig. 4A shows that as early as 1 min after stimulation, there was a significant increase in surface fluorescence associated with MHC class II expression which then decayed back to resting levels after ~ 60 min of incubation at 37 $^{\circ}$ C. The increase in mean fluorescence intensity was reproducible and was specifically generated via DHPR-RyR1 signaling because (i) it also occurred after the addition of necrotic cell extracts and 100 mM KCl and (ii) the latter effects could be blocked by pretreatment of iDCs with dantrolene and nifedipine (Fig. 4B), (iii) it did not occur in cells treated with high levels (1 μ g/ml) of LPS or with ATP, the latter agonist also generating a Ca^{2+} signal, but via inositol 1,4,5-trisphosphate receptor activation (35), and (iv) KCl and necrotic extracts did not affect surface expression of MHC class I molecules (Fig. 4C). Such an effect may represent a specific and

physiological pathway utilized by iDCs to rapidly express MHC class II molecules on their surface. The above-mentioned experiments were performed on "in vitro" generated DCs; when the same experiments were carried out on naturally occurring DCs isolated from mouse spleens, the addition of 100 mM KCl and necrotic cell extracts also caused a significant increase in surface expression of MHC class II molecules (Fig. 5A).

These findings are intriguing because of their rapid time course and because of their specificity but yield no information regarding their physiological role. We wondered whether the activation of the RyR1 signaling system could be important under specific conditions, namely when iDCs are present in an inflamed environment containing antigens as well as T cells. Notably, the classical pathways for T cell activation is via the inositol trisphosphate signaling pathway which leads to an increase in the $[Ca^{2+}]_i$ by releasing Ca^{2+} from intracellular stores and by opening Ca^{2+} channels on the plasma membrane (36). To compensate for the change in

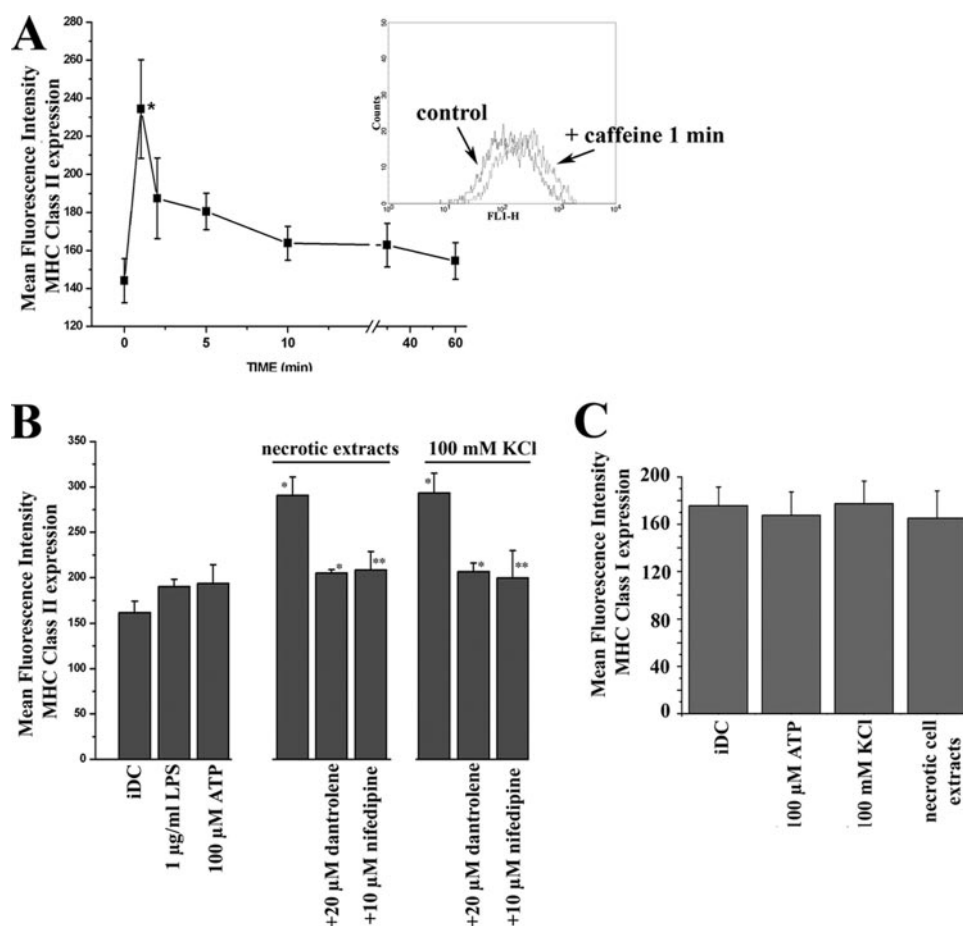


FIGURE 4. Pharmacological activation of RyR induces a rapid increase in membrane-associated MHC class II molecules in iDC. *A*, iDCs were treated with 10 mM caffeine for the indicated time, labeled with FITC-labeled anti-human HLA DR, fixed with paraformaldehyde, and analyzed by fluorescence-activated cell sorter as detailed under "Experimental Procedures." Results represent the mean fluorescent intensity (\pm S.E.) of four experiments carried out on different donors. *, $p < 0.015$. The inset shows a fluorescence-activated cell sorter histogram showing FITC fluorescence in immature DCs (black line) and in iDCs after the addition of 10 mM caffeine for 1 min (gray line). *B*, iDCs were treated for 1 min with the indicated substance and processed as described in *A*. Results represent the mean \pm S.E. of 4–6 experiments. Significant differences were observed in the mean fluorescence intensity between iDCs and cells treated with necrotic cell extracts and between iDCs and cells treated with 100 mM KCl; significant differences in mean fluorescence intensity were observed between iDCs treated with necrotic cell extracts and KCl as compared with the mean fluorescence intensity of cells receiving similar treatments but preincubated with 10 μ M nifedipine or 20 μ M dantrolene; *, $p < 0.03$; **, $p < 0.05$. *C*, iDCs were treated for 1 min as indicated, labeled with FITC-labeled anti-human HLA A, B, C, and processed for fluorescence-activated cell sorter analysis as described for *A*. Results represent the mean fluorescence intensity (\pm S.E.) of five experiments carried out on different DC donors. Mean fluorescence intensity values were not significantly different in treated cells and iDC.

membrane potential caused by the Ca^{2+} influx, K^+ channels (Kv1.3 and K_{Ca}) open, allowing efflux of K^+ ions out of the T cells, thus repolarizing the T cell membrane potential (37).

To determine whether these events (*i.e.* the K^+ efflux from T cells and DHPR-RyR1 activation in DCs) are functionally coupled *in vivo*, we studied if the direct interaction of antigen-specific T cells with DCs causes an increase in MHC II surface expression as well as an increase in the $[\text{Ca}^{2+}]_i$ of the DCs. To carry out the *in vivo* experiments, we exploited the fact that T lymphocytes from ABM $\text{Rg}^{-/-}$ mice express a transgenic T cell receptor which recognizes the class II MHC protein I-A^{bm12} expressed on the surface of DCs from BM12Ly5.1 mice but not class II MHC protein I-A^b expressed on the surface of control B6.Ly5.1 mice (24). CD11c-positive splenic DCs isolated from B6.Ly5.1 or BM12Ly5.1 mice were co-centrifuged with T cells

from ABM $\text{Rg}^{-/-}$ mice and incubated an additional 5 min at 37 °C. Cells were then diluted with ice-cold PBS, stained with fluorescent Abs, and analyzed by flow cytometry. A further control consisting of T cells pretreated with charybdotoxin to block K^+ channels on T cells was also included. This toxin specifically blocks $\text{Kv1.3}/\text{K}_{\text{Ca}}$ channels at nM concentrations and inhibits K^+ efflux (25). When DCs from B6.Ly5.1 were incubated with T cells, there was an approximate 2.5-fold increase in the level of MHC class II molecules expressed on splenic DCs, indicating that co-centrifugation may non-specifically activate to a low extent both cell types. Interestingly, when BM12Ly5.1 DCs were co-centrifuged with untreated ABM $\text{Rg}^{-/-}$ T cells, there was a 5-fold increase in the level of MHC class II surface expression on splenic DCs (Fig. 5*B*). This 5-fold increase in class II MHC expression is specific as it was inhibited in the charybdotoxin-treated T cell group, supporting the idea that the full increase in MHC II expression is due to specific T cell K^+ channel opening occurring as a consequence of the T cell/DC interaction.

We used a similar approach to confirm that the interaction of BM12Ly5.1 DCs with ABM $\text{Rg}^{-/-}$ T cells causes a ryanodine-sensitive increase in the $[\text{Ca}^{2+}]_i$ of DCs. Fig. 5*C* shows a typical result obtained after the addition of ABM $\text{Rg}^{-/-}$ T cells to Fluo-4-loaded BM12DCs. As can be seen, the $[\text{Ca}^{2+}]_i$ of those DCs which were found to have T cells attached to them at the end of

the experiment (inset, Fig. 5*C*) was found to increase in an oscillatory manner. This event was not synchronized in the responding cells as the moment of interaction between the two populations of cells was not coordinated. In line with our hypothesis, the increase in $[\text{Ca}^{2+}]_i$ induced by the BM12Ly5.1DC $\text{Rg}^{-/-}$ T cell interaction was most likely due to opening of K^+ channels on the T cells, as the Ca^{2+} transients in the DCs were profoundly diminished after pretreatment of T cells with charybdotoxin (Fig. 5*D*). Finally, pretreatment of DCs with 500 μ M ryanodine completely blocked the changes in $[\text{Ca}^{2+}]_i$ (Fig. 5*E*).

DISCUSSION

In the present paper we investigated the signaling system involving the RyR in iDCs and show that the upstream events

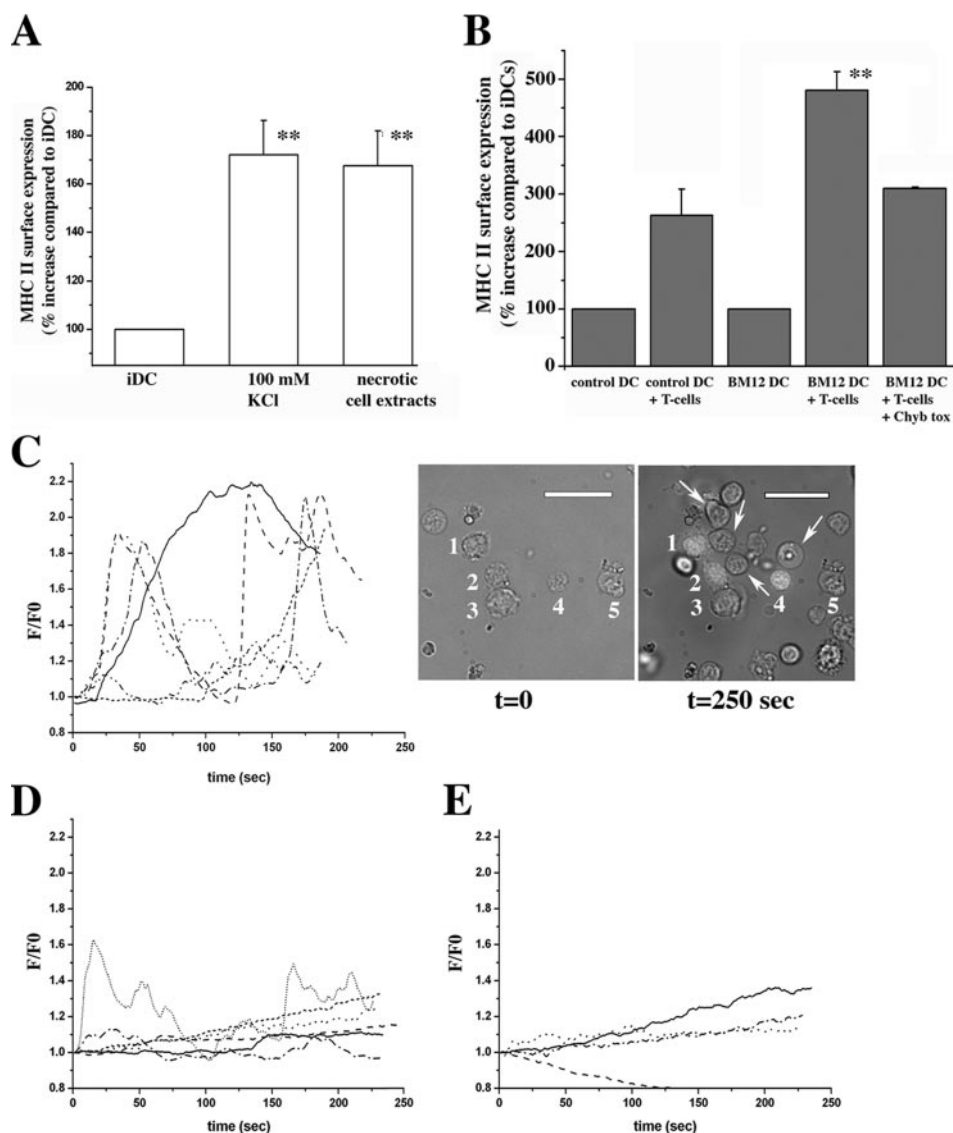


FIGURE 5. Surface expression of MHC class II molecules is promoted by specific T cell-DC interaction or by KCl and necrotic cell extracts and is accompanied by an increase in the $[Ca^{2+}]_i$ in the DCs. *A*, % induction in MHC II surface expression in CD11c-purified DCs isolated from mouse spleen cells after the addition of 100 mM KCl or necrotic cell extracts (mean \pm S.E., $n = 3-4$ experiments); **, $p < 0.007$. *B*, CD11c-positive dendritic cells were isolated from the spleens of either B6.C-H-2bm12Ly5.1 mice (BM12 DC) or B6.Ly5.1 mice (control DC) and co-centrifuged with T cells isolated from lymph nodes of ABM Rg^{-/-} mice. T cells were either untreated or preincubated with 100 nM charybdotoxin (*Chyb tox*) for 45 min to block $K_{v1.3}$ and IK_{Ca1} channels. After co-centrifugation, DC and T cells were incubated an additional 5 min at 37 °C. Cells were then diluted with ice-cold PBS, washed, and stained with FITC-labeled anti-mouse I-A^b monoclonal antibody, biotin-labeled anti-mouse CD11c (Integrin α_x chain) monoclonal antibody, and PE-labeled anti-mouse CD45.1 monoclonal antibody. After selection of triple positive cells by fluorescence-activated cell sorter, MHC II expression was analyzed. Results are expressed as % increase in the mean fluorescent intensity compared with iDC (\pm S.E. of three experiments; **, $p < 0.007$). *C-E* show changes in the $[Ca^{2+}]_i$ in fluo-4-loaded BM12DC after the addition of ABM Rg^{-/-} T cells. Experiments were performed as described under "Experimental Procedures." *C*, BM12DC + T cells. *D* is as in *C* except that T cells were preincubated with 100 nM charybdotoxin before addition to DCs. *E*, as in *C*, except DCs were incubated with 500 μ M ryanodine during fluo-4 loading. Results are expressed as F/F_0 where F is the fluorescent value at any given time, and F_0 is the initial fluorescence level obtained at time 0. Panels represent typical results obtained in six different experiments. *Insets* in panel *C* show brightfield photomicrograph of BM12DC at $t = 0$ and brightfield + epifluorescence of fluo-4-loaded BM12DC at the end of the experiment (250 s). *Numbers* indicate DCs that were analyzed and had T cells (*arrows*) adjacent to them. The *bar* indicates 10 μ m.

leading to Ca^{2+} release via the RyR1 are similar to those occurring in striated muscles and involve the functional interaction with the DHPR L-type Ca^{2+} channel. We also show that RyR1 activation has direct and rapid physiological consequences leading to an increase in the level of MHC class II molecules on

the surface of iDCs within seconds. Such a system may be important in the very early stages of an infection whereby prompt activation of the adaptive immune system could occur allowing rapid priming of T cells without having to wait for iDCs to undergo full functional maturation.

Although the expression of the RyR1 isoform in human and mouse dendritic cells has been clearly established (14, 16–17, 19), little information if any is available concerning its physiological mode of activation. In fact, RyRs are intracellular Ca^{2+} channels localized on sarcoplasmic reticulum/ER membranes, and at least in excitable cells, their activation is coupled to DHPR L-type Ca^{2+} channels present on the plasma membrane (3, 4). The latter channels have been characterized at the molecular, physiological, pharmacological, and biophysical level; they require strong depolarizing signals to open, can be blocked specifically by dihydropyridines and other organic Ca^{2+} channel blockers, act as voltage sensors mediating Ca^{2+} influx in response to membrane depolarization, and regulate a number of processes including muscle contraction, insulin secretion, neurotransmission, and gene transcription (4). DHPRs are macromolecular structures made up of four or five distinct subunits that are encoded by multiple genes. The $\alpha 1$ subunit constitutes the voltage sensor and the pore and usually associates with the $\beta 1$ and $\alpha 2\delta$ subunits. Although DHPRs are predominantly expressed in excitable tissues such as neurons and muscle cells, pancreatic cells, and endocrine cells as well as T-lymphocytes have been shown to express the $Ca_v1.2$ isoform of L-type Ca^{2+} channels (38–40).

In an early report Poggi *et al.* (33) showed that human DC express the $\beta 1$ subunit of the DHPR as well an α subunit because they were stained with the fluorescent dihydropyridine analogue DM-BODIPY-DHP. They also demonstrated the involvement of DHPR-sensitive Ca^{2+} channels in some DC functions such as apoptotic body engulfment and interleukin-12 production. We have extended these results and report that DCs have evolved a chi-

meric configuration, expressing the cardiac isoform of the $\alpha 1$ subunit (*i.e.* the $\text{Ca}_v1.2$ isoform), which functionally interacts with the skeletal isoform of the RyR. The first question arising is how can a functional coupling between the “cardiac” $\text{Ca}_v1.2$ isoform and the “skeletal” RyR1 isoform operate? In muscle cells depolarization of the plasma membrane is sensed by the Ca_v1 , which acts as a voltage sensor activating the RyR to release Ca^{2+} from intracellular stores. In skeletal muscle the $\text{Ca}_v1.1$ subunit and RyR1 interact directly (41–43), whereas in heart cells, which express type 2 RyR, the $\text{Ca}_v1.2$ subunit acts both as a voltage sensor and as a Ca^{2+} channel, and the depolarizing signal allows Ca^{2+} to flow into the cells from the extracellular environment (44). It is the influx of Ca^{2+} which activates RyR2 through a mechanism of Ca^{2+} -induced Ca^{2+} release. We suggest that in DCs, coupling between the DHPR and the RyR1 occurs as outlined in Fig. 9 of Schuhmeier *et al.* (45); membrane depolarization caused by an increase in K^+ is sensed by $\text{Ca}_v1.2$ present on the plasma membrane of DCs. Once activated, these channels allow Ca^{2+} influx. In turn, this local increase in $[\text{Ca}^{2+}]_i$ in the DCs activates RyR1 through a Ca^{2+} induced Ca^{2+} release mechanism. Such a configuration is supported by the fact that RyR activation in DCs is strongly dependent on extracellular Ca^{2+} and can be blocked by nifedipine. That this chimeric arrangement could function is supported by (i) the observation that electrical stimulation of dysgenic myotubes (which express RyR1 but lack endogenous DHPR), reconstituted with the cardiac $\text{Ca}_v1.2$, evokes myotube contraction albeit only in the presence of Ca^{2+} -containing medium (41) and (ii) by a report of Schuhmeier *et al.* (45) who showed that different Ca_v channel isoforms (1.1, 1.2, and 2.1) can functionally interact with RyR1.

The most intriguing questions arising from the observation that DCs express DHPRs are how and when would these voltage-sensor-activated Ca^{2+} channels be activated physiologically? Indeed DCs are not typically classified as electrically excitable cells, yet we show that the addition of either necrotic cell extracts or KCl both cause (i) plasma membrane depolarization, (ii) nifedipine-sensitive increase in $[\text{Ca}^{2+}]_i$, and (iii) rapid and nifedipine-sensitive increase in surface expression of MHC class II molecules. Necrotic and dying cells are present in any tissue after extensive injury due to physical or mechanical traumas, inflammation, or infections, and they can release a number of factors and proteins including uric acid crystals, nuclear-mobility group box 1 protein, and heat shock proteins (HSP96, -90, -70 and calreticulin) which can all induce DC maturation (46–48). In addition, because the intracellular K^+ concentration is ~ 140 mM, dying cells will necessarily release K^+ ions into the extracellular medium; our results support the hypothesis that necrotic cells may lead to activation of the DHPR-RyR signaling pathway by releasing a number of factors, including K^+ . This is supported by the finding that necrotic extracts passed through a $0.22\text{-}\mu\text{m}$ filter caused a nifedipine- and ryanodine-sensitive increase in the $[\text{Ca}^{2+}]_i$ as well as membrane depolarization, but extracts dialyzed against PBS using a 3000-kDa cut-off membrane did not alter the membrane potential. Because ions would be removed by dialysis, these data suggest that K^+ released from the dead cells may be physiologically involved in the *in vivo* activation of the DHPR-RyR1 signaling pathway.

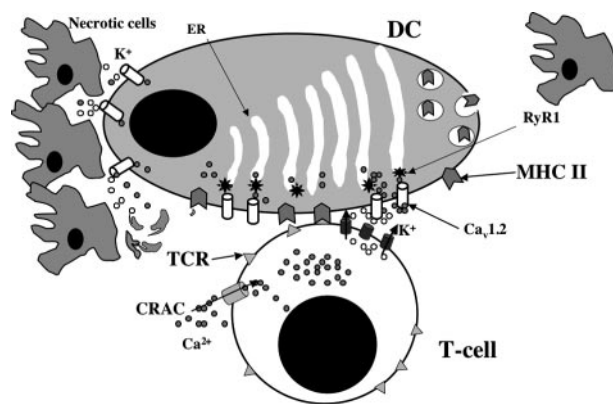


FIGURE 6. Schematic depicting the model of RyR1-dependent signaling pathways in DC. KCl released from dead cells in the vicinity of DCs causes membrane depolarization, which is sensed by the DHPR voltage sensor. Alternatively, interaction of T cells with iDC, strong enough to activate an increase in the $[\text{Ca}^{2+}]_i$, via release from intracellular stores and activation of Ca^{2+} influx, is accompanied by efflux of K^+ to repolarize the T cell membrane potential. This K^+ is released onto the iDCs and can be sensed by the DHPR. This leads to activation of the RyR1 signaling pathway causing the rapid expression of MHC class II molecules onto the surface of iDCs. The latter molecules could be loaded with antigenic peptides and interact *in situ* with T cells to initiate an early and rapid specific immune response. TCR, T cell receptor; CRAC, Ca^{2+} release activated Ca^{2+} channel.

Another important question is whether the DHPR-RyR1 signaling pathway is only involved in the generation of co-stimulatory signals leading to DC maturation or whether it can rapidly and directly activate specific functions. Our results exclude that endocytosis, a process intimately connected with iDC function, and expression of MHC class I molecules on the plasma membrane are influenced by activation of the RyR signaling pathway. On the other hand, our results show that surface expression of MHC class II molecules is rapidly (within seconds) and significantly increased by the activation of the RyR1 signaling pathway. DCs synthesize large quantities of MHC class II molecules which classically bind peptides derived from endocytosed proteins and present them on their surface for interaction with T cells to initiate a specific immune response. They also express empty MHC class II molecules on their surface as well as sequestered MHC class II molecules within intracellular compartments (22, 49). These sequestered molecules apparently reside unproductively within the cell. The results of the present study indicate that activation of the DHPR-RyR1 pathway causes expression of preformed MHC class II molecules on the surface of DCs. Empty surface MHC II molecules can be loaded with antigenic peptides from the extracellular medium, allowing even immature DCs to present peptides to T cells without intracellular processing (50, 51). We hypothesize that RyR1 activation in DCs leads to the rapid surface expression of sequestered MHC II molecules. This would be particularly important for iDC and T cells to interact efficiently directly in an inflamed tissue where dead or dying cells are present, leading to the rapid amplification of a specific immune response. Such a rapid activation must be strictly controlled and most likely requires T cells and iDCs to generate orthograde and retrograde signals, which would strengthen the intracellular signals generated and lead to T cell-dependent immune responses. That T cells are capable of releasing soluble factors which trigger DCs is substantiated by our findings that

the direct interaction of murine T cells with a transgenic T cell receptor specific for the I-A^{bm12} protein and BM12Ly5.1DC (which express the I-A^{bm12}) causes (i) a 5-fold increase in surface expression of MHC class II molecules and (ii) an increase in the Ca²⁺ in the DCs which is sensitive to high concentrations of ryanodine, which inactivate the RyR Ca²⁺ channel (30, 31), and charybdotoxin, which blocks K⁺ channels on T cells. We suggest that the increase in MHC II surface expression is promoted by efflux of K⁺ via channels present on the surface of T cells which open after the increase in [Ca²⁺]_i triggered by engagement of the T cell receptor. This idea is supported by the observation that up-regulation of MHC II could be blocked by pretreatment of T cells with the K⁺ channel toxin charybdotoxin. A schematic outlining this hypothesis is depicted in Fig. 6.

In conclusion we present evidence that the DHPR-RyR1 signaling machinery plays an important role in up-regulation of MHC class II molecules on the surface of DCs, and this signaling pathway could be an important target for drugs aimed at improving the immune system by increasing the efficiency of antigen presentation or at impairing the immune system by decreasing presentation of autoantigens responsible for the induction of autoimmune disorders.

Acknowledgments—We acknowledge the support of the Departments of Anesthesia and Surgery of the Basel University Hospital. We thank Prof. Ed Palmer for supplying the B6.C-H-2bm12Ly5.1, B6.Ly5.1, and ABM Rg^{-/-} mice and for constructive suggestions, Prof. Isaac Pessah for helpful suggestions, Prof. Gennaro DeLiberio for helpful discussion, and Natalia Gomez-Ospina and Prof. Ricardo Dolmetsch for providing the purified anti-Ca_v1.2 (anti-CCAT) antibodies.

REFERENCES

- Berridge, M. J., Lipp, P., and Bootman, M. D. (2000) *Nat. Rev. Mol. Cell Biol.* **1**, 11–21
- Berridge, M., Bootman, M. D., and Roderick, H. L. (2003) *Nat. Rev. Mol. Cell Biol.* **4**, 517–529
- Catterall, W. A. (2000) *Annu. Rev. Cell Dev. Biol.* **16**, 521–555
- Catterall, W. A., Perez-Reyes, E., Snutch, T. P., and Striessnig, J. (2005) *Pharmacol. Rev.* **57**, 411–425
- Sutko, J. L., and Airey, J. A. (1996) *Physiol. Rev.* **76**, 1027–1071
- Franzini-Armstrong, C., and Protasi, F. (1997) *Physiol. Rev.* **77**, 699–729
- Bers, D. M. (2004) *J. Mol. Cell. Cardiol.* **37**, 417–429
- Treves, S., Anderson, A. A., Ducreux, S., Divet, A., Bleunven, C., Grasso, C., Paesante, S., and Zorzato, F. (2005) *Neuromuscul. Disord.* **15**, 577–587
- Robinson, R., Carpenter, D., Shaw, M. A., Halsall, J., and Hopkins, P. (2006) *Hum. Mutat.* **27**, 977–989
- Wehrens, X. H., and Marks, A. R. (2003) *Trends Biochem. Sci.* **28**, 671–678
- George, C. H., Jundi, H., Thomas, N. L., Fry, D. L., and Lai, F. A. (2007) *J. Mol. Cell. Cardiol.* **42**, 34–50
- Tarroni, P., Rossi, D., Conti, A., and Sorrentino, V. (1997) *J. Biol. Chem.* **272**, 19808–19813
- Hosoi, E., Nishizaki, C., Gallagher, K. L., Wyre, H. W., Matsuo, Y., and Sei, Y. (2001) *J. Immunol.* **167**, 4887–4894
- O'Connell P. J., Klyachko, V. A., and Ahern, G. P. (2002) *FEBS Lett.* **512**, 67–70
- Ducreux, S., Zorzato, F., Ferreiro, A., Jungbluth, H., Muntoni, F., Monnier, N., Müller, C. R., and Treves, S. (2006) *Biochem. J.* **395**, 259–266
- Goth, S. R., Chu, R. A., Gregg, J. P., Cjerednichenko, G., and Pessah, I. N. (2006) *Environ. Health Perspect.* **114**, 1083–1091
- Bracci, L., Vukcevic, M., Spagnoli, G., Ducreux, S., Zorzato, F., and Treves, S. (2007) *J. Cell Sci.* **120**, 2232–2240
- Sei, Y., Gallagher, K. L., and Basile, A. S. (1999) *J. Biol. Chem.* **274**, 5995–6002
- Uemura, Y., Liu, T. Y., Narita, Y., Suzuki, M., Ohshima, S., Mizukami, S., Ichihara, Y., Kikuchi, H., and Matsushita, S. (2007) *Biochem. Biophys. Res. Commun.* **362**, 510–515
- Trombetta, S. E., and Mellman, I. (2005) *Annu. Rev. Immunol.* **23**, 975–1028
- Lanzavecchia, A. (1996) *Curr. Opin. Immunol.* **8**, 348–354
- Cella, M., Engering, A., Pinet, V., Pieters, J., and Lanzavecchia, A. (1997) *Nature* **388**, 782–787
- Dauer, M., Obermaier, B., Herten, J., Haerle, C., Pohl, K., Rothenfusser, S., Schnurr, M., Endres, S., and Eigler, A. (2003) *J. Immunol.* **170**, 4069–4076
- Bäckström, B. T., Müller, U., Hausmann, B. T., and Palmer, E. (1998) *Science* **281**, 835–838
- Chandy, G. K., Wulff, H., Beeton, C., Pennington, M., Gutman, G. A., and Cahalan, M. D. (2004) *Trends Pharmacol. Sci.* **25**, 280–289
- Sauter, B. B., Albert, M. L., Francisco, L., Larsson, M., Somersan, S., and Bhardwaj, N. (2000) *J. Exp. Med.* **191**, 423–433
- Zhou, L. J., and Tedder, T. F. (1996) *Proc. Natl. Acad. Sci. U. S. A.* **93**, 2588–2592
- Lachmann M., Berchtold S., Hauber, J., and Steinkasserer, A. (2002) *Trends Immunol.* **23**, 273–275
- Zhao, F., Li, P., Chen, S. R., Louis, C. F., and Fruen, B. R. (2001) *J. Biol. Chem.* **276**, 13810–13816
- Meissner, G. (1986) *J. Biol. Chem.* **261**, 6300–6306
- Zimanyi, I., Buck, J., Abranson, J. J., Mack, M. M., and Pessah, I. (1992) *Mol. Pharmacol.* **42**, 1049–1067
- Kwan, C. Y., Takemura, H., Obie, J. F., Thastrup, O., and Putney, J. W., Jr. (1990) *Am. J. Physiol.* **258**, C1006–C1015
- Poggi, A., Rubartelli, A., and Zocchi, R. (1998) *J. Biol. Chem.* **273**, 7205–7209
- Gomez-Ospina, N., Tsuruta, F., Barreto-Chang, O., Hu, L., and Dolmetsch, R. (2006) *Cell* **127**, 591–606
- Ralevic, R., and Burnstock, G. (1998) *Pharmacol. Rev.* **50**, 413–455
- Lewis, R. S. (2001) *Annu. Rev. Immunol.* **19**, 497–521
- Panyi, G., Varga, Z., and Gaspar, R. (2004) *Immunol. Lett.* **92**, 55–66
- Vignali, S., Leiss, V., Karl, R., Hofmann, F., and Welling, A. (2006) *J. Physiol. (Lond.)* **572**, 691–706
- Sedej, S., Tsujimoto, T., Zorec, R., and Rupnik, M. (2004) *J. Physiol. (Lond.)* **555**, 769–782
- Badou A., Jha, M. K., Matza, D., Mehal, W. Z., Freichel, M., Flockerzi, V., and Flavell, R. A. (2006) *Proc. Natl. Acad. Sci. U. S. A.* **103**, 15529–15534
- Tanabe, T., Beam, K. G., Adams B. A., Niidome, T., and Numa, S. (1990) *Nature* **346**, 567–569
- Nakai, J., Tanabe, T., Konno, T., Adams, B., and Beam, K. G. (1998) *J. Biol. Chem.* **273**, 24983–24986
- Grabner, M., Dirksen, R. T., Suda, N., and Beam, K. G. (1999) *J. Biol. Chem.* **274**, 21913–21919
- Näbauer, M., Callewaert, G., Cleemann, L., and Morad, M. (1989) *Science* **244**, 800–803
- Schuhmeier, R. P., Goudadon, E., Ursu, D., Kaseielke, N., Flucher, B. E., Grabner, M., and Melzer, W. (2005) *Biophys. J.* **88**, 1765–1777
- Basu, S., Binder, R. J., Suto, R., Anderson, K. M., and Srivastava, P. K. (2000) *Int. Immunol.* **12**, 1539–1546
- Shi, Y., Evans, J. E., and Rock, K. L. (2003) *Nature* **425**, 516–521
- Rovere-Querini, P., Capobianco, A., Scaffidi, P., Valentini, B., Catalanotti, F., Giazton, M., Dumitriu, I. E., Müller, S., Iannacone, M., Traversari, C., and Bianchi, M. E. (2004) *EMBO Rep.* **5**, 825–830
- Chow, A., Toomre, D., Garrett, W., and Mellman, I. (2002) *Nature* **418**, 988–994
- Santambrogio, L., Sato, A. K., Fischer, F. R., Dorf, M. E., and Stern, L. J. (1999) *Proc. Natl. Acad. Sci. U. S. A.* **96**, 15050–15055
- Santambrogio, L., Sato, A. K., Carven, G. J., Belyasnkaya, S. L., Strominger, J. L., and Stern, L. J. (1999) *Proc. Natl. Acad. Sci. U. S. A.* **96**, 15056–15061

Frequent Calcium Oscillations Lead to NFAT Activation in Human Immature Dendritic Cells*

Received for publication, September 16, 2009, and in revised form, March 25, 2010. Published, JBC Papers in Press, March 26, 2010, DOI 10.1074/jbc.M109.066704

Mirko Vukcevic[‡], Francesco Zorzato^{‡§}, Giulio Spagnoli[¶], and Susan Treves^{‡§1}

From the [‡]Departments of Anaesthesia and Biomedicine and the [¶]Institute of Surgical Research, Basel University Hospital, Basel 4031, Switzerland and the [§]Department of Experimental and Diagnostic Medicine, General Pathology Section, University of Ferrara, Ferrara 44100, Italy

Spontaneous Ca^{2+} oscillations have been observed in a number of excitable and non-excitable cells, but in most cases their biological role remains elusive. In the present study we demonstrate that spontaneous Ca^{2+} oscillations occur in immature human monocyte-derived dendritic cells but not in dendritic cells stimulated to undergo maturation with lipopolysaccharide or other toll like-receptor agonists. We investigated the mechanism and role of spontaneous Ca^{2+} oscillations in immature dendritic cells and found that they are mediated by the inositol 1,4,5-trisphosphate receptor as they were blocked by pretreatment of cells with the inositol 1,4,5-trisphosphate receptor antagonist Xestospongin C and 2-aminoethoxydiphenylborate. A component of the Ca^{2+} signal is also due to influx from the extracellular environment and may be involved in maintaining the level of the intracellular Ca^{2+} stores. As to their biological role, our results indicate that they are intimately linked to the “immature” phenotype and are associated with the translocation of the transcription factor NFAT into the nucleus. In fact, once the Ca^{2+} oscillations are blocked with 2-aminoethoxydiphenylborate or by treating the cells with lipopolysaccharide, NFAT remains cytoplasmic. The results presented in this report provide novel insights into the physiology of monocyte-derived dendritic cells and into the mechanisms involved in maintaining the cells in the immature stage.

Dendritic cells (DCs)² are the most potent antigen presenting cells and are thought to be the initiators and modulators of the immune response (1). In general, DCs exist in two forms, immature DCs (iDC) and mature DCs. Immature DCs are extremely efficient at endocytosis; they reside in the peripheral tissues and continuously sample their environment for the presence of foreign antigens. After capturing antigens, they become activated and migrate to the lymphoid tissues and in the process lose the ability to take up new antigens, increase

their surface expression of major histocompatibility complex II molecules and co-stimulatory molecules involved in antigen presentation to T cells, and reach their full maturation stage (1–3). Although generally correct, this picture is now proving to be too simple. For example, it was recently found that iDCs are also involved in induction and maintenance of T cell tolerance in peripheral tissues (4).

Immature DCs, produced by culturing monocytes for 5 days in medium containing granulocyte-macrophage stimulating factor and interleukin-4 (IL-4), are phenotypically, morphologically, and functionally identical with iDCs occurring *in vivo* (5). Their maturation is controlled by Toll-like receptors (TLRs), one of the best characterized classes of pattern recognition receptors of mammalian species. Most mammalian species express about 10–15 different TLRs that are encoded by a yet to be defined number of genes. Interestingly, distinct subsets of DCs express different TLRs, and their engagement results in DC maturation (6). In fact, monocyte-derived DCs can be induced to mature very efficiently by incubating them with nanogram to microgram (per ml) concentrations of lipopolysaccharide (LPS) through engagement of TLR4 receptors (7). In addition, other ligands such as the synthetic TLR7 ligand imidazoquinoline, a reagent already used as adjuvant in the treatment of viral infections and skin tumors (8–10), can also induce maturation of iDCs *in vitro*. The signaling pathways leading to DC maturation are complex and involve nuclear translocation of the transcription factor NF- κ B as well as increases in the cytoplasmic Ca^{2+} concentration ($[\text{Ca}^{2+}]$) (11–15). Ca^{2+} is one of the most ubiquitous second messengers underlying cellular responses such as secretion, motility, proliferation, and death. Interestingly, Ca^{2+} -sensitive transcription factors including NFAT and NF- κ B regulate the expression of Ca^{2+} -sensitive genes including IL-2, IL-3, IL-4, tumor necrosis factor- α , and interferon- γ (16, 17). Some cell types exhibit oscillatory changes of their cytosolic Ca^{2+} , and these have been correlated to a variety of cellular functions. For example, in T-cells, depending on their frequency, oscillations trigger Ca^{2+} -dependent activation of the transcription factors NFAT, NF- κ B, and c-Jun N-terminal kinase (JNK) (18). In human bone marrow-derived mesenchymal stem cells, Ca^{2+} oscillations have been implicated in differentiation (19), in embryonic stem cell-derived primitive endodermal cells, oscillations have been implicated in the exo/endocytotic vesicle shuttle (20), and in human astrocytoma cells Ca^{2+} oscillations have been implicated in cell migration (21). Ca^{2+} signaling is also known to be involved in the regulation of immune cell function, and its

* This work was supported by Swiss National Science Foundation Grants SNF 3200B0-114597 and 3200B0-104060.

¹ To whom correspondence should be addressed: Depts. of Anesthesia and Biomedical Research, Basel University Hospital, Hebelstrasse 20, 4031 Basel, Switzerland. Tel.: 41-61-2652373; Fax: 41-61-2653702; E-mail: susan.treves@unibas.ch.

² The abbreviations used are: DC, dendritic cell; $[\text{Ca}^{2+}]$, intracellular calcium concentration; iDC, immature DC; LPS, lipopolysaccharide; NFAT, nuclear factor of activated T-cells; NF- κ B, nuclear factor κ -light-chain enhancer of activated B cells; DAPI, 4' 6-diamidino-2-phenylindole, dihydrochloride; 2-APB, 2-aminoethoxydiphenyl borate; IL-4, interleukin-4; TLR, Toll-like receptor; InsP₃R, inositol 1,4,5-trisphosphate receptor; TIRF, total internal reflection fluorescence; FITC, fluorescein isothiocyanate.

Immature Dendritic Cells Exhibit Spontaneous Ca^{2+} Oscillations

importance is emphasized by the fact that most immune cells including DCs express several classes of Ca^{2+} channels on their plasma membrane (22) as well as intracellular Ca^{2+} channels belonging to the $InsP_3R$ and ryanodine receptor family (23–28). In this context it is worth mentioning that the involvement of Ca^{2+} signaling events in DC maturation has been postulated for a number of years (14, 15), and we recently demonstrated that ryanodine receptor 1-mediated Ca^{2+} signals can act synergistically with signals generated via Toll-like receptors driving DC maturation (26, 27).

In the present report we show that spontaneous Ca^{2+} oscillations occur in iDCs. These oscillations occur only in iDCs and are lost during the maturation process, and their abrogation leads to the cytoplasmic localization of endogenous NFAT. The results of this study offer additional insights into some of the signaling processes controlling maturation of DCs.

MATERIALS AND METHODS

Generation of Dendritic Cells—iDCs were generated from human peripheral blood mononuclear cells as previously described (29). Briefly, monocytes were purified by positive sorting using anti-CD14-conjugated magnetic microbeads (Miltenyi Biotech, Bergisch Gladbach, Germany). The recovered cells (95–98% purity) were cultured for 5 days at $3\text{--}4 \times 10^5/\text{ml}$ in differentiation medium containing RPMI with 10% fetal calf serum, glutamine, nonessential amino acids, and antibiotics (all from Invitrogen) supplemented with 50 ng/ml granulocyte-macrophage stimulating factor (Laboratory Pablo Casarà, Buenos Aires, Argentina) and 1000 units/ml IL-4 (a gift from A. Lanzavecchia, Institute for Research in Biomedicine, Bellinzona, Switzerland). Maturation was induced by the addition of LPS 1 $\mu\text{g}/\text{ml}$ (from *Salmonella abortus equi*, Sigma) to the culture medium. In some experiments DC maturation was induced by the addition of the synthetic TLR7 agonist, imidazoquinoline (3M-001) (final concentration 3 μM), that was kindly provided by 3M Pharmaceuticals (St. Paul, MN).

Single Cell Intracellular Ca^{2+} Measurements— Ca^{2+} measurements were performed on DCs loaded with fast Ca^{2+} indicator fluo-4 (Invitrogen; 5 μM final concentration). In some experiments cells were incubated with 100 μM 2-aminoethoxydiphenylborate (2-APB) (Calbiochem), 1 μM Xestospongine C (Calbiochem), or 2 μM thapsigargin with 0.5 mM EGTA during the loading procedure. After loading, cells were rinsed once, resuspended in Krebs-Ringer medium, and allowed to adhere to poly-L-lysine (1:60 dilution) (Sigma)-treated glass coverslips that were than mounted onto a 37 °C thermostatted chamber. On-line epifluorescence images were acquired every 100 ms for 50 s using a Nikon Eclipse TE2000-E fluorescent microscope equipped with an oil immersion CFI Plan Apochromat 60 \times TIRF objective (1.45 numerical aperture). Changes in fluorescence were detected by exciting at 488 nm and recording the emission at 510 nm via an electron multiplier C9100–13 Hamamatsu CCD camera which allows fast data acquisition (maximal temporal resolution 1 frame (110 \times 110 pixels/8 ms). Where indicated, either 1 $\mu\text{g}/\text{ml}$ LPS or 2 μM U73122 (Bio Mol) was added during the measurements. To investigate the dynamics of Ca^{2+} influx, we measured fluorescent changes in the TIRF mode; first we identified the focal plane at the cover-

glass/cell membrane contact with a surface reflective interference contrast filter, and this focal plane was maintained throughout the recordings by means of the perfect focus system that exploits an infrared laser beam and a quadrant diode for online control of the microscope focusing motor. Image analysis was performed with the MetaMorph (Molecular Devices) software package.

Endocytosis and Quantitative Gene Expression Analysis—Endocytosis was followed by incubating DCs in RPMI medium containing 0.5 mg/ml fluorescein isothiocyanate (FITC)-labeled dextran (Fluka Biochemicals, Buchs, Switzerland) for 30 min at 37 °C. Cells were washed twice in ice-cold phosphate-buffered saline fixed with 1% paraformaldehyde, and the number of FITC-positive cells was assessed by flow cytometry. In some experiments, before incubation with FITC-dextran, cells were treated for 45 min with 100 μM 2-APB or with LPS (1 $\mu\text{g}/\text{ml}$) or with the TLR-7 agonist 3M-001 (3 μM) for 18 h. Gene expression was quantified by real time PCR as previously described (26). Briefly, $1\text{--}2 \times 10^6$ iDCs were incubated for 18 h with 1 μM Xestospongine C, 100 μM 2-APB, 3 μM imidazoquinoline (3M-001), or 1 $\mu\text{g}/\text{ml}$ LPS. Total RNA was extracted and treated with deoxyribonuclease I (Invitrogen) to eliminate contaminant genomic DNA. After reverse transcription using 500 ng of RNA and the Moloney murine leukemia virus reverse transcriptase (Invitrogen), cDNA was amplified by quantitative real-time PCR in the ABI PrismTM7700 using the TaqMan® technology. Commercially available exon-intron junction-designed primers for glyceraldehyde-3-phosphate dehydrogenase, CD83, CD80 CD86, interferon- α , and IL23A (Applied Biosystems, Foster City, CA) were used. Gene expression was normalized using self-glyceraldehyde-3-phosphate dehydrogenase as reference (26). The data from DCs isolated from five donors were pooled and are expressed as -fold increase in gene expression compared with untreated iDCs.

Immunofluorescence—Indirect immunofluorescence was performed on methanol:acetone (1:1)-fixed DCs using rabbit anti-NFATc1 (sc-13033) or rabbit anti-NF- κ B p65 antibody (sc-109, Santa Cruz Biotechnology) followed by Alexa fluor 488-conjugated chicken anti-rabbit antibody (Invitrogen). Nuclei were visualized by 4' 6-diamidino-2-phenylindole, dihydrochloride (DAPI; 100 μM) (Invitrogen) staining. Fluorescence was detected using a fluorescent Axiovert S100 TV inverted microscope (Carl Zeiss GmbH, Jena, Germany) equipped with an $\times 40$ FLUAR objective and Zeiss filter sets (BP 475/40, FT 500, and BP 530/50; BP 546, FT 560, and 575–640) for detection of DAPI and FITC fluorescence, respectively.

Immunoblotting Analysis—The cytosolic fraction of 6×10^6 DCs was extracted as described by Healy *et al.* (30). Briefly, cells were washed once and resuspended in 50 μl of ice-cold buffer containing 20 mM HEPES, pH 7.5, 5 mM NaCl, and 2 mM EDTA to which 50 μl of 20 mM HEPES, pH 7.5, 4 mM NaCl, 2 mM EDTA, and 0.8% Nonidet P-40 were added. Cells were incubated on ice for 2 min, and the nuclear and membrane fractions were removed by centrifugation (600 $\times g$, 10 min, 4 °C). Laemmli loading buffer (10% glycerol, 1% β -mercaptoethanol, 2% SDS, 65 mM Tris-HCl, pH 6.8) was added to the supernatant (cytosolic fraction) which was boiled for 5 min and then loaded onto a 7.5% SDS-polyacrylamide gel. Proteins were transferred

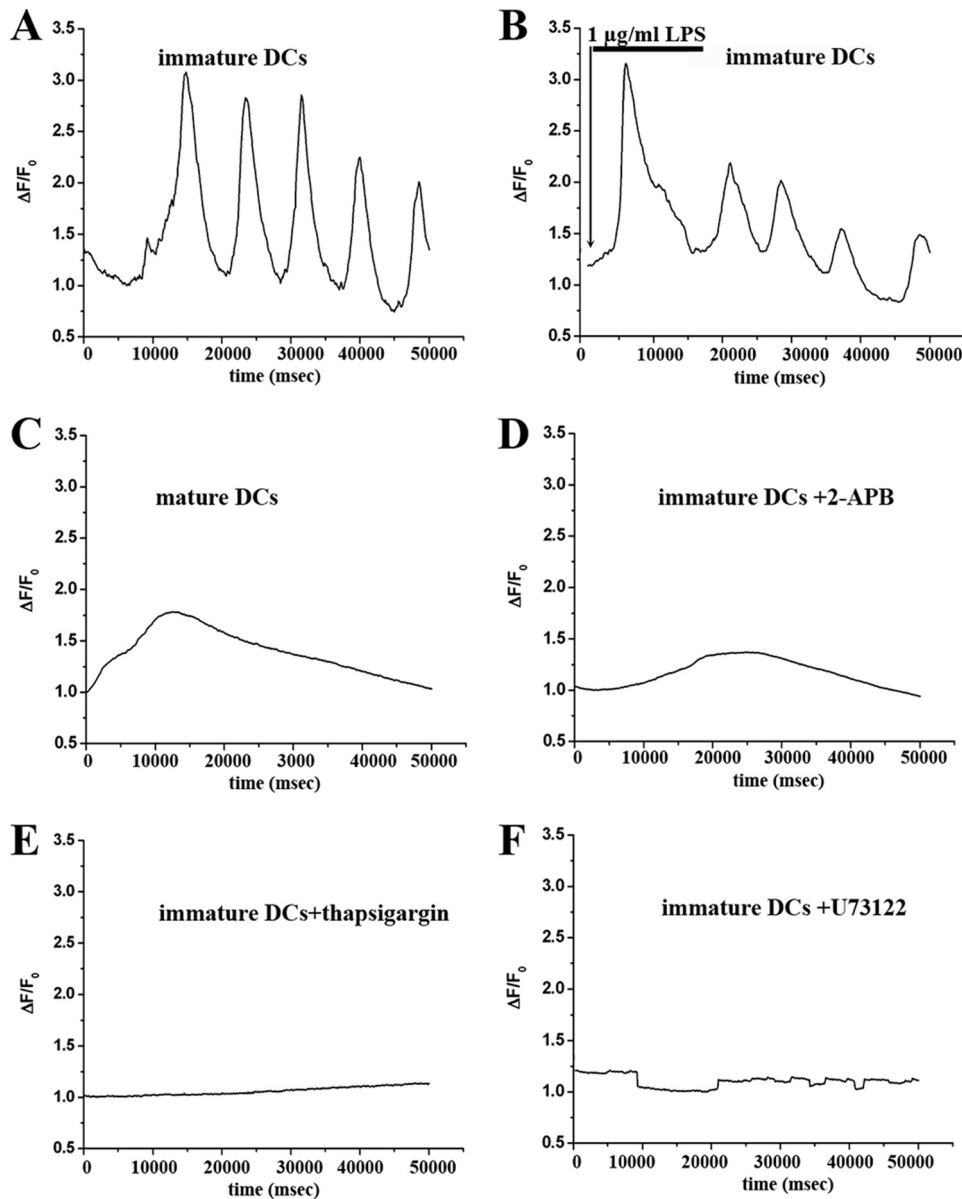


FIGURE 1. Immature human dendritic cells show spontaneous Ca^{2+} oscillations. Fluo-4-loaded dendritic cells were allowed to deposit on poly-L-lysine-treated coverslips, and the changes in fluo-4 fluorescence were monitored every 100 ms as described under "Materials and Methods." Shown is a representative trace of the oscillations observed in immature DCs (A), in iDCs to which 1 μ g/ml LPS was added (arrow) (B), in dendritic cells treated with LPS (1 μ g/ml) overnight (mature DCs) (C), in iDCs pretreated with 2-APB for 45 min (D), in iDCs pretreated with 2 μ M thapsigargin and 0.5 mM EGTA (E), and in iDCs treated with the PLC-inhibitor U73122 (2 μ M) (F). Traces are representative of experiments carried out on cells from five different donors. Results are expressed as F/F_0 , where F is the fluorescent value at any given time, and F_0 is the initial fluorescence level obtained at time 0.

TABLE 1
Characterization of spontaneous Ca^{2+} oscillations in DCs

Frequency is represented as a percentage of cells with 1, 2–4, and 4–8 peaks during 50 s. Statistical analysis was performed using the χ^2 test. $p < 0.0001$. All groups were significantly different compared to iDC $p < 0.002$.

	Total no. cells	1 peak/ 50 s	2–4 peaks/ 50 s	4–8 peaks/ 50 s
		%	%	%
iDC	83	8.30	51.70	40.00
iDC+ 100 μ M La^{3+}	60	36.70	45	18.33
iDC+ 0.5 mM EGTA	66	28.80	53.80	17.40
iDC+ 100 μ M 2-APB	116	100	0	0
iDC+ 1 μ M Xesto C	56	48.21	41	10.71
LPS-matured DC	162	100	0	0
TLR7-matured DC	266	70.00	20.00	10.00

onto nitrocellulose, and the blots were probed with a rabbit anti-NFATc1 antibody (1:500; sc-13033, Santa Cruz Biotechnology) followed by peroxidase-conjugated protein G (1:250,000) and with mouse anti- β tubulin (Santa Cruz sc-5274) followed by peroxidase-conjugated anti-mouse IgG (1:200,000). The immunopositive bands were visualized by autoradiography using the Super Signal West Dura chemiluminescence kit from Thermo Scientific (for NFAT) and BM chemiluminescence kit from Roche Applied Science (for β -tubulin).

Statistical Analysis and Software Programs—Statistical analysis was performed using Student's t test for paired samples; means were considered statistically significant when the p value was < 0.05 . When more than two samples were compared, analysis was performed by the ANOVA test followed by the Bonferroni post hoc test. The PROC MIXED statistical analysis program (SAS 9.2) on log-transformed data were used for real-time PCR gene expression analysis from independent biological replicates. The Origin computer program (Microcal Software, Inc., Northampton, MA) was used to generate graphs and for statistical analysis. Statistical analysis of categorical data was performed using the χ^2 test for contingency tables with a 0.05 level of significance using R software (R development Core team 2008; R Foundation for Statistical Computing, Vienna, Austria; ISBN 3-900051-07-0) was used to perform χ^2 tests.

RESULTS

Immature DCs were loaded with the fast calcium indicator fluo-4 and were observed by conventional epifluorescence microscopy in the absence of added stimuli. Such cells display large rhythmic fluctuations of their cytoplasmic Ca^{2+} (Fig. 1A) with $\sim 40\%$ of the cells exhibiting oscillations with a frequency of one peak every 12.5 s (Table 1). Interestingly, the addition of LPS (Fig. 1B) or of the TLR-7 agonist (not shown) to iDCs did not affect the high frequency oscillations nor did it cause any immediate changes in the $[Ca^{2+}]_i$. On the other hand, when mature DCs (treated with 1 μ g/ml LPS for 18 h) were observed under identical conditions, the high frequency oscillations were no longer present (Fig. 1C). In the latter case of the 162 individual cells that were monitored,

Immature Dendritic Cells Exhibit Spontaneous Ca^{2+} Oscillations

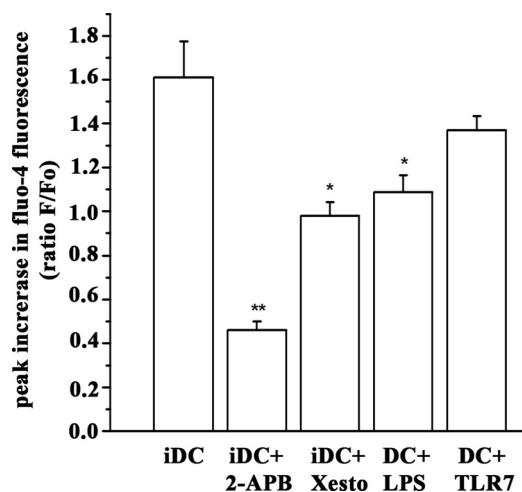


FIGURE 2. **Magnitude of spontaneous Ca^{2+} oscillations in DCs.** The histograms show the peak Ca^{2+} transient ($\Delta F/F_0$) in untreated iDCs or cells treated as indicated with 2-APB (100 μM), Xestospongine C (Xesto; 1 μM), and LPS (1 $\mu\text{g}/\text{ml}$ 18 h). Experiments were performed on cells isolated from at least four different donors, and results are expressed as the mean (\pm S.E.) peak in fluo-4 fluorescence of 26–145 cells. Statistical analysis was performed using the ANOVA test followed by the Bonferroni post hoc test. *, $p < 0.015$; **, $p < 0.0005$.

100% responded with a single, small increase of the $[\text{Ca}^{2+}]_i$ within the 50-s measurement (Table 1). To determine the source of Ca^{2+} in the oscillations, iDCs were treated with (i) 100 μM 2-APB, a blocker of store-operated Ca^{2+} entry, and of InsP_3 -mediated Ca^{2+} release, (ii) 2 μM thapsigargin, a SERCA (sarco(endo)plasmic reticulum calcium ATPase) inhibitor that leads to depletion of intracellular Ca^{2+} stores, and (iii) 2 μM U73122, an inhibitor of phospholipase C. The addition of these compounds completely abolished the spontaneous Ca^{2+} oscillations (Fig. 1, D–F). DCs were also incubated with other pharmacological agents as shown in Table 1; the addition of 100 μM La^{3+} or 0.5 mM EGTA significantly reduced the frequency of oscillations from 40% cells showing 4–8 peaks/50 s to about 18% cells showing 4–8 peaks/50 s, indicating that Ca^{2+} influx plays some role in the oscillatory events. The addition of 1 μM Xestospongine C (an inhibitor of InsP_3 -mediated Ca^{2+} release) significantly diminished the frequency of the oscillations (Table 1) as well as the peak fluo-4 fluorescence in iDCs (Fig. 2). These results strongly suggest that the oscillations are mainly due to InsP_3 -mediated release of Ca^{2+} from intracellular stores, with a component (probably involved in store refilling) due to influx from the extracellular environment. The phenotype of mature DCs, on the other hand, was quite different irrespective of whether the cells had been induced to mature via TLR-4 activation (by overnight incubation with 1 $\mu\text{g}/\text{ml}$ LPS) or via activation of TLR-7 (by overnight incubation with 3 μM imidazoquinoline (3M-001)). In fact, LPS-matured DCs did not show the high frequency oscillations but rather small and slow (1 peak/50 s) spontaneous fluctuations of their $[\text{Ca}^{2+}]_i$. Interestingly, incubation with imidazoquinoline, which does not transmit a maturation signal as strong as that conveyed by LPS (see CD83 expression in Fig. 5A), resulted in DCs with an intermediate phenotype; that is, with only a small proportion of cells showing 2–8 oscillations/min whose magnitude is comparable with that exhibited by iDCs (Table 1 and Fig. 2). The slow peak

Ca^{2+} increase observed in mature DCs was reduced by more than 50% by the addition of 100 μM 2-APB (Fig. 2), whereas the peak transient observed in the presence of Krebs-Ringer medium containing no additional Ca^{2+} and 0.5 mM EGTA was not different from that observed in the presence of extracellular Ca^{2+} (1.79 \pm 0.31 and 2.10 \pm 0.35 ΔF increase in Ca^{2+} and EGTA containing medium respectively). These results indicate that in mature DCs as well, the slow Ca^{2+} transient is mainly due to release from intracellular stores.

To directly determine whether Ca^{2+} influx accompanies the oscillations, we examined the DCs by TIRF microscopy, which allows one to monitor changes in fluorescence occurring at the plasma membrane or within microdomains close to the plasma membrane. As shown in Fig. 3 oscillations are accompanied by $[\text{Ca}^{2+}]_i$ influx in iDCs. Cells were allowed to attach onto the glass coverslips, and the areas of attachment were identified with the surface reflection interference contrast filter (Fig. 3, panel B). This focal plane was fixed using the perfect focus system, and changes in the $[\text{Ca}^{2+}]_i$, which in this case represent Ca^{2+} events occurring at or very close to the plasma membrane, were monitored (Fig. 3, panel C). The pseudocolor images in panel C represent the changes of fluo-4 fluorescence $\Delta F(F/F_0)$ at four time points, whereas panel D represents the kymographs of three selected cells (arrows in panel C) showing that these changes in $[\text{Ca}^{2+}]_i$ occur at different time points in different cells during the 50 s of recording. The specificity of the signal is demonstrated by the fact that the increase in fluo-4 fluorescence only occurs when cells are bathed in Krebs-Ringer solution containing 2 mM Ca^{2+} but is absent when cells are bathed in Krebs-Ringer solution containing 100 μM La^{3+} (a nonspecific blocker of plasma membrane Ca^{2+} channels) or in LPS-matured DCs (Fig. 3, panel E).

These results support the finding that oscillations of the $[\text{Ca}^{2+}]_i$ are a specific feature of iDC that is lost upon differentiation but convey little information as to their biological role. We hypothesized that oscillations may be implicated in maintaining the immature phenotype by acting on transcription factors, in particular on the Ca^{2+} -sensitive transcription factor NFAT. To dissect the intracellular pathways directly downstream of the spontaneous Ca^{2+} oscillations, we followed the intracellular localization of endogenous NFAT in oscillating iDCs or in DCs in which oscillations had been inhibited by 2-APB and in mature DCs. The cytosolic fraction of DCs was obtained from untreated iDCs, iDCs treated for 15 and 45 min with 2-APB, LPS-matured DCs, and iDCs treated with cyclosporine, a drug that reduces the nuclear translocation of NFAT by inhibiting the Ca^{2+} -dependent phosphatase calcineurin. Fig. 4A shows a representative Western blot and Fig. 4B shows a bar graph of the intensities of the immunopositive bands of the cytosolic content of NFATc1. LPS-matured DCs, which lack the high frequency Ca^{2+} oscillations, show the highest level of cytoplasmic expression of NFAT. Similarly, its cytoplasmic level is high in cyclosporine-treated iDCs but is significantly reduced in the cytoplasm of untreated iDCs. Treatment of the latter cells with 2-APB induced the cytoplasmic localization of NFATc1. Fig. 4C shows the subcellular localization of NFATc1 by immunofluorescence; indeed, in iDCs a number of cells exhibit nuclear distribution of NFAT (arrows), whereas iDCs

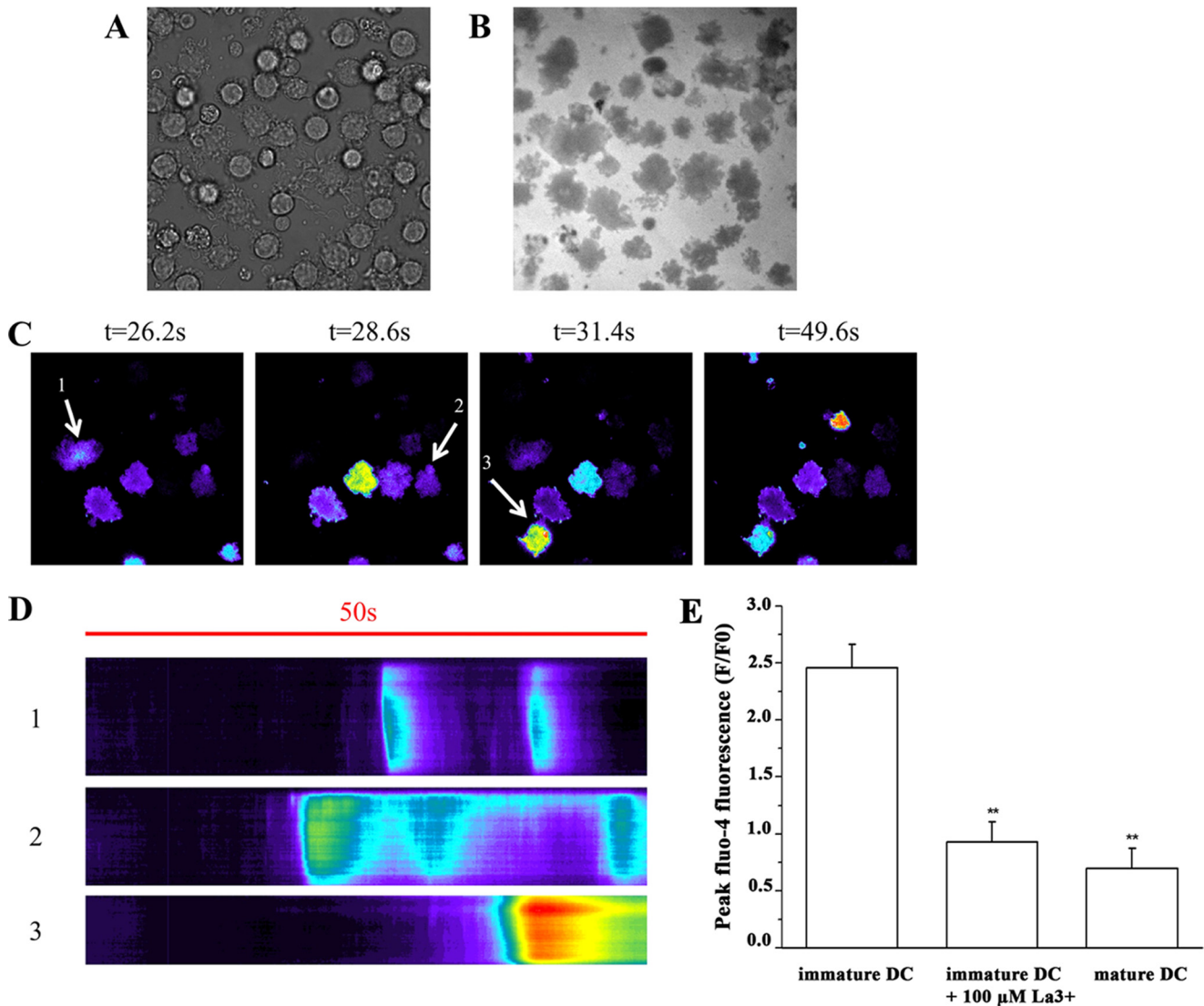


FIGURE 3. Calcium influx in iDCs monitored by TIRF microscopy. Fluo-4 loaded iDCs were resuspended in Krebs-Ringer medium containing 2 mM Ca^{2+} or 100 μM La^{3+} and allowed to attach to poly-L-lysine-coated glass coverslips. Once attached, cells were monitored by brightfield (*panel A*) with a surface reflection interference contrast filter to monitor glass coverslip/cell membrane attachment site (*panel B*) or by TIRF microscopy (*panel C*). Images in *panel C* show pseudocolored ratiometric (F/F_0) changes in membrane-associated $[\text{Ca}^{2+}]_i$ at four time points. *Panel D* shows the kymograph representation of the Ca^{2+} changes in 50 s in 3 selected cells from *panel C*. *Panel E* shows the mean (\pm S.E.) increase in fluo-4 fluorescence ratio (F/F_0) of iDCs bathed in 2 mM Ca^{2+} containing Krebs-Ringer medium ($n = 57$ cells), in iDCs bathed in Krebs-Ringer medium containing 100 μM La^{3+} ($n = 45$ cells), and in LPS-matured DCs ($n = 20$ cells). Experiments were performed on cells isolated from at least four different donors. **, statistical analysis was performed using the ANOVA test followed by the Bonferroni post hoc test $p < 0.0002$.

treated with cyclosporine or in mature DCs the fluorescence is distributed throughout the cytoplasm. These results indicate that most of the transcription factor NFAT is targeted to the nucleus in oscillating iDCs but that abrogation of Ca^{2+} oscillations with 2-APB results in the preservation of NFATc1 within the cytoplasm. To determine whether this was specifically related to the transcription factor NFAT or a general effect, we also followed the subcellular distribution of p65 (RelA), a component of the NF- κ B transcription complex (NF- κ B1+RelA+I κ B) detectable in the cytoplasm of iDCs that translocates to the nucleus upon DC maturation (12, 13, 26). As shown in Fig. 4D, in LPS-matured DCs NF- κ B is translocated to the nucleus, whereas in iDCs it shows a cytoplasmic distribution. Blocking high frequency oscillations with 2-APB does not result in the nuclear translocation of NF- κ B. Thus, the simple

abrogation of spontaneous Ca^{2+} oscillations is not sufficient to stimulate the cells to undergo maturation, whereas the oscillations appear to regulate nuclear targeting of NFAT and may be intimately linked to the immature phenotype. The latter hypothesis was tested by following the effect of abolishing the high frequency oscillations on the transcription of several genes characteristic of mature DCs. As shown in Fig. 5A, iDCs exhibit low transcription levels of CD80, CD86, CD83, interferon- α , and IL23A, genes that are characteristically transcribed in mature DCs (1, 26, 31). Inhibition of high frequency Ca^{2+} oscillations with Xestospongin C or 2-APB caused a significant (2–20-fold) increase in their levels of expression.

Finally we studied whether the high frequency oscillations are linked to endocytosis, an essential phenotypic characteristic of iDCs (2, 3), by comparing the capacity of iDCs, 2-APB-

Immature Dendritic Cells Exhibit Spontaneous Ca^{2+} Oscillations

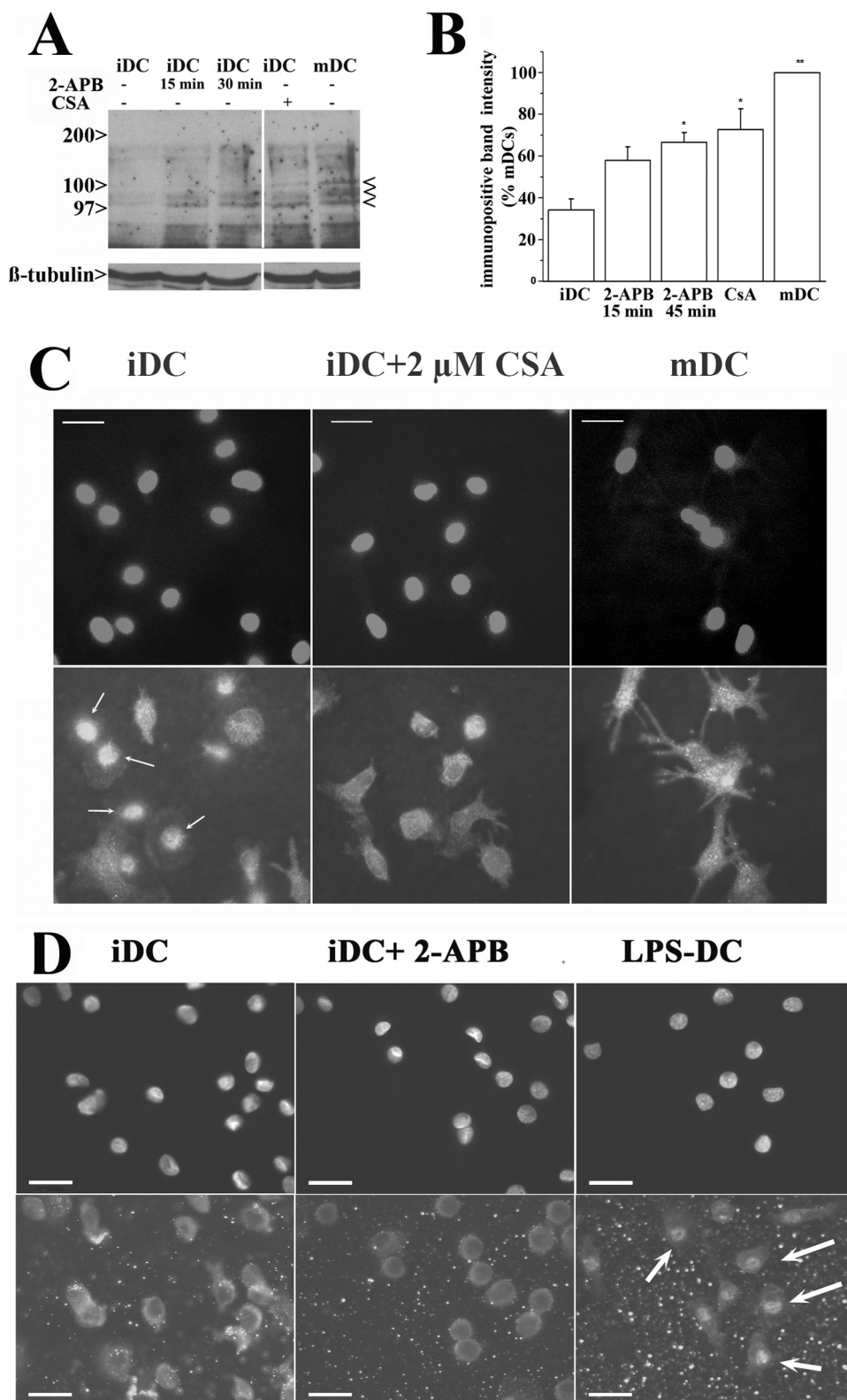
treated iDCs, and mature DCs to endocytose FITC-labeled dextran. Fig. 5B shows that although 2-APB reduces the percentage of FITC-positive cells by 40%, thus significantly reducing the endocytic activity of iDCs, it does not result in a loss of endocytosis comparable with that seen in mature DCs (loss of ~80%). These results strongly suggest that abolishing the Ca^{2+} oscillations generates a signal(s) required for DC maturation.

DISCUSSION

Spontaneous Ca^{2+} oscillations, which are rhythmic changes in $[Ca^{2+}]_i$ in the absence of stimulation, have been reported in certain types of excitable and non-excitable cells such as mesenchymal stem cells, endodermal cells, human astrocytoma cells, astrocytes, pancreatic acinar cells, cardiac myocytes, oocytes, and fibroblasts (19–21, 32–35), although their intracellular mediators and biological role(s) and the functional consequence of their inhibition have in many cases not been elucidated. In the present study we show that spontaneous Ca^{2+} oscillations also occur in human DCs and that these Ca^{2+} events are an exclusive characteristic of cells in the immature stage. In fact, the addition of LPS as well as maturation triggered by other stimuli leads to the loss of the spontaneous high frequency Ca^{2+} transients. A similar finding concerning the loss of spontaneous Ca^{2+} oscillations induced by differentiation was reported in human mesenchymal stem cells upon differentiation into adipocytes (19) and in osteogenic cells upon differentiation into osteoblasts (36, 37). Interestingly, in stem cells Ca^{2+} oscillations occur during the G_1 to S transition, suggesting their involvement in cell cycle progression (38, 39). On the other hand, *in vitro* monocyte-derived DCs do not actively proliferate but, rather, acquire the biochemical and immunological characteristics of naturally occurring iDCs (5) indicating that in these cells the oscillations are probably not involved in cell division.

In immature dendritic cells, intracellular Ca^{2+} stores and $InsP_3$ are intimately connected with the high frequency oscillations, as they were completely abolished by depleting

stores with the Ca^{2+} -ATPase inhibitor thapsigargin ($2 \mu M$) in the presence of EGTA (0.5 mM). The lack of high frequency Ca^{2+} oscillations in mature LPS-treated DCs could not be explained by different levels of expression of functional $InsP_3R$ as mature DCs respond to ATP an $InsP_3$ -mobilizing agonist (23) with a Ca^{2+} transient of comparable magnitude in the



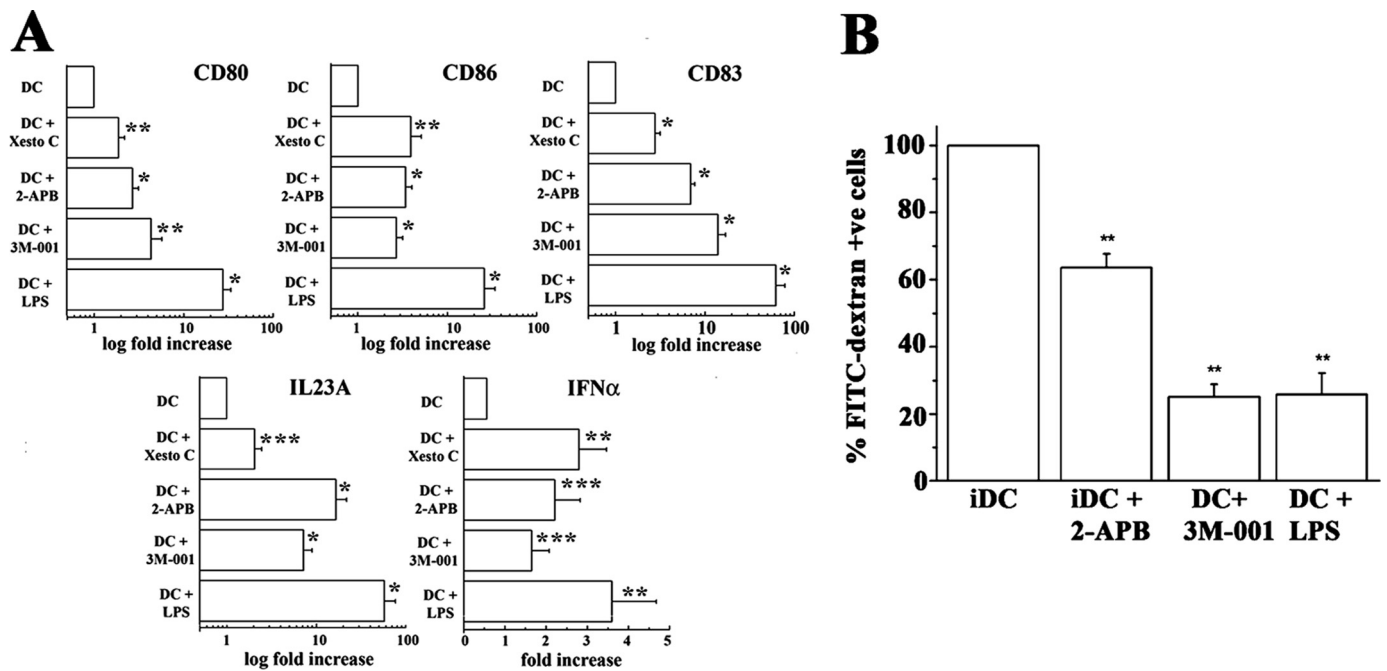


FIGURE 5. Maturation markers of DCs after inhibition of oscillations. *A*, real-time PCR analysis of genes involved in DC maturation in untreated cells or DCs treated for 18 h with Xestospongins C (1 μM), 2-APB (100 μM), TLR-7 agonist 3M-001 (3 μM), or LPS (1 $\mu\text{g}/\text{ml}$). Total RNA was extracted from $1\text{--}2 \times 10^6$ cells, and CD80, CD86, interferon- α , and IL23A gene expression was evaluated by quantitative real-time PCR. Gene expression results are expressed as mean (\pm S.E.)-fold increase as compared with values obtained in iDCs treated with medium. Pooled data are from experiments carried out on cells from five different donors except for CD83 (DC + 3M-001), INF α (DC + 2-APB, 3M-001, LPS), IL23A (DC + Xesto C, DC + 2-APB), where data from four donors were pooled, and CD83 (DC + 2-APB), where data from three donors were pooled. Statistical analysis was performed using the PROC MIXED SAS 9.2 statistical analysis program. *, $p < 0.0001$; **, $p < 0.00025$; ***, $p < 0.001$. *B*, endocytosis of FITC-labeled dextran is shown. Cells treated as described for *panel A* were plated in 12-well plate and incubated at 37 $^{\circ}\text{C}$ for 30 min with 0.5 mg/ml of FITC-labeled dextran. Negative controls were also incubated with FITC-labeled dextran but kept for 30 min at 4 $^{\circ}\text{C}$. Cells were washed 2 times with ice-cold phosphate-buffered saline and fixed with 1% paraformaldehyde, and the % of FITC-positive (+ve) cells was assessed by flow cytometry. *Bar graphs* represent the mean (\pm S.E.) % of fluorescent cells; fluorescent value obtained for iDC was considered 100%. Results from 3–8 experiments from 3–8 different donors were pooled and averaged. Statistical analysis was performed using the ANOVA test followed by the Bonferroni post hoc test. *, $p < 0.018$; **, $p < 0.0003$.

mature and immature stage (results not shown). As to the intracellular mediator(s) of the Ca^{2+} oscillations, U73122, an inhibitor of phospholipase C (40), completely blocked Ca^{2+} transients, whereas both 2-APB, a rather unspecific inhibitor of the InsP_3R also inhibiting Ca^{2+} entry (41, 42), and Xestospongins C, an inhibitor of InsP_3R -mediated Ca^{2+} release (43), significantly decreased the frequency and magnitude of these events. The differences in response to these compounds could be explained by the contribution of Ca^{2+} influx to the maintenance of the Ca^{2+} oscillations. To further address this question, we performed intracellular Ca^{2+} measurements in medium containing 2 mM Ca^{2+} or in the presence of 100 μM La^{3+} to block Ca^{2+} entry. Under these conditions Ca^{2+} fluctuations were still present, but there was a reduction in the percentage of cells

showing high frequency (>4 transients/50 s) Ca^{2+} transients. This result together with the TIRF Ca^{2+} measurements support the hypothesis that Ca^{2+} influx is necessary to maintain the high frequency Ca^{2+} oscillations characteristic of immature dendritic cells through a refilling mechanism.

The most intriguing question arising from the observation that monocyte-derived dendritic cells in the immature stage show frequent Ca^{2+} oscillations concerns the biological role(s) of the oscillations. In macrophages, Ca^{2+} oscillations have been reported to accompany phagocytosis, suggesting a relationship between Ca^{2+} oscillations and uptake of foreign particles (44, 45). *In vivo*, immature DCs continuously sample their environment for foreign antigens, and indeed one of the main functions of iDCs is antigen capture by endocytosis. We originally

FIGURE 4. Influence of Ca^{2+} oscillations on the intracellular localization of NFAT and NF- κB . *A*, shown is a representative Western blot of the cytoplasmic fraction of iDCs treated as indicated and LPS (1 $\mu\text{g}/\text{ml}$)-matured DC (mDCs). In each lane the proteins present in the cytoplasmic extract of 6×10^6 cells was separated on 7.5% SDS-polyacrylamide gel and blotted onto nitrocellulose. The blot was cut into two; the upper portion (>60 kDa) was incubated with rabbit anti-NFATc1 followed by peroxidase-conjugated anti-rabbit IgG. The lower portion was used as a control for protein loading and developed with β -tubulin. Immunopositive bands were visualized by chemiluminescence; $<$ indicates bands corresponding to NFAT. The experiment was repeated five times on DCs from different donors. *B*, the intensity of the immunopositive bands from five experiments was quantified by densitometry using Bio-Rad GelDoc 2000; the intensities were corrected for β -tubulin content. Values are expressed as % intensity of immunopositive bands of mature DCs. Statistical analysis was performed using the ANOVA test followed by the Bonferroni post hoc test. *, $p < 0.04$; **, $p < 0.00005$. *C*, shown is an immunofluorescence analysis of NFATc1 subcellular distribution in iDCs (untreated or treated with 2 μM cyclosporine (CSA)) and mature DC. Cells were fixed with an ice-cold solution of acetone:methanol (1:1) for 20 min at -20 $^{\circ}\text{C}$. Cells were then incubated with rabbit anti-NFAT followed by Alexa fluor 488-labeled anti-rabbit IgG. Before mounting, DAPI staining was performed to visualize nuclei. The scale bar indicates 25 μm . Arrows indicate nuclear localization of NFAT in iDCs. *D*, NF- κB subcellular distribution in iDCs (untreated or incubated with 100 μM 2-APB for 45 min or with 1 $\mu\text{g}/\text{ml}$ LPS for 60 min) is shown. Cells were fixed with an ice-cold solution of acetone:methanol (1:1) for 20 min at -20 $^{\circ}\text{C}$. Cells were then incubated with rabbit anti-NF- κB p65 polyclonal antibody followed by Alexa fluor 488-labeled anti-rabbit IgG. Before mounting, DAPI staining was performed to visualize nuclei. The scale bar indicates 25 μm . Arrows indicate nuclear translocation of NF- κB in LPS-treated DCs.

Immature Dendritic Cells Exhibit Spontaneous Ca^{2+} Oscillations

hypothesized that the high frequency Ca^{2+} oscillations may be involved in activation of endocytosis, and blocking Ca^{2+} oscillations with 2-APB resulted in a significant but partial decrease of FITC-dextran endocytosis, suggesting that the high frequency oscillations may not be essential for endocytosis as reported in embryonic stem cell-derived primitive endodermal cells (20). Alternatively, the inhibitory effect of 2-APB may reflect the fact that endocytosis is a Ca^{2+} -dependent event requiring InsP_3R activation and/or Ca^{2+} influx (46, 47). On the other hand, the involvement of Ca^{2+} signaling in maturation had been previously documented (26, 28), and it was shown that DC maturation is enhanced by activation of ryanodine receptor-mediated Ca^{2+} release. The results obtained by real time PCR strongly suggest that pharmacological interventions, which decrease the high frequency oscillations, activate signals that are necessary but not sufficient to induce full DC maturation.

We next turned our attention to Ca^{2+} -sensitive transcription factors as Ca^{2+} oscillations have been shown to promote the expression of specific genes in other cell systems (39, 48). We focused our attention on NFAT, a calcineurin-dependent transcription factor, as early work demonstrated that NFAT has the remarkable capacity to sense dynamic changes in the $[\text{Ca}^{2+}]_i$ and is especially tuned to detect high frequent Ca^{2+} oscillations occurring within cells (48, 49). In fact, high frequency oscillations have been shown to activate NFAT by keeping the transcription factor in the nucleus at high enough levels to bind to enhancer sites long enough to allow initiation of transcription. Because in our case only iDCs possess these high frequency Ca^{2+} fluctuations, NFAT should be active and translocated into the nucleus only in iDCs and not in LPS-matured DCs. Western blot analysis of endogenous NFAT indeed showed that the cytosolic fraction of iDCs contains considerable less immunopositive band compared with that present in mature DCs; furthermore, by shutting off the Ca^{2+} oscillations with 2-APB, NFAT is retained in the cytoplasm. As opposed to what was observed for NFAT, the transcription factor NF- κB is activated and translocated into the nucleus in LPS-matured DCs but not in iDCs nor in 2-APB-treated DCs. Thus, simply blocking the high frequency Ca^{2+} oscillations or blocking nuclear translocation of NFAT is not sufficient to induce either nuclear translocation of NF- κB or DC maturation.

Altogether these results indicate that the high frequency Ca^{2+} oscillations depend on the maturation stage of DCs, and we suggest that they act as "frequency encoding" (as opposed to amplitude encoding) signals, whereby through the activation of NFAT, DCs maintain their immature phenotype. Our data do not support recent results showing that LPS induces a transient increase in $[\text{Ca}^{2+}]_i$ in DCs (50–52). We directly tested whether the addition of LPS (1 $\mu\text{g}/\text{ml}$) to iDCs causes an increase in the cytoplasmic $[\text{Ca}^{2+}]_i$, but failed to obtain any response. Similarly, no changes in the $[\text{Ca}^{2+}]_i$ on plasma membrane microdomains after the addition of LPS were observed by TIRF microscopy (data not shown). The differences between our results and those presented in Refs. 50–52 are most likely due to the different experimental models that were used; that is, human monocyte-derived DCs in this study *versus* mouse bone marrow-derived DCs. In fact, as opposed to mouse DCs, immature human

DCs express very low levels of CD14, and thus, the CD14-dependent Ca^{2+} signaling pathways may be absent in our system. Our possibility of using the TIRF microscope has enabled us to directly monitor membrane-associated events, and our results together with those of Matzner *et al.* (51) argue against a major role of Ca^{2+} influx in LPS-mediated Ca^{2+} signaling.

In conclusion, we report that human monocyte-derived iDCs exhibit spontaneous $[\text{Ca}^{2+}]_i$ oscillations that are linked to InsP_3R activation and to, a lesser extent, to Ca^{2+} influx. These high frequency events are lost during maturation and appear to be an endogenous characteristic of the immature phenotype, possibly activating nuclear translocation of NFAT and, thus, enhancing the transcription of genes involved in maintaining the cells immature. The results of the present investigation are important because they point out novel aspects of intracellular signaling in human DC and may open new areas of research that could be developed in the future to help patients requiring modulation of their immune response.

Acknowledgments—We thank Dr. Andrija Tomovic for help with the statistical analysis. We also acknowledge the support of the Departments of Anesthesia and Surgery of Basel University Hospital.

REFERENCES

1. Banchereau, J., and Steinman, R. M. (1998) *Nature* **392**, 245–252
2. Trombetta, E. S., and Mellman, I. (2005) *Annu. Rev. Immunol.* **23**, 975–1028
3. Lanzavecchia, A. (1996) *Curr. Opin. Immunol.* **8**, 348–354
4. Mahnke, K., Schmitt, E., Bonifaz, L., Enk, A. H., and Jonuleit, H. (2002) *Immunol. Cell Biol.* **80**, 477–483
5. Sallusto, F., and Lanzavecchia, A. (1994) *J. Exp. Med.* **179**, 1109–1118
6. Iwasaki, A., and Medzhitov, R. (2004) *Nat. Immunol.* **5**, 987–995
7. Langenkamp, A., Messi, M., Lanzavecchia, A., and Sallusto, F. (2000) *Nat. Immunol.* **1**, 311–316
8. Hengge, U. R., and Ruzicka, T. (2004) *Dermatol. Surg.* **30**, 1101–1112
9. Urošević, M., and Dummer, R. (2004) *Am. J. Clin. Dermatol.* **5**, 453–458
10. Bracci, L., Schumacher, R., Provenzano, M., Adamina, M., Rosenthal, R., Groeper, C., Zajac, P., Iezzi, G., Proietti, E., Belardelli, F., and Spagnoli, G. C. (2008) *J. Immunother.* **31**, 466–474
11. Bagley, K. C., Abdelwahab, S. F., Tuskan, R. G., and Lewis, G. K. (2004) *Clin. Diagn. Lab. Immunol.* **11**, 77–82
12. Ghosh, S., May, M. J., and Kopp, E. B. (1998) *Annu. Rev. Immunol.* **16**, 225–260
13. Lee, J. I., Ganster, R. W., Geller, D. A., Burckart, G. J., Thomson, A. W., and Lu, L. (1999) *Transplantation* **68**, 1255–1263
14. Koski, G. K., Schwartz, G. N., Weng, D. E., Czerniecki, B. J., Carter, C., Gress, R. E., and Cohen, P. A. (1999) *J. Immunol.* **163**, 82–92
15. Czerniecki, B. J., Carter, C., Rivoltini, L., Koski, G. K., Kim, H. I., Weng, D. E., Roros, J. G., Hijazi, Y. M., Xu, S., Rosenberg, S. A., and Cohen, P. A. (1997) *J. Immunol.* **159**, 3823–3837
16. Rao, A. (1994) *Immunol. Today* **15**, 274–281
17. Baeuerle, P. A., and Henkel, T. (1994) *Annu. Rev. Immunol.* **12**, 141–179
18. Lewis, R. S. (2003) *Biochem. Soc. Trans.* **31**, 925–929
19. Kawano, S., Otsu, K., Kuruma, A., Shoji, S., Yanagida, E., Muto, Y., Yoshikawa, F., Hirayama, Y., Mikoshiba, K., and Furuichi, T. (2006) *Cell Calcium* **39**, 313–324
20. Sauer, H., Hofmann, C., Wartenberg, M., Wobus, A. M., and Hescheler, J. (1998) *Exp. Cell Res.* **238**, 13–22
21. Rondé, P., Giannone, G., Gerasymova, I., Stoeckel, H., Takeda, K., and Haiech, J. (2000) *Biochim. Biophys. Acta* **1498**, 273–280
22. Hsu, S. F., O'Connell, P. J., Klyachko, V. A., Badminton, M. N., Thomson, A. W., Jackson, M. B., Clapham, D. E., and Ahern, G. P. (2001) *J. Immunol.* **166**, 6126–6133

23. Schnurr, M., Toy, T., Stoitzner, P., Cameron, P., Shin, A., Beecroft, T., Davis, I. D., Cebon, J., and Maraskovsky, E. (2003) *Blood* **102**, 613–620
24. Goth, S. R., Chu, R. A., Gregg, J. P., Cherednichenko, G., and Pessah, I. N. (2006) *Environ. Health Perspect.* **114**, 1083–1091
25. O'Connell, P. J., Klyachko, V. A., and Ahern, G. P. (2002) *FEBS Lett.* **512**, 67–70
26. Bracci, L., Vukcevic, M., Spagnoli, G., Ducreux, S., Zorzato, F., and Treves, S. (2007) *J. Cell Sci.* **120**, 2232–2240
27. Vukcevic, M., Spagnoli, G. C., Iezzi, G., Zorzato, F., and Treves, S. (2008) *J. Biol. Chem.* **283**, 34913–34922
28. Uemura, Y., Liu, T. Y., Narita, Y., Suzuki, M., Ohshima, S., Mizukami, S., Ichihara, Y., Kikuchi, H., and Matsushita, S. (2007) *Biochem. Biophys. Res. Commun.* **362**, 510–515
29. Schnurr, M., Toy, T., Shin, A., Hartmann, G., Rothenfusser, S., Soellner, J., Davis, I. D., Cebon, J., and Maraskovsky, E. (2004) *Blood* **103**, 1391–1397
30. Healy, J. I., Dolmetsch, R. E., Timmerman, L. A., Cyster, J. G., Thomas, M. L., Crabtree, G. R., Lewis, R. S., and Goodnow, C. C. (1997) *Immunity.* **6**, 419–428
31. Lutz, M. B., and Schuler, G. (2002) *Trends Immunol.* **23**, 445–449
32. Parri, H. R., Gould, T. M., and Crunelli, V. (2001) *Nat. Neurosci.* **4**, 803–812
33. Wang, T. F., Zhou, C., Tang, A. H., Wang, S. Q., and Chai, Z. (2006) *Acta Pharmacol. Sin.* **27**, 861–868
34. Fewtrell, C. (1993) *Annu. Rev. Physiol.* **55**, 427–454
35. Osipchuk, Y. V., Wakui, M., Yule, D. I., Gallacher, D. V., and Petersen, O. H. (1990) *EMBO J.* **9**, 697–704
36. Sun, S., Liu, Y., Lipsky, S., and Cho, M. (2007) *FASEB J.* **21**, 1472–1480
37. Kim, T. J., Seong, J., Ouyang, M., Sun, J., Lu, S., Hong, J. P., Wang, N., and Wang, Y. (2009) *J. Cell Physiol.* **218**, 285–293
38. Kapur, N., Mignery, G. A., and Banach, K. (2007) *Am. J. Physiol. Cell Physiol.* **292**, C1510–1518
39. Resende, R. R., Adhikari, A., da Costa, J. L., Lorençon, E., Ladeira, M. S., Guatimosim, S., Kihara, A. H., and Ladeira, L. O. (2010) *Biochim. Biophys. Acta* **1803**, 246–260
40. Smith, R. J., Sam, L. M., Justen, J. M., Bundy, G. L., Bala, G. A., and Bleasdale, J. E. (1990) *J. Pharmacol. Exp. Ther.* **253**, 688–697
41. Harks, E. G., Camiña, J. P., Peters, P. H., Ypey, D. L., Scheenen, W. J., van Zoelen, E. J., and Theuvenet, A. P. (2003) *FASEB J.* **17**, 941–943
42. Peppiatt, C. M., Collins, T. J., Mackenzie, L., Conway, S. J., Holmes, A. B., Bootman, M. D., Berridge, M. J., Seo, J. T., and Roderick, H. L. (2003) *Cell Calcium* **34**, 97–108
43. Gafni, J., Munsch, J. A., Lam, T. H., Catlin, M. C., Costa, L. G., Molinski, T. F., and Pessah, I. N. (1997) *Neuron* **19**, 723–733
44. Kruskal, B. A., and Maxfield, F. R. (1987) *J. Cell Biol.* **105**, 2685–2693
45. Myers, J. T., and Swanson, J. A. (2002) *J. Leukoc. Biol.* **72**, 677–684
46. Falcone, S., Cocucci, E., Podini, P., Kirchhausen, T., Clementi, E., and Meldolesi, J. (2006) *J. Cell Sci.* **119**, 4758–4769
47. Balaji, J., Armbruster, M., and Ryan, T. A. (2008) *J. Neurosci.* **28**, 6742–6749
48. Dolmetsch, R. E., Xu, K., and Lewis, R. S. (1998) *Nature* **392**, 933–936
49. Dolmetsch, R. E., Lewis, R. S., Goodnow, C. C., and Healy, J. I. (1997) *Nature* **386**, 855–858
50. Zanon, I., Ostuni, R., Capuano, G., Collini, M., Caccia, M., Ronchi, A. E., Rocchetti, M., Mingozzi, F., Foti, M., Chirico, G., Costa, B., Zaza, A., Ricciardi-Castagnoli, P., and Granucci, F. (2009) *Nature* **460**, 264–268
51. Matzner, N., Zemtsova, I. M., Nguyen, T. X., Duszenko, M., Shumilina, E., and Lang, F. (2008) *J. Immunol.* **181**, 6803–6809
52. Aki, D., Minoda, Y., Yoshida, H., Watanabe, S., Yoshida, R., Takaesu, G., Chinen, T., Inaba, T., Hikida, M., Kurosaki, T., Saeki, K., and Yoshimura, A. (2008) *Genes Cells* **13**, 199–208

II. Functional properties of RyR1 mutations linked to malignant hyperthermia and central core disease

II.1 Introduction to publications

Dominant point mutations in the gene encoding *RYR1* have been linked to Malignant Hyperthermia (MH) and Central core disease (CCD). MH is a pharmacogenetic disorder with autosomal dominant inheritance and abnormal Ca^{2+} homeostasis in skeletal muscle in response to triggering agents. CCD is a slowly progressive myopathy characterized by muscle weakness and hypotonia. CCD is characterized histologically by the presence of central cores running along longitudinal axis of the muscle fibre.

In this section of my thesis we describe results obtained on EBV immortalized B-lymphocyte cell lines. The aim of these studies is to develop a parallel diagnostic tool aimed at identifying functional defects in RyR1 caused by mutations. In fact to date the “gold standard” for defining MH susceptibility is an invasive in vitro contracture test (IVST) and clinical histopathological examination of muscle fibres in the case of CCD. The study of the functional properties of RyR channels carrying mutations linked to neuromuscular disorders is important from a diagnostic point of view but also to understand the basic pathophysiological mechanism leading to these different diseases. In fact understanding the mechanisms leading to dysregulation of Ca^{2+} homeostasis is of fundamental importance if one is to develop a pharmacological treatment to improve the quality of life of affected patients.

In this section, we investigated the Ca^{2+} homeostasis of EBV-transformed lymphocytes carrying 9 distinct *RYR1* mutations (p.D544Y, p.R2336H, p.E2404K and p.D2730G, p.E1058K, p.R1679H, p.H382N, p.K1393R and p.R2508G) associated with MHS and CCD cases from Swiss and Swedish population.

In order to assess the functional effects of these mutations we compared Ca^{2+} homeostasis in EBV cells from patients and healthy donors (used as controls).

We determined if mutation affect the resting Ca^{2+} concentration, the size of thapsigargin-sensitive stores and the channel sensitivity to RyR1 agonists.

II.2 publications

1. Soledad Levano*, Mirko Vukcevic*, Martine Singer, Anja Matter, Susan Treves, Albert Urwyler and Thierry Girard. Increasing the Number of Diagnostic Mutations in Malignant Hyperthermia
Hum Mutat. 2009 Apr; 30(4): 590-8.

*These authors contributed equally to this work

2. Mirko Vukcevic*, Marcus Broman*, Gunilla Islander, Mikael Bodelsson, Eva Ranklev-Twetman, Clemens R. Müller and Susan Treves. Functional Properties of RyR1 Mutations Identified in Swedish Malignant Hyperthermia and Central Core Disease Patients
Anesth Analg. 2010 Feb 8. [Epub ahead of print]

*These authors contributed equally to this work

Increasing the Number of Diagnostic Mutations in Malignant Hyperthermia

Soledad Levano,^{1,2*} Mirko Vukcevic,^{1,2} Martine Singer,^{1,2} Anja Matter,^{1,2} Susan Treves,^{1,2} Albert Urwyler,^{1,2} and Thierry Girard^{1,2}

¹Department of Biomedicine, University Hospital Basel, Basel, Switzerland

²Department of Anesthesia, University Hospital Basel, Basel, Switzerland

Communicated by William Oetting

Received 21 February 2008; accepted revised manuscript 16 July 2008.

Published online 3 February 2009 in Wiley InterScience (www.interscience.wiley.com). DOI 10.1002/humu.20878

ABSTRACT: Malignant hyperthermia (MH) is an autosomal dominant disorder characterized by abnormal calcium homeostasis in skeletal muscle in response to triggering agents. Today, genetic investigations on ryanodine receptor type 1 (RYR1) gene and $\alpha 1$ subunit of the dihydropyridine receptor (DHPR) (CACNA1S) gene have improved the procedures associated with MH diagnosis. In approximately 50% of MH cases a causative RYR1 mutation was found. Molecular genetic testing based on RYR1 mutations for MH diagnosis is challenging, because the causative mutations, most of which are private, are distributed throughout the RYR1 gene. A more comprehensive genetic testing procedure is needed. Therefore, we aim to expand the genetic information related to MH and to evaluate the effect of mutations on the MH phenotype. Performing an in-depth mutation screening of the RYR1 transcript sequence in 36 unrelated MH susceptible (MHS) patients, we identified 17 novel, five rare, and eight non-disease-causing variants in 23 patients. The 13 remaining MHS patients presented no known variants, neither in RYR1 nor in the CACNA1S binding regions to RYR1. The 17 novel variants were found to affect highly conserved amino acids and were absent in 100 controls. Excellent genotype-phenotype correlations were found by investigating 21 MHS families—a total of 186 individuals. Epstein-Barr virus (EBV) lymphoblastoid cells carrying four of these novel mutations showed abnormal calcium homeostasis. The results of this study contribute to the establishment of a robust genetic testing procedure for MH diagnosis. *Hum Mutat* 30, 590–598, 2009. © 2009 Wiley-Liss, Inc.

KEY WORDS: malignant hyperthermia; MH; ryanodine receptor type 1; RYR1; MH diagnosis; in vitro contracture testing; IVCT; mutation segregation; abnormal calcium homeostasis

Additional Supporting Information may be found in the online version of this article. Soledad Levano and Mirko Vukcevic contributed equally to this work.

*Correspondence to: Soledad Levano, PhD, Department of Biomedicine, ZLF, Hebelstrasse 20, CH-4031 Basel, Switzerland. E-mail: s.levano@unibas.ch

Contract grant sponsor: European Society of Anesthesiology (ESA); Swiss Society of Anesthesia and Resuscitation (SGAR); Association Francaise contre les Myopathies (AFM); Anaesthesieverein, Department of Anesthesia, University Hospital Basel, Switzerland; Contract grant sponsor: Swiss National Science Foundation; Grant numbers: 405340-104853; and 320080-114597.

Introduction

Malignant hyperthermia (MH; MIM# 145600) is an autosomal dominant pharmacogenetic disorder triggered by volatile halogenated anesthetics and/or succinylcholine. An MH crisis reflects a disturbance of skeletal muscle calcium homeostasis. Genetic linkage studies mapped six different loci for MH, and two candidate genes have been identified, namely the ryanodine receptor type 1 gene (RYR1; MIM# 180901) located on chromosome 19q13.1 [MacLennan et al., 1990] and the CACNA1S gene (MIM# 114208), encoding the $\alpha 1$ subunit of the voltage-gated dihydropyridine receptor (DHPR), located on chromosome 1q32 [Monnier et al., 1997; Robinson et al., 1997]. Both channels are known to be involved in the regulation of calcium release from the sarcoplasmic reticulum [Endo, 1989].

A number of studies in different populations reported that mutations in the RYR1 gene account for approximately 50% of MH cases, while 1% are linked to mutations in CACNA1S gene [Brandt et al., 1999; Girard et al., 2001b; Monnier et al., 1997; Rueffert et al., 2002; Sei et al., 2004; Stewart et al., 2001]. These studies are mostly based on the mutation screening of the three previously identified hotspot regions of RYR1 and of the CACNA1S binding region to RYR1. In studies involving extensive mutation screening of the genomic sequence of RYR1, a number of variants were also found outside the hotspot regions [Galli et al., 2006; Ibarra et al., 2006; Sambuughin et al., 2005; Tammaro et al., 2003]. Such in-depth genetic analysis of the whole coding region seems to be essential, as most of the mutations have been detected in single families or/and specific populations. However, the cost of such analysis is high because of the large size of the RYR1 gene, which comprises 106 exons and transcribes a 15-kb-long RNA molecule. As an alternative approach, two reports recently described the genetic screening of cDNA samples [Robinson et al., 2006; Sambuughin et al., 2005]. A mutation screening of the RYR1 gene is a challenge, not only because of its large size but also on account of sequence heterogeneity. Several missense, nondisease variants, and multiple silent polymorphisms are present, in addition to mutations associated with MH. Recently, Robinson's group reviewed all known RYR1 mutations, which included 178 missense variants, of which 28 mutations have been functionally characterized [Robinson et al., 2006]. Therefore, we selected automated sequencing technology as an optimal method for the detection and differentiation of single-nucleotide variations, providing more accurate information in a highly polymorphic sequence like the RYR1 gene.

Testing for MH susceptibility can be performed using molecular genetic methods [Urwyler et al., 2001]. However, only mutations with a proven MH causative effect are to be used for diagnostic investigations. According to the guidelines of the European MH

Group (EMHG), novel mutations must be genetically and functionally characterized, providing evidence of MH causality prior to such use (www.emhg.org). In this context, we report a comprehensive mutation study including detailed molecular genetic examinations of all detected variants, genotype-phenotype correlation analysis, and functional characterization of four newly-identified MH-linked mutations.

Materials and Methods

Patient Selection and In Vitro Contracture Testing Phenotyping

From the register of the Swiss MH Investigation Unit, 36 MH families were selected that did not present any known causative RYR1 mutation when they were analyzed using restriction fragment length polymorphisms (RFLP) [Girard et al., 2004]. Each family included at least one individual who had experienced a MH crisis. Susceptibility to MH was diagnosed on the basis of in vitro contracture testing (IVCT), which is performed on muscle bundles exposed to increased concentrations of halothane and caffeine. Contractures of ≥ 2 mN following 2% halothane or 2 mM caffeine are considered pathological. Depending on the contracture response measured after drug treatment, patients are diagnosed as MH normal (MHN) if no pathological contracture occurs, MH susceptible (MHS) if pathological contractures occur following administration of caffeine and halothane, or MH equivocal (MHE) if either caffeine or halothane lead to pathological contractures [European Malignant Hyperpyrexia Group, 1984]. For patient safety, MHE individuals are clinically treated as MH positive, although this group is scientifically classified as a group of unclear MH diagnosis. To achieve a high confidence of true-positive MH diagnosis, we selected one MHS patient per family who presented a muscle contracture of ≥ 5 mN at 2% halothane and/or 2 mM caffeine. For most of the MH families, relatives were available for the mutation segregation and the genotype-phenotype analyses. A random sample of 100 anonymous blood donors from the general population was included. This study was approved by the regional ethical committee (Ethikkommission beider Basel [EKBB]).

Isolation of Total RNA and Genomic DNA

Muscle biopsies, which were not exposed to either halothane or caffeine, were used for RNA isolation using RNeasy Mini Kit (Qiagen GmbH, Hilden, Germany) according to the manufacturer's protocol. Genomic DNA was isolated either from whole blood or untreated muscle tissue using QIAamp DNA mini kit (Qiagen AG) according to the manufacturer's protocol.

Mutation Screening

RYR1 Transcript

Total RNA was transcribed to cDNA using the first-strand cDNA kit (Roche Diagnostics, Rotkreuz, Switzerland) according to the manufacturer's protocol. The 23 primer pairs for the amplification of the whole RYR1 transcript were previously published by McCarthy's Group [Schulte am Esch et al., 2000]. One universal condition was established and applied to 23 PCR reactions using Pwo Super Yield DNA polymerase (Roche Diagnostics). The PCR products were cleaned by ultrafiltration using a 96-well filter plate (Roche Diagnostics) and sequenced in both directions by commercial services (Microsynth Sequencing Group, Balgach, Switzerland). The analyses of the sequences were performed using the Staden package (www.mrc-lmb.cam.ac.uk/pubseq/staden_home.html) and the wild-

type human RYR1 transcript sequence (GenBank accession number NM_000540.1) starting with +1 corresponding to A of the ATG initiation codon. All observed variations in the cDNA sequence were verified by additional analysis of genomic DNA.

CACNA1S Transcript

Using cDNA as a template, exons 14 to 18 and 25 to 27 of CACNA1S were amplified by PCR. The PCR products were cleaned as described above and sequenced using the BigDye terminator cycle sequencing kit and the ABI Prism 3100 Avant Genetic Analyzer (Applied Biosystems, Foster City, CA) according to the manufacturer's instructions. The sequences were analyzed and compared with the wild-type sequence of CACNA1S (NM_000069.1) as described above.

Molecular Genetic Analysis of Detected Mutations

The mutation segregation was systematically investigated in DNA samples of available relatives. The isolated genomic DNA was amplified by PCR using 1 × Eppendorf Master Mix (Eppendorf AG, Hamburg, Germany) and primer pairs flanking the RYR1 exons of interest. The mutation detection scanning was performed by RFLP and denaturing high-performance liquid chromatography (dHPLC) (Table 1). Using the same procedure, the mutation occurrences in 100 DNA samples of random blood donors were investigated to assess their possible polymorphic status.

Bioinformatic Tools

For the analysis of the conservative status across the evolution of the gene, a protein multiple sequence alignment was performed using ClustalW v1.82 (www.ebi.ac.uk/clustalw). Two open-source programs (MUpro [www.ics.uci.edu/~baldig/mutation.html] and Pmut [<http://mmb2.pcb.ub.es:8080/PMut/>]) available through web servers were used to predict the effect of single amino acid mutations on the RYR1 protein in silico. MUpro is a program based on support vector machines that uses primary sequence information to predict protein stability through single amino acid mutations [Cheng et al., 2006]. The recommended value to use is the predicted energy change ($\Delta\Delta G$). A negative $\Delta\Delta G$ value indicates that a given mutation decreases protein stability. The web-based Pmut tool is based on the use of neural networks trained with human mutational data, such as sequence-derived information (structure, evolutionary conservation, data, and residue properties). The prediction, whether a given mutation is pathological or neutral, is described according to a pathological index ranging from 0 to 1, where an index > 0.5 indicates a pathological character.

Functional Assay

Changes in the intracellular Ca^{2+} concentration in Epstein-Barr virus (EBV)-immortalized lymphoblastoid cells from healthy controls and in MHS patients carrying the mutation of interest were monitored with the fluorescent Ca^{2+} indicator fura-2/AM. Experiments were carried out on populations of cells in a LS50 spectrofluorimeter (Perkin Elmer Instruments, Shelton, CT) at 37°C, as previously described [Girard et al., 2001a], or at the single-cell level by digital imaging microscopy, also at 37°C, as previously described [Ducreux et al., 2006]. In the latter case, lymphoblastoid cells loaded with 5 μ M fura-2 were allowed to attach to poly-L-lysine-treated glass coverslips for 10 minutes prior to the experiments. Individual cells were stimulated with a 12-way 100-mm-diameter quartz micromanifold computer-con-

Table 1. RYR1 Variants Detected in Our MHS Patients and the Methods Used for the Genetic Analysis in the Family Members and Controls*

Nucleotide change	Amino acid change	Exon	Analysis method ^a	Family	References
c.38T>G	p.L13R	1	Seq	S1	Ibarra et al. [2006]
c.677T>A	p.M226K	8	dHPLC	S2	This study
c.1100G>T	p.R367L	11	dHPLC/RFLP	S3	This study
c.1589G>A	p.R530H	15	RFLP	S4	This study
c.1630G>T	p.D544Y	15	RFLP	S5	This study
c.3127C>T	p.R1043C	24	dHPLC/RFLP	S6	This study
c.4055C>G	p.A1352G	28	dHPLC/RFLP	S7	This study
c.7007G>A	p.R2336H	43	dHPLC/RFLP	S6, S8–S14	This study
c.7210G>A	p.E2404K	44	dHPLC/RFLP	S15	This study
c.8026C>T	p.R2676W	50	RFLP	S7	Guis et al. [2004]
c.8189A>G	p.D2730G	51	dHPLC/RFLP	S16	This study
c.8360C>G	p.T2787S	53	RFLP	S7	Guis et al. [2004]
c.8638G>A	p.E2880K	56	dHPLC	S17, S18	This study
c.9649T>C	p.S3217P	65	dHPLC	S3	This study
c.9868G>A	p.E3290K	66	dHPLC	S18	This study
c.11314C>T	p.R3772W	79	dHPLC	S19	This study
c.11416G>A	p.G3806R	80	dHPLC	S20	This study
c.12861_12869dupCACGGCGGC	p.T4288_A4290dup	91	dHPLC	S2	This study
c.13502C>T	p.P4501L	92	dHPLC/RFLP	S7	This study
c.14512C>G	p.L4838V	101	dHPLC/RFLP	S21	Oyamada et al. [2002]
c.14627A>G	p.K4876R	101	dHPLC	S22	Monnier et al. [2005]
c.14813T>C	p.I4938T	103	dHPLC/RFLP	S23	This study

*Numbering of the transcript sequence starts with +1 corresponding to A of the ATG initiation codon and corresponds to the GenBank accession number NM_000540.1. The amino acid numbering corresponds to the GenBank accession number NP_000531.1.

^aFor segregation analysis and DNA controls.

dHPLC, denaturing high-performance liquid chromatography; RFLP, restriction fragment length polymorphism.

trolled microperfuser (ALA Scientific, Westbury, NY). Online (340 nm, 380 nm, and ratio) measurements were recorded using a fluorescent Axiovert S100 TV inverted microscope (Carl Zeiss GmbH, Jena, Germany) equipped with a 40 × oil-immersion Plan-NEOFLUAR objective (0.17 NA; Carl Zeiss GmbH) and filters (BP 340/380, FT 425, and BP 500/530). The cells were analyzed using an Openlab (Improvision, Coventry, UK) imaging system and the average pixel value for each cell was measured at excitation wavelengths of 340 and 380 nm.

The presence of the mutation in the lymphoblastoid cell lines was confirmed by PCR and automated sequencing.

Statistical Analysis

Statistical analyses were performed using the Student's *t*-test for paired samples, or analysis of variance (ANOVA) when more than two groups were compared. Origin software (version 6.0; Microcal Software, Inc., Northampton, MA) was used for statistical analysis and to generate dose-response curves according to the Hill equation. From these curves, the effective concentration 50% (EC50) was calculated. ANOVA was used to compare EC50 values. If they were significantly different, Dunnett's multiple comparison test was used for post-hoc analysis. *P* values below 5% were considered significant.

Results

Mutations in RYR1 and CACNA1S Transcripts

The entire coding region of RYR1 was analyzed in 36 unrelated MHS patients. In 23 of these patients we found 22 variants (64%). Of these 22 variants, 17 (78%) were novel, one was a rare causative MH mutation (p.L4838V) [Oyamada et al., 2002], and four were previously reported variants (p.L13R, p.R2676W, p.T2787S, and p.K4876R) [Guis et al., 2004; Ibarra et al., 2006; Monnier et al., 2005; Sambuughin et al., 2005]. All novel variants were found

in the heterozygous state and were characterized as single-nucleotide changes, but one was an in-frame duplication of nine nucleotides (Table 1). The 17 novel variants were absent in 100 control DNA samples. The variants p.R2336H and p.E2280K were recurrent in eight and two families, respectively (Table 1). Four MHS patients of unrelated families were double-variant carriers (p.R1043C/p.R2336H, p.E2880K/p.E3290K, p.R367/p.S3217P, and p.M226K/p.T4288_A4290dup), and one MHS patient even presented quadruple variants (p.S1352G/p.R2676W/p.T2787S/p.P4501L).

Eight noncausative variants were previously reported (p.P1787L, p.A1832G, p.G2060C, p.V2550L, p.E3583Q, and p.Q3756E) [Robinson et al., 2006] or were already described as polymorphisms, p.S1342G (rs34694816:A>G) and p.I2321V (rs34390345:A>G), in the NCBI SNP database (www.ncbi.nlm.nih.gov/projects/SNP). Some of these variants not associated with MH were present alone, in combination with each other, or with novel variants described here. In this context, five MHS patients were identified as double carriers, who belong to Family S1 (p.L13R/p.I2321V), Family S17 (p.E2880K/p.E3583Q), Family S21 (p.G2060C/p.L4838V), and Families S24 and S25 (p.P1787L/p.G2060C). One MHS patient from Family S4 presented p.R530H, together with p.G2060C and p.E3583Q.

In addition, silent polymorphisms were also detected. With the exception of 11 polymorphisms, 30 have been previously listed in the SNP database. Regarding splicing variants of RYR1, we observed splicing transcripts lacking exons 70 and 83 in all of our samples. A similar observation was recently reported [Robinson et al., 2006].

In the remaining 13 of the 36 selected MHS patients who did not present any known RYR1 variants, we further analyzed the sequence of the interacting region of CACNA1S to RYR1. We found the silent polymorphism T2630C (rs7415038) coding for p.F801. This polymorphism was present in all samples.

Localization and Predicted Effect of RYR1 Mutations

The detected variants were distributed along the whole coding region of RYR1 (Fig. 1). Ten out of the 17 novel variants were localized outside of the previously reported hotspot regions. Similarly, 15 out of 17 variants were confined to different domains of RYR1 according to the SwissPfam protein database (www.sanger.ac.uk/cgi-bin/Pfam).

The 16 novel point mutations caused amino acid changes that were highly conserved throughout the evolution of RYR1 and among different human isoforms (Table 2). Using two different prediction programs, the novel amino acid changes, when analyzed individually, were predicted to affect the protein stability and to have a pathological character. For five variants (p.A1352G, p.R1043C, p.R2676W, p.E3290K, and p.K4876R), the predictions generated using MUpro and Pmut were divergent (Table 2).

Functional Assay of Novel Mutations

To perform functional analysis, we needed to use a variant that was present in at least two MHS patients. Although eight variants met this criterion, available fresh blood samples allowed analysis of only four novel mutations (p.D544Y, p.R2336H, p.E2404K, and p.D2730G). The resting Ca^{2+} concentration in cells from patients carrying one of the novel mutations was significantly higher than that observed in cells from control individuals (Fig. 2A). To assess whether the mutations affected the amount of Ca^{2+} present in intracellular stores, we treated the cells with the sarcoplasmic/endoplasmic reticulum Ca^{2+} -ATPase (SERCA) inhibitor thapsigargin in the presence of 0.5 mM ethylene glycol tetraacetic acid (EGTA). As shown in Figure 2B, none of the mutations affected the amount of Ca^{2+} released from rapidly releasable stores. Next, we assessed whether the mutations affected the sensitivity of RYR1 to pharmacological stimulation. Figure 3 shows the dose-response curves to 4-chloro-*m*-cresol and caffeine. The presence of all mutations shifted the dose-response curves to lower agonist concentrations compared to that observed in cells from control individuals. This shift in the dose-response curve was statistically significant for all four mutations with at least 1 out of the 2 agonists (Fig. 3).

Segregation and Phenotype-Genotype Analysis

A total of 186 individuals (including the 21 selected MHS patients) from 213 members of 21 MH families were available for

the segregation analysis (Table 3). One MH family (Family S2) with no available relatives carried two variants. As a consequence, 19 out of 22 variants were further investigated for segregation.

Few (30%, 15/51) MHE patients were carriers of the novel variants (Table 3). Excluding MHE individuals, a high overall concordance of 0.94 (95% confidence interval [CI], 0.89–0.98) was observed between the phenotype and genotype. Of the 69 MHS individuals, 65 were carriers, corresponding to a sensitivity of 0.94 (95% CI, 0.85–0.98), whereas 3 out of the 66 MHN individuals carried RYR1 variants, resulting in a specificity of 0.95 (95% CI, 0.86–0.99). These numbers would be substantially lower after inclusion of the MHE patients. Although these patients must clinically be considered MH-positive, they belong to a group with unclear MH diagnosis. Therefore, we only considered unambiguous IVCT diagnoses for the above calculations.

From the eight families (Families S6 and S8–S14) carrying p.R2336H, a total of 80 individuals were investigated. The p.R2336H segregation was observed in family members across three- and two-generation pedigrees and was transmitted to 22 out of 26 MHS patients and to 3 out of 21 MHE patients. The 3 out of 4 MHS noncarriers for R2336H belong to the large Family S11, with 10 MHS carriers (Supplementary Fig. S1; available online at <http://www.interscience.wiley.com/jpages/1059-7794/suppmat>). For two of these patients (Supplementary Fig. S1, Patients S11-1 and S11-2) the mutation inheritance was initially assumed to be maternal. However, the mother of Patient S11-2 was diagnosed as MHN and did not carry p.R2336H. Unfortunately, neither the parents nor any grandparents were available for analysis. The third MHS noncarrier (Supplementary Fig. S1; Patient S11-3) was identified in a different branch not carrying p.R2336H. The fourth MHS noncarrier (Supplementary Fig. S2; Patient S14-1) was the husband of an MHS patient, who carries the p.R2336H. The analysis of the full RYR1 transcript in these four MHS patients revealed no novel variants. As expected, the p.R2336H was not detected in any of the 34 MHN individuals. The index patient of Family S6 coexpressed p.R2336H together with p.R1043C. After genetic analysis, it was found that the mother presented wild-type sequences whereas the father carried both variants. This suggests that the variants lie on the same chromosome. The second most frequent variant, p.E2880K, was examined in two families (Families S17 and S18) comprising 11 relatives with five MHS patients. One of the three MHS patients

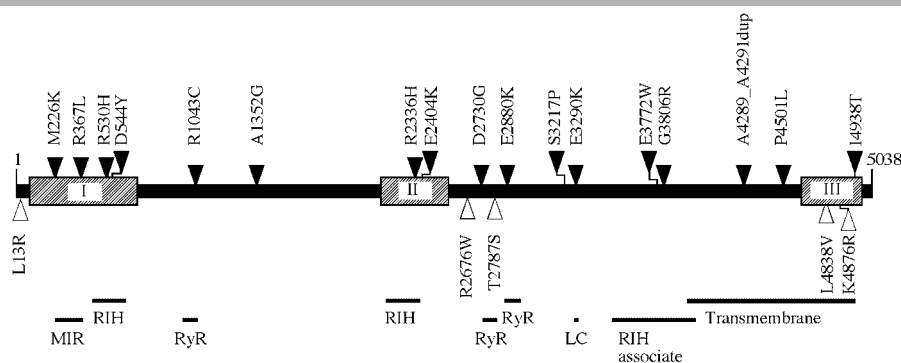


Figure 1. Location of the RYR1 variants found in this study along the protein sequence. Novel variants are indicated by filled triangles and known variants by open triangles. The hatched boxes represent the three putative hotspot regions. Selected domains according to the SwissPfam protein database are represented by thin horizontal bars and are described as the following: MIR = domain in ryanodine and inositol trisphosphate receptors (IP3R) and protein O-mannosyltransferases; RIH = RYR and IP3R homology domains (this extracellular domain may form a binding site for IP3); RyR = ryanodine receptor domain; RIH associate = RyR and IP3R homology associated (this domain is found in RYR and IP3R); and LC = low complexity region.

Table 2. Analysis of Detected RYR1 Variants*

Protein name	13R	226K	367L	530H	544Y	1043C	1352G	2336H	2404K	2676W	2730G	2787S	2880K	3217P	3290K	3772W	3806R	4501L	4838V	4876R	4938T	
A.																						
Human RYR1	L	M	R	R	D	R	A	R	E	R	D	T	E	S	E	R	G	P	L	K	I	I
Pig RYR1	L	M	R	R	D	R	A	R	E	R	D	T	E	S	E	R	G	P	L	K	K	I
Rabbit RYR1	L	M	R	R	D	R	A	R	E	R	D	T	E	S	E	R	G	P	L	K	K	I
Mouse RYR1	L	M	R	R	D	R	A	R	E	R	D	T	E	S	E	R	G	P	L	K	K	I
Human RYR2	L	M	R	R	D	R	A	R	K	R	D	V	E	S	E	R	G	—	L	K	K	I
Human RYR3	L	—	R	R	D	R	A	R	V	R	D	T	E	S	E	R	G	—	L	K	K	I
B.																						
MUpro	-2.1	-1.5	-0.7	-1.2	-1.4	-0.5	-1.6	-1.3	-1.8	-1.1	-0.9	-0.9	-1.4	-1.0	-0.3	-0.7	-0.8	0.0	-0.6	-0.8	-2.2	
PMut	0.9	0.8	0.8	0.8	0.9	0.9	0.1	0.8	0.8	1.0	0.8	0.0	0.8	0.8	0.4	1.0	0.9	0.9	0.5	0.1	0.7	

* A: Protein alignment of human RYR1 in diverse species and other RYR proteins. GenBank accession numbers: NP_000531.1 for human, P11716 for rabbit, P16960 for pig, and NP_033135.1 for *Mus musculus* RYR1, as well as NP_001026.1 for human RYR2 and NP_001027.2 for human RYR3. B: Predicted effect of the detected variants of RYR1 by using MUpro and PMut programs. The protein stability using MUpro is given through G values, where the negative values predict the pathological effect. Likewise, PMut predicts the pathological effect by means of the index > 0.5.

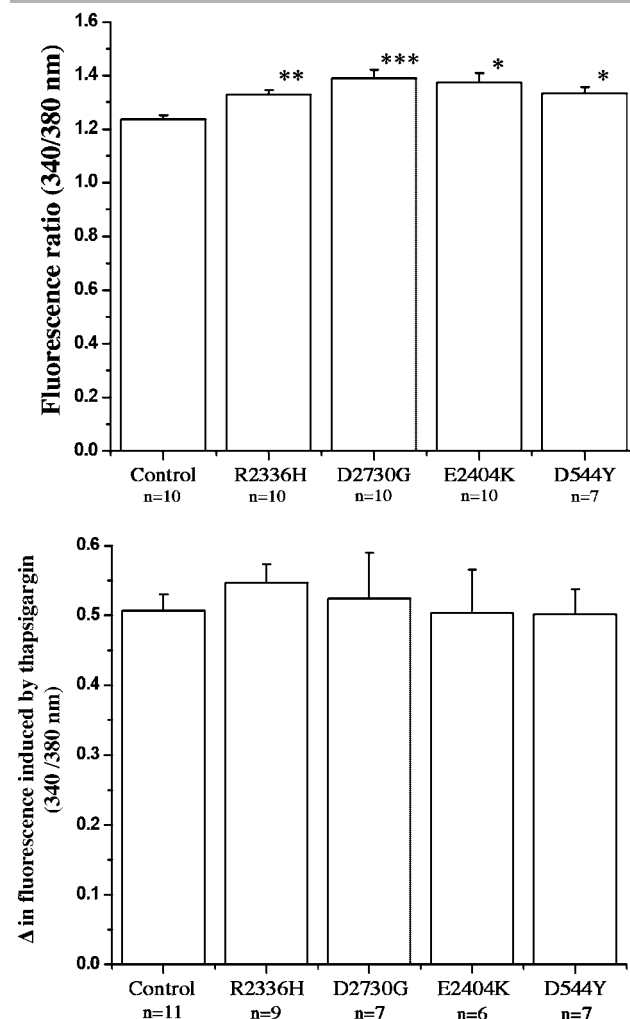


Figure 2. Comparison of the resting Ca^{2+} concentration and the status of thapsigargin-sensitive Ca^{2+} stores in lymphoblastoid cells from control and MHS individuals carrying the novel RYR1 mutations. (A) Resting fluorescent values and (B) change in fluorescence (peak resting fluorescence ratio 340/380 nm) induced by addition of 400 nM thapsigargin. Fluorescence measurements were performed on fura-2 loaded lymphoblastoid cells (1×10^6 cells/ml) in a Perkin Elmer LS50 spectrofluorimeter thermostatted at 37°C and equipped with a magnetic stirrer. Results represent the mean \pm standard error of the mean (SEM) of the indicated number of experiments. * $P = 0.002$, ** $P = 0.001$, *** $P = 0.0003$.

from Family S18, carrying p.E2880K, exhibited an additional change of glutamic acid to lysine, namely p.E3290K. The single MHN sister harbored no variants.

An MHS double carrier in Family S3 carried p.R367L and p.S3217P, whereas his MHE mother was a carrier of only p.S3217P. This suggests that the father, who was not available for analysis, is a possible carrier of p.R367L.

Discordances were found in two families carrying p.P4501L and p.I4938T, in which these variants were harbored by MHN patients. In Family S7 (Supplementary Fig. S3; Patients S7-1 and S7-2) an MHS father was a carrier for four variants (p.A1352G, p.P4501L, p.R2676W, and p.T2787S), while both of his MHN siblings carried solely p.P4501L. Another discordance was identified in Family S23 (Supplementary Fig. S4), in which Patient S23-1 carried p.I4938T, while being diagnosed MHN by IVCT. In all MHN patients, the IVCT results were unambiguous, with viable muscle samples contracting to neither caffeine nor halothane.

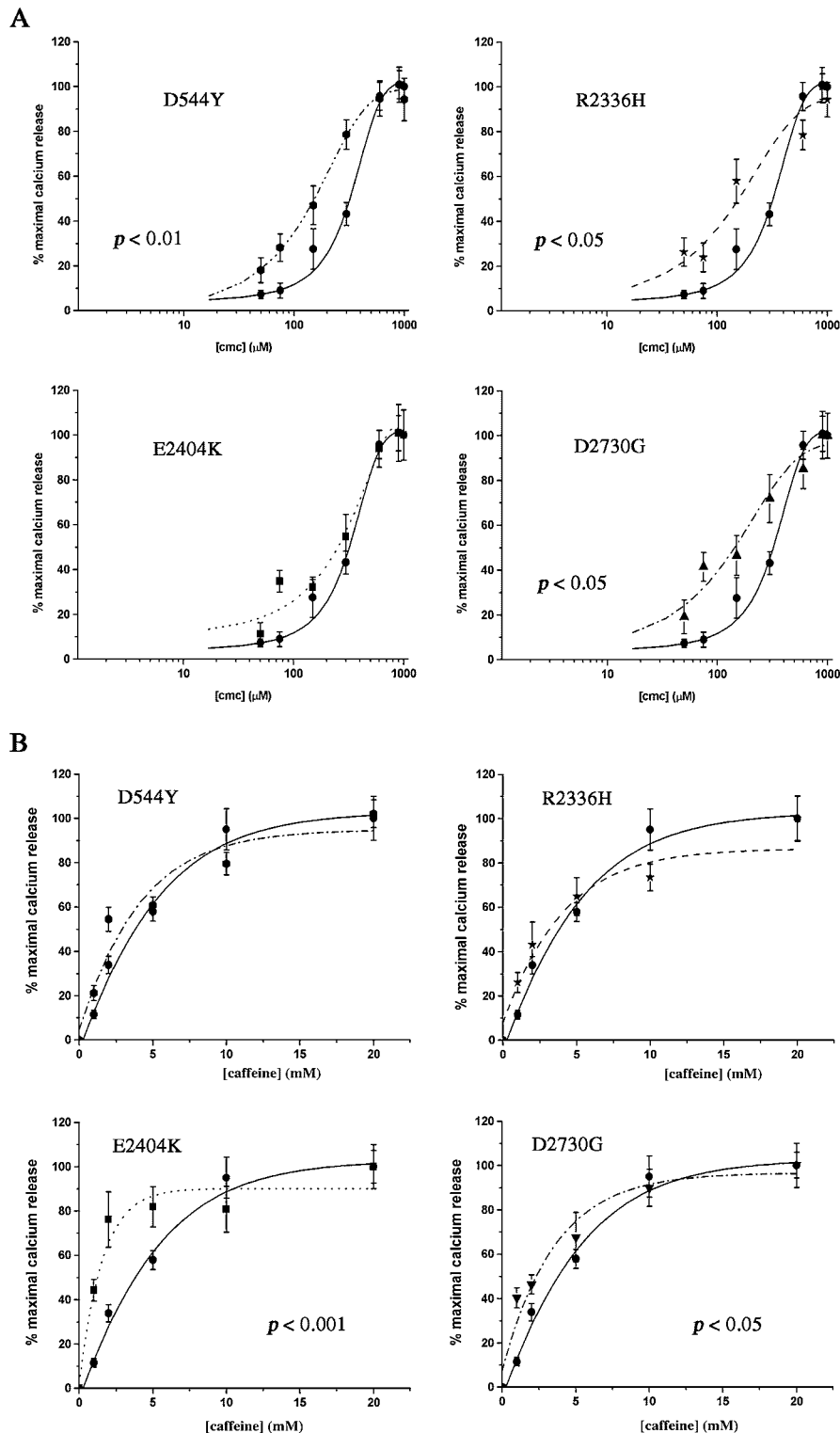


Figure 3. Dose-dependent changes in intracellular Ca^{2+} concentrations induced by pharmacological RyR1 activation in lymphoblastoid cells from control individuals and patients carrying the indicated RYR1 mutations. Single-cell intracellular Ca^{2+} measurements of fura-2-loaded cells were measured before and after the addition of the indicated concentration of 4-chloro-*m*-cresol (**A**) or caffeine (**B**). The curves show the changes in intracellular Ca^{2+} concentrations expressed as change in fluorescence ratio (peak ratio 340/380 nm; resting ratio 340/380 nm). Results are mean \pm standard error of the mean (SEM) of the change in fluorescence of 10 to 53 individual cells. The curves were generated using a sigmoidal dose-response curve function included in Origin software. cmc = 4-chloro-*m*-cresol; solid lines = controls; dashed lines = patients.

Discussion

The RYR1 gene is the major locus of MH susceptibility. As such, this gene is the principal focus on the genetic research of this

pharmacogenetic disease. The advantage of molecular genetic testing for MH susceptibility, as well as the pathophysiological understanding of MH, has led to a continued search for new mutations in MH families with formerly unknown genotypes.

Table 3. Total Individuals Included in the Genetic Screening Analysis

Amino acid change	Family	Available generations	MHS ^a	MHN ^a	MHE ^a	Total IVCT	No IVCT ^b
p.L13R	S1	2	2/2	1/0	0/0	3	
p.M226K	S2	1	1/1	0/0	0/0	1	
p.R367L	S3	2	1/1	0/0	1/0	2	
p.R530H	S4	2	1/1	0/0	2/0	3	
p.D544Y	S5	3	4/4	2/0	1/0	8	4
p.R1043C	S6	2	2/2	1/0	3/0	6	
p.A1352G	S7	2	1/1	2/0	4/4	7	
p.R2336H	S6	2	2/2	1/0	3/0	6	
	S8	2	2/2	0/0	0/0	3	
	S9	2	1/1	1/0	1/0	4	
	S10	1	2/2	1/0	1/0	4	
	S11	3	10/7	23/0	9/0	53	
	S12	2	1/1	1/0	2/1	4	
	S13	3	5/5	4/0	4/1	22	
	S14	2	3/2	3/0	1/1	7	
p.E2404K	S15	2	3/3	1/0	2/1	6	
p.R2676W	S7	2	1/1	2/0	4/4	7	
p.D2730G	S16	3	17/17	6/0	5/0	28	2
p.T2787S	S7	2	1/1	2/0	4/4	7	
p.E2880K	S17	3	1/1	2/0	2/1	5	2
	S18	1	3/3	1/0	0/0	4	
p.S3217P	S3	1	1/1	0/0	1/1	2	
p.E3290K	S18	1	3/1	1/0	0/0	4	
p.R3772W	S19	2	1/1	0/0	0/0	1	
p.G3806R	S20	2	5/5	12/0	9/3	29	
p.T4288_A4290dup	S2	1	1/1	0/0	0/0	1	
p.P4501L	S7	2	1/1	2/2	4/2	7	
p.L4838V	S21	2	1/1	0/0	0/0	1	1
p.K4876R	S22	2	2/2	0/0	1/1	3	
p.I4938T	S23	2	2/2	5/1	3/2	11	

^aTotal genotyped/total carrier.

^bAdditional patients were available, without IVCT diagnosis.

However, the hunt for the causative mutations in the RYR1 gene is challenging because of its sequence heterogeneity and the presence of numerous rare mutations distributed across the whole RYR1 gene [Robinson et al., 2006]. This demonstrates the importance of investigating the entire gene rather than hotspot regions. The analysis of the coding region at the genomic DNA level by current protocols is time-consuming. However, a stepwise approach seems reasonable for the clarification of the MH genetic status in affected individuals. Taking these facts into consideration, we first examined MH families by screening the frequent causative RYR1 mutations [Girard et al., 2004] and further investigated those families without RYR1 mutations by amplification of the RYR1 transcript sequences and automated sequencing, as described in this study.

Novel Mutations and Their Frequencies

The strict selection criteria based on the IVCT data (contractions ≥ 5 mN) might have contributed to the high detection rate of RYR1 variants (64%, 23/36). A high proportion of novel variants (78%, 17/22) was expected, as the MH patients were prescreened for RYR1 mutations [Girard et al., 2004].

Interestingly, variant p.R2336H was detected with the highest frequency, suggesting it to be a common mutation, similar to p.V2168M in the Swiss population [Girard et al., 2001b]. As previously reported, the prevalence of a specific mutation is high in some populations and low in others. While p.V2168M is the most prevalent mutation in Switzerland [Girard et al., 2001b], p.G2434R is more common in the United Kingdom [Robinson et al., 2002], p.G341R in the Caucasian population living in France [Quane et al., 1994], and p.R614C in German and French families [Brandt et al., 1999; Monnier et al., 2005].

Although all variants except for two were detected in single MH families, most of the variants were found in more than one MHS patient and were absent in MHN patients. Furthermore, p.L13R and p.K4876R, which we detected in single families, were each recently reported in a Japanese [Ibarra et al., 2006], a French [Monnier et al., 2005], and a North American family [Monnier et al., 2005; Sambuughin et al., 2005]. Similarly, D2730G and I4938T variants were previously described with different amino acid alterations in single UK (I4938M) and Japanese (D2730M) MH families [Ibarra et al., 2006; Shepherd et al., 2004].

Characterization of Novel RYR1 Mutations

Novel mutations localized along the transcript could certainly affect the function of RYR1, taking into account the fact that the RYR1 gene contains several ligand binding sites as well as conserved domains according to the SwissPfam protein database and previously reported findings [Dulhunty and Pouliquin, 2003]. The N-terminal region (216–572) has been reported to have a similar structure as the IP3R core region and to be involved in the regulation of Ca²⁺ channel activity [Serysheva et al., 2005]. In this region, we detected four novel variants (p.M226L, p.R367L, p.R530H, and p.D544Y) that could affect channel regulation. Furthermore, two sequence regions (1924–2446 and 2644–3223) have been found to be critical for excitation-contraction (E-C) coupling [Perez et al., 2003]. In these regions we found five novel variants (p.R2336H, p.E2404K, p.D2730G, p.E2880K, and p.S3217P) that could alter the coupling mechanism. In addition, p.E2404K could be one of the glutamate residues belonging to a region (1641–2437) rich in glutamate and aspartate residues, and

may be involved in the ion conduction and regulation of the channel [Bhat et al., 1997].

Taking advantage of bioinformatics tools, the novel variants have been shown to affect well-conserved amino acid residues. Furthermore, all novel variants were predicted to destabilize the protein structure according to the results from MUp. They are also predicted to be pathological according to the results from Pmut.

Functional Assay of Novel Mutations

Alterations of intracellular calcium homeostasis in EBV cells from carriers of four mutations are a strong indication of the causative role in the susceptibility to MH. The four RYR1 mutations we functionally characterized significantly increased the resting calcium concentration; such a finding is consistent with a previous report [Ducreux et al., 2006]. These four mutations were also found to significantly affect either 4-chloro-*m*-cresol or caffeine dose-response curve to pharmacological activation. Only one mutation (p.D2730G) showed a significant reduction in EC50 of both caffeine and 4-chloro-*m*-cresol. We do not have experimental explanations for the different agonistic effects in these four mutations, but this might be influenced by the different conformational state induced by each mutation, depending on the position and the property of the amino acid substitution. In this regard, the sensitivity of RYR1 to a particular agonist would also be affected differently. In mutation p.E2404K, there was no significant reduction in the EC50 of 4-chloro-*m*-cresol compared to cells from control individuals. It is interesting to note that although this residue is conserved throughout evolution, the cardiac RYR isoform (RYR2) has lysine in position 2404.

Phenotype-Genotype Correlations

We found an excellent overall concordance of 93% between IVCT-phenotype and genotype in 186 individuals from 21 MHS families. There were six discordant MHS individuals that did not carry the familial variant. Contracture data from IVCT were not different from mutation carriers and the probability of an alternative RYR1 mutation was ruled out by sequencing the full coding region. In four MHS patients the absence of p.R2336H was clarified by analyzing their pedigrees. Thus, the MH susceptibility of these noncarriers could be due to involvement of other genes, or represent false-positive IVCT diagnoses. The two remaining discordant MHS patients were noncarriers for p.E3290K, but carriers for p.E2880K. This might suggest that the p.E2880K could be the causative mutation in this family. An additive effect of the p.E3290K on the RYR1 would be possible; however, single and double MHS carriers presented similar IVCT data. The implications of this variant remain indeterminate, as unfortunately the other 2 of the 4 brothers who manifested MH events, as well as the parents, were unavailable for genetic testing. The absence of p.E3290K in the healthy controls ($n = 100$) was confirmed.

We also identified three discordant MHN patients carrying the familial variant. For patient safety, identification of RYR1 mutations in patients diagnosed MHN by IVCT is crucial. If the mutation is confirmed to be causative for MH, the MH status of these patients will need to be corrected. The MHN individual presenting p.I4938T was the only discordant patient in Family S23. As his mother is MHE by IVCT, this might suggest a variable penetrance of p.I4938T or the participation of additional genes in this family. Although the causative effect of p.I4938T has yet to be proven, a variant at this position (p.I4938M) was previously found to be linked to MH [Shepherd et al., 2004]. The last two

discordant MHN individuals carried the variant p.P4501L. In this family (Family S7) with four different variants, p.P4501L does not segregate with the IVCT phenotype. In spite of the absence of p.P4501L in healthy controls, this variant does not seem to be linked to MH susceptibility.

Recently, allelic silencing was proposed as an explanation for phenotype-genotype discordances in multimicore disease [Zhou et al., 2006]. However, discordances of our study population cannot be explained by allelic silencing, as genotyping on genomic and cDNA level was concordant.

Unfortunately, segregation analysis could not be performed in 3 out of the 22 identified variants, as additional family members were not available. Of interest might be the case of the duplication of nine nucleotides, as these residues are localized in a protein region (4187–4381) suggested to be involved in calcium inactivation [Du et al., 2000]. To expand the characterization of novel mutations and to clarify arising discordance, in-depth molecular genetic analysis should be performed in all members of affected families. However, enrollment of patients is one of the acute problems in genetic studies. Multicenter and international collaborations could overcome this limitation, and mutations identified in single families within different populations could be characterized in an international effort.

In summary, this study describes novel RYR1 variants expressed in patients registered in our MH investigation unit and four of these mutations (p.D544Y, p.R2336H, p.E2404K, and p.D2730G) that were functionally tested and seem to have a causative effect. These results expand the number of MH mutations to be of value in the molecular genetic diagnosis of MH susceptibility. Furthermore, the presented novel mutations contribute to the update of the international mutation database of the RYR1 gene and emphasize the importance of international collaboration to characterize rare mutations. Finally, the identification and characterization of novel MH causative mutations is important, to increase our understanding of the molecular mechanisms underlying MH susceptibility.

Acknowledgments

We thank Prof. Raija Lindberg and Dr. Fabrice Schoumacher for critically reading the manuscript, and Allison Dwileski for editorial support.

References

- Bhat MB, Zhao J, Hayek S, Freeman EC, Takeshima H, Ma J. 1997. Deletion of amino acids 1641-2437 from the foot region of skeletal muscle ryanodine receptor alters the conduction properties of the Ca release channel. *Biophys J* 73:1320-1328.
- Brandt A, Schleithoff L, Jurkat-Rott K, Klingler W, Baur C, Lehmann-Horn F. 1999. Screening of the ryanodine receptor gene in 105 malignant hyperthermia families: novel mutations and concordance with the in vitro contracture test. *Hum Mol Genet* 8:2055-2062.
- Cheng J, Randall A, Baldi P. 2006. Prediction of protein stability changes for single-site mutations using support vector machines. *Proteins* 62:1125-1132.
- Du G, Khanna V, MacLennan D. 2000. Mutation of divergent region 1 alters caffeine and Ca(2+) sensitivity of the skeletal muscle Ca(2+) release channel (ryanodine receptor). *J Biol Chem* 275:11778-11783.
- Ducreux S, Zorzato F, Ferreiro A, Jungbluth H, Muntoni F, Monnier N, Muller CR, Treves S. 2006. Functional properties of ryanodine receptors carrying three amino acid substitutions identified in patients affected by multi-micore disease and central core disease, expressed in immortalized lymphocytes. *Biochem J* 395:259-266.
- Dulhunty AF, Pouliquin P. 2003. What we don't know about the structure of ryanodine receptor calcium release channels. *Clin Exp Pharmacol Physiol* 30:713-723.
- Endo M. 1989. [Mechanisms and their pharmacology of mobilization of calcium ion in muscle cells]. *Nippon Yakurigaku Zasshi* 94:329-338. [Japanese]

- European Malignant Hyperpyrexia Group. 1984. A protocol for the investigation of malignant hyperpyrexia (MH) susceptibility. The European Malignant Hyperpyrexia Group. *Br J Anaesth* 56:1267–1269.
- Galli L, Orrico A, Lorenzini S, Censini S, Falciani M, Covacci A, Tegazzin V, Sorrentino V. 2006. Frequency and localization of mutations in the 106 exons of the RYR1 gene in 50 individuals with malignant hyperthermia. *Hum Mutat* 27:830.
- Girard T, Cavagna D, Padovan E, Spagnoli G, Urwyler A, Zorzato F, Treves S. 2001a. B-lymphocytes from malignant hyperthermia-susceptible patients have an increased sensitivity to skeletal muscle ryanodine receptor activators. *J Biol Chem* 276:48077–48082.
- Girard T, Urwyler A, Censier K, Mueller CR, Zorzato F, Treves S. 2001b. Genotype-phenotype comparison of the Swiss malignant hyperthermia population. *Hum Mutat* 18:357–358.
- Girard T, Treves S, Voronkov E, Siegemund M, Urwyler A. 2004. Molecular genetic testing for malignant hyperthermia susceptibility. *Anesthesiology* 100:1076–1080.
- Guis S, Figarella-Branger D, Monnier N, Bendahan D, Kozak-Ribbens G, Mattei JP, Lunardi J, Cozzone PJ, Pellissier JF. 2004. Multiminicore disease in a family susceptible to malignant hyperthermia: histology, in vitro contracture tests, and genetic characterization. *Arch Neurol* 61:106–113.
- Ibarra MC, Wu S, Murayama K, Minami N, Ichihara Y, Kikuchi H, Noguchi S, Hayashi YK, Ochiai R, Nishino I. 2006. Malignant hyperthermia in Japan: mutation screening of the entire ryanodine receptor type 1 gene coding region by direct sequencing. *Anesthesiology* 104:1146–1154.
- MacLennan DH, Duff C, Zorzato F, Fujii J, Phillips M, Korneluk RG, Frodis W, Britt BA, Worton RG. 1990. Ryanodine receptor gene is a candidate for predisposition to malignant hyperthermia. *Nature* 343:559–561.
- Monnier N, Procaccio V, Stieglitz P, Lunardi J. 1997. Malignant-hyperthermia susceptibility is associated with a mutation of the alpha 1-subunit of the human dihydropyridine-sensitive L-type voltage-dependent calcium-channel receptor in skeletal muscle. *Am J Hum Genet* 60:1316–1325.
- Monnier N, Kozak-Ribbens G, Krivosic-Horber R, Nivoche Y, Qi D, Kraev N, Loke J, Sharma P, Tegazzin V, Figarella-Branger D, Romero N, Mezin P, Bendahan D, Payen JF, Depret T, MacLennan DH, Lunardi J. 2005. Correlations between genotype and pharmacological, histological, functional, and clinical phenotypes in malignant hyperthermia susceptibility. *Hum Mutat* 26:413–425.
- Oyamada H, Oguchi K, Saitoh N, Yamazawa T, Hirose K, Kawana Y, Wakatsuki K, Tagami M, Hanaoka K, Endo M, Iino M. 2002. Novel mutations in C-terminal channel region of the ryanodine receptor in malignant hyperthermia patients. *Jpn J Pharmacol* 88:159–166.
- Perez CE, Voss A, Pessah IN, Allen PD. 2003. RyR1/RyR3 chimeras reveal that multiple domains of RyR1 are involved in skeletal-type E-C coupling. *Biophys J* 84:2655–2663.
- Quane KA, Keating KE, Manning BM, Healy JM, Monsieurs K, Heffron JJ, Lehane M, Heytens L, Krivosic-Horber R, Adnet P, Ellis FR, Monnler N, Lunardi J, McCarthy TV. 1994. Detection of a novel common mutation in the ryanodine receptor gene in malignant hyperthermia: implications for diagnosis and heterogeneity studies. *Hum Mol Genet* 3:471–476.
- Robinson RL, Monnier N, Wolz W, Jung M, Reis A, Nuernberg G, Curran JL, Monsieurs K, Stieglitz P, Heytens L, Fricker R, van Broeckhoven C, Deufel T, Hopkins PM, Lunardi J, Mueller CR. 1997. A genome wide search for susceptibility loci in three European malignant hyperthermia pedigrees. *Hum Mol Genet* 6:953–961.
- Robinson RL, Brooks C, Brown SL, Ellis FR, Halsall PJ, Quinell RJ, Shaw MA, Hopkins PM. 2002. RYR1 mutations causing central core disease are associated with more severe malignant hyperthermia in vitro contracture test phenotypes. *Hum Mutat* 20:88–97.
- Robinson R, Carpenter D, Shaw MA, Halsall J, Hopkins P. 2006. Mutations in RYR1 in malignant hyperthermia and central core disease. *Hum Mutat* 27:977–989.
- Rueffert H, Olthoff D, Deutrich C, Meinecke CD, Froster UG. 2002. Mutation screening in the ryanodine receptor 1 gene (RYR1) in patients susceptible to malignant hyperthermia who show definite IVCT results: identification of three novel mutations. *Acta Anaesthesiol Scand* 46:692–698.
- Sambuughin N, Holley H, Muldoon S, Brandom BW, de Bantel AM, Tobin JR, Nelson TE, Goldfarb LG. 2005. Screening of the entire ryanodine receptor type 1 coding region for sequence variants associated with malignant hyperthermia susceptibility in the North American population. *Anesthesiology* 102:515–521.
- Schulte am Esch J, Scholz J, Wappler F, editors. 2000. Malignant hyperthermia. Lengerich, Germany: Pabst Science Publishers. 425 p.
- Sei Y, Sambuughin NN, Davis EJ, Sachs D, Cuenca PB, Brandom BW, Tautz T, Rosenberg H, Nelson TE, Muldoon SM. 2004. Malignant hyperthermia in North America: genetic screening of the three hot spots in the type I ryanodine receptor gene. *Anesthesiology* 101:824–830.
- Serysheva II, Hamilton SL, Chiu W, Ludtke SJ. 2005. Structure of Ca²⁺ release channel at 14 Å resolution. *J Mol Biol* 345:427–431.
- Shepherd S, Ellis F, Halsall J, Hopkins P, Robinson R. 2004. RYR1 mutations in UK central core disease patients: more than just the C-terminal transmembrane region of the RYR1 gene. *J Med Genet* 41:e33.
- Stewart SL, Hogan K, Rosenberg H, Fletcher JE. 2001. Identification of the Arg1086His mutation in the alpha subunit of the voltage-dependent calcium channel (CACNA1S) in a North American family with malignant hyperthermia. *Clin Genet* 59:178–184.
- Tammara A, Bracco A, Cozzolino S, Esposito M, Di Martino A, Savoia G, Zeuli L, Piluso G, Aurino S, Nigro V. 2003. Scanning for mutations of the ryanodine receptor (RYR1) gene by denaturing HPLC: detection of three novel malignant hyperthermia alleles. *Clin Chem* 49:761–768.
- Urwyler A, Deufel T, McCarthy T, West S. 2001. Guidelines for molecular genetic detection of susceptibility to malignant hyperthermia. *Br J Anaesth* 86:283–287.
- Zhou H, Brockington M, Jungbluth H, Monk D, Stanier P, Sewry CA, Moore GE, Muntoni F. 2006. Epigenetic allele silencing unveils recessive RYR1 mutations in core myopathies. *Am J Hum Genet* 79:859–868.

Functional Properties of *RYR1* Mutations Identified in Swedish Patients with Malignant Hyperthermia and Central Core Disease

Mirko Vukcevic, PhD,*§ Marcus Broman, MD,†§ Gunilla Islander, MD, PhD,†
Mikael Bodelsson, MD, PhD,† Eva Ranklev-Twetman, MD, PhD,† Clemens R. Müller, PhD,‡
Susan Treves, PhD*

BACKGROUND: A diagnosis of malignant hyperthermia susceptibility by in vitro contraction testing can often only be performed at specialized laboratories far away from where patients live. Therefore, we have designed a protocol for genetic screening of the *RYR1*-cDNA and for functional testing of newly identified ryanodine receptor 1 (*RYR1*) gene variants in B lymphocytes isolated from peripheral blood samples drawn at local primary care centers.

METHODS: B lymphocytes were isolated for the extraction of *RYR1*-mRNA and genomic DNA and for establishment of lymphoblastoid B cell lines in 5 patients carrying yet unclassified mutations in the *RYR1*. The B lymphoblastoid cell lines were used to study resting cytoplasmic calcium concentration, the peak calcium transient induced by the sarco(endo)plasmic reticulum Ca-ATPase inhibitor thapsigargin, and the dose-dependent calcium release induced by the ryanodine receptor agonist 4-chloro-*m*-cresol.

RESULTS: It was possible to extract mRNA for cDNA synthesis and to create B lymphocyte clones from all samples. All B lymphoblastoid cell lines carrying *RYR1* candidate mutations showed significantly increased resting cytoplasmic calcium levels as well as a shift to lower concentrations of 4-chloro-*m*-cresol inducing calcium release compared with controls.

CONCLUSIONS: Peripheral blood samples are stable regarding RNA and DNA extraction and establishment of lymphoblastoid B cell lines after transportation at ambient temperature over large distances by ordinary mail. Functional tests on B cells harboring the newly identified amino acid substitutions indicate that they alter intracellular Ca²⁺ homeostasis and are most likely causative of malignant hyperthermia. (Anesth Analg 2010;X:●●●-●●●)

In individuals who are genetically malignant hyperthermia (MH) susceptible (MHS) (Online Mendelian Inheritance in Man [OMIM] 145600), volatile anesthetics and/or succinylcholine can induce a severe decompensation of muscle calcium homeostasis leading to a life-threatening crisis including hyperthermia, tachycardia, coagulation disturbances, generalized muscle rigidity, oliguria, and eventually death.¹ The diagnosis of MHS is traditionally made by an in vitro contraction test (IVCT). This investigation is highly invasive, requiring an open muscle biopsy from musculus quadriceps and specialized testing equipment.²

The clinical presentation of central core disease (CCD) (OMIM 117000) is highly variable and symptoms can vary from clinically very mild to severe congenital myopathy with hypotonia, skeletal abnormalities, and scoliosis.^{3,4}

The ryanodine receptor 1 (*RYR1*) is encoded by the *RYR1* gene located on chromosome 19q13.1. The gene comprises 159,000 base pairs that are distributed over 106 exons. The *RYR1*-cDNA has a length of 15,117 kb and encodes a protein monomer of 5038 amino acids.^{5,6} More than 200 sequence variants in the *RYR1* gene have been identified and linked to MHS, CCD, and other neuromuscular disorders, yet the functional impact of only a minority of these amino acid substitutions has been elucidated (www.emhg.org). The vast majority of these variants have been found in individual patients and their families, and only a few recurrent variants each account for <10% of the MHS subjects.^{5,6}

Ca²⁺ is a second messenger in skeletal muscle cells. It is stored in the sarcoplasmic reticulum, an organelle whose function is intimately linked to regulating the myoplasmic Ca²⁺ concentration,⁷⁻¹¹ and is released via a process known as excitation-contraction coupling. When the dihydropyridine receptor (DHPR), the voltage sensor on the plasmalemma, senses a change in membrane potential, it undergoes a conformational change and directly interacts with the *RYR1* Ca²⁺ channel, causing it to open. DHPR and *RYR1* form highly organized structures on their respective membranes: 4 DHPR units on the transverse tubular membrane face corresponding *RYR1* tetramers located on the junctional face membrane of the terminal cisternae.¹² Because Ca²⁺ can act as a second messenger in many biological functions, its intracellular concentration is tightly regulated and maintained in a typical resting mammalian cell at about 60 to 120 nM, whereas the extracellular free

From the *Department of Anaesthesia and Biomedicine, Basel University Hospital, Basel, Switzerland; †Department of Anaesthesiology and Intensive Care, Lund University Hospital, Lund, Sweden; and ‡Department of Human Genetics, Biocentre, University of Würzburg, Würzburg, Germany.

§Drs. M. Vukcevic and M. Broman contributed equally to the study.

Accepted for publication November 12, 2009.

Supplemental digital content is available for this article. Direct URL citations appear in the printed text and are provided in the HTML and PDF versions of this article on the journal's Web site (www.anesthesia-analgesia.org).

Study funding: Funding information is provided at the end of the article.

Disclosure: The authors report no conflicts of interest.

Address correspondence and reprint requests to Marcus Broman, MD, Department of Anaesthesiology and Intensive Care, Lund University Hospital, S-22185 Lund, Sweden. Address e-mail to marcus.broman@skane.se.

Copyright © 2010 International Anesthesia Research Society

DOI: 10.1213/ANE.0b013e3181cbd815

Table 1. Clinical Details, In Vitro Contraction Test (IVCT), and Genetic Results of the Malignant Hyperthermia Susceptible (MHS) and Central Core Disease (CCD) Individuals Studied

Age at MH crisis	Gender	Surgery	IVCT result, caffeine (g)	IVCT result, halothane (g)	MH rank	Candidate mutation and exon found on cDNA and verified on genomic DNA
Patient 1, 29 y	Female	Cesarean delivery	6.2	7.55	6	p.Glu1058Lys in exon 24
Patient 2, 39 y	Male	Nasal septoplasty	2.4	4.1	5	p.Arg1679His in exon 34
Patient 3, 29 y	Female	Explorative laparotomy	2.8	1.8	4	p.His382Asn in exon 12
Patient 4, 5 y	Male	Achilles tendon elongation	0.5	1.15	6	p.Lys1393Arg in exon 29
Patient 5	Male	—	7.2	7.3	—	p.Arg2508Gly in exon 47

Maximal contractures in IVCT at the threshold concentrations of caffeine (2.0 mmol/L) and halothane (0.44 mmol/L) and the *RYR1* candidate mutations are given. The MH rank describes the likelihood that the clinical adverse reaction is MH.¹⁷

Ca²⁺ concentration is about 2 mM.^{8,9} Any alteration of Ca²⁺ homeostasis can affect the function of cells. In muscle cells, genetic disturbances of Ca²⁺ handling result in a variety of neuromuscular disorders such as MHS, CCD, some forms of multiminicore disease and centronuclear myopathy, and Brody disease.^{4,6,13}

Although the *RYR1* is mainly expressed in striated muscle cells, it is now well established that B lymphocytes also express this calcium channel.^{14,15}

The aim of this study was to develop an alternative protocol for diagnostic studies on MHS individuals by transporting blood samples instead of the patients themselves to the specialized testing center. This increases the opportunity of MHS diagnosis even if a patient's health service provider is far away from the MH laboratory. We designed a simple and practical protocol for the collection of blood samples to be drawn at the patients' local primary care centers. Three venous peripheral blood samples of 5 mL each were collected in different test tubes for mRNA and genomic DNA extraction and for establishment of B lymphoblastoid cell lines. Genetic screening and functional studies were successfully performed on these samples.

METHODS

Clinical Presentation

With Regional Ethics Committee approval, the patients participating in the study were informed by telephone and also signed a written consent to the study. All patients carried 1 candidate *RYR1* mutation each: patient 1: p.Glu1058Lys, patient 2: p.Arg1679His, patient 3: p.His382Asn, patient 4: p.Lys1393Arg, and patient 5: p.Arg2508Gly. These patients are from a cohort of 15 Scandinavian MHS patients, who were screened for the *RYR1* total coding region in our previous study¹⁶ and found to carry a novel or yet unclassified sequence variant.

Details of the clinical presentation of the patients with the reported *RYR1* amino acid substitutions are given in Table 1 and in Appendix 1 (see Supplemental Digital Content 1, <http://links.lww.com/AA/A61>).

For patients 1 to 4, the MH rank was assessed. The MH rank describes the qualitative likelihood, from 1 = almost never to 6 = almost certain, that an adverse anesthetic event represents MH. This clinical grading scale requires the anesthesiologist to judge whether specific clinical signs are appropriate for the patient's medical condition, anesthetic technique, or surgical procedure.¹⁷ The MH rank scores are presented in Table 1 and in Appendix 1 (see Supplemental

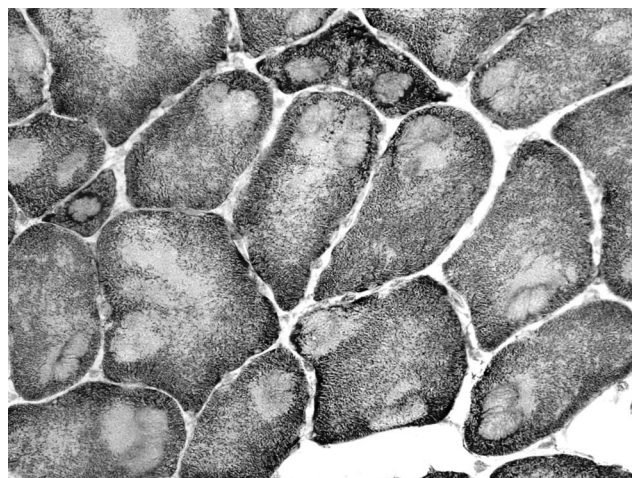


Figure 1. Histopathologic picture of the muscle biopsy taken from musculus vastus lateralis showing cores and degradation of the myosin around the cores in a nicotinamide adenine dinucleotide stain from patient 5, whose main disability is muscle weakness in his lower extremities and scoliosis. Cores are the light structures, devoid of mitochondria inside the cells. The sequence variant p.Arg2508Gly found has been reported previously in a Japanese patient with central core disease.²²

Digital Content 1, <http://links.lww.com/AA/A61>). Patient 5 has an established CCD diagnosis and his main symptoms are scoliosis and muscle weakness in the lower extremities. A microscopic histopathologic picture of his muscle tissue is shown in Figure 1.

In Vitro Contraction Test

Patients 1 to 4 had experienced serious MH clinical reactions and thereafter were tested by IVCT and classified as MHS. The patient with CCD (patient 5) was tested by the IVCT as part of standard diagnostic investigations to establish his diagnosis and was also classified as MHS. All IVCTs were performed at the National Swedish Malignant Hyperthermia Laboratory of Lund University Hospital according to the European Malignant Hyperthermia group protocol.² The results of the IVCTs are presented in Table 1 and in Appendix 1 (see Supplemental Digital Content 1, <http://links.lww.com/AA/A61>).

Blood Sampling

The patients were provided with written information about the sampling process. Peripheral venous blood samples

were drawn by the local family doctor in an EDTA tube, a PAXgene tube (BD, Stockholm, Sweden), and a heparin tube. The tubes were sent by normal mail without further handling or cooling to the laboratory in Würzburg, Germany, a distance up to 2000 km and a transportation time up to 6 days. Because PAXgene tubes are not normally available at Swedish primary care centers, they were provided to the patients.

Genetics

Total RNA was extracted from the PAXgene tubes according to the manufacturer's instructions, and genomic DNA of leukocytes was extracted from the EDTA tubes according to standard protocols. First-strand cDNA was synthesized using SuperScript™ II (Invitrogen, Carlsbad, CA) according to the manufacturer's instructions. Because of the size of the RYR1-mRNA, the first cDNA strand was synthesized using 3 mixes of specific primers. The resulting first strands were then amplified in 500 to 700 base pairs overlapping fragments using a second set of primers (primer sequences are available from the authors on request). Sequencing was performed by using the BigDye 1.1 kit on an ABI 3130 XL (Applied Biosystems, Darmstadt, Germany). All cDNA sequence variants leading to amino acid substitutions were confirmed on genomic DNA from the same patient.^{16,18}

Establishment of Epstein-Barr Virus Immortalized B Lymphoblastoid Cell Lines

B lymphocytes were isolated from the blood collected in the heparin tubes and transformed by the Epstein-Barr virus, as previously described.¹⁸

Functional Tests

Changes in the intracellular Ca^{2+} concentration ($[Ca^{2+}]_i$) of the B lymphoblastoid cells from patients carrying the candidate mutations and from healthy controls were assessed as previously described^{14,18} after loading cells with the fluorescent Ca^{2+} indicator fura-2/AM (5- μ M final concentration). Experiments were performed on cell populations (1.0×10^6 cells/mL, final volume 1.5 mL) in a thermostated LS-50 Perkin-Elmer (Waltham, MA) spectrofluorimeter equipped with a magnetic stirrer. The peak increase of the Ca^{2+} transient obtained after addition of a given concentration of 4-chloro-*m*-cresol on the linear part of the fura-2 calcium-sensitive curve was expressed as percentage of the peak Ca^{2+} released by maximal concentrations (1000 μ M) of 4-chloro-*m*-cresol. To assess the size of the intracellular Ca^{2+} stores, the area under the curve (AUC) obtained after addition of 400 nM thapsigargin, which represents the total amount of Ca^{2+} present in the rapidly releasable intracellular Ca^{2+} stores, was also calculated.

Statistical Analysis

Statistical analysis was performed using Student *t* test for paired samples or ANOVA when >2 groups were compared. The Origin computer program (Microcal Software, Northampton, MA) was used for statistical analysis and dose-response curve generation. The AUC values were calculated from the dose-response curves, whereas the 50%

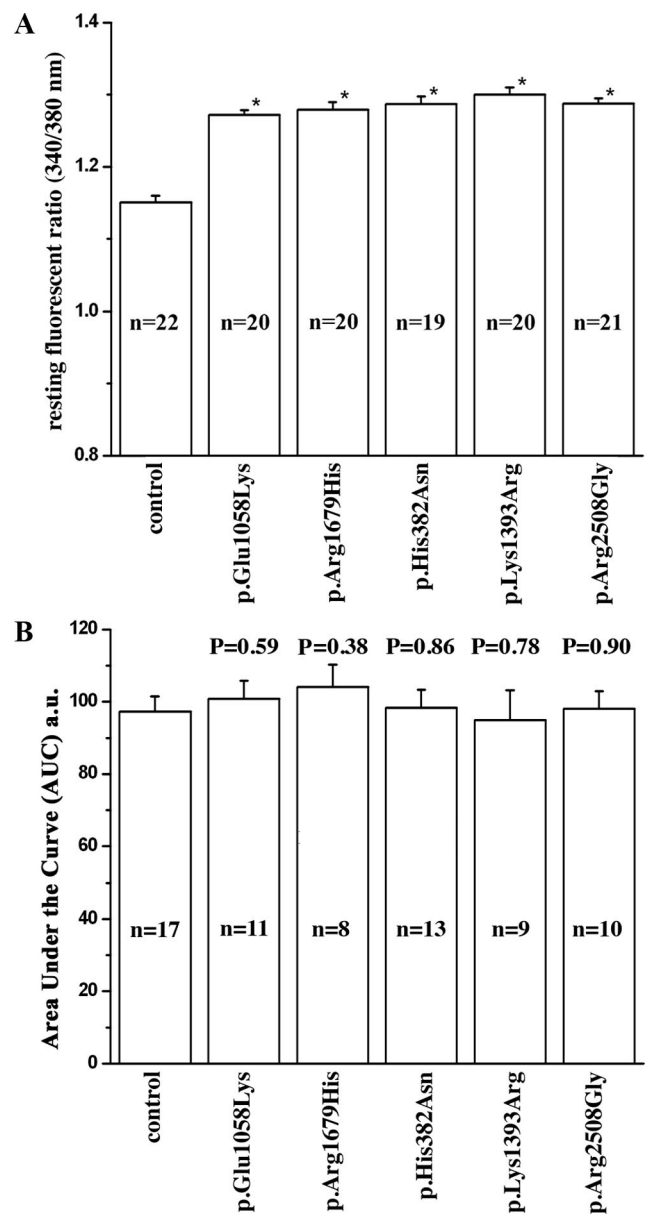


Figure 2. Comparison of the resting $[Ca^{2+}]_i$ and of the thapsigargin-induced Ca^{2+} release in lymphoblastoid B cells from healthy controls and 5 patients carrying the reported RYR1 candidate mutations. A, In all cases, resting fluorescence was significantly higher ($*P < 10^{-11}$) in patients' cell lines compared with healthy controls. B, The thapsigargin-induced Ca^{2+} release measurements are given as area under the curve (AUC) units; these were calculated by integrating the differences of the fluorescence values (the peak ratio 340/380 nm obtained after the addition of 400 nM thapsigargin – the resting ratio 340/380 nm). All cell lines show the same magnitude of Ca^{2+} content within the thapsigargin-sensitive intracellular Ca^{2+} stores. Fluorescence measurements were performed on fura-2-loaded cells as described in the Methods section. Values are the mean (\pm SEM) of the indicated *n* independent measurements. *P* values were obtained by performing the Student *t* test on values obtained from cells carrying the indicated mutation compared with controls.

effective concentration (EC_{50}) and R_{max} values were calculated from sigmoidal curve fitting of all data points. Results are expressed as mean value (\pm SEM) of *n* results, where *n* is the number of measurements.

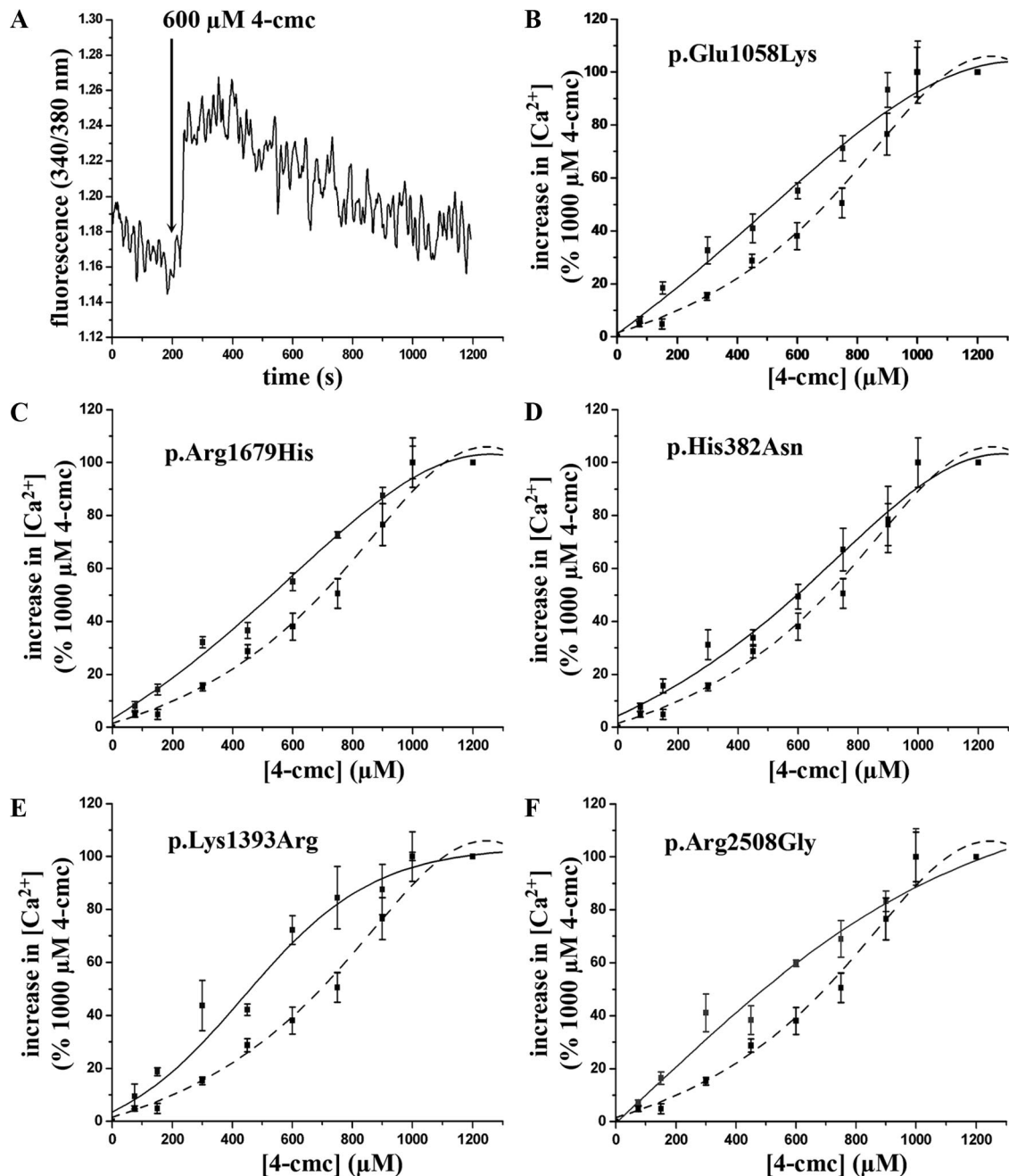


Figure 3. Dose-dependent 4-chloro-*m*-cresol-induced Ca^{2+} release in lymphoblastoid B cells from control individuals and from patients carrying candidate *RYR1* mutations. A, Representative trace of the effect of 4-chloro-*m*-cresol on the $[\text{Ca}^{2+}]_i$ of B lymphoblastoid cells from a control individual. Once the resting steady state was obtained, 600 μM 4-chloro-*m*-cresol was added as indicated by the arrow. B, p.Glu1058Lys (solid line) compared with control (dashed line). C, p.Arg1679His. D, p.His382Asn. E, p.Lys1393Arg. F, p.Arg2508Gly. Conditions as described in Figure 2. The peak increase of the Ca^{2+} transient, obtained after addition of a given concentration of 4-chloro-*m*-cresol on the linear part of the fura-2 calcium-sensitive curve, was expressed as percentage of the peak Ca^{2+} released by maximal concentrations (1000 μM) of 4-chloro-*m*-cresol. Results are expressed as mean \pm SEM ($n = 4-9$), where n indicates the number of independent measurements each performed on 1.5×10^6 cells. Sigmoidal dose-response curves were generated using Origin software.

RESULTS

After the sampling protocol as outlined in Methods section, peripheral blood samples proved to be sufficiently stable during transportation by ordinary mail at ambient temperatures over a period of up to 6 days for RNA and DNA extraction and establishment of lymphoblastoid B cell lines. Genetic screening for the presence of *RYR1* mutations¹⁶ and

calcium measurements on B lymphocytes could successfully be performed on these samples.

We first examined the resting $[\text{Ca}^{2+}]_i$ of the B lymphocytes carrying the newly identified sequence variants and compared it with the resting $[\text{Ca}^{2+}]_i$ of healthy controls (Fig. 2). All cell lines carrying a candidate mutation showed statistically significantly higher resting $[\text{Ca}^{2+}]_i$ compared

Table 2. EC₅₀ for 4-Chloro-*m*-Cresol (4-cmc)-Induced Calcium Release from Immortalized B Lymphoblastoid Cell Lines from Controls and Patients with the Indicated RYR1 Candidate Mutations

RYR1 mutant cell line	EC ₅₀ 4-cmc (μM)
Control	717.8 ± 65.0
p.Glu1058Lys	550.0 ± 28.3*
p.Arg1679His	480.9 ± 65.3*
p.His382Asn	615.9 ± 52.2*
p.Lys1393Arg	435.7 ± 27.5*
p.Arg2508Gly	501.3 ± 39.3*

Results are means ± SEM (of *n* experiments) compared with controls.

**P* < 0.05.

with cell lines from healthy controls. However, the AUC calculations of the Ca²⁺ transient obtained after stimulating the B lymphocytes with 400 nM thapsigargin were all within the same range, irrespective of whether the cells were obtained from controls or from individuals carrying the indicated RYR1 candidate mutations (Fig. 2). These results imply that none of the mutations affect the size of the intracellular Ca²⁺ stores in a way that could not be compensated by the cells. Nevertheless, all the amino acid substitutions affect Ca²⁺ homeostasis because they cause a small but significant increase in the resting Ca²⁺, a result that has been previously shown for B lymphocytes from individuals with the MHS phenotype.^{15,19–21}

We next determined whether the newly identified mutations affect the sensitivity of Ca²⁺ release induced by the RYR1 agonist 4-chloro-*m*-cresol. Figure 3A shows the typical increase in cytoplasmic [Ca²⁺]_i obtained in control cells after the addition of 600 μM 4-chloro-*m*-cresol. The trace, which represents the mean change in fluorescence of 1.5 × 10⁶ cells, shows that addition of the RYR1 agonist is accompanied by a transient increase in the 340/380 nm fluorescent ratio, which returns to resting levels within about 10 minutes. We then constructed 4-chloro-*m*-cresol dose-response curves by calculating the peak Ca²⁺ released by 4-chloro-*m*-cresol in a population (1.5 × 10⁶ cells) of fura-2-loaded lymphoblastoid B cells as a percentage of the maximal amount that could be released by 1000 μM 4-chloro-*m*-cresol. Results are given as means ± SEM. The dose-response curves from the cell lines carrying each of the candidate mutations showed a significant shift to the left compared with the curves from the cell lines from healthy controls. Table 2 shows the EC₅₀ values for 4-chloro-*m*-cresol-induced Ca²⁺ release.

DISCUSSION

In this study, we used a practical protocol to draw peripheral blood samples from MHS individuals at their local primary care centers to screen and identify RYR1 variants and to perform functional tests on the newly identified candidate mutations. Blood samples were sent by ordinary mail from different locations in Sweden to the laboratory in Würzburg, Germany, from September to January, which is autumn and winter in Northern Europe. Thus, the samples were not exposed to extreme heat, which could have compromised their viability.

Four of the substitutions described in the present report were identified in MHS patients who had developed life-threatening MH reactions during anesthesia (p.Glu1058Lys, p.Arg1679His, p.His382Asn, and p.Lys1393Arg). None of these substitutions have been reported in former patients. The fifth substitution (p.Arg2508Gly), occurring in the patient with CCD, has been identified before in a cohort of patients with CCD from Japan.²²

Patient 1 (p.Glu1058Lys) has shown signs of a mild muscular disease (Appendix 1, see Supplemental Digital Content 1, <http://links.lww.com/AA/A61>), but despite intensive investigations, a definitive diagnosis has not been established. Patients with myotonic muscle disease can especially react to succinylcholine²³ and thus one could argue the reaction she experienced was not true MH. However, her clinical reaction scores were high on the Larach scale and she had symptoms that are not first line in myotonic patients reacting to succinylcholine and inhalation anesthetics.

In our previous study,¹⁶ the substitution p.Arg1679His was found in 1 of 150 healthy anonymized German subjects and p.Lys1393Arg in 1 of 100 Swedish subjects leaving the possibility of rare polymorphisms. However, the population prevalence of a genetic MH disposition has never been studied. Therefore, these control subjects could likewise be as yet unidentified MH carriers. Ideal controls would of course be individuals with known IVCT status not MHS.

After the report by Sei et al.¹⁴ that B lymphocytes also express a functional type 1 RYR, we and others have exploited such a system to investigate the functional effect of candidate mutations linked to MHS and CCD phenotypes.^{15,18,20–22,24–27} These studies have revealed that most MH-causing mutations disturb normal calcium homeostasis by (1) shifting the sensitivity of pharmacologic RYR1 activation to lower agonist concentrations, and (2) by causing an increase in the resting [Ca²⁺]_i.^{15,20,21,24} Overall, the results compared well with the IVCT data of the same subjects. Likewise, the results of this study demonstrate a significant alteration of intracellular Ca²⁺ handling for all 5 candidate mutations and compare well with other studies.²⁸

Assessing Ca²⁺ homeostasis in the immortalized B lymphocyte system offers several advantages such as (1) cells can be grown in large numbers, (2) are easy to handle, and (3) can be assayed using a simple methodology such as fluorimetric analysis of cells loaded with the fluorescent Ca²⁺ indicator fura-2 and stimulated with the RYR1 agonist 4-chloro-*m*-cresol. In this context, it should be emphasized that this system is only useful for assessing RYR1 mutations and not, for example, mutations found in the α-1 subunit gene encoding the DHPR, which has been found to harbor mutations in a small number of MHS families²⁹ because this isoform of the voltage sensor is probably not expressed in B lymphocytes. Furthermore, it has been estimated that up to 30% of MH families might not link to RYR1 and thus will not benefit from this method.^{5,16}

We conclude from our results that the RYR1 amino acid substitutions studied are highly likely to be associated with the MH status in these patients. According to the guidelines of the European Malignant Hyperthermia Group,³⁰ RYR1 mutations should only be regarded as causative of MH if functional tests have been performed on tissues from at

least 2 unrelated individuals carrying the same candidate mutation. This, however, is impeded by the rarity of most RYR1 mutations.

We propose our protocol as a complementary approach for the diagnosis of MH-suspected subjects living far away from an MH diagnostic center. ■■

STUDY FUNDING

This work was supported by grants 3200B0–114597 from SNF and grants from the Swiss Muscle Foundation and Association Française Contre les Myopathies.

ACKNOWLEDGMENTS

The authors acknowledge the support of the Departments of Anesthesia of the Basel University Hospital, Switzerland and of Lund University Hospital, Sweden. The authors acknowledge Dr. Olof Danielsson, MD, PhD, Neuromuscular Unit, Linköping University Hospital, Sweden, for assistance with Figure 1. The authors also acknowledge the patients participating in the study

REFERENCES

- Hopkins PM. Malignant hyperthermia. *Advances in clinical management and diagnosis*. *Br J Anaesth* 2000;85:118–28
- Ording H, Brancadoro V, Cozzolino S, Ellis FR, Glauber V, Gonano EF, Halsall PJ, Hartung E, Heffron JJ, Heytens L, Kozak-Ribbens G, Kress H, Krivosic-Horber R, Lehmann-Horn F, Mortier W, Nivoche Y, Ranklev-Twetman E, Sigurdsson S, Snoeck M, Stiegliz M, Tegazzin V, Urwyler A, Wappler F. In vitro contracture test for diagnosis of malignant hyperthermia following the protocol of the European MH group: results of testing patients surviving fulminant MH and unrelated low-risk subjects. The European Malignant Hyperthermia group. *Acta Anaesthesiol Scand* 1997;41:955–66
- Quinlivan RM, Müller C, Davis M, Laing NG, Evans GA, Dove J, Roberts AP, Sewry CA. Central core disease: clinical, pathological, and genetic features. *Arch Dis Child* 2003;88:1051–5
- Treves S, Jungbluth H, Muntoni F, Zorzato F. Congenital muscle disorders with cores: the ryanodine receptor calcium channel paradigm. *Curr Opin Pharmacol* 2008;8:319–26
- Robinson R, Carpenter D, Shaw MA, Halsall J, Hopkins P. Mutations in RYR1 in malignant hyperthermia and central core disease. *Hum Mutat* 2006;27:977–89
- Treves S, Anderson AA, Ducreux S, Divet A, Bleunven C, Grasso C, Paesante S, Zorzato F. Ryanodine receptor 1 mutations, dysregulation of calcium homeostasis and neuromuscular disorders. *Neuromuscul Disord* 2005;15:577–87
- Carafoli E. Intracellular calcium homeostasis. *Ann Rev Biochem* 1987;56:395–433
- Berridge MJ, Lipp P, Bootman MD. The versatility and universality of calcium signaling. *Nat Rev Mol Cell Biol* 2000;1:11–21
- Berridge M, Bootman MD, Roderick HL. Calcium signaling: dynamics, homeostasis and remodeling. *Nat Rev Mol Cell Biol* 2003;4:817–21
- Rossi AE, Dirksen RT. Sarcoplasmic reticulum: the dynamic calcium governor of muscle. *Muscle Nerve* 2006;33:715–31
- Divet A, Paesante S, Bleunven C, Anderson A, Treves S, Zorzato F. Novel sarco(endo)plasmic reticulum proteins and calcium homeostasis in striated muscles. *J Muscle Res Cell Motil* 2005;26:7–12
- Protasi F, Franzini-Armstrong C, Allen PD. Role of ryanodine receptors in the assembly of calcium release units in skeletal muscle. *J Cell Biol* 1998;140:831–42
- Monnier N, Kozak-Ribbens G, Krivosic-Horber R, Nivoche Y, Qi D, Kraev N, Loke J, Sharma P, Tegazzin V, Figarella-Branger D, Romero N, Mezin P, Bendahan D, Payen JF, Depret T, MacLennan DH, Lunardi J. Correlations between genotype and pharmacological, histological, functional and clinical phenotypes in malignant hyperthermia susceptibility. *Hum Mutat* 2005;26:413–25
- Sei Y, Gallagher KL, Basile AS. Skeletal muscle type ryanodine receptor is involved in calcium signaling in human B lymphocytes. *J Biol Chem* 1999;274:5995–6002
- Girard T, Cavagna D, Padovan E, Spagnoli G, Urwyler A, Zorzato F, Treves S. B-lymphocytes from malignant hyperthermia-susceptible patients have an increased sensitivity to skeletal muscle ryanodine receptor activators. *J Biol Chem* 2001;276:48077–82
- Broman M, Gehrig A, Bodelsson M, Ranklev-Twetman E, Ruffert H, Müller C. Mutation screening of the RYR1-cDNA from peripheral B lymphocytes in 15 Swedish malignant hyperthermia index cases. *Br J Anaesth* 2009;102:642–9
- Larach MG, Localio AR, Allen GC, Denborough MA, Ellis R, Gronert GA, Kaplan RF, Muldoon SM, Nelson TE, Ording H. A clinical grading scale to predict malignant hyperthermia susceptibility. *Anesthesiology* 1994;80:771–9
- Tilgen N, Zorzato F, Halliger-Keller B, Muntoni F, Sewry C, Palmucci LM, Schneider C, Hauser E, Lehmann-Horn F, Müller CR, Treves S. Identification of four novel mutations in the C-terminal membrane spanning domain of the ryanodine receptor 1: association with central core disease and alteration of calcium homeostasis. *Hum Mol Genet* 2001;10:2879–87
- McKinney LC, Butler T, Mullen SP, Klein MG. Characterization of ryanodine receptor-mediated calcium release in human B cells: relevance to diagnostic testing for malignant hyperthermia. *Anesthesiology* 2006;104:1191–1201
- Lopez JR, Contreras J, Linares N, Allen PD. Hypersensitivity of malignant hyperthermia susceptible swine skeletal muscle to caffeine is mediated by high resting myoplasmic $[Ca^{2+}]_i$. *Anesthesiology* 2000;92:1799–1806
- Lopez JR, Linares N, Pessah IN, Allen PD. Enhanced response to caffeine and 4-chloro-*m*-cresol in malignant hyperthermia susceptible muscle is related in part to chronically elevated resting $[Ca^{2+}]_i$. *Am J Physiol Cell Physiol* 2005;288:606–12
- Wu S, Ibarra MC, McIcldan MC, Murayama K, Ichihara Y, Kikuchi H, Nonaka I, Noguchi S, Hayashi YK, Nishino I. Central core disease is due to RYR1 mutations in more than 90% of patients. *Brain* 2006;129:1470–80
- Driessen J. Neuromuscular and mitochondrial disorders: what is relevant to the anaesthesiologist? *Curr Opin Anaesthesiol* 2008;21:350–5
- Ducreaux S, Zorzato F, Müller CR, Sewry C, Muntoni F, Quinlivan R, Restagno G, Girard T, Treves S. Effect of ryanodine receptor mutations on IL-6 release and intracellular calcium homeostasis in human myotubes from malignant hyperthermia susceptible individuals and patients affected by central core disease. *J Biol Chem* 2004;279:43838–46
- Ducreux S, Zorzato F, Ferreiro A, Jungbluth H, Muntoni F, Monnier N, Müller CR, Treves S. Functional properties of ryanodine receptors carrying 3 amino acid substitutions identified in patients affected by multi-minicore disease and central core disease, expressed in immortalised lymphocytes. *Biochem J* 2006;395:259–66
- Anderson AA, Brown RL, Polster B, Pollock N, Stowell KM. Identification and biochemical characterization of a novel ryanodine receptor gene mutation associated with malignant hyperthermia. *Anesthesiology* 2008;108:208–15
- Lyfenko AD, Ducreux S, Wang Y, Xu L, Zorzato F, Ferreiro A, Meissner G, Treves S, Dirksen RT. Two central core disease (CCD) deletions in the C-terminal region of RYR1 alter muscle EC coupling by distinct mechanisms. *Hum Mutat* 2007;28:61–8
- Levano S, Vukcevic M, Singer M, Matter A, Treves S, Urwyler A, Girard T. Increasing the number of diagnostic mutations in malignant hyperthermia. *Hum Mutat* 2009;30:590–8
- Weiss R, O'Connell K, Flucher B, Allen P, Grabner M, Dirksen R. Functional analysis of the R1068H malignant hyperthermia mutation in the DHPR reveals an unexpected influence of the III–IV loop on skeletal muscle EC coupling. *Am J Physiol Cell Physiol* 2004;287:1094–102
- Urwyler A, Deufel T, McCarthy T, West S. Guidelines for molecular genetic detection of susceptibility to malignant hyperthermia. *Br J Anaesth* 2001;86:283–7

CHAPTER 3: GENERAL CONCLUSION AND PERSPECTIVES

Calcium is as an important second messenger, directing cells in their response to different agonists. The cell in turn is equipped with a variety of proteins to decode the information contained within the Ca^{2+} signal, in order to respond to the different signals coming from the extracellular environment. In this thesis we identified novel aspects of Ca^{2+} signalling in dendritic cells. We not only show that DCs express functional RyR1s, important players in calcium homeostasis in excitable cells, but we also investigated the role of RyR1 in DC biology and the mechanism through which this channel can be activated physiologically in these cells. Since the involvement of Ca^{2+} dependent events in DCs activation and maturation processes had been previously established, our first idea was to investigate downstream events induced by Ca^{2+} release by pharmacological stimulation of the RyR1. Our data demonstrate that activation of RyR1 in iDCs generates signals, which act in synergy with TLRs in promoting DC maturation. Although DCs are not excitable cells they express the cardiac isoform of L-type Ca^{2+} channel on the plasma membrane and they use a Ca^{2+} induce Ca^{2+} release mechanism to activate Ca^{2+} release from the RyR1. One of the intriguing questions prompting our research was that since DCs as non-excitable cells why are they are equipped with such a machinery capable of responding to signals within milliseconds? The solution to this question may come from the following facts: DCs synthesize large quantities of MHC class II molecules which classically bind peptides derived from endocytosed proteins and present them on their surface for interaction with T cells in order to initiate a specific immune response. Those empty MHC II molecules are expressed on the surface as well as sequestered within intracellular compartments and these sequestered molecules apparently reside unproductively within the cell. We now propose a direct role of DHPR-RyR1 signalling in the rapid surface expression of MHC class II molecules. Since MHC II molecules are crucial for antigen presentation and thus for the activation of a specific immune response

we think that DHPR-RyR1 signalling in DCs is important for very early and rapid activation of the immune system.

From our studies, several interesting points have emerged: firstly even if DCs are not excitable cells depolarizing the plasma membrane by addition of 100mM KCl leads to intracellular Ca^{2+} release. Thus plasma membrane depolarization in DCs could be a physiological route of DHPR-RyR1 activation *in vivo*. Secondly, since the main intracellular cation is potassium and by using necrotic cells extract we were able to activate DHPR-RyR1 signalling pathway, we postulate that cells dying within an inflamed tissue may release their K^+ in the vicinity of DCs and so activate the DHPR-RyR1 signalling pathway. Alternatively, if the interaction between T cells and DCs is strong enough, it can lead to activation of Ca^{2+} release from the intracellular stores of T cells and activation of Ca^{2+} influx. In T cells this is accompanied by efflux of K^+ to repolarise the T cell membrane potential. This K^+ could be released into the immunological synapse where molecules involved in cross signalling between T cells and DCs are concentrated and could be sensed by the DHPR on iDCs leading to activation of the RyR1 signalling pathway and bringing about the rapid release of MHC class II molecules onto the surface of iDCs. A schematic diagram outlining this hypothesis is depicted in (Fig.3-1).

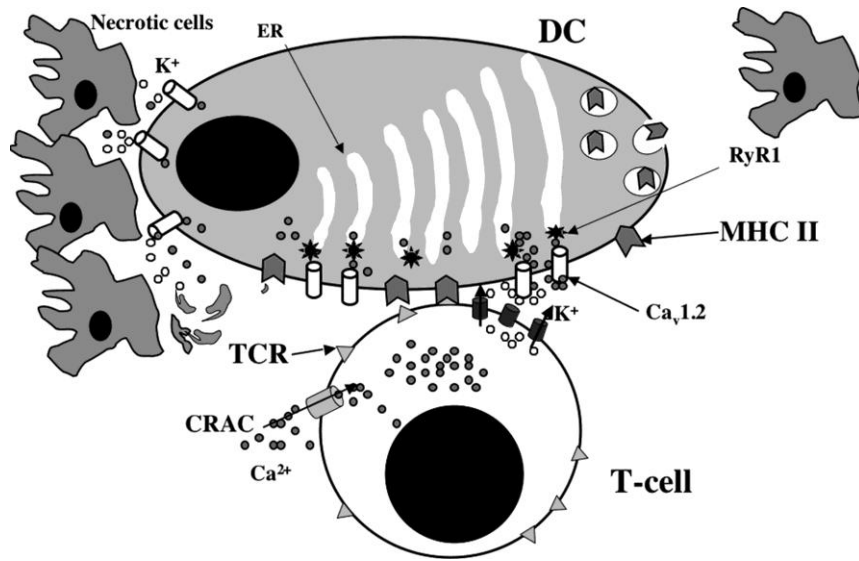


Figure 3-1: Schematic diagram depicting the model of RyR1-dependent signalling pathways in DC. Local depolarization of dendritic cell plasma membrane and activation of DHPR-RyR1 signalling by local increases of K^+ concentration released from dying cells or activated T cells into immunological synapse could cause the rapid release of recycling MHC class II molecules on the surface of dendritic cells.

A possible outlook from these results of the DHPR-RyR1 signalling pathway could be the development of drugs aimed at improving the immune system by increasing the efficiency of Ag presentation of DCs or at impairing the immune system in case of induction of autoimmune disorders.

During our investigations of Ca^{2+} homeostasis in DCs we noticed that spontaneous oscillations of the intracellular Ca^{2+} are exhibited by immature DCs. In contrast DCs, which had undergone the maturation process had lost these high frequency oscillations. Since these events are exclusively connected with the immature phenotype we suggest that these fluctuations in intracellular Ca^{2+} may be involved in maintaining the cells in the immature stage. As to their biological role, our results indicate that they are associated with the translocation of the transcription factor NFAT into the nucleus. These results are important because they point out novel aspects of intracellular Ca^{2+} signalling in human

DC and may open new areas of research important to help patients requiring modulations of the immune system.

The second part of my thesis focuses on the functional consequences of *RYR1* mutations on Ca^{2+} homeostasis and the possible use of EBV-immortalized B-lymphocytes expressing endogenous *RYR1* mutation linked to neuromuscular disorders to prove the functional effect of a mutation.

Unfortunately, muscle biopsies are not always available or their size is not sufficient for both histological diagnosis and generation of cell lines. Since RyR1 is also expressed in human B-lymphocytes we investigated whether EBV-immortalized B-lymphocytes could be used as a model system to study the functional impact of *RYR1* mutations identified in patients with neuromuscular disorders. All the *RYR1* mutations, which we functionally characterized in the present work, cause a significant increase of the resting Ca^{2+} concentration underlying their probable causative pathological role.

Furthermore the sensitivity of mutated RyR1 to pharmacological activation was increased in all mutations, also suggesting altered functional properties of these mutated RyR1. Thus the results from this study contribute to the establishment of a robust genetic/functional testing procedure for MH and we propose our protocol as a complementary approach for the diagnosis of MH.

As an outlook from these studies, we may hypothesize that mutations in *RYR1* associated with MH and CCD are also present in B-lymphocytes and DCs and one of the roles of these cells in the immune response is to release inflammatory cytokines thus one of the downstream events of *RYR1* mutations may be on the levels of circulating cytokines which may ultimately be involved in the pathology of these diseases. Since activation of the RyR1 leads to release of IL-6 and IL-1 α + IL-6 from muscle cells and B-cells, respectively and since mutation in *RYR1* result in significantly different amounts of pro-inflammatory cytokines released by B-lymphocytes and differentiated myotubes *in vitro*, it is possible that *RYR1* mutations found in patients with CCD and MH may affect the amount of circulating pro-inflammatory cytokines without an underlining infection. One of our future aims and ongoing studies are to determine the levels of IL-1 and IL-6 in the

serum of patients carrying *RYR1* mutations. Our future work will also focus on the impact of *RYR1* mutations on dendritic cell function and generally on the immune system. In order to study in greater detail the function of the RyR1 in cells of immune system, we think it is important to use an animal model in which a mutation linked to MH/CCD has been knocked-in.

We think that the results of these future studies will show us if there is a gain of immunological function connected with *RYR1* mutation. In addition such studies may provide answers if alterations of the immune function bears any role in the pathophysiology of ryanodinopathies.

REFERENCES:

- Abramson, J.J., E. Buck, G. Salama, J.E. Casida, and I.N. Pessah. 1988. Mechanism of anthraquinone-induced calcium release from skeletal muscle sarcoplasmic reticulum. *J Biol Chem* 263:18750-8.
- Allen, G.C., M.G. Larach, and A.R. Kunselman. 1998. The sensitivity and specificity of the caffeine-halothane contracture test: a report from the North American Malignant Hyperthermia Registry. The North American Malignant Hyperthermia Registry of MHAUS. *Anesthesiology* 88:579-88.
- Araki, N., M.T. Johnson, and J.A. Swanson. 1996. A role for phosphoinositide 3-kinase in the completion of macropinocytosis and phagocytosis by macrophages. *J Cell Biol* 135:1249-60.
- Aramburu, J., J. Heitman, and G.R. Crabtree. 2004. Calcineurin: a central controller of signalling in eukaryotes. *EMBO Rep* 5:343-8.
- Asselin-Paturel, C., and G. Trinchieri. 2005. Production of type I interferons: plasmacytoid dendritic cells and beyond. *J Exp Med* 202:461-5.
- Badou, A., M.K. Jha, D. Matza, W.Z. Mehal, M. Freichel, V. Flockerzi, and R.A. Flavell. 2006. Critical role for the beta regulatory subunits of Cav channels in T lymphocyte function. *Proc Natl Acad Sci U S A* 103:15529-34.
- Banchereau, J., and R.M. Steinman. 1998. Dendritic cells and the control of immunity. *Nature* 392:245-52.
- Bannister, R.A., I.N. Pessah, and K.G. Beam. 2009. The skeletal L-type Ca(2+) current is a major contributor to excitation-coupled Ca(2+) entry. *J Gen Physiol* 133:79-91.
- Barone, V., O. Massa, E. Intravaia, A. Bracco, A. Di Martino, V. Tegazzin, S. Cozzolino, and V. Sorrentino. 1999. Mutation screening of the RYR1 gene and identification of two novel mutations in Italian malignant hyperthermia families. *J Med Genet* 36:115-8.
- Baumeister, W., J. Walz, F. Zuhl, and E. Seemuller. 1998. The proteasome: paradigm of a self-compartmentalizing protease. *Cell* 92:367-80.

- Bendahan, D., S. Guis, N. Monnier, G. Kozak-Ribbens, J. Lunardi, B. Ghattas, J.P. Mattei, and P.J. Cozzone. 2004. Comparative analysis of in vitro contracture tests with ryanodine and a combination of ryanodine with either halothane or caffeine: a comparative investigation in malignant hyperthermia. *Acta Anaesthesiol Scand* 48:1019-27.
- Bernardi, P. 1999. Mitochondrial transport of cations: channels, exchangers, and permeability transition. *Physiol Rev* 79:1127-55.
- Berridge, M.J., M.D. Bootman, and P. Lipp. 1998. Calcium--a life and death signal. *Nature* 395:645-8.
- Berridge, M.J., P. Lipp, and M.D. Bootman. 2000. The versatility and universality of calcium signalling. *Nat Rev Mol Cell Biol* 1:11-21.
- Berridge, M.J., M.D. Bootman, and H.L. Roderick. 2003. Calcium signalling: dynamics, homeostasis and remodelling. *Nat Rev Mol Cell Biol* 4:517-29.
- Bers, D.M. 2002. Cardiac excitation-contraction coupling. *Nature* 415:198-205.
- Bers, D.M. 2004. Macromolecular complexes regulating cardiac ryanodine receptor function. *J Mol Cell Cardiol* 37:417-29.
- Bers, D.M. 2006. Cardiac ryanodine receptor phosphorylation: target sites and functional consequences. *Biochem J* 396:e1-3.
- Bers, D.M., and V.M. Stiffel. 1993. Ratio of ryanodine to dihydropyridine receptors in cardiac and skeletal muscle and implications for E-C coupling. *Am J Physiol* 264:C1587-93.
- Bevan, M.J. 1976. Minor H antigens introduced on H-2 different stimulating cells cross-react at the cytotoxic T cell level during in vivo priming. *J Immunol* 117:2233-8.
- Bitoun, M., S. Maugenre, P.Y. Jeannet, E. Lacene, X. Ferrer, P. Laforet, J.J. Martin, J. Laporte, H. Lochmuller, A.H. Beggs, M. Fardeau, B. Eymard, N.B. Romero, and P. Guicheney. 2005. Mutations in dynamin 2 cause dominant centronuclear myopathy. *Nat Genet* 37:1207-9.
- Bjorkman, P.J., M.A. Saper, B. Samraoui, W.S. Bennett, J.L. Strominger, and D.C. Wiley. 1987. Structure of the human class I histocompatibility antigen, HLA-A2. *Nature* 329:506-12.

- Bracci, L., M. Vukcevic, G. Spagnoli, S. Ducreux, F. Zorzato, and S. Treves. 2007. Ca²⁺ signaling through ryanodine receptor 1 enhances maturation and activation of human dendritic cells. *J Cell Sci* 120:2232-40.
- Brady, J.E., L.S. Sun, H. Rosenberg, and G. Li. 2009. Prevalence of malignant hyperthermia due to anesthesia in New York State, 2001-2005. *Anesth Analg* 109:1162-6.
- Brandman, O., J. Liou, W.S. Park, and T. Meyer. 2007. STIM2 is a feedback regulator that stabilizes basal cytosolic and endoplasmic reticulum Ca²⁺ levels. *Cell* 131:1327-39.
- Britt, B.A. 1985. Malignant hyperthermia. *Can Anaesth Soc J* 32:666-78.
- Brody, I.A. 1969. Muscle contracture induced by exercise. A syndrome attributable to decreased relaxing factor. *N Engl J Med* 281:187-92.
- Bromley, S.K., W.R. Burack, K.G. Johnson, K. Somersalo, T.N. Sims, C. Sumen, M.M. Davis, A.S. Shaw, P.M. Allen, and M.L. Dustin. 2001. The immunological synapse. *Annu Rev Immunol* 19:375-96.
- Brose, N., A. Betz, and H. Wegmeyer. 2004. Divergent and convergent signaling by the diacylglycerol second messenger pathway in mammals. *Curr Opin Neurobiol* 14:328-40.
- Brownell, A.K., R.T. Paasuke, A. Elash, S.B. Fowlow, C.G. Seagram, R.J. Diewold, and C. Friesen. 1983. Malignant hyperthermia in Duchenne muscular dystrophy. *Anesthesiology* 58:180-2.
- Cantrell, D. 1996. T cell antigen receptor signal transduction pathways. *Annu Rev Immunol* 14:259-74.
- Carafoli, E., L. Santella, D. Branca, and M. Brini. 2001. Generation, control, and processing of cellular calcium signals. *Crit Rev Biochem Mol Biol* 36:107-260.
- Catterall, W.A. 2000. Structure and regulation of voltage-gated Ca²⁺ channels. *Annu Rev Cell Dev Biol* 16:521-55.
- Catterall, W.A., E. Perez-Reyes, T.P. Snutch, and J. Striessnig. 2005. International Union of Pharmacology. XLVIII. Nomenclature and structure-function relationships of voltage-gated calcium channels. *Pharmacol Rev* 57:411-25.

- Chakrabarti, R., and R. Chakrabarti. 2006. Calcium signaling in non-excitabile cells: Ca²⁺ release and influx are independent events linked to two plasma membrane Ca²⁺ entry channels. *J Cell Biochem* 99:1503-16.
- Chamberlain, B.K., P. Volpe, and S. Fleischer. 1984. Inhibition of calcium-induced calcium release from purified cardiac sarcoplasmic reticulum vesicles. *J Biol Chem* 259:7547-53.
- Chapman, H.A. 1998. Endosomal proteolysis and MHC class II function. *Curr Opin Immunol* 10:93-102.
- Chen, S.R., and D.H. MacLennan. 1994. Identification of calmodulin-, Ca(2+)-, and ruthenium red-binding domains in the Ca²⁺ release channel (ryanodine receptor) of rabbit skeletal muscle sarcoplasmic reticulum. *J Biol Chem* 269:22698-704.
- Cherednichenko, G., A.M. Hurne, J.D. Fessenden, E.H. Lee, P.D. Allen, K.G. Beam, and I.N. Pessah. 2004. Conformational activation of Ca²⁺ entry by depolarization of skeletal myotubes. *Proc Natl Acad Sci U S A* 101:15793-8.
- Chiesi, M., R. Schwaller, and G. Calviello. 1988. Inhibition of rapid Ca-release from isolated skeletal and cardiac sarcoplasmic reticulum (SR) membranes. *Biochem Biophys Res Commun* 154:1-8.
- Clapham, D.E. 1995. Calcium signaling. *Cell* 80:259-68.
- Clipstone, N.A., and G.R. Crabtree. 1992. Identification of calcineurin as a key signalling enzyme in T-lymphocyte activation. *Nature* 357:695-7.
- Colonna, M., G. Trinchieri, and Y.J. Liu. 2004. Plasmacytoid dendritic cells in immunity. *Nat Immunol* 5:1219-26.
- Colucci, A., R. Giunti, S. Senesi, F.L. Bygrave, A. Benedetti, and A. Gamberucci. 2009. Effect of nifedipine on capacitive calcium entry in Jurkat T lymphocytes. *Arch Biochem Biophys* 481:80-5.
- Cristillo, A.D., and B.E. Bierer. 2002. Identification of novel targets of immunosuppressive agents by cDNA-based microarray analysis. *J Biol Chem* 277:4465-76.
- Czerniecki, B.J., C. Carter, L. Rivoltini, G.K. Koski, H.I. Kim, D.E. Weng, J.G. Roros, Y.M. Hijazi, S. Xu, S.A. Rosenberg, and P.A. Cohen. 1997. Calcium ionophore-

- treated peripheral blood monocytes and dendritic cells rapidly display characteristics of activated dendritic cells. *J Immunol* 159:3823-37.
- D'Arcy, C.E., A. Bjorksten, E.M. Yiu, A. Bankier, R. Gillies, C.A. McLean, L.K. Shield, and M.M. Ryan. 2008. King-denborough syndrome caused by a novel mutation in the ryanodine receptor gene. *Neurology* 71:776-7.
- Delon, J., N. Bercovici, R. Liblau, and A. Trautmann. 1998. Imaging antigen recognition by naive CD4+ T cells: compulsory cytoskeletal alterations for the triggering of an intracellular calcium response. *Eur J Immunol* 28:716-29.
- Denborough, M.A., X. Dennett, and R.M. Anderson. 1973. Central-core disease and malignant hyperpyrexia. *Br Med J* 1:272-3.
- Diebold, S.S., T. Kaisho, H. Hemmi, S. Akira, and C. Reis e Sousa. 2004. Innate antiviral responses by means of TLR7-mediated recognition of single-stranded RNA. *Science* 303:1529-31.
- Dirksen, R.T., and G. Avila. 2004. Distinct effects on Ca²⁺ handling caused by malignant hyperthermia and central core disease mutations in RyR1. *Biophys J* 87:3193-204.
- Dolmetsch, R.E., R.S. Lewis, C.C. Goodnow, and J.I. Healy. 1997. Differential activation of transcription factors induced by Ca²⁺ response amplitude and duration. *Nature* 386:855-8.
- Donoso, P., P. Aracena, and C. Hidalgo. 2000. Sulfhydryl oxidation overrides Mg(2+) inhibition of calcium-induced calcium release in skeletal muscle triads. *Biophys J* 79:279-86.
- Du, G.G., B. Sandhu, V.K. Khanna, X.H. Guo, and D.H. MacLennan. 2002. Topology of the Ca²⁺ release channel of skeletal muscle sarcoplasmic reticulum (RyR1). *Proc Natl Acad Sci U S A* 99:16725-30.
- Dubowitz, V., and A.G. Pearse. 1960. Oxidative enzymes and phosphorylase in central-core disease of muscle. *Lancet* 2:23-4.
- Duchen, M.R. 1999. Contributions of mitochondria to animal physiology: from homeostatic sensor to calcium signalling and cell death. *J Physiol* 516 (Pt 1):1-17.

- Ducreux, S., F. Zorzato, A. Ferreiro, H. Jungbluth, F. Muntoni, N. Monnier, C.R. Muller, and S. Treves. 2006. Functional properties of ryanodine receptors carrying three amino acid substitutions identified in patients affected by multi-minicore disease and central core disease, expressed in immortalized lymphocytes. *Biochem J* 395:259-66.
- Ducreux, S., F. Zorzato, C. Muller, C. Sewry, F. Muntoni, R. Quinlivan, G. Restagno, T. Girard, and S. Treves. 2004. Effect of ryanodine receptor mutations on interleukin-6 release and intracellular calcium homeostasis in human myotubes from malignant hyperthermia-susceptible individuals and patients affected by central core disease. *J Biol Chem* 279:43838-46.
- Dunnett, J., and W.G. Nayler. 1978. Calcium efflux from cardiac sarcoplasmic reticulum: effects of calcium and magnesium. *J Mol Cell Cardiol* 10:487-98.
- Ebashi, S., M. Endo, and I. Otsuki. 1969. Control of muscle contraction. *Q Rev Biophys* 2:351-84.
- Eng, G.D., B.S. Epstein, W.K. Engel, D.W. McKay, and R. McKay. 1978. Malignant hyperthermia and central core disease in a child with congenital dislocating hips. *Arch Neurol* 35:189-97.
- Engel, A.G., M.R. Gomez, and R.V. Groover. 1971. Multicore disease. A recently recognized congenital myopathy associated with multifocal degeneration of muscle fibers. *Mayo Clin Proc* 46:666-81.
- Ertel, E.A., K.P. Campbell, M.M. Harpold, F. Hofmann, Y. Mori, E. Perez-Reyes, A. Schwartz, T.P. Snutch, T. Tanabe, L. Birnbaumer, R.W. Tsien, and W.A. Catterall. 2000. Nomenclature of voltage-gated calcium channels. *Neuron* 25:533-5.
- Eu, J.P., J. Sun, L. Xu, J.S. Stamler, and G. Meissner. 2000. The skeletal muscle calcium release channel: coupled O₂ sensor and NO signaling functions. *Cell* 102:499-509.
- Ferreiro, A., N. Monnier, N.B. Romero, J.P. Leroy, C. Bonnemann, C.A. Haenggeli, V. Straub, W.D. Voss, Y. Nivoche, H. Jungbluth, A. Lemainque, T. Voit, J. Lunardi, M. Fardeau, and P. Guicheney. 2002. A recessive form of central core disease,

- transiently presenting as multi-minicore disease, is associated with a homozygous mutation in the ryanodine receptor type 1 gene. *Ann Neurol* 51:750-9.
- Feske, S., J. Giltneane, R. Dolmetsch, L.M. Staudt, and A. Rao. 2001. Gene regulation mediated by calcium signals in T lymphocytes. *Nat Immunol* 2:316-24.
- Feske, S., Y. Gwack, M. Prakriya, S. Srikanth, S.H. Puppel, B. Tanasa, P.G. Hogan, R.S. Lewis, M. Daly, and A. Rao. 2006. A mutation in *Orai1* causes immune deficiency by abrogating CRAC channel function. *Nature* 441:179-85.
- Fill, M., and J.A. Copello. 2002. Ryanodine receptor calcium release channels. *Physiol Rev* 82:893-922.
- Fletcher, J.E., G.E. Conner, G.C. Allen, F.J. Huggins, and H. Rosenberg. 1990. Importance of fasting in the lymphocyte calcium test for malignant hyperthermia. *Acta Anaesthesiol Scand* 34:636-9.
- Flewellen, E.H., T.E. Nelson, W.P. Jones, J.F. Arens, and D.L. Wagner. 1983. Dantrolene dose response in awake man: implications for management of malignant hyperthermia. *Anesthesiology* 59:275-80.
- Frank, J.P., Y. Harati, I.J. Butler, T.E. Nelson, and C.I. Scott. 1980. Central core disease and malignant hyperthermia syndrome. *Ann Neurol* 7:11-7.
- Franzini-Armstrong, C., and F. Protasi. 1997. Ryanodine receptors of striated muscles: a complex channel capable of multiple interactions. *Physiol Rev* 77:699-729.
- Franzini-Armstrong, C., F. Protasi, and V. Ramesh. 1998. Comparative ultrastructure of Ca²⁺ release units in skeletal and cardiac muscle. *Ann N Y Acad Sci* 853:20-30.
- Fryer, M.W., G.D. Lamb, and I.R. Neering. 1989. The action of ryanodine on rat fast and slow intact skeletal muscles. *J Physiol* 414:399-413.
- Galione, A., and G.C. Churchill. 2000. Cyclic ADP ribose as a calcium-mobilizing messenger. *Sci STKE* 2000:pe1.
- Gamble, J.G., L.A. Rinsky, and J.H. Lee. 1988. Orthopaedic aspects of central core disease. *J Bone Joint Surg Am* 70:1061-6.
- George, C.H., H. Jundi, N.L. Thomas, D.L. Fry, and F.A. Lai. 2007. Ryanodine receptors and ventricular arrhythmias: emerging trends in mutations, mechanisms and therapies. *J Mol Cell Cardiol* 42:34-50.

- Germain, R.N. 2004. An innately interesting decade of research in immunology. *Nat Med* 10:1307-20.
- Ghassemi, F., M. Vukcevic, L. Xu, H. Zhou, G. Meissner, F. Muntoni, H. Jungbluth, F. Zorzato, and S. Treves. 2009. A recessive ryanodine receptor 1 mutation in a CCD patient increases channel activity. *Cell Calcium* 45:192-7.
- Girard, T., D. Cavagna, E. Padovan, G. Spagnoli, A. Urwyler, F. Zorzato, and S. Treves. 2001. B-lymphocytes from malignant hyperthermia-susceptible patients have an increased sensitivity to skeletal muscle ryanodine receptor activators. *J Biol Chem* 276:48077-82.
- Godfrey, C., D. Escolar, M. Brockington, E.M. Clement, R. Mein, C. Jimenez-Mallebrera, S. Torelli, L. Feng, S.C. Brown, C.A. Sewry, M. Rutherford, Y. Shapira, S. Abbs, and F. Muntoni. 2006. Fukutin gene mutations in steroid-responsive limb girdle muscular dystrophy. *Ann Neurol* 60:603-10.
- Gomes, B., M. Savignac, M. Moreau, C. Leclerc, P. Lory, J.C. Guery, and L. Pelletier. 2004. Lymphocyte calcium signaling involves dihydropyridine-sensitive L-type calcium channels: facts and controversies. *Crit Rev Immunol* 24:425-47.
- Goth, S.R., R.A. Chu, J.P. Gregg, G. Cherednichenko, and I.N. Pessah. 2006. Uncoupling of ATP-mediated calcium signaling and dysregulated interleukin-6 secretion in dendritic cells by nanomolar thimerosal. *Environ Health Perspect* 114:1083-91.
- Grafton, G., and L. Thwaite. 2001. Calcium channels in lymphocytes. *Immunology* 104:119-26.
- Grafton, G., L. Stokes, K.M. Toellner, and J. Gordon. 2003. A non-voltage-gated calcium channel with L-type characteristics activated by B cell receptor ligation. *Biochem Pharmacol* 66:2001-9.
- Guis, S., D. Figarella-Branger, N. Monnier, D. Bendahan, G. Kozak-Ribbens, J.P. Mattei, J. Lunardi, P.J. Cozzzone, and J.F. Pellissier. 2004. Multimicore disease in a family susceptible to malignant hyperthermia: histology, in vitro contracture tests, and genetic characterization. *Arch Neurol* 61:106-13.
- Hamilton, S.L., and M.B. Reid. 2000. RyR1 modulation by oxidation and calmodulin. *Antioxid Redox Signal* 2:41-5.

- Hamilton, S.L., and Serysheva, II. 2009. Ryanodine receptor structure: progress and challenges. *J Biol Chem* 284:4047-51.
- Harrison, G.G. 1975. Control of the malignant hyperpyrexia syndrome in MHS swine by dantrolene sodium. *Br J Anaesth* 47:62-5.
- Hasselbach, W. 1964. Atp-Driven Active Transport of Calcium in the Membranes of the Sarcoplasmic Reticulum. *Proc R Soc Lond B Biol Sci* 160:501-4.
- Hayashi, F., K.D. Smith, A. Ozinsky, T.R. Hawn, E.C. Yi, D.R. Goodlett, J.K. Eng, S. Akira, D.M. Underhill, and A. Aderem. 2001. The innate immune response to bacterial flagellin is mediated by Toll-like receptor 5. *Nature* 410:1099-103.
- Hayek, S.M., X. Zhu, M.B. Bhat, J. Zhao, H. Takeshima, H.H. Valdivia, and J. Ma. 2000. Characterization of a calcium-regulation domain of the skeletal-muscle ryanodine receptor. *Biochem J* 351:57-65.
- Heil, F., H. Hemmi, H. Hochrein, F. Ampenberger, C. Kirschning, S. Akira, G. Lipford, H. Wagner, and S. Bauer. 2004. Species-specific recognition of single-stranded RNA via toll-like receptor 7 and 8. *Science* 303:1526-9.
- Herrmann-Frank, A., M. Richter, S. Sarkozi, U. Mohr, and F. Lehmann-Horn. 1996. 4-Chloro-m-cresol, a potent and specific activator of the skeletal muscle ryanodine receptor. *Biochim Biophys Acta* 1289:31-40.
- Hidalgo, C., P. Donoso, and M.A. Carrasco. 2005. The ryanodine receptors Ca²⁺ release channels: cellular redox sensors? *IUBMB Life* 57:315-22.
- Hidalgo, C., P. Aracena, G. Sanchez, and P. Donoso. 2002. Redox regulation of calcium release in skeletal and cardiac muscle. *Biol Res* 35:183-93.
- Hidalgo, C., R. Bull, M.I. Behrens, and P. Donoso. 2004. Redox regulation of RyR-mediated Ca²⁺ release in muscle and neurons. *Biol Res* 37:539-52.
- Hidalgo, C., R. Bull, J.J. Marengo, C.F. Perez, and P. Donoso. 2000. SH oxidation stimulates calcium release channels (ryanodine receptors) from excitable cells. *Biol Res* 33:113-24.
- Hopf, F.W., P. Reddy, J. Hong, and R.A. Steinhardt. 1996. A capacitative calcium current in cultured skeletal muscle cells is mediated by the calcium-specific leak channel and inhibited by dihydropyridine compounds. *J Biol Chem* 271:22358-67.

- Hoshino, K., O. Takeuchi, T. Kawai, H. Sanjo, T. Ogawa, Y. Takeda, K. Takeda, and S. Akira. 1999. Cutting edge: Toll-like receptor 4 (TLR4)-deficient mice are hyporesponsive to lipopolysaccharide: evidence for TLR4 as the Lps gene product. *J Immunol* 162:3749-52.
- Hosoi, E., C. Nishizaki, K.L. Gallagher, H.W. Wyre, Y. Matsuo, and Y. Sei. 2001. Expression of the ryanodine receptor isoforms in immune cells. *J Immunol* 167:4887-94.
- Hoth, M., and R. Penner. 1992. Depletion of intracellular calcium stores activates a calcium current in mast cells. *Nature* 355:353-6.
- Hsu, S., P.J. O'Connell, V.A. Klyachko, M.N. Badminton, A.W. Thomson, M.B. Jackson, D.E. Clapham, and G.P. Ahern. 2001. Fundamental Ca²⁺ signaling mechanisms in mouse dendritic cells: CRAC is the major Ca²⁺ entry pathway. *J Immunol* 166:6126-33.
- Hu, Z., J.M. Bonifas, J. Beech, G. Bench, T. Shigihara, H. Ogawa, S. Ikeda, T. Mauro, and E.H. Epstein, Jr. 2000. Mutations in ATP2C1, encoding a calcium pump, cause Hailey-Hailey disease. *Nat Genet* 24:61-5.
- Huang, Q., D. Liu, P. Majewski, L.C. Schulte, J.M. Korn, R.A. Young, E.S. Lander, and N. Hacohen. 2001. The plasticity of dendritic cell responses to pathogens and their components. *Science* 294:870-5.
- Iaizzo, P.A., M.J. Seewald, R. Olsen, D.J. Wedel, D.E. Chapman, M. Berggren, H.M. Eichinger, and G. Powis. 1991. Enhanced mobilization of intracellular Ca²⁺ induced by halothane in hepatocytes isolated from swine susceptible to malignant hyperthermia. *Anesthesiology* 74:531-8.
- Ibarra, M.C., S. Wu, K. Murayama, N. Minami, Y. Ichihara, H. Kikuchi, S. Noguchi, Y.K. Hayashi, R. Ochiai, and I. Nishino. 2006. Malignant hyperthermia in Japan: mutation screening of the entire ryanodine receptor type 1 gene coding region by direct sequencing. *Anesthesiology* 104:1146-54.
- Ichas, F., L.S. Jouaville, and J.P. Mazat. 1997. Mitochondria are excitable organelles capable of generating and conveying electrical and calcium signals. *Cell* 89:1145-53.

- Ikemoto, N., and R. el-Hayek. 1998. Signal transmission and transduction in excitation-contraction coupling. *Adv Exp Med Biol* 453:199-207.
- Ikemoto, N., M. Yano, R. el-Hayek, B. Antoniu, and M. Morii. 1994. Chemical depolarization-induced SR calcium release in triads isolated from rabbit skeletal muscle. *Biochemistry* 33:10961-8.
- Inaba, K., M. Pack, M. Inaba, H. Sakuta, F. Isdell, and R.M. Steinman. 1997. High levels of a major histocompatibility complex II-self peptide complex on dendritic cells from the T cell areas of lymph nodes. *J Exp Med* 186:665-72.
- Iwasaki, A., and R. Medzhitov. 2004. Toll-like receptor control of the adaptive immune responses. *Nat Immunol* 5:987-95.
- Janeway, C.A., Jr., and R. Medzhitov. 2002. Innate immune recognition. *Annu Rev Immunol* 20:197-216.
- Jiang, W., W.J. Swiggard, C. Heufler, M. Peng, A. Mirza, R.M. Steinman, and M.C. Nussenzweig. 1995. The receptor DEC-205 expressed by dendritic cells and thymic epithelial cells is involved in antigen processing. *Nature* 375:151-5.
- John, L.M., M. Mosquera-Caro, P. Camacho, and J.D. Lechleiter. 2001. Control of IP(3)-mediated Ca²⁺ puffs in *Xenopus laevis* oocytes by the Ca²⁺-binding protein parvalbumin. *J Physiol* 535:3-16.
- Jolles, S. 2002. Paul Langerhans. *J Clin Pathol* 55:243.
- Jungbluth, H. 2007. Central core disease. *Orphanet J Rare Dis* 2:25.
- Jungbluth, H., H. Zhou, C.A. Sewry, S. Robb, S. Treves, M. Bitoun, P. Guicheney, A. Buj-Bello, C. Bonnemann, and F. Muntoni. 2007. Centronuclear myopathy due to a de novo dominant mutation in the skeletal muscle ryanodine receptor (RYR1) gene. *Neuromuscul Disord* 17:338-45.
- Jungbluth, H., C.R. Muller, B. Halliger-Keller, M. Brockington, S.C. Brown, L. Feng, A. Chattopadhyay, E. Mercuri, A.Y. Manzur, A. Ferreira, N.G. Laing, M.R. Davis, H.P. Roper, V. Dubowitz, G. Bydder, C.A. Sewry, and F. Muntoni. 2002. Autosomal recessive inheritance of RYR1 mutations in a congenital myopathy with cores. *Neurology* 59:284-7.
- Karin, M., and E. Gallagher. 2005. From JNK to pay dirt: jun kinases, their biochemistry, physiology and clinical importance. *IUBMB Life* 57:283-95.

- Kaus, S.J., and M.A. Rockoff. 1994. Malignant hyperthermia. *Pediatr Clin North Am* 41:221-37.
- Kermode, H., A.J. Williams, and R. Sitsapesan. 1998. The interactions of ATP, ADP, and inorganic phosphate with the sheep cardiac ryanodine receptor. *Biophys J* 74:1296-304.
- Kim, D.H., F.A. Sreter, S.T. Ohnishi, J.F. Ryan, J. Roberts, P.D. Allen, L.G. Meszaros, B. Antoniu, and N. Ikemoto. 1984. Kinetic studies of Ca²⁺ release from sarcoplasmic reticulum of normal and malignant hyperthermia susceptible pig muscles. *Biochim Biophys Acta* 775:320-7.
- Kimber, I., M. Cumberbatch, and R.J. Dearman. 2009. Langerhans cell migration: not necessarily always at the center of the skin sensitization universe. *J Invest Dermatol* 129:1852-3.
- Klip, A., T. Ramlal, D. Walker, B.A. Britt, and M.E. Elliott. 1987. Selective increase in cytoplasmic calcium by anesthetic in lymphocytes from malignant hyperthermia-susceptible pigs. *Anesth Analg* 66:381-5.
- Klip, A., B.A. Britt, M.E. Elliott, D. Walker, T. Ramlal, and W. Pegg. 1986. Changes in cytoplasmic free calcium caused by halothane. Role of the plasma membrane and intracellular Ca²⁺ stores. *Biochem Cell Biol* 64:1181-9.
- Koch, B.M., T.E. Bertorini, G.D. Eng, and R. Boehm. 1985. Severe multicore disease associated with reaction to anesthesia. *Arch Neurol* 42:1204-6.
- Kopp, E., and R. Medzhitov. 2003. Recognition of microbial infection by Toll-like receptors. *Curr Opin Immunol* 15:396-401.
- Koski, G.K., G.N. Schwartz, D.E. Weng, B.J. Czerniecki, C. Carter, R.E. Gress, and P.A. Cohen. 1999. Calcium mobilization in human myeloid cells results in acquisition of individual dendritic cell-like characteristics through discrete signaling pathways. *J Immunol* 163:82-92.
- Kossugue, P.M., J.F. Paim, M.M. Navarro, H.C. Silva, R.C. Pavanello, J. Gurgel-Giannetti, M. Zatz, and M. Vainzof. 2007. Central core disease due to recessive mutations in RYR1 gene: is it more common than described? *Muscle Nerve* 35:670-4.

- Kotturi, M.F., D.A. Carlow, J.C. Lee, H.J. Ziltener, and W.A. Jefferies. 2003. Identification and functional characterization of voltage-dependent calcium channels in T lymphocytes. *J Biol Chem* 278:46949-60.
- Kurebayashi, N., and Y. Ogawa. 2001. Depletion of Ca²⁺ in the sarcoplasmic reticulum stimulates Ca²⁺ entry into mouse skeletal muscle fibres. *J Physiol* 533:185-99.
- Lai, F.A., M. Misra, L. Xu, H.A. Smith, and G. Meissner. 1989. The ryanodine receptor-Ca²⁺ release channel complex of skeletal muscle sarcoplasmic reticulum. Evidence for a cooperatively coupled, negatively charged homotetramer. *J Biol Chem* 264:16776-85.
- Lamb, G.D., and D.G. Stephenson. 1991. Effect of Mg²⁺ on the control of Ca²⁺ release in skeletal muscle fibres of the toad. *J Physiol* 434:507-28.
- Lamb, G.D., and D.G. Stephenson. 1992. Control of calcium release from the sarcoplasmic reticulum. *Adv Exp Med Biol* 311:289-303.
- Lamb, G.D., and D.G. Stephenson. 1994. Effects of intracellular pH and [Mg²⁺] on excitation-contraction coupling in skeletal muscle fibres of the rat. *J Physiol* 478 (Pt 2):331-9.
- Lanahan, A., and P. Worley. 1998. Immediate-early genes and synaptic function. *Neurobiol Learn Mem* 70:37-43.
- Lanzavecchia, A. 1990. Receptor-mediated antigen uptake and its effect on antigen presentation to class II-restricted T lymphocytes. *Annu Rev Immunol* 8:773-93.
- Lanzavecchia, A. 1996. Mechanisms of antigen uptake for presentation. *Curr Opin Immunol* 8:348-54.
- Lanzavecchia, A., and F. Sallusto. 2001. Regulation of T cell immunity by dendritic cells. *Cell* 106:263-6.
- Laporte, J., L.J. Hu, C. Kretz, J.L. Mandel, P. Kioschis, J.F. Coy, S.M. Klauck, A. Poustka, and N. Dahl. 1996. A gene mutated in X-linked myotubular myopathy defines a new putative tyrosine phosphatase family conserved in yeast. *Nat Genet* 13:175-82.
- Laporte, J., C. Guiraud-Chaumeil, M.C. Vincent, J.L. Mandel, S.M. Tanner, S. Liechti-Gallati, C. Wallgren-Pettersson, N. Dahl, W. Kress, P.A. Bolhuis, M. Fardeau, F. Samson, and E. Bertini. 1997. Mutations in the MTM1 gene implicated in X-

- linked myotubular myopathy. ENMC International Consortium on Myotubular Myopathy. European Neuro-Muscular Center. *Hum Mol Genet* 6:1505-11.
- Laver, D.R., T.M. Baynes, and A.F. Dulhunty. 1997. Magnesium inhibition of ryanodine-receptor calcium channels: evidence for two independent mechanisms. *J Membr Biol* 156:213-29.
- Laver, D.R., E.R. O'Neill, and G.D. Lamb. 2004. Luminal Ca²⁺-regulated Mg²⁺ inhibition of skeletal RyRs reconstituted as isolated channels or coupled clusters. *J Gen Physiol* 124:741-58.
- Laver, D.R., L.D. Roden, G.P. Ahern, K.R. Eager, P.R. Junankar, and A.F. Dulhunty. 1995. Cytoplasmic Ca²⁺ inhibits the ryanodine receptor from cardiac muscle. *J Membr Biol* 147:7-22.
- Lewis, R.S. 2003. Calcium oscillations in T-cells: mechanisms and consequences for gene expression. *Biochem Soc Trans* 31:925-9.
- Lewis, R.S., and M.D. Cahalan. 1989. Mitogen-induced oscillations of cytosolic Ca²⁺ and transmembrane Ca²⁺ current in human leukemic T cells. *Cell Regul* 1:99-112.
- Liou, J., M.L. Kim, W.D. Heo, J.T. Jones, J.W. Myers, J.E. Ferrell, Jr., and T. Meyer. 2005. STIM is a Ca²⁺ sensor essential for Ca²⁺-store-depletion-triggered Ca²⁺ influx. *Curr Biol* 15:1235-41.
- Liu, G., J.J. Abramson, A.C. Zable, and I.N. Pessah. 1994. Direct evidence for the existence and functional role of hyperreactive sulfhydryls on the ryanodine receptor-triadin complex selectively labeled by the coumarin maleimide 7-diethylamino-3-(4'-maleimidylphenyl)-4-methylcoumarin. *Mol Pharmacol* 45:189-200.
- Loke, J., and D.H. MacLennan. 1998. Malignant hyperthermia and central core disease: disorders of Ca²⁺ release channels. *Am J Med* 104:470-86.
- Lopez, J.R., J. Contreras, N. Linares, and P.D. Allen. 2000. Hypersensitivity of malignant hyperthermia-susceptible swine skeletal muscle to caffeine is mediated by high resting myoplasmic [Ca²⁺]. *Anesthesiology* 92:1799-806.
- Ludtke, S.J., Serysheva, II, S.L. Hamilton, and W. Chiu. 2005. The pore structure of the closed RyR1 channel. *Structure* 13:1203-11.

- Lukyanenko, V., I. Gyorke, T.F. Wiesner, and S. Gyorke. 2001. Potentiation of Ca²⁺ release by cADP-ribose in the heart is mediated by enhanced SR Ca²⁺ uptake into the sarcoplasmic reticulum. *Circ Res* 89:614-22.
- Lund, J.M., L. Alexopoulou, A. Sato, M. Karow, N.C. Adams, N.W. Gale, A. Iwasaki, and R.A. Flavell. 2004. Recognition of single-stranded RNA viruses by Toll-like receptor 7. *Proc Natl Acad Sci U S A* 101:5598-603.
- Lynch, P.J., J. Tong, M. Lehane, A. Mallet, L. Giblin, J.J. Heffron, P. Vaughan, G. Zafra, D.H. MacLennan, and T.V. McCarthy. 1999. A mutation in the transmembrane/luminal domain of the ryanodine receptor is associated with abnormal Ca²⁺ release channel function and severe central core disease. *Proc Natl Acad Sci U S A* 96:4164-9.
- Lyubchenko, T.A., G.A. Wurth, and A. Zweifach. 2001. Role of calcium influx in cytotoxic T lymphocyte lytic granule exocytosis during target cell killing. *Immunity* 15:847-59.
- MacKrell, J.J. 1999. Protein-protein interactions in intracellular Ca²⁺-release channel function. *Biochem J* 337 (Pt 3):345-61.
- MacLennan, D.H. 2000. Ca²⁺ signalling and muscle disease. *Eur J Biochem* 267:5291-7.
- Manoury, B., E.W. Hewitt, N. Morrice, P.M. Dando, A.J. Barrett, and C. Watts. 1998. An asparaginyl endopeptidase processes a microbial antigen for class II MHC presentation. *Nature* 396:695-9.
- Marengo, J.J., C. Hidalgo, and R. Bull. 1998. Sulfhydryl oxidation modifies the calcium dependence of ryanodine-sensitive calcium channels of excitable cells. *Biophys J* 74:1263-77.
- Marty, I., M. Robert, M. Villaz, K. De Jongh, Y. Lai, W.A. Catterall, and M. Ronjat. 1994. Biochemical evidence for a complex involving dihydropyridine receptor and ryanodine receptor in triad junctions of skeletal muscle. *Proc Natl Acad Sci U S A* 91:2270-4.
- Marx, S.O., S. Reiken, Y. Hisamatsu, T. Jayaraman, D. Burkhoff, N. Rosemblyt, and A.R. Marks. 2000. PKA phosphorylation dissociates FKBP12.6 from the calcium release channel (ryanodine receptor): defective regulation in failing hearts. *Cell* 101:365-76.

- Matza, D., and R.A. Flavell. 2009. Roles of Ca(v) channels and AHNAK1 in T cells: the beauty and the beast. *Immunol Rev* 231:257-64.
- Matzinger, P. 1994. Tolerance, danger, and the extended family. *Annu Rev Immunol* 12:991-1045.
- Matzinger, P. 2002. The danger model: a renewed sense of self. *Science* 296:301-5.
- McPherson, P.S., and K.P. Campbell. 1993. Characterization of the major brain form of the ryanodine receptor/Ca²⁺ release channel. *J Biol Chem* 268:19785-90.
- Meissner, G. 1986. Ryanodine activation and inhibition of the Ca²⁺ release channel of sarcoplasmic reticulum. *J Biol Chem* 261:6300-6.
- Meissner, G. 1994. Ryanodine receptor/Ca²⁺ release channels and their regulation by endogenous effectors. *Annu Rev Physiol* 56:485-508.
- Meissner, G., E. Rios, A. Tripathy, and D.A. Pasek. 1997. Regulation of skeletal muscle Ca²⁺ release channel (ryanodine receptor) by Ca²⁺ and monovalent cations and anions. *J Biol Chem* 272:1628-38.
- Meissner, G., E. Rousseau, F.A. Lai, Q.Y. Liu, and K.A. Anderson. 1988. Biochemical characterization of the Ca²⁺ release channel of skeletal and cardiac sarcoplasmic reticulum. *Mol Cell Biochem* 82:59-65.
- Merlini, L., P. Mattutini, S. Bonfiglioli, and C. Granata. 1987. Non-progressive central core disease with severe congenital scoliosis: a case report. *Dev Med Child Neurol* 29:106-9.
- Moghadaszadeh, B., N. Petit, C. Jaillard, M. Brockington, S.Q. Roy, L. Merlini, N. Romero, B. Estournet, I. Desguerre, D. Chaigne, F. Muntoni, H. Topaloglu, and P. Guicheney. 2001. Mutations in SEPNI cause congenital muscular dystrophy with spinal rigidity and restrictive respiratory syndrome. *Nat Genet* 29:17-8.
- Monnier, N., A. Ferreira, I. Marty, A. Labarre-Vila, P. Mezin, and J. Lunardi. 2003. A homozygous splicing mutation causing a depletion of skeletal muscle RYR1 is associated with multi-minicore disease congenital myopathy with ophthalmoplegia. *Hum Mol Genet* 12:1171-8.
- Monnier, N., I. Marty, J. Faure, C. Castiglioni, C. Desnuelle, S. Sacconi, B. Estournet, A. Ferreira, N. Romero, A. Laquerriere, L. Lazaro, J.J. Martin, E. Morava, A. Rossi, A. Van der Kooi, M. de Visser, C. Verschuuren, and J. Lunardi. 2008. Null

- mutations causing depletion of the type 1 ryanodine receptor (RYR1) are commonly associated with recessive structural congenital myopathies with cores. *Hum Mutat* 29:670-8.
- Mosmann, T.R., and A.M. Livingstone. 2004. Dendritic cells: the immune information management experts. *Nat Immunol* 5:564-6.
- Nadif Kasri, N., G. Bultynck, I. Sienaert, G. Callewaert, C. Erneux, L. Missiaen, J.B. Parys, and H. De Smedt. 2002. The role of calmodulin for inositol 1,4,5-trisphosphate receptor function. *Biochim Biophys Acta* 1600:19-31.
- Negulescu, P.A., T.B. Krasieva, A. Khan, H.H. Kerschbaum, and M.D. Cahalan. 1996. Polarity of T cell shape, motility, and sensitivity to antigen. *Immunity* 4:421-30.
- O'Connell, P.J., V.A. Klyachko, and G.P. Ahern. 2002. Identification of functional type 1 ryanodine receptors in mouse dendritic cells. *FEBS Lett* 512:67-70.
- Odermatt, A., P.E. Taschner, V.K. Khanna, H.F. Busch, G. Karpati, C.K. Jablecki, M.H. Breuning, and D.H. MacLennan. 1996. Mutations in the gene-encoding SERCA1, the fast-twitch skeletal muscle sarcoplasmic reticulum Ca²⁺ ATPase, are associated with Brody disease. *Nat Genet* 14:191-4.
- Oh-hora, M. 2009. Calcium signaling in the development and function of T-lineage cells. *Immunol Rev* 231:210-24.
- Oh-Hora, M., M. Yamashita, P.G. Hogan, S. Sharma, E. Lamperti, W. Chung, M. Prakriya, S. Feske, and A. Rao. 2008. Dual functions for the endoplasmic reticulum calcium sensors STIM1 and STIM2 in T cell activation and tolerance. *Nat Immunol* 9:432-43.
- Okamura, H., and A. Rao. 2001. Transcriptional regulation in lymphocytes. *Curr Opin Cell Biol* 13:239-43.
- Ording, H., B. Foder, and O. Scharff. 1990. Cytosolic free calcium concentrations in lymphocytes from malignant hyperthermia susceptible patients. *Br J Anaesth* 64:341-5.
- Ording, H., V. Brancadoro, S. Cozzolino, F.R. Ellis, V. Glauber, E.F. Gonano, P.J. Halsall, E. Hartung, J.J. Heffron, L. Heytens, G. Kozak-Ribbens, H. Kress, R. Krivosic-Horber, F. Lehmann-Horn, W. Mortier, Y. Nivoche, E. Ranklev-Twetman, S. Sigurdsson, M. Snoeck, P. Stieglitz, V. Tegazzin, A. Urwyler, and F.

- Wappler. 1997. In vitro contracture test for diagnosis of malignant hyperthermia following the protocol of the European MH Group: results of testing patients surviving fulminant MH and unrelated low-risk subjects. The European Malignant Hyperthermia Group. *Acta Anaesthesiol Scand* 41:955-66.
- Osada, H., K. Masuda, K. Seki, and S. Sekiya. 2004. Multi-minicore disease with susceptibility to malignant hyperthermia in pregnancy. *Gynecol Obstet Invest* 58:32-5.
- Otsu, K., H.F. Willard, V.K. Khanna, F. Zorzato, N.M. Green, and D.H. MacLennan. 1990. Molecular cloning of cDNA encoding the Ca²⁺ release channel (ryanodine receptor) of rabbit cardiac muscle sarcoplasmic reticulum. *J Biol Chem* 265:13472-83.
- Owen, V.J., N.L. Taske, and G.D. Lamb. 1997. Reduced Mg²⁺ inhibition of Ca²⁺ release in muscle fibers of pigs susceptible to malignant hyperthermia. *Am J Physiol* 272:C203-11.
- Peinelt, C., M. Vig, D.L. Koomoa, A. Beck, M.J. Nadler, M. Koblan-Huberson, A. Lis, A. Fleig, R. Penner, and J.P. Kinet. 2006. Amplification of CRAC current by STIM1 and CRACM1 (Orai1). *Nat Cell Biol* 8:771-3.
- Perrimon, N., and B. Mathey-Prevot. 2007. Applications of high-throughput RNA interference screens to problems in cell and developmental biology. *Genetics* 175:7-16.
- Pessah, I.N., R.A. Stambuk, and J.E. Casida. 1987. Ca²⁺-activated ryanodine binding: mechanisms of sensitivity and intensity modulation by Mg²⁺, caffeine, and adenine nucleotides. *Mol Pharmacol* 31:232-8.
- Pessah, I.N., K.H. Kim, and W. Feng. 2002. Redox sensing properties of the ryanodine receptor complex. *Front Biosci* 7:a72-9.
- Pessah, I.N., E.L. Durie, M.J. Schiedt, and I. Zimanyi. 1990. Anthraquinone-sensitized Ca²⁺ release channel from rat cardiac sarcoplasmic reticulum: possible receptor-mediated mechanism of doxorubicin cardiomyopathy. *Mol Pharmacol* 37:503-14.
- Petersen, O.H., M. Michalak, and A. Verkhratsky. 2005. Calcium signalling: past, present and future. *Cell Calcium* 38:161-9.

- Poenie, M., R.Y. Tsien, and A.M. Schmitt-Verhulst. 1987. Sequential activation and lethal hit measured by $[Ca^{2+}]_i$ in individual cytolytic T cells and targets. *Embo J* 6:2223-32.
- Prakriya, M., S. Feske, Y. Gwack, S. Srikanth, A. Rao, and P.G. Hogan. 2006. Orai1 is an essential pore subunit of the CRAC channel. *Nature* 443:230-3.
- Putney, J.W., Jr. 1986. A model for receptor-regulated calcium entry. *Cell Calcium* 7:1-12.
- Ramsey, P.L., and R.N. Hensinger. 1975. Congenital dislocation of the hip associated with central core disease. *J Bone Joint Surg Am* 57:648-51.
- Rhee, S.G. 2001. Regulation of phosphoinositide-specific phospholipase C. *Annu Rev Biochem* 70:281-312.
- Ringer, S. 1883. A further Contribution regarding the influence of the different Constituents of the Blood on the Contraction of the Heart. *J Physiol* 4:29-42 3.
- Rios, E., B.S. Launikonis, L. Royer, G. Brum, and J. Zhou. 2006. The elusive role of store depletion in the control of intracellular calcium release. *J Muscle Res Cell Motil* 27:337-50.
- Rizzuto, R., M. Brini, M. Murgia, and T. Pozzan. 1993. Microdomains with high Ca^{2+} close to IP_3 -sensitive channels that are sensed by neighboring mitochondria. *Science* 262:744-7.
- Robinson, R., D. Carpenter, M.A. Shaw, J. Halsall, and P. Hopkins. 2006. Mutations in RYR1 in malignant hyperthermia and central core disease. *Hum Mutat* 27:977-89.
- Robinson, R.L., C. Brooks, S.L. Brown, F.R. Ellis, P.J. Halsall, R.J. Quinell, M.A. Shaw, and P.M. Hopkins. 2002. RYR1 mutations causing central core disease are associated with more severe malignant hyperthermia in vitro contracture test phenotypes. *Hum Mutat* 20:88-97.
- Romero, N.B., N. Monnier, L. Viollet, A. Cortey, M. Chevally, J.P. Leroy, J. Lunardi, and M. Fardeau. 2003. Dominant and recessive central core disease associated with RYR1 mutations and fetal akinesia. *Brain* 126:2341-9.
- Roos, J., P.J. DiGregorio, A.V. Yeromin, K. Ohlsen, M. Liudyno, S. Zhang, O. Safrina, J.A. Kozak, S.L. Wagner, M.D. Cahalan, G. Velicelebi, and K.A. Stauderman.

2005. STIM1, an essential and conserved component of store-operated Ca²⁺ channel function. *J Cell Biol* 169:435-45.
- Rosenberg, H., M. Davis, D. James, N. Pollock, and K. Stowell. 2007. Malignant hyperthermia. *Orphanet J Rare Dis* 2:21.
- Rossi, A.E., and R.T. Dirksen. 2006. Sarcoplasmic reticulum: the dynamic calcium governor of muscle. *Muscle Nerve* 33:715-31.
- Rueffert, H., D. Olthoff, C. Deutrich, C.D. Meinecke, and U.G. Froster. 2002. Mutation screening in the ryanodine receptor 1 gene (RYR1) in patients susceptible to malignant hyperthermia who show definite IVCT results: identification of three novel mutations. *Acta Anaesthesiol Scand* 46:692-8.
- Salama, G., E.V. Menshikova, and J.J. Abramson. 2000. Molecular interaction between nitric oxide and ryanodine receptors of skeletal and cardiac sarcoplasmic reticulum. *Antioxid Redox Signal* 2:5-16.
- Sallusto, F., and A. Lanzavecchia. 1994. Efficient presentation of soluble antigen by cultured human dendritic cells is maintained by granulocyte/macrophage colony-stimulating factor plus interleukin 4 and downregulated by tumor necrosis factor alpha. *J Exp Med* 179:1109-18.
- Sallusto, F., M. Cella, C. Danieli, and A. Lanzavecchia. 1995. Dendritic cells use macropinocytosis and the mannose receptor to concentrate macromolecules in the major histocompatibility complex class II compartment: downregulation by cytokines and bacterial products. *J Exp Med* 182:389-400.
- Samso, M., and T. Wagenknecht. 1998. Contributions of electron microscopy and single-particle techniques to the determination of the ryanodine receptor three-dimensional structure. *J Struct Biol* 121:172-80.
- Samso, M., T. Wagenknecht, and P.D. Allen. 2005. Internal structure and visualization of transmembrane domains of the RyR1 calcium release channel by cryo-EM. *Nat Struct Mol Biol* 12:539-44.
- Sandow, A. 1965. Excitation-contraction coupling in skeletal muscle. *Pharmacol Rev* 17:265-320.
- Schulze-Luehrmann, J., and S. Ghosh. 2006. Antigen-receptor signaling to nuclear factor kappa B. *Immunity* 25:701-15.

- Sei, Y., K.L. Gallagher, and A.S. Basile. 1999. Skeletal muscle type ryanodine receptor is involved in calcium signaling in human B lymphocytes. *J Biol Chem* 274:5995-6002.
- Serysheva, II, S.L. Hamilton, W. Chiu, and S.J. Ludtke. 2005. Structure of Ca²⁺ release channel at 14 Å resolution. *J Mol Biol* 345:427-31.
- Shibasaki, F., E.R. Price, D. Milan, and F. McKeon. 1996. Role of kinases and the phosphatase calcineurin in the nuclear shuttling of transcription factor NF-AT4. *Nature* 382:370-3.
- Shimamoto, S., M. Takata, M. Tokuda, F. Oohira, H. Tokumitsu, and R. Kobayashi. 2008. Interactions of S100A2 and S100A6 with the tetratricopeptide repeat proteins, Hsp90/Hsp70-organizing protein and kinesin light chain. *J Biol Chem* 283:28246-58.
- Shuaib, A., R.T. Paasuke, and K.W. Brownell. 1987. Central core disease. Clinical features in 13 patients. *Medicine (Baltimore)* 66:389-96.
- Soler, F., F. Fernandez-Belda, and J.C. Gomez-Fernandez. 1992. The Ca²⁺ release channel in junctional sarcoplasmic reticulum: gating and blockade by cations. *Int J Biochem* 24:903-9.
- Sorrentino, V., G. Giannini, P. Malzac, and M.G. Mattei. 1993. Localization of a novel ryanodine receptor gene (RYR3) to human chromosome 15q14-q15 by in situ hybridization. *Genomics* 18:163-5.
- Stancovski, I., and D. Baltimore. 1997. NF-kappaB activation: the I kappaB kinase revealed? *Cell* 91:299-302.
- Stathopoulos, P.B., L. Zheng, G.Y. Li, M.J. Plevin, and M. Ikura. 2008. Structural and mechanistic insights into STIM1-mediated initiation of store-operated calcium entry. *Cell* 135:110-22.
- Steinbach, J.H. 2008. Pharmacology: Unready for action. *Nature* 454:704-5.
- Steinman, R.M., and Z.A. Cohn. 1973. Identification of a novel cell type in peripheral lymphoid organs of mice. I. Morphology, quantitation, tissue distribution. *J Exp Med* 137:1142-62.
- Steinman, R.M., M. Pack, and K. Inaba. 1997. Dendritic cells in the T-cell areas of lymphoid organs. *Immunol Rev* 156:25-37.

- Strazis, K.P., and A.W. Fox. 1993. Malignant hyperthermia: a review of published cases. *Anesth Analg* 77:297-304.
- Suko, J., H. Drobny, and G. Hellmann. 1999. Activation and inhibition of purified skeletal muscle calcium release channel by NO donors in single channel current recordings. *Biochim Biophys Acta* 1451:271-87.
- Suko, J., I. Maurer-Fogy, B. Plank, O. Bertel, W. Wyskovsky, M. Hohenegger, and G. Hellmann. 1993. Phosphorylation of serine 2843 in ryanodine receptor-calcium release channel of skeletal muscle by cAMP-, cGMP- and CaM-dependent protein kinase. *Biochim Biophys Acta* 1175:193-206.
- Sutko, J.L., and J.A. Airey. 1996. Ryanodine receptor Ca²⁺ release channels: does diversity in form equal diversity in function? *Physiol Rev* 76:1027-71.
- Takeshima, H., S. Nishimura, T. Matsumoto, H. Ishida, K. Kangawa, N. Minamino, H. Matsuo, M. Ueda, M. Hanaoka, T. Hirose, and et al. 1989. Primary structure and expression from complementary DNA of skeletal muscle ryanodine receptor. *Nature* 339:439-45.
- Tarroni, P., D. Rossi, A. Conti, and V. Sorrentino. 1997. Expression of the ryanodine receptor type 3 calcium release channel during development and differentiation of mammalian skeletal muscle cells. *J Biol Chem* 272:19808-13.
- Taylor, C.W., and A.J. Laude. 2002. IP₃ receptors and their regulation by calmodulin and cytosolic Ca²⁺. *Cell Calcium* 32:321-34.
- Tilgen, N., F. Zorzato, B. Halliger-Keller, F. Muntoni, C. Sewry, L.M. Palmucci, C. Schneider, E. Hauser, F. Lehmann-Horn, C.R. Muller, and S. Treves. 2001. Identification of four novel mutations in the C-terminal membrane spanning domain of the ryanodine receptor 1: association with central core disease and alteration of calcium homeostasis. *Hum Mol Genet* 10:2879-87.
- Treves, S., H. Jungbluth, F. Muntoni, and F. Zorzato. 2008. Congenital muscle disorders with cores: the ryanodine receptor calcium channel paradigm. *Curr Opin Pharmacol* 8:319-26.
- Treves, S., F. Di Virgilio, V. Cerundolo, P. Zanovello, D. Collavo, and T. Pozzan. 1987. Calcium and inositolphosphates in the activation of T cell-mediated cytotoxicity. *J Exp Med* 166:33-42.

- Treves, S., A.A. Anderson, S. Ducreux, A. Divet, C. Bleunven, C. Grasso, S. Paesante, and F. Zorzato. 2005. Ryanodine receptor 1 mutations, dysregulation of calcium homeostasis and neuromuscular disorders. *Neuromuscul Disord* 15:577-87.
- Trombetta, E.S., and I. Mellman. 2005. Cell biology of antigen processing in vitro and in vivo. *Annu Rev Immunol* 23:975-1028.
- Varsanyi, M., and H.E. Meyer. 1995. Sarcoplasmic reticular Ca²⁺ release channel is phosphorylated at serine 2843 in intact rabbit skeletal muscle. *Biol Chem Hoppe Seyler* 376:45-9.
- Vig, M., A. Beck, J.M. Billingsley, A. Lis, S. Parvez, C. Peinelt, D.L. Koomoa, J. Soboloff, D.L. Gill, A. Fleig, J.P. Kinet, and R. Penner. 2006. CRACM1 multimers form the ion-selective pore of the CRAC channel. *Curr Biol* 16:2073-9.
- Vukcevic, M., G.C. Spagnoli, G. Iezzi, F. Zorzato, and S. Treves. 2008. Ryanodine receptor activation by Ca^v 1.2 is involved in dendritic cell major histocompatibility complex class II surface expression. *J Biol Chem* 283:34913-22.
- Wagenknecht, T., R. Grassucci, J. Berkowitz, G.J. Wiederrecht, H.B. Xin, and S. Fleischer. 1996. Cryoelectron microscopy resolves FK506-binding protein sites on the skeletal muscle ryanodine receptor. *Biophys J* 70:1709-15.
- Wehrens, X.H., and A.R. Marks. 2003. Altered function and regulation of cardiac ryanodine receptors in cardiac disease. *Trends Biochem Sci* 28:671-8.
- Wu, S., M.C. Ibarra, M.C. Malicdan, K. Murayama, Y. Ichihara, H. Kikuchi, I. Nonaka, S. Noguchi, Y.K. Hayashi, and I. Nishino. 2006. Central core disease is due to RYR1 mutations in more than 90% of patients. *Brain* 129:1470-80.
- Xiong, H., X. Feng, L. Gao, L. Xu, D.A. Pasek, J.H. Seok, and G. Meissner. 1998. Identification of a two EF-hand Ca²⁺ binding domain in lobster skeletal muscle ryanodine receptor/Ca²⁺ release channel. *Biochemistry* 37:4804-14.
- Xu, L., J.P. Eu, G. Meissner, and J.S. Stamler. 1998a. Activation of the cardiac calcium release channel (ryanodine receptor) by poly-S-nitrosylation. *Science* 279:234-7.
- Xu, L., A. Tripathy, D.A. Pasek, and G. Meissner. 1998b. Potential for pharmacology of ryanodine receptor/calcium release channels. *Ann N Y Acad Sci* 853:130-48.

- Xu, L., Y. Wang, N. Yamaguchi, D.A. Pasek, and G. Meissner. 2008. Single channel properties of heterotetrameric mutant RyR1 ion channels linked to core myopathies. *J Biol Chem* 283:6321-9.
- Yeromin, A.V., S.L. Zhang, W. Jiang, Y. Yu, O. Safrina, and M.D. Cahalan. 2006. Molecular identification of the CRAC channel by altered ion selectivity in a mutant of Orai. *Nature* 443:226-9.
- Zahradnikova, A., I. Minarovic, R.C. Venema, and L.G. Meszaros. 1997. Inactivation of the cardiac ryanodine receptor calcium release channel by nitric oxide. *Cell Calcium* 22:447-54.
- Zhao, F., P. Li, S.R. Chen, C.F. Louis, and B.R. Fruen. 2001. Dantrolene inhibition of ryanodine receptor Ca²⁺ release channels. Molecular mechanism and isoform selectivity. *J Biol Chem* 276:13810-6.
- Zhou, H., M. Brockington, H. Jungbluth, D. Monk, P. Stanier, C.A. Sewry, G.E. Moore, and F. Muntoni. 2006a. Epigenetic allele silencing unveils recessive RYR1 mutations in core myopathies. *Am J Hum Genet* 79:859-68.
- Zhou, H., N. Yamaguchi, L. Xu, Y. Wang, C. Sewry, H. Jungbluth, F. Zorzato, E. Bertini, F. Muntoni, G. Meissner, and S. Treves. 2006b. Characterization of recessive RYR1 mutations in core myopathies. *Hum Mol Genet* 15:2791-803.
- Zhou, H., H. Jungbluth, C.A. Sewry, L. Feng, E. Bertini, K. Bushby, V. Straub, H. Roper, M.R. Rose, M. Brockington, M. Kinali, A. Manzur, S. Robb, R. Appleton, S. Messina, A. D'Amico, R. Quinlivan, M. Swash, C.R. Muller, S. Brown, S. Treves, and F. Muntoni. 2007. Molecular mechanisms and phenotypic variation in RYR1-related congenital myopathies. *Brain* 130:2024-36.
- Zorzato, F., G. Salviati, T. Facchinetti, and P. Volpe. 1985. Doxorubicin induces calcium release from terminal cisternae of skeletal muscle. A study on isolated sarcoplasmic reticulum and chemically skinned fibers. *J Biol Chem* 260:7349-55.
- Zorzato, F., P. Menegazzi, S. Treves, and M. Ronjat. 1996. Role of malignant hyperthermia domain in the regulation of Ca²⁺ release channel (ryanodine receptor) of skeletal muscle sarcoplasmic reticulum. *J Biol Chem* 271:22759-63.

- Zorzato, F., E. Scutari, V. Tegazzin, E. Clementi, and S. Treves. 1993. Chlorocresol: an activator of ryanodine receptor-mediated Ca²⁺ release. *Mol Pharmacol* 44:1192-201.
- Zorzato, F., J. Fujii, K. Otsu, M. Phillips, N.M. Green, F.A. Lai, G. Meissner, and D.H. MacLennan. 1990. Molecular cloning of cDNA encoding human and rabbit forms of the Ca²⁺ release channel (ryanodine receptor) of skeletal muscle sarcoplasmic reticulum. *J Biol Chem* 265:2244-56.
- Zorzato, F., N. Yamaguchi, L. Xu, G. Meissner, C.R. Muller, P. Pouliquin, F. Muntoni, C. Sewry, T. Girard, and S. Treves. 2003. Clinical and functional effects of a deletion in a COOH-terminal luminal loop of the skeletal muscle ryanodine receptor. *Hum Mol Genet* 12:379-88.
- Zweifach, A., and R.S. Lewis. 1993. Mitogen-regulated Ca²⁺ current of T lymphocytes is activated by depletion of intracellular Ca²⁺ stores. *Proc Natl Acad Sci U S A* 90:6295-9.

CURRICULUM VITAE

Name: Vukcevic
First name: Mirko
Birth Date/Place: 14/04/1977, Belgrade

EDUCATION:

July, 2006 – Feb, 2010 PhD study, Laboratory: Perioperative Patient Safety, Department of Biomedicine, University Hospital, University of Basel

24.02.2004 Pharmacy Board Certification, Serbian Ministry of Health

1996-2002 Faculty of Pharmacy, University of Belgrade
/5 years + diploma/master thesis/
Final exam grade 10 (out of 10)
Grade point average 8.68 (out of 10.00)

1992-1996 Grammar school, Belgrade /main courses: chemistry, biology, mathematics, physics /

WORKING EXPERIENCE:

March, 2010-present PostDoc, Laboratory: Perioperative Patient Safety, Department of Biomedicine, University Hospital, University of Basel

2005, July 1st – 2006, June Trainee, Novartis Institute for Biomedical Research, Department: Musculoskeletal Diseases / Bone Metabolism, Basel, Switzerland

2003, April 1st – 2005, June

Pharmacist, Pharmanova Pharmaceutical
Company, Belgrade

2004, June 1st - 2005, June

Trainee, Central Pharmacy, Special Hospital for
Cerebral Diseases, Belgrade

PUBLICATIONS:

1. Mirko Vukcevic, Francesco Zorzato, Giulio Spagnoli and Susan Treves.
Frequent calcium oscillations lead to NFAT activation in human immature dendritic cells. *J. Biol Chem.* 2010 May 21;285(21):16003-11. Epub 2010 Mar 26.
2. Mirko Vukcevic*, Marcus Broman*, Gunilla Islander, Mikael Bodelsson, Eva Ranklev-Twetman, Clemens R. Müller and Susan Treves.
Functional Properties of RyR1 Mutations Identified in Swedish Malignant Hyperthermia and Central Core Disease Patients
Anesth Analg. 2010 Feb 8. [Epub ahead of print]
*These authors contributed equally to this work
3. Treves S, Vukcevic M, Maj M, Thurnheer R, Mosca B, Zorzato F.
Minor sarcoplasmic reticulum membrane components that modulate excitation-contraction coupling in striated muscles. *J Physiol.* 2009 Jul 1;587(Pt 13):3071-9. Epub 2009 Apr 29. Review.
4. Soledad Levano*, Mirko Vukcevic*, Martine Singer, Anja Matter, Susan Treves, Albert Urwyler, Thierry Girard
Increasing the Number of Diagnostic Mutations in Malignant Hyperthermia. *Hum Mutat.* 2009 Apr;30(4):590-8
* These authors contributed equally to this work
5. Farshid Ghassemia, Mirko Vukcevic, Le Xua, Haiyan Zhoue, Gerhard Meissnera, Francesco Muntonie, Heinz Jungbluthf, Francesco Zorzato, Susan Treves.
A recessive ryanodine receptor 1 mutation in a CCD patient increase channel activity. *Cell Calcium.* 2009 Feb;45(2):192-7. Epub 2008 Nov 21.
6. Mirko Vukcevic, Giulio C. Spagnoli, Giandomenica Iezzi, Francesco Zorzato and Susan Treves.
Ryanodine Receptor Activation by Cav1.2 Is Involved in Dendritic Cell Major Histocompatibility Complex Class II Surface Expression.
J Biol Chem. 2008 Dec 12;283(50):34913-22. Epub 2008 Oct 16.
7. Laura Bracci*, Mirko Vukcevic*, Giulio Spagnoli, Sylvie Ducreux, Francesco Zorzato and Susan Treves.

Ca²⁺ signalling through ryanodine receptor 1 enhances maturation and activation of human dendritic cells. *J Cell Sci.* 2007 Jul 1;120(Pt 13):2232-40. Epub 2007 Jun 13. Erratum in: *J Cell Sci.* 2007 Jul 15;120(Pt 14):2468.

* These authors contributed equally to this work

8. Rishard Salie, Michaela Kneissel, Mirko Vukevic, Natasa Zamurovic, Ina Kramer, Glenda Evans, Nicole Gerwin, Matthias Mueller, Bernd Kinzel, Mira Susa. Ubiquitous overexpression of Hey1 transcription factor leads to osteopenia and chondrocyte hypertrophy in bone. *Bone.* 2010 Mar;46(3):680-94. Epub 2009 Oct 24.
9. Soledad Levano, Albert Urwyler, Susan Treves, Mirko Vukcevic, Thierry Girard. Maligne Hyperthermie: Gentests statt Muskelbiopsien *Schweiz Med Forum* 2008;8(44):849–851
10. Vukcevic M, Zamurovic N, Luong-Nguyen N, Geffers N, Gossler A, Susa M. BMP-2 Induces Hey1 and HES1 in Osteoblastic Cells via Notch-Dependent and -Independent Signalling Pathways. Poster presentation, 28th Annual Meeting of the American Society for Bone and Mineral Research, September 15-19 2006, Philadelphia, Pennsylvania, USA.
11. Susa M, Zamurovic N, Salie R, Rohner D, Evans G, Vukcevic M, Mueller M, Kinzel B, Kneissel M. Overexpression of Hey1, a Notch Target Gene, Leads to Osteopenia in Mice Due to Decreased Osteoblast Performance. Oral presentation, 28th Annual Meeting of the American Society for Bone and Mineral Research, September 15-19 2006, Philadelphia, Pennsylvania, USA.